GEOPHYSICAL INVESTIGATION OF THE INNER MORAY FIRTH AND ST GEORGE'S CHANNEL BASINS

by

Konstantinos Dimitropoulos
B.Sc., Athens University

Thesis presented for the degree of
Doctor of Philosophy
of the University of Edinburgh in the
Faculty of Science

SEPTEMBER 1981

DECLARATION

I hereby declare that the work presented in this thesis is my own unless otherwise stated in the text, and that the thesis has been composed by myself.

.....

Konstantinos Dimitropoulos

To

Elena

ACKNOWLEDGEMENTS

I am grateful to Professor K M Creer, Head of the Geophysics Department for accepting me as a post-graduate student in his department. I am further indebted to Mr R McQuillin, Head of the Marine Geophysics Unit of the Institute of Geological Sciences, not only for allowing me full use of the Unit's facilities to carry out my project, but also for his continuous encouragement, useful discussions and suggestions and constructive comments on my manuscript. It has been a great pleasure and joy for me to work with him.

My knowledge of the English language does not allow me to properly express my gratitude to Dr J A Donato. For more than three and a half years he has always been available to help me, comment on my work and discuss whatever problems I have had, always happily, always smiling. Any value that attaches to this thesis must to a great degree reflect his continuous help and encouragement. Many thanks John.

I wish also to express my sincere thanks to Dr R A Scutton for his help and supervision over the years. His vast academic experience and quick anticipation has always helped me to keep working along the right direction and to avoid spending time pursuing less fruitful lines of research to little avail. I shall always be indebted to him for his continuous effort and the encouragement he has given me.

I am deeply indebted to my wife Helen for her strong support and encouragement throughout.

I would like to thank Mr G A Day for his useful comments and discussions and for always willingly checking my manuscripts, also Dr R Thompson for his help when I needed to deal with palaeomagnetic data.

My gratitude is due to Dr W Mykura of IGS Edinburgh for helping me with geological information for the Moray Firth area, his constructive comments and for allowing me to use figure 2/3 in my thesis.

I would like to thank Dr R Hipkin and Dr A Hussein of the Geophysics Department, Edinburgh University, the first for his useful comments and discussions, the second for assistance with the three-dimensional gravity computer program.

I am indebted to Dr R Whittington of the University of Wales, Aberystwyth, for his useful and constructive comments and for helping me with geological information for the south Irish Sea area.

I wish to express my gratitude to my colleagues of the Marine Geophysics Unit at the Institute of Geological Sciences, Edinburgh for their help and continuous encouragement and mention especially Miss L Nisbet, Miss M Glen and Mr R Walker. I also thank Mr D Smythe of the Hydrocarbons Unit for his useful suggestions and for helping me with the ray-tracing computer program used in the thesis.

I am indebted to my Greek colleagues Dr E Lagios and Dr Papamarinopoulos, the first for useful discussions and help with computer contouring routines, the second for suggesting Edinburgh University to me for continuation of my studies and especially for suggesting that I work in the Marine Geophysics Unit of IGS Edinburgh.

My thanks are due to Dr V Colter of British Gas and to the Phillips Petroleum Company for providing and allowing me to publish selected exploration data of critical value to this thesis; also the Continental Shelf Division of IGS for allowing me free access to open files.

Finally I would like to thank again Linda Nisbet who kindly gave up many of her hours to type this thesis, an achievement for which I am particularly indebted to her.

ABSTRACT

This principally geophysical study involves the examination of two Mesozoic sedimentary basins, the Inner Moray Firth Basin in north-east Scotland and the St George's Channel Basin in the south Irish Sea. The long-standing buoyancy of the Grampian Highlands is also examined.

In the Inner Moray Firth Basin the gravity effect of the Mesozoic sediments along two-dimensional profiles is calculated using deep seismic reflection records to obtain layer geometry and well density data. The difference between observed and calculated gravity varies from -12 to -30mGal and is partly attributed to the presence of Old Red Sandstone sediments under the Mesozoic cover having an average thickness of about 3km, and partly to the presence of granite batholiths under the basin. The buoyancy of one such granite at the centre of the basin is thought to support the Central Ridge, a horst-like feature which divides the basin into two sub-basins.

Long gravity profiles through the Grampian Highlands show that the area is characterised by low gravity values compared to surrounding areas. A regional magnetic anomaly as well as some uncertainties in the results of refraction data over the area lead to production of a combined gravity, magnetic and seismic interpretation along the LISPB refraction line through the area. This indicated the abundant presence of granite batholiths at mid-crustal depths with an average total thickness of 12km. The presence of these granites is thought to have caused the long-standing persistence of the area above sea level and a northwards tilt of the Grampian Highlands during the tensional regime of Mesozoic times. This tilted movement is believed to be a major factor in the initiation and development of the Inner Moray Firth Basin.

Gravity modelling across the St George's Channel Basin indicated a difference in the wavelength of the observed and calculated anomaly, the latter being narrower. This difference is explained in terms of salt migration from the centre towards the flanks of the basin

and is supported by a deep seismic reflection section. The regional gravity field over the Irish Sea is studied and the results show an anomalous high of 25mGal amplitude centred over the south Irish Sea which is attributed to the presence of a high density layer at the base of the crust having a maximum thickness of 5.5km. This layer is thought to have intruded the crust in early Permian times resulting in an uplift of the area and consequent fracture of the upper crust. This mechanism is believed to have led to the formation of the Permo-Triassic basins within and around the south Irish Sea. The St George's Channel Basin is considered to be one of these basins. Lying as it does at the centre of the uplifted area it has been subject to the greatest subsidence and reaches a depth of about 11km.

CONTENTS

List of Figures

CHAPTER 1

INTRODUCTION

"In the preparation of dishes for the connoisseurs of World Tectonics we seem to have become obsessed by plates and neglected basins"

- A Hallam 1975

In the celebrity lecture of the Geological Societies of Edinburgh and Glasgow in 1977 Sir Peter Kent summarised the knowledge existing at the time on the development of the Mesozoic sedimentary basins in Britain and pointed to the significance of vertical movements in creating basins in an Atlantic type continental shelf. Here are some extracts from his talk (Kent, 1977).

> "Epeirogenic movements are the most widespread but one of the least-well understood tectonic agencies. In some degree they must relate to the new global tectonics, but as has been stressed elsewhere they tend to be far longer lasting, and have a tendency to show analogous features independently of relation to plate margins."

> "Simple basin development on either a continental or country-wide scale is subject to modification due to discontinuities and variation within the crystalline basement. Ancient fractures in particular provide lines of weakness which persist for long periods in shelf (foreland) areas, in contrast to the dominant effect of the sedimentary load in miogeosynclinal basins."

> "Modern Britain shows a scatter of mountains or hilly areas of old rocks, separated by basins of Permian and Mesozoic sediments. ...This is for the most part a long-existing relationship: some areas - the Scottish

Highlands, the Southern Uplands, the Pennines (with the Lake District), Wales and Cornubia - were marginal to the main basins from the Trias onwards (Kent, 1949)."

"Most of these were probably near sea-level in Mesozoic times, suffering an alternation of shallow submergence with minor erosion, as in the case of East Anglia; probably only the Scottish Highlands provided a continuing large scale source of sediment. They are sometimes referred to as "Hercynian massifs" but with the exception of Cornubia all have histories as positive structures extending back at least into the Lower Carboniferous and are mainly blocks essentially Caledonian in structure."

"The widespread continued emergence of these areas of Palaeozoic rocks (which themselves show a history of buoyancy throughout the Upper Palaeozoic) emphasises the basic fact that the British area was part of a broad Mesozoic shelf, and that the various basins are due to inter-cratonic subsidence. No true geosyncline is known in Britain or beneath the British seas after the Armorican geosynclinal subsidence, now largely concealed beneath southern England and the Channel."

"The Mesozoic history of the British area has been essentially one of vertical tectonics in a cratonic environment, with widespread basin subsidence which was initially fault-controlled but later developed by simple downwarping aggregating 3-8km or more in different areas."

"The fault-controlled phase of the vertical movements in the British seas pre-dated the opening of the North Atlantic, demonstrating that here (as fairly universally on the world's Atlantic-type coasts) the lateral opening was preceded by a much longer period of gentle tension than subsequently marked the

development of new oceanic crust. The pre-opening tension ended late in the early Cretaceous - again world-wide - with a date much more uniform than the times of the opening of adjacent oceans (Kent 1977)."

"Thus, fundamental processes are more complicated in space and time than the simple plate tectonic concept would indicate, and continued investigation of deep-seated relationships on the margin of northwest Europe should make a major contribution to their understanding, and hence to interpretation of the structure of other continental margins."

The main theme of this thesis is in accordance with the last suggestion by Sir Peter Kent. More specifically the scope of the thesis is to improve our understanding of why and how deep sedimentary basins of relatively small size were developed by examining two examples, for which there were available data, using a range of geophysical methods. In particular, the thesis seeks a better understanding of the way the basement of such basins has behaved and influenced their subsidence.

1.1 A mechanism of graben formation

In order to explain the widely observed graben-like subsidence, a particularly appealing mechanism based on stretching in response to tension was put forward in 1976 by M H P Bott (Bott, 1976). This mechanism was developed following previous ideas of Vening Meinesz (1950), Artemjev and Artyushkov (1971), Bott (1971), Fuchs (1974) and Whiteman et al (1975) and can briefly be discussed as follows.

The mechanism depends on two main factors, the subdivision of the continental crust into brittle and ductile layers, and the wedge subsidence hypothesis of Vening Meinesz (1950) applied to the brittle layer only rather than to the crust as a whole as in the original version. According to this mechansim normal faulting occurs when the strength of the brittle layer is exceeded, and the wedge subsides incrementally with complementary rim uplift. As the

tensile stress in the brittle layer drops on faulting, there is an immediate complementary increase in tension in the ductile layer below. This causes incremental stretching and thinning of the ductile layer, as a result of which the tensile stress again increases in the brittle layer towards the critical value to re-initiate faulting.

Bott states that theoretical graben width can be approximately estimated by calculating the position of the second fault by the theory of elastic bending of a thin two-dimensional elastic plate. (Vening Meinesz, 1950; Heiskanen and Meinesz, 1958; Walcott, 1970.) It can be shown that the predicted graben base width is between $\pi a/4$ and $2\pi a/4$ and the width of the rim uplifts lies between $2\pi a/4$ and $3\pi a/4$, where a is the flexural parameter of the layer,

$$a = \sqrt[4]{Et^3/3g\rho_d(1-\sigma^2)}$$

E is the Young's modulus, t is the thickness of the (brittle) layer, g is the acceleration of gravity, ρ_d is the density of the underlying (ductile) layer and σ is Poisson's ratio. Putting $E = 7.10^{10}$ Nt/m^2, ρ_d = 2800kg/m^3, g = 9.8Nt/kg and σ = 0.25, then for three different values of t the following widths are predicted:

t (km)	a (km)	Graben Width (km)	Rim Width (km)
10	31	24-48	48-72
15	42	33-66	66-99
20	52	41-82	82-123

The ranges indicated above are theoretical predictions. In reality deviations from these ranges may occur as a result of pre-existing basement weaknesses, or because density inequalities occur in the brittle layer, or because only a single fault develops. Pre-

existent zones of weakness, such as major transcurrent faults, are expected to define the location of the initial fracturing as long as their trends are about normal to the direction of maximum tension.

Bott (1976) calculated the maximum possible graben subsidence in cases where horst structures rise on one or both sides of the subsiding graben, when this is either filled or unfilled with sediments. The results of these calculations are shown in Table 1.

TABLE 1

Maximum possible graben subsidence in kilometres computed for horst model

Width of graben (km)	Without sediments		With sediments	
	T = 50MPa	T = 100MPa	T = 50MPa	T = 100MPa
20	0.93	1.84	2.54(2.96)	4.73(5.58)
30	0.65	1.28	1.50(1.95)	2.90(3.78)
40	0.49	0.98	1.01(1.42)	1.98(2.78)
50	0.40	0.80	0.74(1.10)	1.47(2.18)

Column 1 shows the surface width of the graben at the start of subsidence; surface width of horst = 40km; brittle layer thickness = 10km, density = 2700kg/m^3; fault hade = 25^o; ductile layer density = 2800kg/m^3; sediment density = 2000kg/m^3. The computations have been carried out for the single-horst model except those shown in parentheses which are for the double-horst model. T is the applied tension (after Bott, 1976).

Some important implications emerge from the calculations by Bott (1976) referred to above. The theoretical amount of subsidence possible is greater for a narrower than a wider graben. The subsidence is increased considerably by sediment loading and also increases almost linearly with increase in the applied tensile

stress. The tensile stress system needed to cause graben formation must persist throughout the whole period of subsidence. As examples of grabens formed by this mechanism, Bott referred to those of East Africa, the Rhinegraben, the Baikal rift zone and in the British region the north-south orientated Permo-Triassic basins and Mesozoic grabens of the North Sea.

1.2 The basins of the present study and data sources used

The basins chosen for investigation here are the Inner Moray Firth and St George's Channel basins (figure 1/1). The reasons for choosing these basins are that they are of relatively small size and quite deep and that commercial deep reflection seismic data for these areas were available at the Institute of Geological Sciences.

The Inner Moray Firth Basin is of triangular shape, fault-controlled at its north-west margin by the Great Glen and Helmsdale Faults. The south margin is of onlap type on Devonian strata along the north coast of the Grampian Highlands. To the east the basin runs into the Outer Moray Firth Basin which is an extension of the Buchan and Witchground graben system in the North Sea. The deepest parts of the basin run along the Great Glen Fault, the maximum depth being between 3.5 and 4.5km (Sunderland, 1972). Thus the basin is of a generally half-graben type similar to one expected when only one fault develops in the mechanism described above. The age of the sediments filling the basin extends from Permo-Triassic to Lower Cretaceous.

The St George's Channel Basin is an elongated (about 100km long) and narrow (30-35km wide) basin trending NE-SW in the south Irish Sea area. The sedimentary infill of the basin, which ranges in age from Permo-Triassic to Quaternary was thought to be 5 to 8km thick at maximum (Blundell et al, 1971). The basin was thought to be fault-controlled along its south-eastern margin by the Bala Fault. To the north-east the basin runs into the Cardigan Bay Basin and to the south-west into the north Celtic Sea Basin. Both these transitions are of anticlinal type. The north-western margin of the basin is formed by the Irish Sea Geanticline which is a Palaeozoic ridge

FIGURE 1/1

Regional structure of Britain: massifs and basins. D or ORS Devonian, C Carboniferous, P Permian, Tr Triassic, J Jurassic, K Cretaceous, T Tertiary. After Kent (1977).

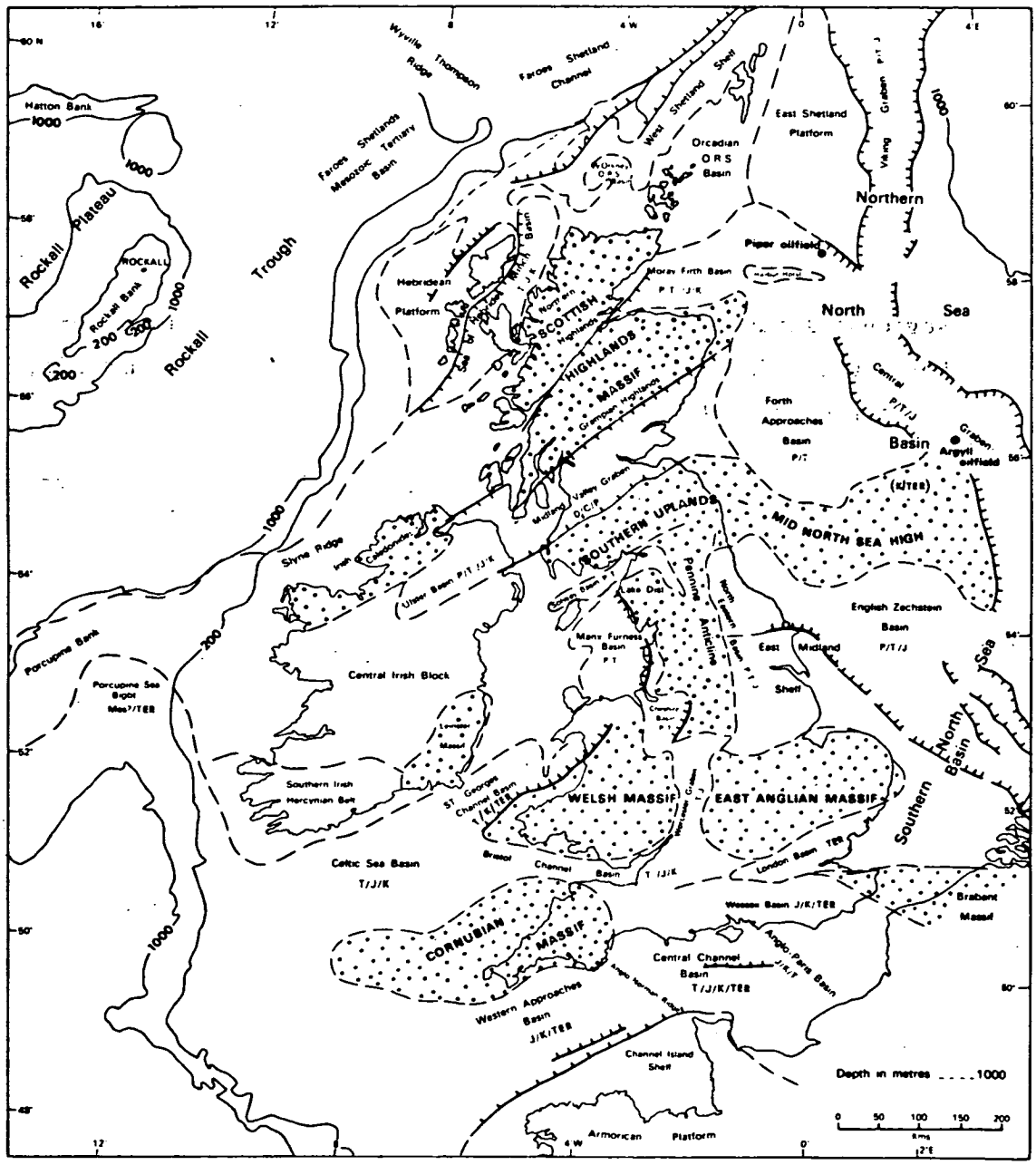
Wyville Thomson Ridge
Faroes Shetland Channel
Hatton Bank
1000
Faroes Shetlands Mesozoic Tertiary Basin
Rockall Plateau
ROCKALL
Rockall Bank
200
Rockall Trough
West Shetland Shelf
Orcadian ORS Basin
East Shetland Platform
Viking Graben
Northern North Sea
Piper oilfield
Hebridean Platform
Moray Firth Basin
SCOTTISH HIGHLANDS MASSIF
Forth Approaches Basin
Central Basin
Argyll oilfield
Midland Valley Graben
SOUTHERN UPLANDS
MID NORTH SEA HIGH
Slyne Ridge
Ulster Basin
Porcupine Bank
Porcupine Sea Bight
Central Irish Block
Manx Furness Basin
Penning Anticline
East Midland Shelf
English Zechstein Basin
Southern North Sea Basin
Southern Irish Mercymian Belt
St Georges Channel Basin
WELSH MASSIF
EAST ANGLIAN MASSIF
Celtic Sea Basin
Bristol Channel Basin
London Basin
Brabant Massif
CORNUBIAN MASSIF
Western Approaches Basin
Central Channel Basin
Anglo-Paris Basin
Channel Island Shelf
Armorican Platform
Depth in metres 1000
0 50 100 150 200

covered by thin sediments (Dobson et al, 1973). It is not clear if this margin is fault-controlled in which case the basin is a graben type basin, or is one of onlap type in which case the basin is of half-graben type. In the case that the basin is of a graben type, it should be mentioned that its depth is one and a half to two times the theoretical depth predicted in Table 1. This thickness would require a similar increase in the applied tension ($T \simeq$ (150-2000)MPa) throughout the subsidence of the basin, although the higher average sediment density in the basin compared with that used for the theoretical calculations (2400kg/m^3 instead of 2000kg/m^3) would make up some of the difference. The persistence of such a high tensional stress for so long a period of time is questionable.

Previous studies of sedimentary basin development have used a wide range of methods incorporating all available geophysical techniques. The deep structure of basins has mainly been deduced using refraction data and through the introduction of tectonic information from the surrounding area. The use of deep seismic reflection data in the interpretation of the two basins examined in this thesis is not an innovation, since an interpretation of the deep seismic survey over the Inner Moray Firth Basin had already been published by the time this thesis started. Nevertheless, these data had not yet been used in order to evaluate the way the basins were initiated although they established the subsidence history and the associated faulting of the basins during the Mesozoic. The present work incorporates the deep seismic information along with other geophysical and geological information in order to evaluate the deep structure and the mechanism responsible for the formation of the basins bearing earlier work, such as Bott's (1976) in mind. The method used is based on the removal of the sediments' gravity effect based on the deep seismic information and well density data, and interpretation of the "residual" anomalies (if any) in terms of those basement features which controlled the development of the basins. The latter stage incorporates all the other data available. Thus the following sources of data have been used in this thesis.

(a) Marine geophysical data including deep seismic reflection records and gravity data either collected by the Marine Geophysics Unit of IGS or published by other authors. Well information (mainly density) and refraction results published for the areas of interest.

(b) Marine geological data in the form of the solid geology maps of the areas and well information.

(c) Aeromagnetic data, when useful, including the aeromagnetic map of Great Britain and its smoothed version.

(d) Land geophysical information, including gravity maps produced by IGS, refraction work onshore (LISPB), densities of measured samples and magnetic information (susceptibilities - palaeomagnetic information).

(e) Land geological information including solid geology maps, geological information on the origin of different rocks onshore, and tectonic information.

The author was not involved in the collection of any of the above mentioned data used in this thesis. However, he actively took part in two regional geophysical surveys with the Marine Geophysics Unit of the Institute of Geological Sciences as part of his training (see Appendix I).

The computer programs used in this thesis include two-dimensional gravity and magnetic and a three-dimensional gravity modelling program. Another program correlating the total magnetisation vector of a body causing a magnetic anomaly to palaeopole positions known from palaeomagnetic data, developed for this thesis, is described in Appendix II.

CHAPTER 2

THE GEOLOGY OF THE MORAY FIRTH AREA

2.1 Introduction

The geology of the area surrounding the Moray Firth basin was in general terms well known long before the first offshore exploration was carried out. Figure 2/1 shows the first geological map of the area, which includes Mesozoic sediments along the north-west and south coasts of the Firth and which was published more than a hundred years ago (Judd, 1873). Since that time the knowledge of the geology of the area has vastly increased, and a summary account of it is presented in this chapter. Before describing the onshore geology, it is worth noting that even at the time of the first offshore surveys, knowledge of this geology was not sufficient to allow a correct interpretation of new offshore data.

The first offshore geophysical survey of the area was a gravity survey undertaken by the Netherlands Geodetic Commission in 1956 and 1957. This survey revealed a gravity low over the Moray Firth which was interpreted as being caused by a shallow seated granite covered with thin Mesozoic sediments (Collette, 1960). The alternative interpretation of a large sedimentary basin lying beneath the Moray Firth, which had been proposed in 1933 (Arkell, 1933) was preferred by many authors (Donovan, 1963; Hallam, 1965; Peacock et al, 1968) and further strengthened by the publication of an aeromagnetic map of the area (IGS, 1968). The latter showed magnetic anomalies of long wavelength and relatively low amplitude over the Firth.

Marine research in the Moray Firth by the Institute of Geological Sciences commenced in 1966 with a reconnaissance shallow seismic survey on m.v. "Rosherville." A regional shallow seismic survey was undertaken in 1970 on m.v. "Surveyor" on a rectangular grid of north-west to south-east and north-east to south-west traverse lines spaced approximately 10km apart. A shallow sampling programme followed later in 1970 aboard m.v. "Vickers Venturer." Drilling together with additional sampling and geophysical work was completed

FIGURE 2/1

First geological map of the coastal areas around the Inner Moray Firth. After Judd (1873).

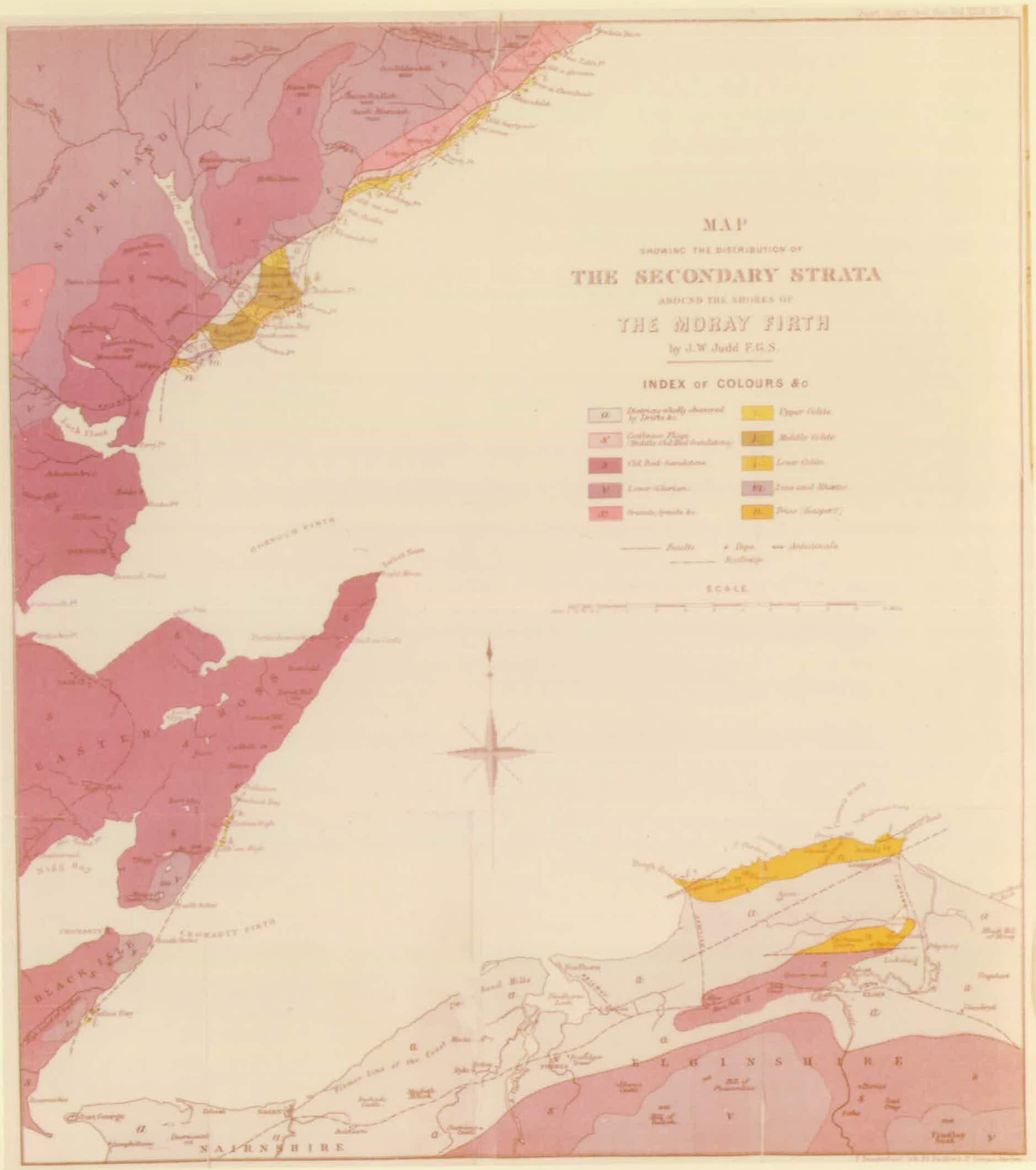
MAP
SHOWING THE DISTRIBUTION OF
THE SECONDARY STRATA
AROUND THE SHORES OF
THE MORAY FIRTH
by J.W Judd F.G.S.
INDEX OF COLOURS &c
SUTHERLAND
EASTER ROSS
NAIRNSHIRE
MORAY FIRTH
DORNOCH FIRTH
CROMARTY FIRTH
BLACK ISLE
MORAY BAY

on m.v. "Whitethorn" during the period 1971 to 1974, and detailed descriptions of the boreholes drilled have been published by Chesher et al (1972) and Evans et al (1980). A deep seismic survey was carried out in 1972 aboard m.v. "Caribe Tide" to evaluate the deep structure of the inner Moray Firth. The IGS report (Chesher and Bacon, 1975) on the interpretation of these deep seismic data together with all the above mentioned investigations confirmed the existence of a deep Mesozoic sedimentary basin as the offshore continuation of Mesozoic outcrops around the Firth onshore.

2.2 The Rocks of the Moray Firth Area

2.2.1 Basement rocks

Basement rocks enter the study presented here as the high density moderately magnetised formations which underlie and enclose the Old Red Sandstone and younger sedimentary rocks. The basement is composed of crystalline, metamorphic rocks of the Late Precambrian Moine Series in the northern Highlands and of both the Moine Series and the Dalradian Supergroup in the Grampian Highlands. Typical stratigraphic logs of these two formations are shown in figure 2/2. The Dalradian is a succession of sediments many kilometres thick, containing towards its top basic volcanic rocks, all now metamorphosed to a greater or lesser degree. Fossil evidence (Downie et al, 1971) suggests that the youngest Dalradian rocks are of Lower Ordovician age. The metamorphic rocks of the Grampian Highlands in fact form a late Precambrian to Lower Palaeozoic succession which underwent deformation and metamorphism probably during the Lower Ordovician. This was after the formation of the Newer Gabbros of Banffshire and Aberdeenshire (501 ± 17Ma - Pankhurst, 1970). Although these gabbros post-date the earliest stages of deformation and metamorphism, they are folded during the later stages. No earlier orogenic event has been demonstrated in the Grampian Highlands metamorphic rocks but in the Northern Highlands many Moine rocks have yielded radiometric ages which suggest a Precambrian orogenic event, the Morarian (Johnson, 1975). Thus although the Northern and Grampian Highlands metamorphic rocks share a Caledonian orogenic event and exhibit a common Caledonian thermal cooling pattern (Dewey and Pankhurst, 1970; Winchester, 1974), the Northern Highland rocks

FIGURE 2/2

Generalised stratigraphic successions of the Moinian (Northern Highlands) and Dalradian (Grampian Highlands) Series. After Anderton et al (1979).

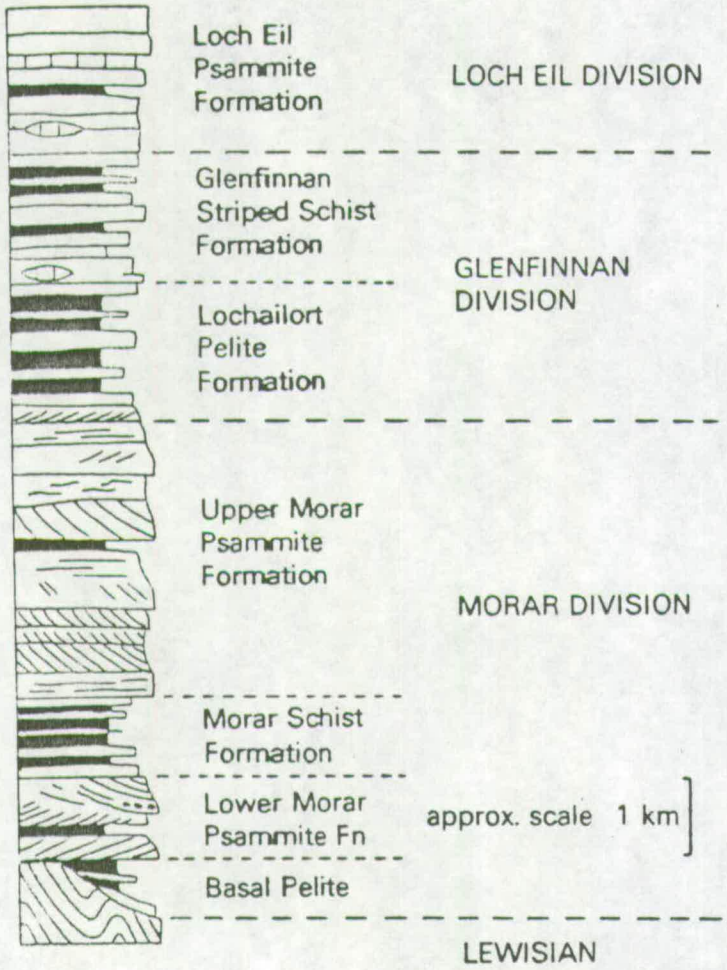
Loch Eil
Psammite
Formation
LOCH EIL DIVISION
Glenfinnan
Striped Schist
Formation
GLENFINNAN
DIVISION
Lochailort
Pelite
Formation
Upper Morar
Psammite
Formation
MORAR DIVISION
Morar Schist
Formation
Lower Morar
Psammite Fn
approx. scale 1 km
Basal Pelite
LEWISIAN

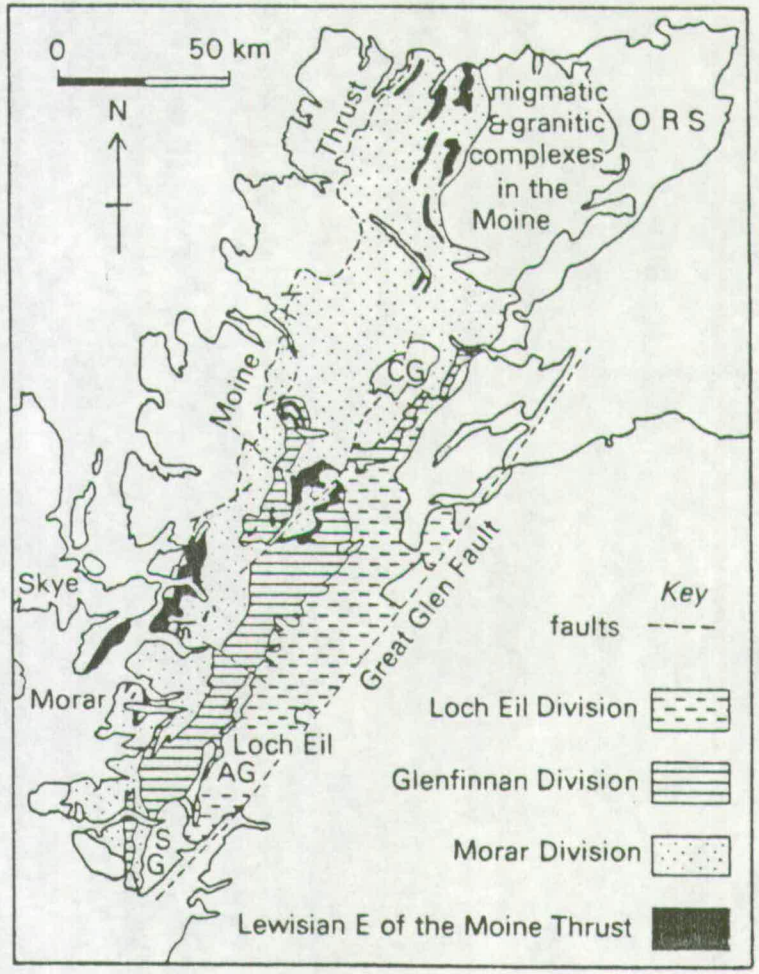
0
50 km
N
Thrust
migmatic
&granitic
complexes
in the
Moine
O R S
Moine
CG
Skye
Great Glen Fault
Key
faults
Morar
Loch Eil
AG
Loch Eil Division
Glenfinnan Division
Morar Division
S
G
Lewisian E of the Moine Thrust

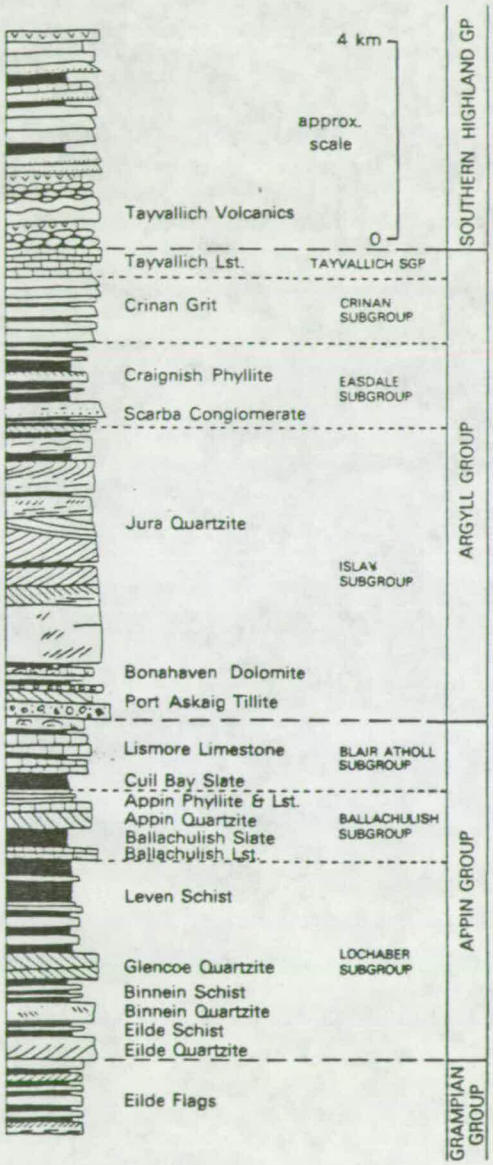
4 km
approx.
scale
0
Tayvallich Volcanics
Tayvallich Lst.
TAYVALLICH SGP
Crinan Grit
CRINAN SUBGROUP
Craignish Phyllite
EASDALE SUBGROUP
Scarba Conglomerate
Jura Quartzite
ISLAY SUBGROUP
Bonahaven Dolomite
Port Askaig Tillite
Lismore Limestone
BLAIR ATHOLL SUBGROUP
Cuil Bay Slate
Appin Phyllite & Lst.
Appin Quartzite
Ballachulish Slate
Ballachulish Lst.
BALLACHULISH SUBGROUP
Leven Schist
Glencoe Quartzite
Binnein Schist
Binnein Quartzite
Eilde Schist
Eilde Quartzite
LOCHABER SUBGROUP
Eilde Flags
SOUTHERN HIGHLAND GP
ARGYLL GROUP
APPIN GROUP
GRAMPIAN GROUP

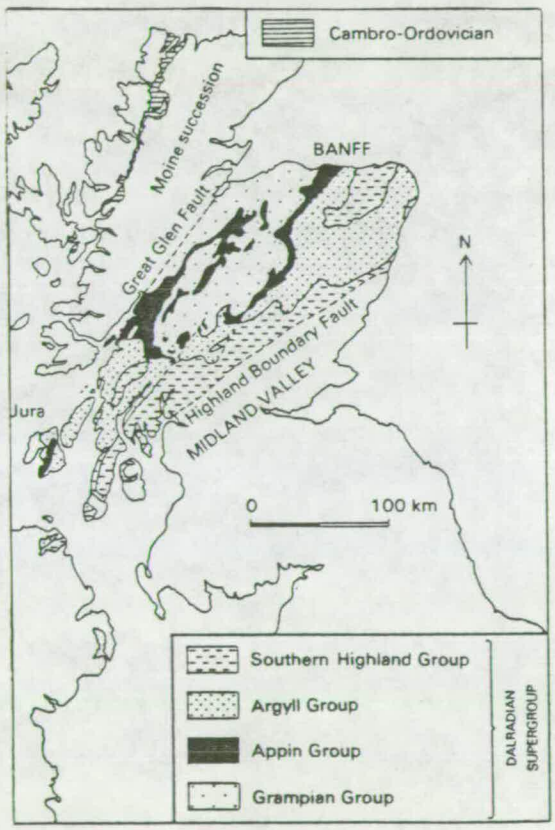
Cambro-Ordovician
Moine succession
Great Glen Fault
BANFF
N
Highland Boundary Fault
MIDLAND VALLEY
Jura
0
100 km
Southern Highland Group
Argyll Group
Appin Group
Grampian Group
DALRADIAN SUPERGROUP

seem to have suffered a longer and more complex orogenic history than those of the Central and Eastern Highlands. This distinction between basement on either side of the Great Glen Fault emphasises the importance of that structure, which has remained the most significant element in the tectonic history of the area from Caledonian to the present times.

A further contrast between the Northern and Grampian Highland metamorphic rocks lies in the presence in the former of slices of Lewisian basement gneisses which are interleaved in fold cores and along slides with Moine metasediments (Tanner et al, 1970; Watson, 1975). Such interleaving has not been recorded in the Dalradian of the Grampian Highlands, and on the Scottish mainland, at least, Lewisian rocks do not crop out to the south-east of the Great Glen Fault. On the other hand, associated with the Caledonian Orogeny is a great suite of igneous rocks both intrusive and extrusive that predominate in the area south of the Great Glen Fault. A grouping of these rocks (Johnstone, 1978) is:

a. The Older Igneous rocks (pre- or early-Tectonic) comprising basic rocks extruded in the developing Caledonian geosyncline, together with certain basic and granitic intrusions which either pre-date the general Caledonian folding or are associated with its early phases.

b. Syntectonic migmatites consisting mainly of composite gneisses which developed during the main movement phase of the orogeny and which were associated with the metamorphism.

c. The Newer Igneous rocks (late- to post-Tectonic) comprising basic, acid and complex plutonic intrusions, minor intrusions and volcanic rocks. The earlier members of the group appear to have been involved to some extent in late Caledonian movements; the later members are completely post-Tectonic.

Of these groups, of special interest is the group of the Newer Igneous rocks and more particularly the granites of the Grampian Highlands. A

further discussion of these granites, in association with some geophysical anomalies observed in this area as well as some tectonic implications deriving from their extent, is given in chapter 4.

In the modelling of structures presented in the next chapter the basement rocks are treated in the first instance as a homogeneous unit on the basis of their similar density. It is clear, however, that they are not homogeneous and the final stages of modelling take that into account.

2.2.2 Old Red Sandstone rocks

The information on the Old Red Sandstone and Mesozoic rocks of the Moray Firth, unless otherwise stated, has been derived from the IGS report with the title: "The geology of the Moray Firth" by Chesher and Lawson (in press).

Extensive outcrops of Old Red Sandstone are present on both the north and south coasts of the Moray Firth. They comprise Lower, Middle and Upper Old Red Sandstone sediments.

Rocks of Lower Old Red Sandstone age are recognised from Glen Urquhart, across the Inner Dornoch Firth, to near the north coast of Caithness and Reay where they consist of up to 900m of conglomerates, breccias, arkoses, flaggy sandstones and mudstones. Lower Old Red Sandstone may also be present along the south coast of the Moray Firth as at Buckie (Peacock et al, 1968). Westoll (1964) suggested that the Rhynie outlier may also be of Lower and not Middle Old Red Sandstone age as previously thought.

The Middle Old Red Sandstone is well developed in Caithness where it consists of the lacustrine Caithness Flagstone, locally underlain by conglomerates and overlain by at least 600m of the friable John O'Groats Sandstone.

Around the Cromarty Firth the lacustrine facies of Caithness are replaced by fluvial braided stream and alluvial plain sandstone deposits, whereas along the southern shore of the Moray Firth from

Inverness to Buckie, the Middle Old Red Sandstone appears to be between 300 and 600m thick (Peacock et al, 1968) and is represented by basal conglomerates overlain by sandstones, flagstones and limestones. Farther east the Middle Old Red Sandstone occurs as a series of outliers along the coast between Buckie and Fraserburgh.

The Upper Old Red Sandstone outcrops at Tarbat Ness and Dornoch, and in a belt of strata stretching from Nairn to Elgin. It comprises an estimated thickness of 1200m (Peacock et al, 1968) of sandstones with intercalated layers and pellets of red clay.

The outliers of Old Red Sandstone continue offshore both in the north and south of the area. Along the south coast of the Moray Firth the Old Red Sandstone continues for a limited distance as a belt of strata five to eight kilometres wide, striking parallel to the coast before being unconformably overlain by the Mesozoic. This belt of strata forming the coastal platform appears as fairly homogeneous on shallow seismic reflection records with only rare irregular traces of bedding. Borehole 71/22 shows it to consist of sandstones, marls and conglomerates. Along the north-west margin of the Moray Firth, the Old Red Sandstone is terminated at the coast by the Great Glen Fault between Ethie and Tarbat Ness, and by the Helmsdale Fault between Golspie and Lybster. Farther north to the east of Wick, the Old Red Sandstone appears to continue for only a limited distance offshore forming a platform less than 10km in width. In this region the Old Red Sandstone is characterised on the seismic records by the general absence of any well developed reflectors and it appears to be unconformably overlain to the east by well-bedded strata of presumed Permo-Triassic age.

The presence of Old Red Sandstone resting with marked unconformity on the metamorphic basement on both the north and south coasts of the Moray Firth, its presence in offshore wells in the outer Moray Firth (12/23-1) and farther to the east, in conjunction with the general basinal disposition and thickness of the formation, leads to the conclusion that it is present throughout the Firth concealed beneath the overlying Mesozoic sediments. The maximum likely extent of the Middle Old Red Sandstone in northern Scotland

FIGURE 2/3

Maximum extent of Middle Old Red Sandstone in northern Scotland. After W Mykura (personal communication).

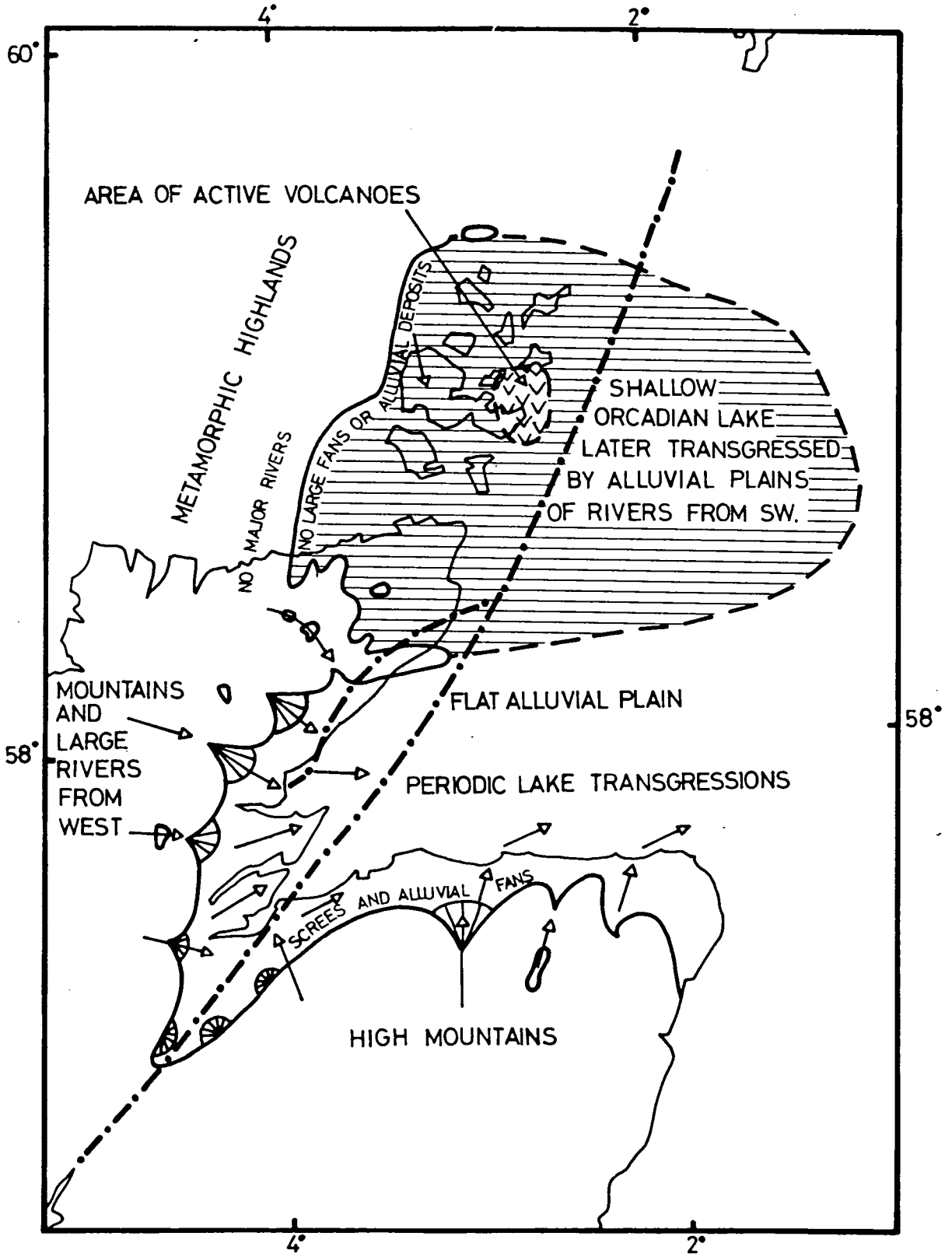
4°
2°
60°
58°
AREA OF ACTIVE VOLCANOES
METAMORPHIC HIGHLANDS
NO MAJOR RIVERS
NO LARGE FANS OR ALLUVIAL DEPOSITS
SHALLOW ORCADIAN LAKE LATER TRANSGRESSED BY ALLUVIAL PLAINS OF RIVERS FROM SW.
MOUNTAINS AND LARGE RIVERS FROM WEST
FLAT ALLUVIAL PLAIN
PERIODIC LAKE TRANSGRESSIONS
SCREES AND ALLUVIAL FANS
HIGH MOUNTAINS

as well as the direction of its deposition are shown in figure 2/3. To date, no precise estimate, based upon geological or geophysical data, of the thickness of the Old Red Sandstone sediments beneath the Mesozoic basin has been given, although it has been suggested that they could be up to 7km thick (Chesher and Lawson, in press; Mykura, personal communication). The thickest section onshore has been estimated to be about 3.5km thick in the area near Forres (Burollet et al, 1969).

2.2.3 Mesozoic rocks

Mesozoic rocks outcrop along both the north-west and south coasts of the Moray Firth. The age of these rocks ranges from Triassic to Upper Jurassic in the north-west and from Permo-Triassic to Liassic in the south. There are no Cretaceous rocks onshore although some glacial erratics of this age have been found in Caithness and in the Aberdeenshire area (Phemister, 1960).

Rocks which are thought to be of Upper Permian or Lower Triassic age crop out around Elgin. They comprise the Burghead and Hopeman Sandstone, about 60m thick (Peacock et al, 1968). They are mainly aeolian in character with some indication of fluvial transport in places. In the Lossiemouth area rocks of Triassic age consist of about 70m of mainly waterlain continental sandstones (Peacock et al, 1968) overlain by a further 35m of section consisting mainly of sandstones of Upper Triassic age. At East Sutherland the Triassic rocks consist of calcareous sandstones, overlain by marls and 70-80m of grits and conglomerates all of Upper Triassic age. The extension of the Permo-Triassic rocks offshore has been confirmed through IGS boreholes 71/15 and 71/23. In borehole 71/15, east of Lossiemouth, the rocks consist of silts with marly bands, rocks of the same composition as those south of Golspie where they form a narrow strip striking south-east (figure 2/4). In borehole 71/23 north of Fraserburgh, the Permo-Triassic rocks are faulted against Cretaceous strata and consist of sandstones and mudstones of Upper Permian age. The Permo-Triassic rocks lie unconformably on the Old Red Sandstone sediments and thicken towards the centre of the basin where they are probably more than 500m thick. Sediments presumably of

FIGURE 2/4

Solid geology map of the Moray Firth area. After Chesher and Lawson, in press.

SEDIMENTARY ROCKS

- Tertiary
- Upper Cretaceous
- Lower Cretaceous
- Upper Jurassic
- Middle Jurassic
- Lower Jurassic
- Permo-Triassic
- Upper Devonian
- Middle Devonian
- Lower Devonian
- Devonian
- Dalradian
- Moine

IGNEOUS ROCKS

- Basic coarse grained (Gabbro)
- Acid coarse grained (Granite)

Universal Transverse Mercator Projection

Statute Miles

Kilometres

Nautical Miles

STRUCTURES

- Geological boundary
- Axial trace of anticline
- Axial trace of synclina
- Fault at surface
- Fault at depth
- Fault zone

The following periods of fault activity have been recognised

- Post Lower Cretaceous
- Post Middle Jurassic – Pre Lower Cretaceous
- Post base Lower Jurassic – Pre Upper Jurassic
- Post base Permo Triassic – Pre Lower Jurassic
- I.G.S. borehole
- I.G.S. sample station solid outcrop
- Commercial borehole

Permo-Triassic age crop out north of the Moray Firth and east of Wick, where they form a shallow basin resting on the Old Red Sandstone of the area.

Outcrops of Lower Jurassic age rocks occur at Dunrobin and Lossiemouth. At Dunrobin they consists of a condensed succession of largely argillaceous sediments, whereas at Lossiemouth, sediments of Lower Lias found in an IGS borehole (Berridge and Ivemey-Cook, 1967) comprise 70m of sandstones, siltstones and shales. The origin of the Lossiemouth rocks is quoted as being both marine and non-marine, suggesting deposition near sea level. Rocks of Middle Jurassic age (Bathonian) are exposed between Brora and Helmsdale and at Balintore and Ethie. In the Brora area they consist of 15m of sandstone overlain by clays and shale, with a similar succession at Balintore. All these sediments are of deltaic origin. Offshore, rocks of Lower and Middle Jurassic age have been found in boreholes 71/16, 71/18 and 71/21. They rest with only a minor disconformity on the Permo-Triassic sediments and generally dip northwards. They consist of soft friable sandstones, with thin interbedded shales. The boundary between Lower and Middle Jurassic is not clear on the shallow seismic records but often forms a strong seismic reflector on the deep seismic records. The thickness of the Lower Jurassic rocks varies from 150m near the coast to 500m in the centre of the basin, while the Middle Jurassic varies from 150m near the coast to 750m at the centre of the basin.

Rocks of Callovian and Oxfordian (Upper Jurassic) age occur onshore at Brora and at Balintore and have been classified into three formations: the Brora Argillaceous Formation, the Brora Arenaceous Formation and the Balintore Formation (Lee and Pringle, 1932; Sykes, 1975). The first formation is about 90m thick at Brora but only 30m thick at Balintore; the second formation is about 60m thick at Brora but 21m at Balintore; finally the third formation is 12m at Brora and 24m at Balintore. Thus no more than 160m of section of this age may be present. The topmost Jurassic rocks on-shore, however, are of Kimmeridgian age and north of Brora they consist of 60m of massive sandstone and shales, overlain by 500m of shales, sandstones, grits and extensive boulder beds. At

Balintore the Kimmeridgian consists of similar rocks with some thin limestones. Offshore, Upper Jurassic rocks of Kimmeridgian age have been found in boreholes 71/20, 71/24 and 71/36. They consist of a thick sequence of shales similar to the ones observed onshore. The Upper Jurassic sediments are separated from those of Lower and Middle Jurassic age by a disconformity and reach a total thickness of 1000m at the centre of the basin.

Rocks of Cretaceous age are not present onshore, apart from the glacial erratics already referred to. Offshore outcrops of Lower Cretaceous cover the central and inner part of the Moray Firth whereas the Upper Cretaceous rocks crop out only in the eastern part of the basin. The Lower Cretaceous sediments are separated from the underlying Kimmeridgian by a minor unconformity and they consist mainly of a sequence of shales and siltstones with sandstones occurring in places. They have been drilled in boreholes 71/17, 71/27, 71/28, 72/24, 72/29 and 74/17. The Upper Cretaceous rocks of the Moray Firth rest with a minor unconformity on the Lower Cretaceous and they dip gently to the east. In borehole 74/19 they consist of 78m of chalk underlain by sandstones and shales.

The rocks which infill the Moray Firth basin are, or can be seen from the above, generally shallow water deposits, sometimes deltaic and sometimes open water in origin. The marginal nature of the Mesozoic rocks along the southern margin of the basin along with evidence from the deep seismic records and the existence of the high grounds of the Grampian Highlands and Northern Highlands all suggest that in the south the maximum extent of the basin has been just beyond the present day coastline. Farther north, however, in the vicinity of Helmsdale, the thickness of the Mesozoic strata downfaulted by the Helmsdale Fault suggests that here the Mesozoic basin was extended much farther to the north-west than the present coast.

2.3 Structural Regime

2.3.1 Structure within the basin

The structure of the Mesozoic basin is well known following the work of Bacon and Chesher (1975), Chesher and Bacon (1975), Chesher (1977)

and Chesher and Lawson (in press). The main structural features and the extent of the basin are shown in figure 2/4.

The margins of the basin are largely fault controlled, the Mesozoic strata being downfaulted against Old Red Sandstone by the Helmsdale and Great Glen Faults along the north-west margin. Along the northern and south-eastern margins the Wick and Banff Faults respectively downthrow the Mesozoic sediments against Old Red Sandstone and Permo-Triassic rocks. These faults can be seen as steep gravity gradients on the Bouguer anomaly map of the area (figure 3/3), and they must have a downthrow of at least 500m (Chesher and Lawson, in press). The southwestern margin of the basin is one of sediment onlap rather than fault control.

It has been possible to recognise five relatively continuous major reflecting horizons within the area. Horizon identifications have been based on shallow and deep seismic surveys, borehole data of IGS and released oil exploration wells and are as follows:-

Horizon A - Intra-Lower Cretaceous
Horizon B - Base Lower Cretaceous
Horizon C - Mid-Jurassic
Horizon E - Base Lower Jurassic
Horizon F - Permo-Trias?

Horizons B and E have been used in the gravity backstripping procedure. Horizon B represents a very strong and continuous event particularly to the east in the deeper parts of the basin. Its reflection character and velocity discontinuity suggest a possible widespread disconformity at this level (Chesher and Bacon, 1975). Horizon C is the strongest deep reflector. The event can be followed reliably through the central and southern parts of the area. The correlation across the Great Glen Fault is poor. Between Horizons B and E two other horizons are recognised. Horizon C is not as strong as either Horizons B and E, but its continuity is generally fairly good in the main basin, whereas the correlation across the Great Glen Fault is again poor. It can probably be correlated with the base of the Kimmeridgian. Horizon D represents a strong

continuous event immediately above Horizon E with which it shows rather similar trends. Horizon F represents the deepest event mapped by Chesher and Bacon (1975). This horizon has been accurately followed only in the south-east part of the area (figure 2/7). The continuity of this event deteriorates as the horizon deepens into the main basin and the correlation across the fault on the south-east side of the Central Ridge is not reliable. This can be seen better on the interpreted picture of line 6 (figure 2/8), where the thickness of the layer between Horizons E and F over the ridge at the centre of the line is double that observed on the downthrown side of the fault, south-east of the ridge. Geological identification of Horizon F is uncertain; it probably represents an event low in the Permo-Trias. Precise knowledge of the Permo-Triassic layer thickness in the basin is of vital importance for the gravity backstripping procedure, especially in the interpretation of the remaining gravity anomaly once the effect of the Cretaceous and Jurassic sediments would have been removed. Two-way time contour maps to Horizons B, E and F as well as the interpreted seismic lines are shown in figures 2/5-2/8 respectively.

The Mesozoic sediments within the Inner Moray Firth basin are generally conformable, although minor disconformities exist at the base of Lower Cretaceous Horizon B and between the mid-Jurassic Horizon C and the base of the Jurassic Horizon E. The following periods of fault activity have been recognised in the basin (figure 2/4):-

a. Post Lower Cretaceous
b. Post Middle Jurassic-Pre Lower Cretaceous
c. Post base Lower Jurassic-Pre Middle Jurassic
d. Post base Permo-Triassic-Pre Lower Jurassic

The intensity of faulting at Horizons B, E and F (figures 2/5-2/7) has been designated by varying thickness of lines. The overall fault pattern is one of block faulting, all the faults being normal in character. The faults vary in trend from north-east in the north-west part of the region to east-north-east in the south-east part, and appear to radiate from a focal point in the innermost part of the basin.

FIGURE 2/5

Two-way time to horizon B, base of the Lower Cretaceous. After Chesher and Bacon (1975).

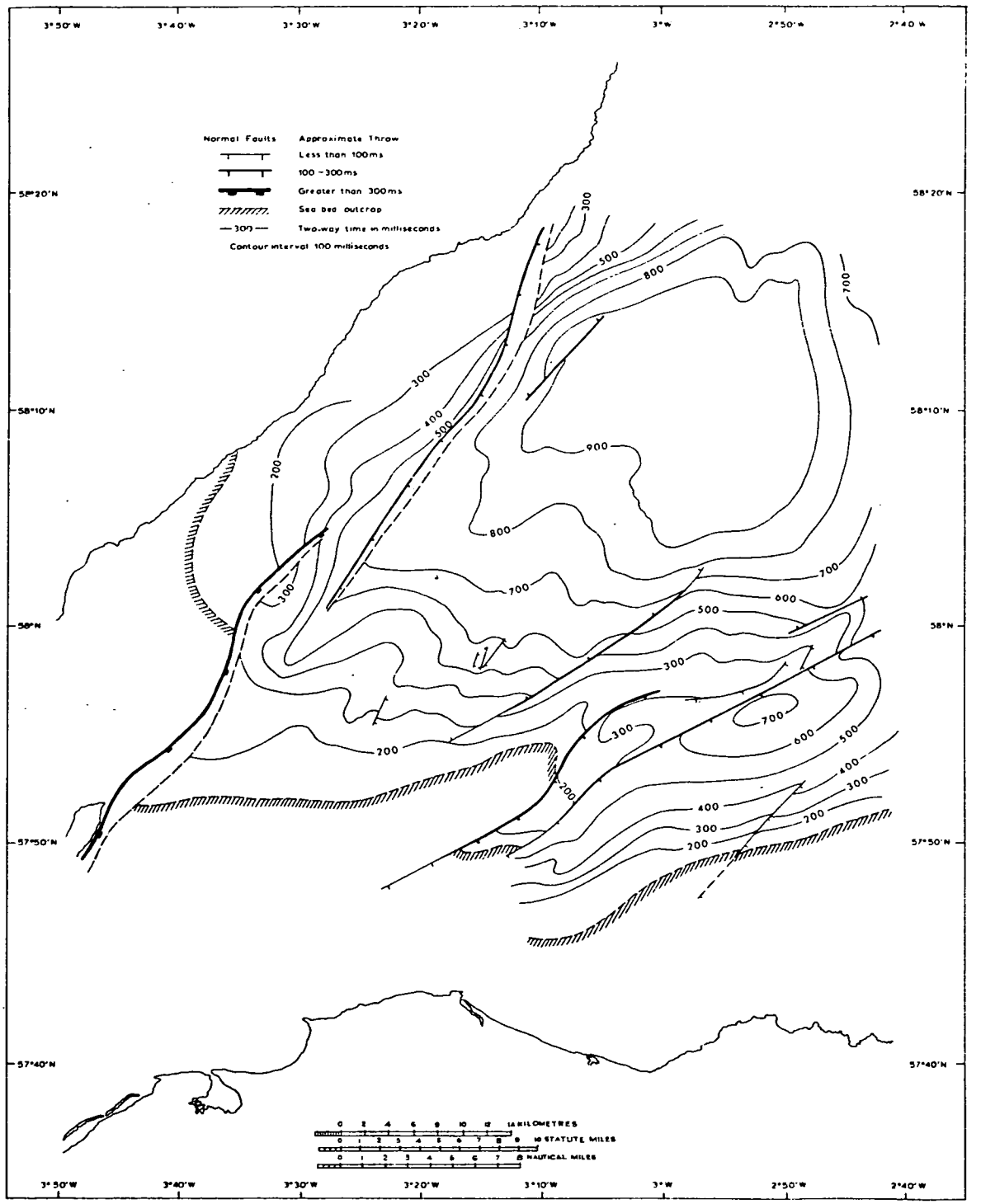
3°50'W
3°40'W
3°30'W
3°20'W
3°10'W
3°W
2°50'W
2°40'W
58°20'N
58°10'N
58°N
57°50'N
57°40'N
Normal Faults
Approximate Throw
Less than 100ms
100 - 300ms
Greater than 300ms
Sea bed outcrop
Two-way time in milliseconds
Contour interval 100 milliseconds
300
500
800
700
900
400
600
200
KILOMETRES
STATUTE MILES
NAUTICAL MILES

FIGURE 2/6

Two-way time to horizon E, base of the Jurassic. After Chesher and Bacon (1975).

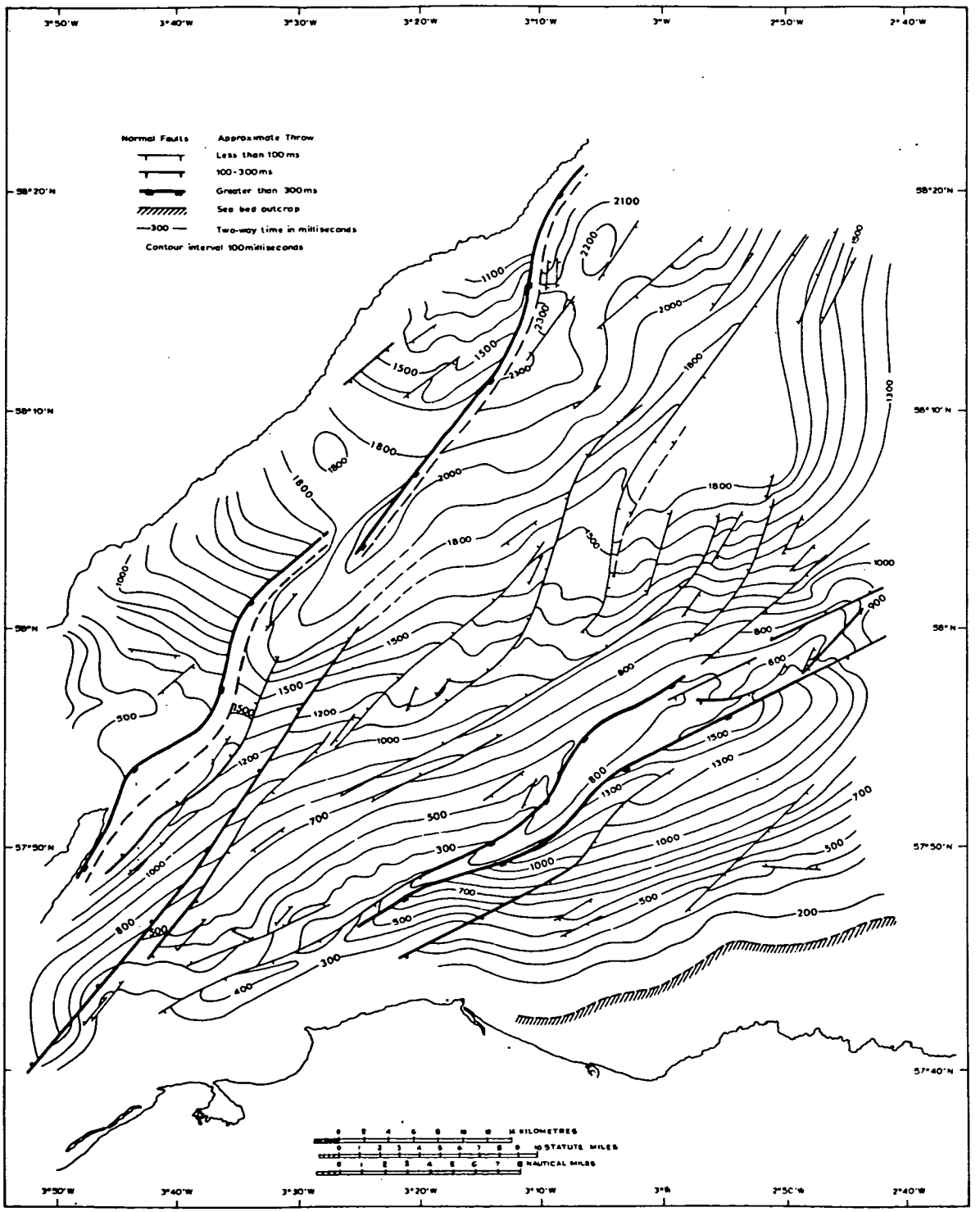
3°50'W
3°40'W
3°30'W
3°20'W
3°10'W
3°W
2°50'W
2°40'W
58°20'N
58°10'N
58°N
57°50'N
57°40'N
Normal Faults
Approximate Throw
Less than 100 ms
100-300 ms
Greater than 300 ms
Sea bed outcrop
—300— Two-way time in milliseconds
Contour interval 100 milliseconds
KILOMETRES
STATUTE MILES
NAUTICAL MILES

FIGURE 2/7

Two-way time to horizon F, base? of the Permo-Trias. After Chesher and Bacon (1975).

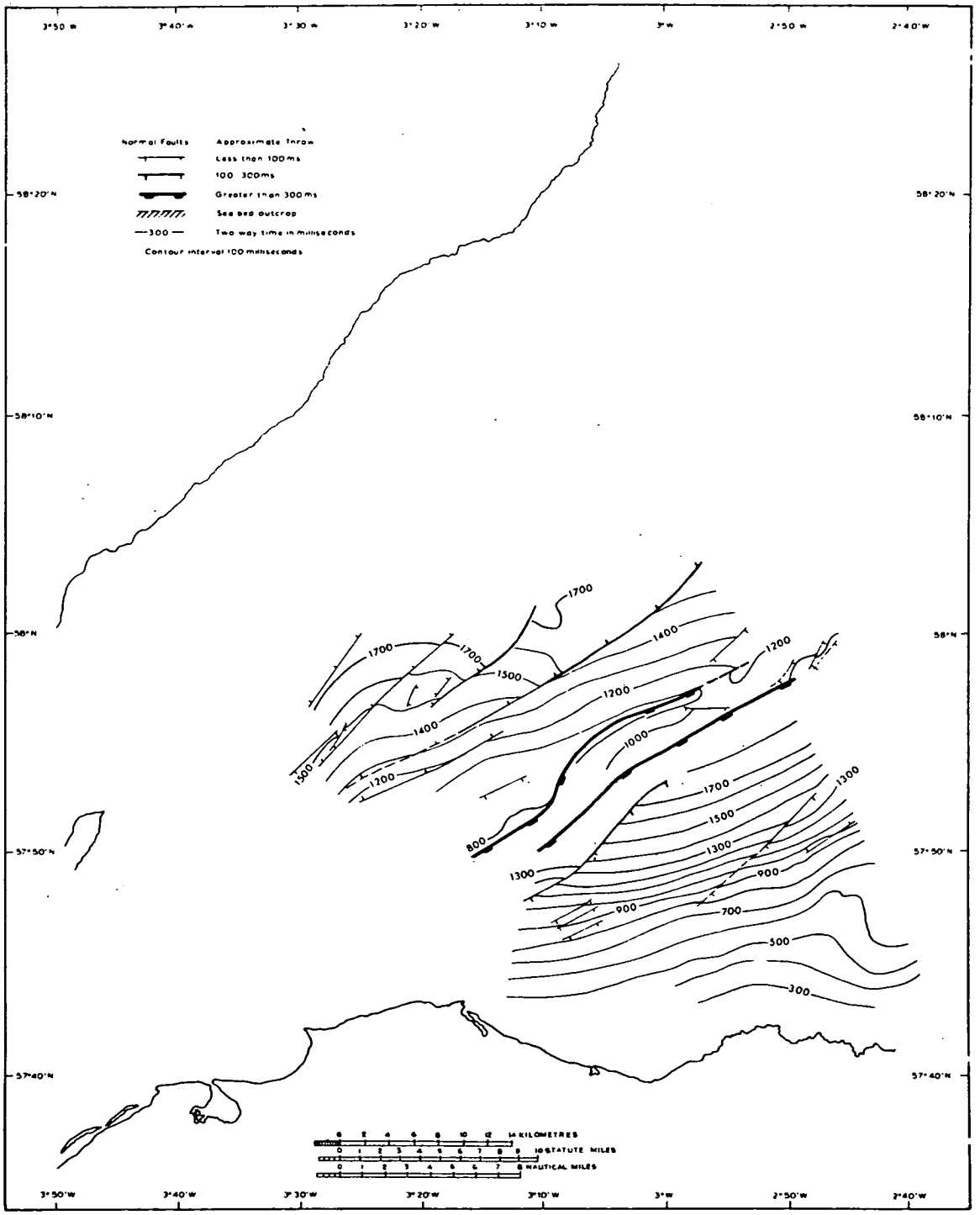
3°50 W
3°40' W
3° 30 W
3°20' W
3°10 W
3°W
2°50 W
2°40'W
58°20'N
58°10'N
58°N
57°50'N
57°40'N
Normal Faults
Approximate Throw
Less than 100 ms
100 300ms
Greater than 300 ms
Sea bed outcrop
—300— Two way time in milliseconds
Contour interval 100 milliseconds
1700
1500
1400
1200
1000
800
1300
900
700
500
300
0 2 4 6 8 10 12 14 KILOMETRES
0 1 2 3 4 5 6 7 8 9 10 STATUTE MILES
0 1 2 3 4 5 6 7 8 NAUTICAL MILES

FIGURE 2/8

Interpreted seismic lines nos. 3, 4, 5, 6 and 11 from the IGS deep reflection seismic survey of the Inner Moray Firth area. For the position of the lines see figure 3/4. After Chesher and Bacon (1975).

LINE 3

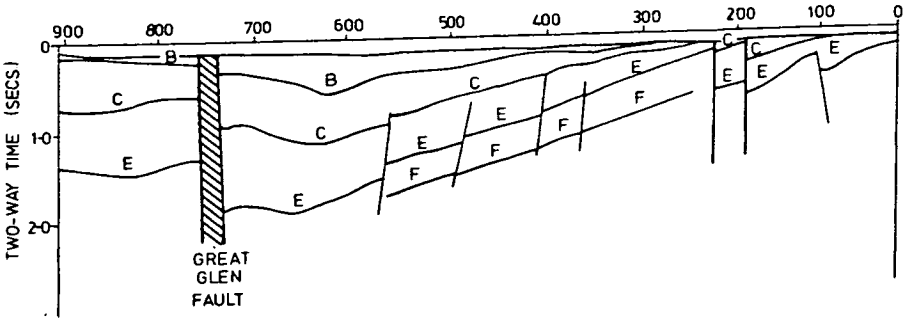

LINE 4

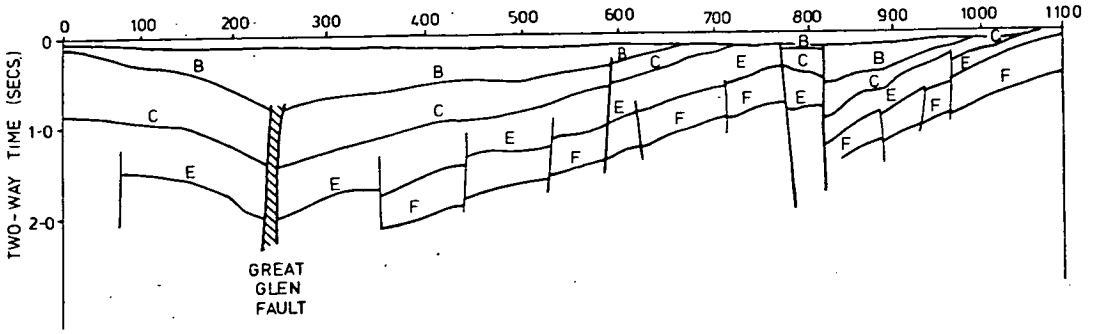

LINE 5

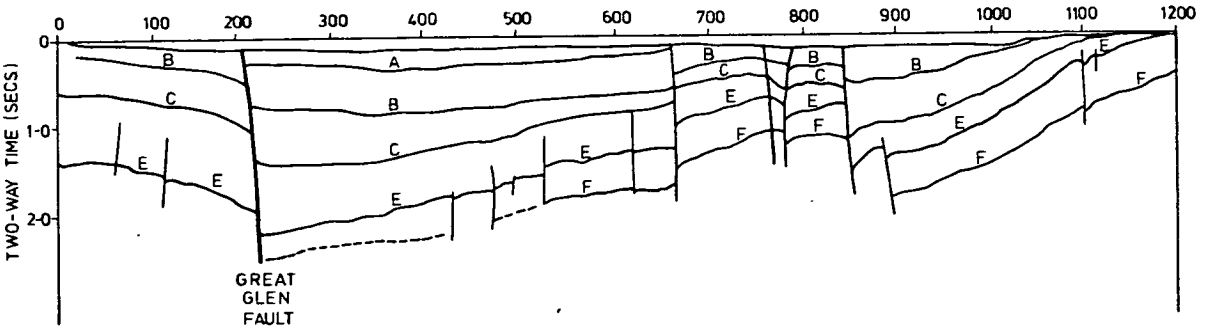

LINE 6

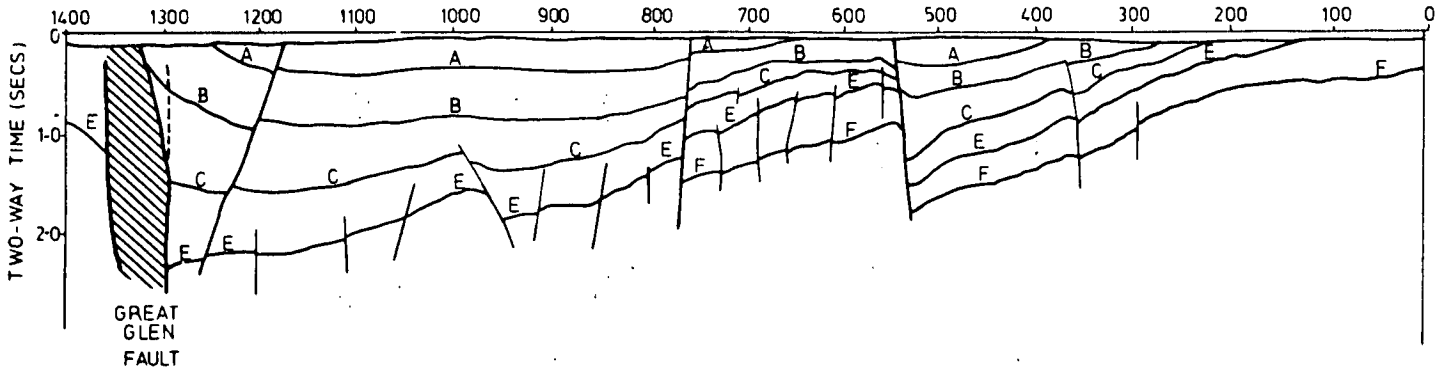

LINE 11

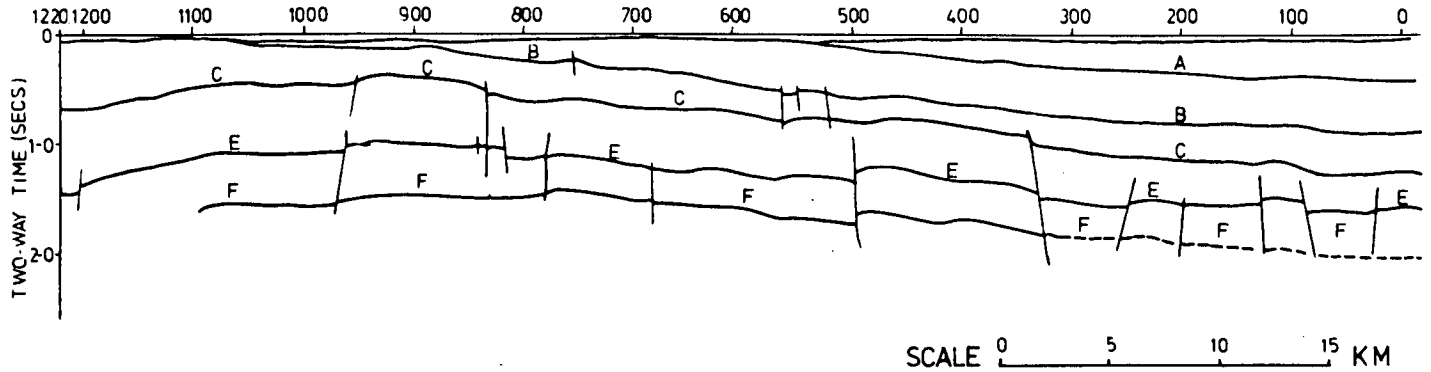

The above ascribed periods of faulting activity represent the climaxes during an era of faulting and reactivation which extended throughout the Mesozoic. The peak of the faulting occurred before mid-Jurassic times and then decreased gradually in intensity until during the Lower Cretaceous only the major fault lines were active (Chesher and Bacon, 1975). The result of all this faulting activity was the formation of a series of horst and graben structures in the basin. The most prominent of these features is a zone of uplift which separates the main basin from a secondary basin in the south. This zone is named the Central Ridge (figure 2/4). The uplifted area is a horst-like basement high which trends east-north-east across the centre of the basin and is clearly fault controlled (Chesher and Lawson, in press). The sediments in general thin over the ridge and thicken to the north and to the south suggesting that the sedimentation was in part fault controlled. This also appears to be the case across the Great Glen Fault in that the main Mesozoic basin is centred to the south-east of this fault zone in the north-east part of the basin. There it reaches a maximum depth equivalent to at least 2500ms two-way reflection time (Chesher and Bacon, 1975). A subsidiary development of the main basin, seen clearly in the isochron contour map of the E Horizon is situated to the south-east of the main basin and is separated from it by another north-east trending fault bounded ridge.

The sediments of the basin are relatively little affected by folding. A major syncline is present along the line of the Great Glen Fault and in the north-east part of the basin the upper Horizons A and B are folded into smooth anticlinal and synclinal flexures as seen on line 6 between shotpoints 800 and 1200. Other folding is generally associated with faulting occurring as tight drag-type folds along the lines of the major faults. A tight anticlinal rise of the Horizons B and C, seen on line 11 at shotpoint 100, is probably the result of horst faulting at depth (Chesher and Bacon, 1975).

Undoubtedly the most important structural feature within the basin is the Great Glen Fault. The fault zone follows the coastline between Ethie and Tarbat Ness downfaulting Jurassic sediments against Old Red Sandstone. It continues within the Mesozoic strata offshore in a north-north-east direction exhibiting a sinuous pattern of outcrop.

Where the fault zone crosses seismic line 1 it is about 2.5km wide and has a downthrow to the south in the regional of 800ms for Horizon E. The width and the downthrow of the fault zone decreases northwards and where the zone crosses line 3 it is 0.8km wide and the downthrow is 500ms for Horizon E. Near line 4 the fault line passes into the northern limb of a broad syncline and the fault movement is then taken up, en echelon, 2km to the south, along the axis of another syncline (figure 2/4). The fault line continues in a north-north-easterly direction gradually increasing in width and downthrow until the north-west end of line 6 where it is 1km wide and has a downthrow of 100ms for Horizon E. North of Wick the continuation of the fault cannot be traced with any degree of accuracy. Movements on the Great Glen Fault line, as they are seen to affect the Mesozoic strata, appear to be predominantly normal, and the pattern of outcrop and character of the fault zone precludes any major Mesozoic phase of transcurrent movement (Chesher and Bacon, 1975).

2.3.2 Regional structure in and around the Moray Firth

The Moray Firth forms a triangular shaped embayment in the coast-line of north-east Scotland between latitudes 57°N and 58°45' and longitudes 2°W and 4°W and its regional setting can be seen in figure 2/9. Although there are some Mesozoic sediments to the west of the Great Glen Fault, the main basin is to the east of the fault within the structural unit which represents the Grampian Highlands. Dalradian rocks presumably continue beneath the Firth since they are sampled in some of the North Sea wells to the north-east (Kent, 1980). The Great Glen Fault separates this unit from the Northern Highlands and is probably tectonically the most significant fault in the area. It was active as a transcurrent fault during Pre-Devonian times with a sinistral displacement of more than 100km and probably some thrusting movements to the north-west. During the Devonian movements were normal along the north-east trending fault line with a throw of the order of hundreds of metres, and local thrusting again observed in some localities. Post-Devonian dextral movements of 27-28km have been postulated along the fault (Donovan et al, 1976; Mykura, in press). These movements occurred probably during Carboniferous and Permo-Triassic times as the movements

FIGURE 2/9

Regional setting of the Inner Moray Firth Basin. 1: Moine Thrust; 2: Great Glen Fault; 3: Highland Boundary Fault; 4: Southern Uplands Fault; 5: Wick Fault; 6: Banff Fault; 7: Halibut Horst; 8: Viking Graben; 9: Central Graben; 10: Northern Highlands; 11: Grampian Highlands; 12: Midland Valley; 13: Southern Uplands; 14: Inner Moray Firth Basin. Modified from Kent (1977).

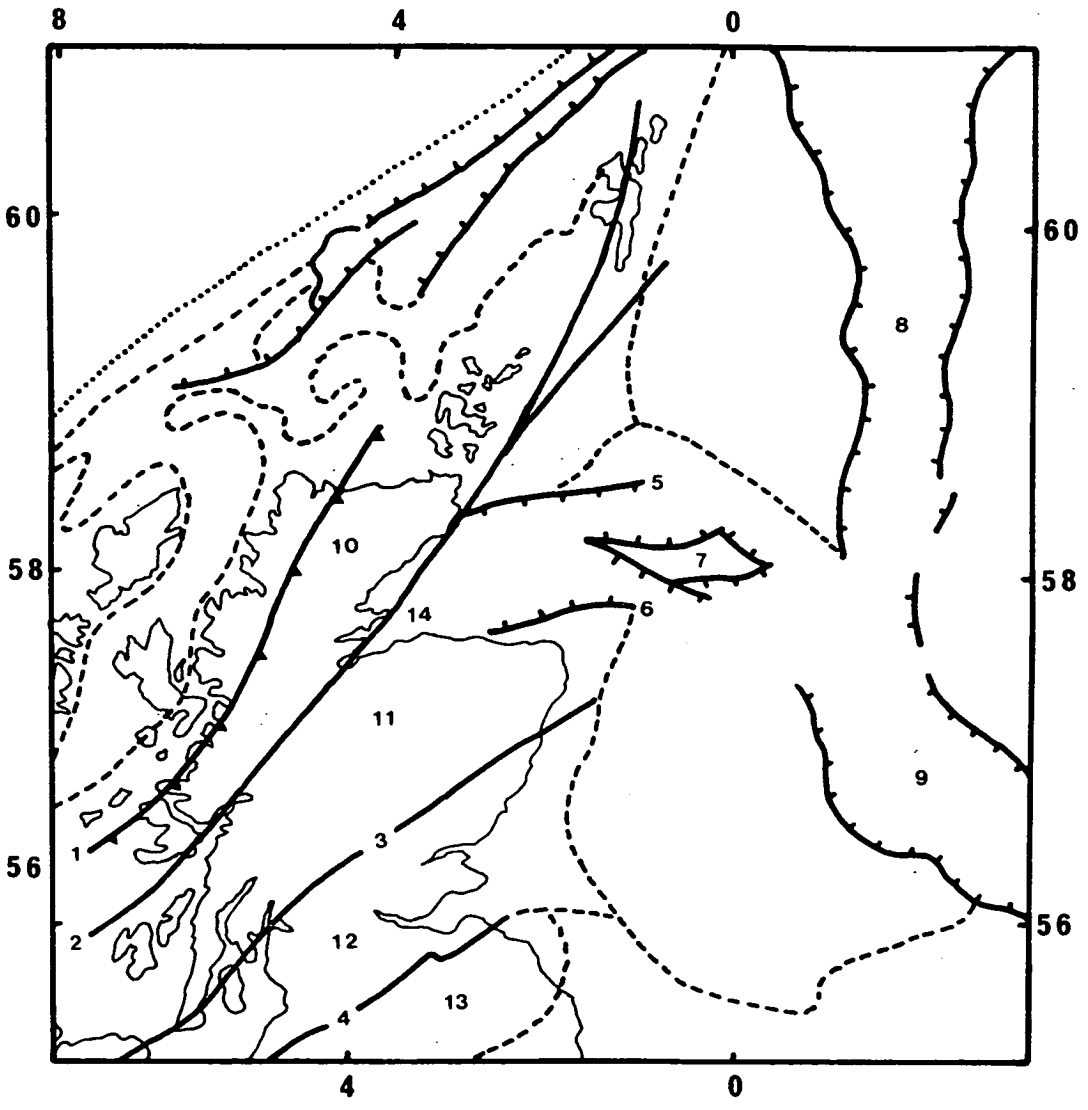
8
4
0
60
58
56
1
2
3
4
5
6
7
8
9
10
11
12
13
14

along the fault during Jurassic and Lower Cretaceous were almost entirely normal and restricted in the Moray Firth area, dying out to the south-west. Eight of the twenty-seven kilometres are definitely post-Carboniferous and McQuillin et al (in preparation) postulate a post-Lower Cretaceous event for this dextral movement. This summary of the movements along the Great Glen Fault is derived mainly from information supplied by W Mykura (personal communication).

The Wick and Banff Faults forming the north and south-east margins of the basin seem to form a graben type structure, and a connection of this graben structure with the Viking and Central Grabens through the Buchan and Witchground Grabens has been proposed (Whiteman et al, 1975). A discussion of the relationship of the Moray Firth basin and the North Sea grabens is given in the last chapter. The fault controlled basement high to the east of the basin (Halibut Horst) and the Moine Thrust, seen in figure 2/9, do not seem to have affected the shape or development of the Mesozoic basin.

2.4 Summary

The Moray Firth basin is a triangular shaped embayment set into the coastline of north-east Scotland. The Mesozoic sediments which fill the basin show their greatest development against normal faults, the thickest section being against the Great Glen Fault in the north-east part of the basin. Faults bound the basin on all sides but the east giving it a "cul-de-sac" shape, and normal faults within the basin form a series of horst and graben structures the most prominent of which is clearly seen on the seismic lines 4, 5 and 6, and is called the "Central Ridge." The peak of the normal faulting activity occurred during the Lower Jurassic, the faulting then reducing in intensity gradually until the movements died out during the Upper Cretaceous. The identification of the base Jurassic and base Cretaceous horizons, which are used in the geophysical modelling, is very good but the base of Permo-Trias is not identifiable. An event believed to be low in the Permo-Triassic can be followed with some difficulty in the main basin. Onshore indications (Johnstone, 1978) suggest that the Permo-Trias does not develop to any great thickness

compared with the Jurassic and Cretaceous strata. The existence of Devonian sediments beneath the Mesozoic cover has been proved in some outer Moray Firth and North Sea wells but the suggested thickness of up to 7km of Old Red Sandstone under the Firth is not considered to be supported by either geological or geophysical evidence. Finally, the basement underlying the Old Red Sandstone sediments is thought to consist of rocks similar to those of the Grampian Highlands. The geology of this area is characterised by the presence of a great suite of igneous rocks, both intrusive and extrusive, within metamorphic rocks of Moinian and Dalradian age.

CHAPTER 3

GEOPHYSICAL INVESTIGATION OF THE INNER MORAY FIRTH AREA

3.1 Introduction

Geophysical exploration in the Moray Firth area started in 1956. During a survey in the north with the Hr.Ms. Submarine "Zeeleeuw" a single pendulum observation within the Moray Firth area was taken. This observation was followed by a gravity survey of the area in 1957 with Hr.Ms. Frigate "Fret," both surveys being undertaken by the Netherlands Geodetic Commission. The observer on "Fret" was B J Collette who published later the isostatic (T = 30km, R = 0) gravity map of the area (Collette, 1960). The main feature of the map, seen in figure 3/1, is a large gravity low of nearly -40mGal over the Inner Moray Firth. Collette proposed the existence of a buried but shallow seated granitic batholith as the cause of this gravity low. Being aware of the presence of Mesozoic sediments onshore he accepted that a thin sedimentary cover might be present over the batholith. Assuming a density contrast of -300kg/m^3 he pointed out that this granitic body needed to be more than 10km thick in order to produce the observed field.

The alternative interpretation that the gravity low was due to a thick Mesozoic sedimentary basin with faulted margins lying close to the present shores was preferred by other authors (Donovan, 1963; Hallam, 1965; Peacock et al, 1968). This interpretation was reinforced by the publication of the aeromagnetic map of the region (IGS, 1968). The anomaly pattern of the Moray Firth area on this map is one of characteristically long wavelength smooth anomalies in contrast to the complicated pattern of very short wavelength anomalies over the metamorphic rocks of the Northern and Grampian Highlands (figure 3/2). Thus the magnetic anomaly pattern is consistent with the presence of thick sedimentary cover over the magnetic basement. The main features on the aeromagnetic map over the Moray Firth area were two elongated anomalies along the Great Glen Fault at Helmsdale and Wick and a positive magnetic zone trending north-south near Lossiemouth and then turning to a north-

FIGURE 3/1

Isostatic gravity map of the Moray Firth area. Contours at 10mGal intervals. After Collette (1960).

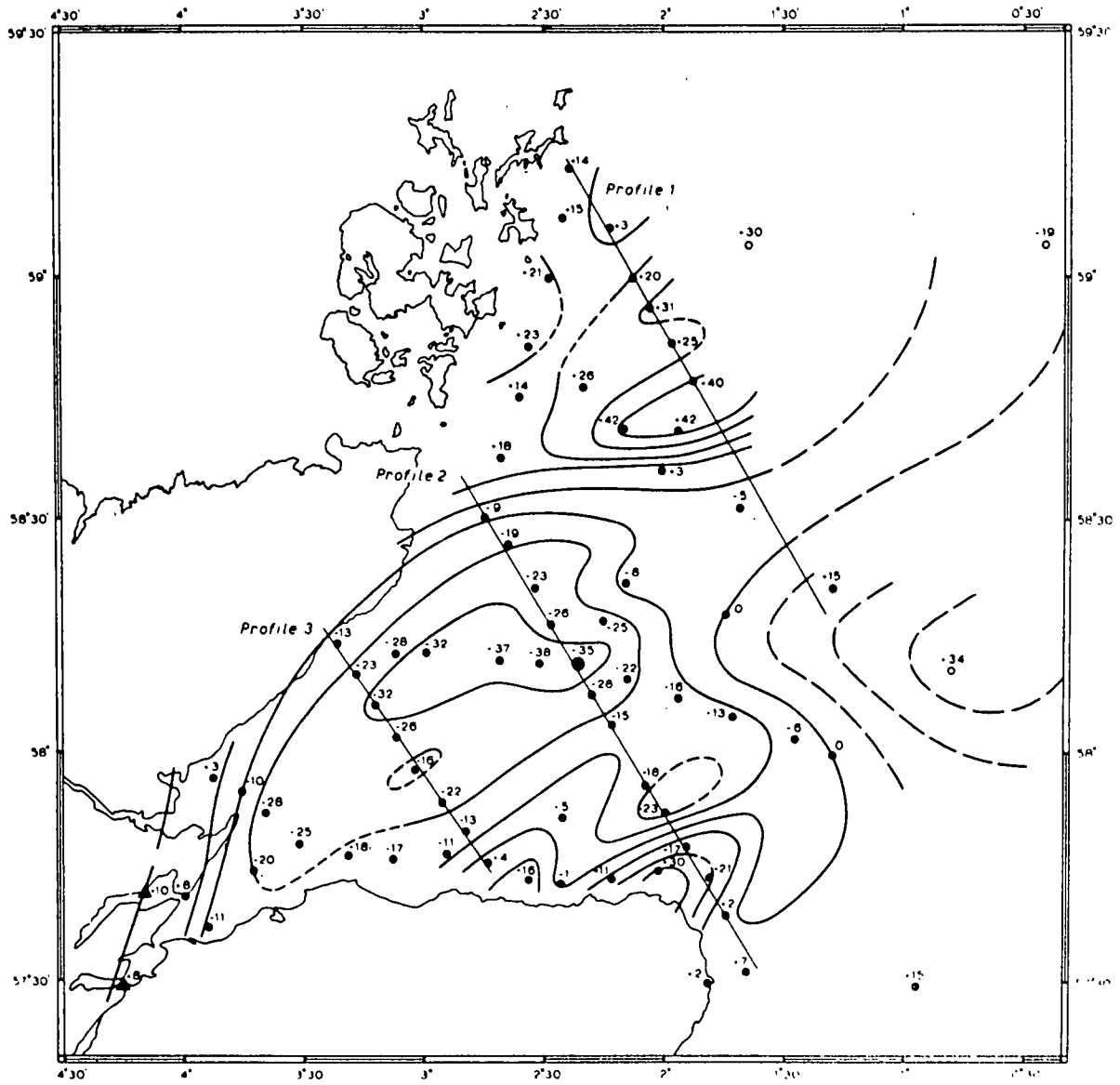
4°30'
4°
3°30'
3°
2°30'
2°
1°30'
1°
0°30'
59°30'
59°
58°30'
58°
57°30'
Profile 1
Profile 2
Profile 3

FIGURE 3/2

Aeromagnetic map of the Moray Firth area. Draughted in simplified form from published IGS aeromagnetic maps. Contours at 100nT intervals. AA', BB', CC' are the modelled profiles.

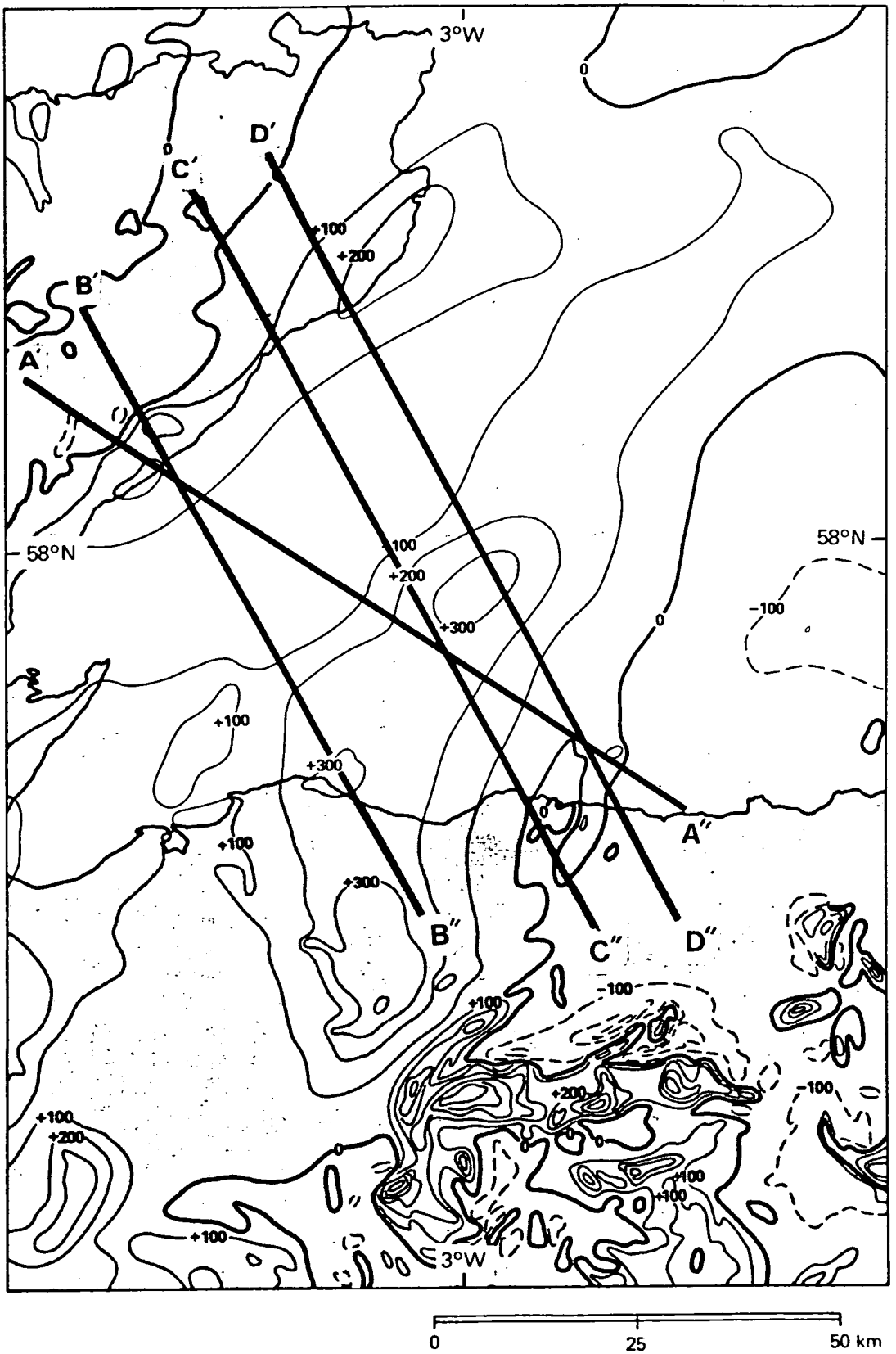
3°W
58°N
A'
B'
C'
D'
A''
B''
C''
D''
0
+100
+200
+300
-100
0
25
50 km

east direction with two peaks of 320nT and 330nT off the coast of Lossiemouth and near the centre of the basin respectively.

Following the IGS surveys in the area in 1970 (see paragraph 2.1) a solid geology map (Chesher et al, 1972) and a Bouguer anomaly gravity map (Sunderland, 1972) were published. The gravity map showed very steep linear gradients on the north, north-west (along the coastline) and south-east sides of the Moray Firth, indicating the existence of large normal faults bounding the basin. A local gravity "high" of -20mGal was indicated near the location of the 330nT magnetic peak in the centre of the basin, the lowest gravity values of the basin being to the east of this "high" and having an amplitude of -40mGal. Sunderland analysed a profile across the basin, running from the north-east edge of the Caithness area to the north-east edge of the Grampians, and pointed out that the observed gradients require density contrasts consistent with a thick sedimentary basin and not with a granitic body. By using a density contrast of -400kg/m^3 between the sediments and the metamorphic basement he proposed a maximum thickness of the sediments of between 3.5 and 4.5km. A basement ridge towards the south-east end of the profile was indicated by the modelled profile as well.

A deep seismic reflection survey, which was carried out by Seiscom-Delta for IGS in 1972, covered the area between latitudes 2°40'W and 4°W and longitudes 57°30'N and 58°30'N. The survey tracks (figure 3/4) form a rectangular grid with spacings of about 10km between north-north-west trending lines and about 13km between the east-north-east trending lines. The survey was carried out by m.v. "Caribe Tide" and the navigational accuracy was probably better than 100m. An array of eight gas guns formed the sound source. Data down to 6s two-way travel time at a 4ms sampling rate were recorded on a 48-channel system. During shooting, 48-fold coverage was obtained, but during the processing this was reduced by summation to an effective 24-fold coverage. The interpretation of the deep seismic data which were processed down to 4s two-way travel time, has been done by Chesher and Bacon (1975) of IGS and some interpreted lines are seen in figure 2/8.

FIGURE 3/3

Bouguer gravity map of the Moray Firth area. Draughted in simplified form from published IGS Bouguer gravity maps. Contours at 5mGal intervals. AA', BB', CC' and DDp are the modelled profiles.

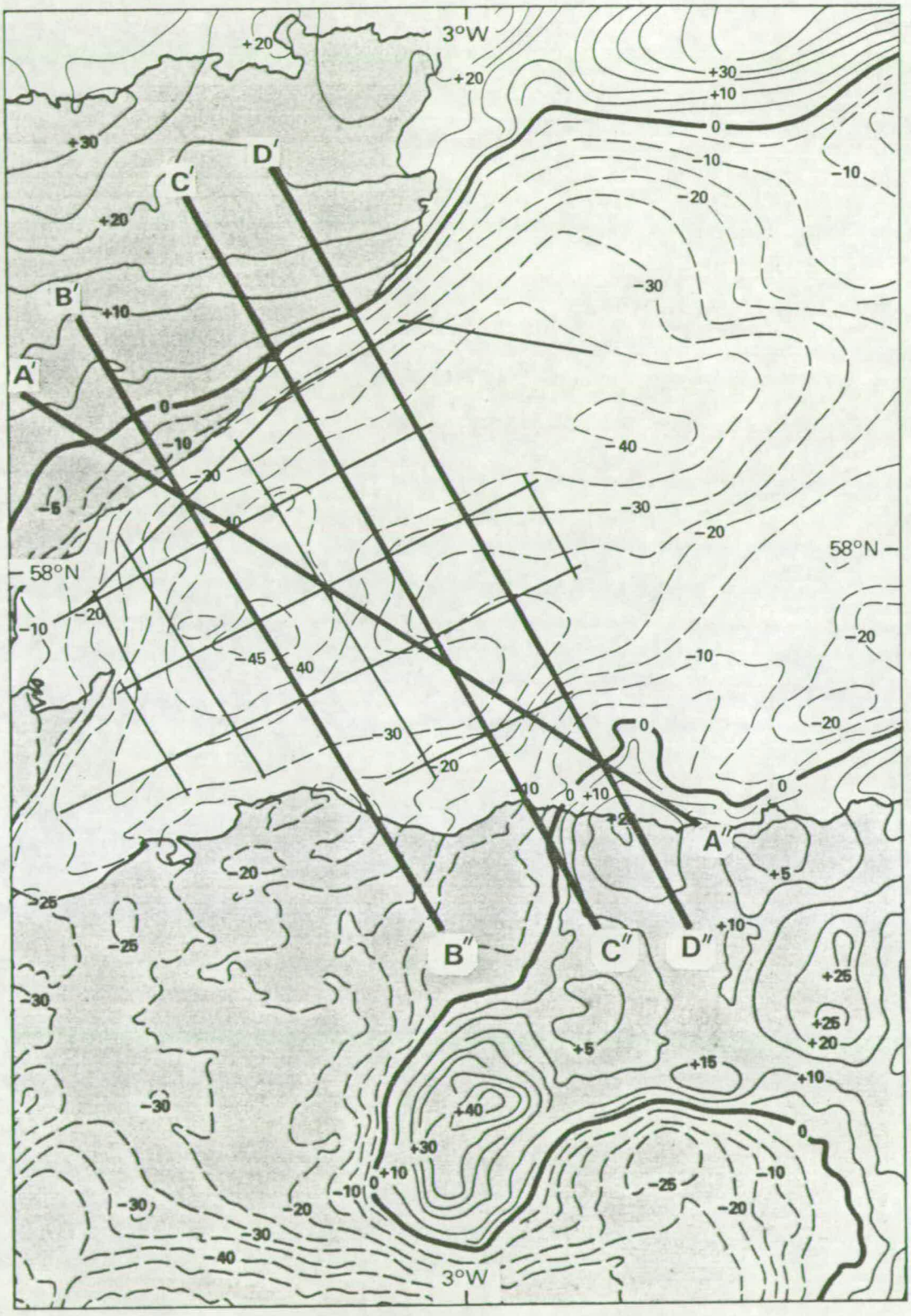
3°W
58°N
A′
B′
C′
D′
A″
B″
C″
D″
IGS deep seismic lines
0
25
50 km

FIGURE 3/4

Track lines of the IGS deep reflection survey of the Inner Moray Firth Basin. After Chesher and Bacon (1975).

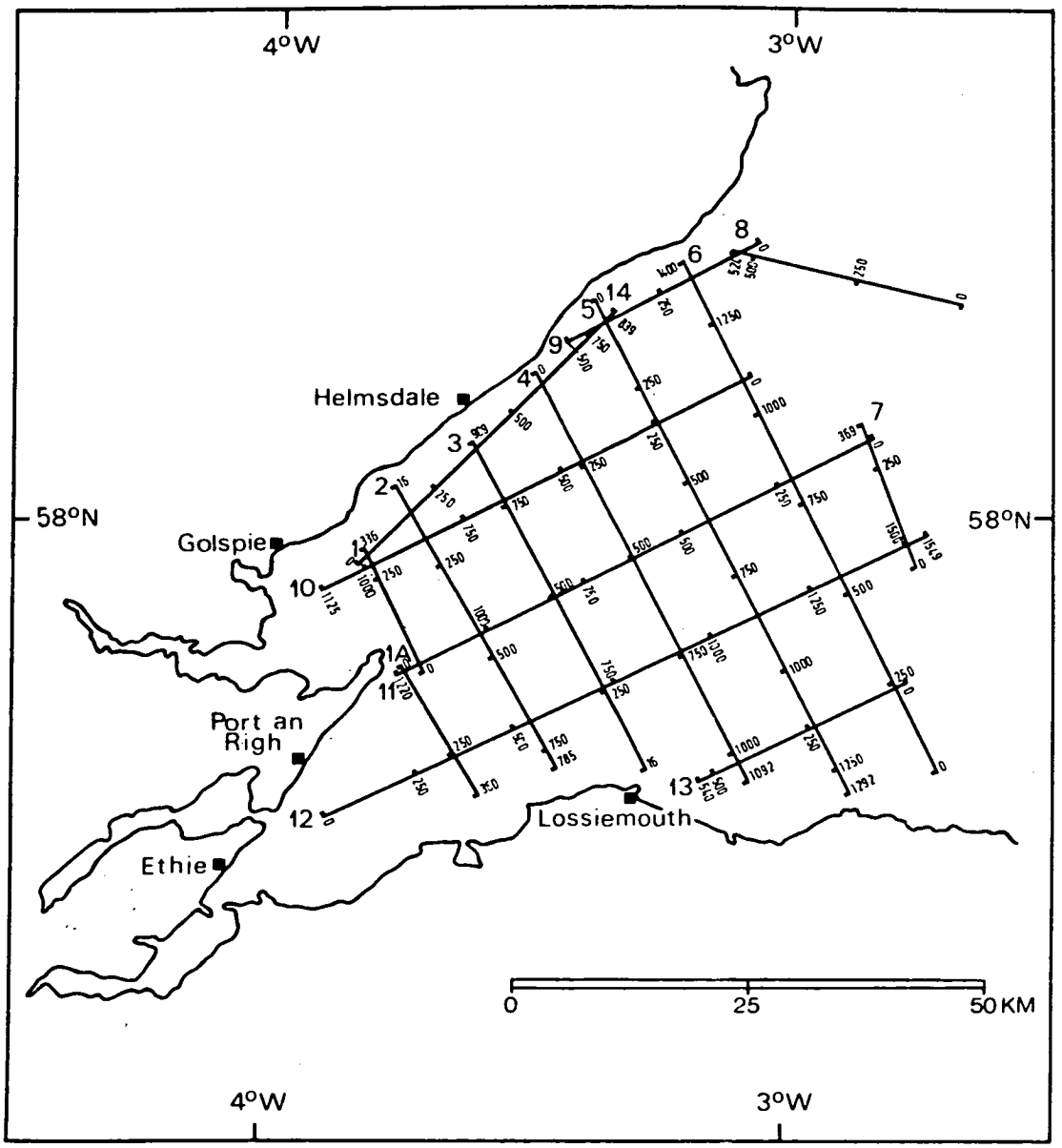
4°W
3°W
58°N
Helmsdale
Golspie
Port an Righ
Ethie
Lossiemouth
1
2
3
4
5
6
7
8
9
10
11
12
13
14
1A
0
25
50 KM

Comparing the thickness of the Mesozoic sediments revealed by the multi-channel seismic data with the gravity map, Chesher and Bacon (1975) noticed that there was a discrepancy between them. The thickest sediments occur in the north-east part of the basin about the intersection of lines 6 and 11 (figure 3/4), whereas the lowest observed gravity anomaly occurs in the south-east part of the basin around the intersection of lines 3 and 11. They went on to calculate the three-dimensional gravity effect of the sediments. The basin structure was approximated by a rectangular matrix of prisms 3km square, the top of each prism being set at sea level (the observed Bouguer anomalies are corrected to sea level) and the bottom of the presumed base of Jurassic. The difference between observed and calculated gravity, assuming a density contrast of $-400kg/m^3$ between the sediments and the metamorphic basement, as well as the observed gravity are shown in figure 3/5. The most prominent discrepancy between observed and calculated gravity occurs in the south of the basin, where over a wide area the observed gravity is much lower than calculated. Lower calculated values occur in the north-west part of the basin. A two-dimensional profile between the two extremes of the difference between observed and calculated gravity is also shown in the same figure. Chesher and Bacon (1975) assumed a linear regional gravity decrease of about 0.85mGal/km along this profile (line AB). Superimposed on this linear regional variation is a low of about 20mGal amplitude, centred around the intersection of lines 3 and 12. No certain explanation of the cause of either the regional gradient or the superimposed gravity low was proposed by the authors, although both variations in density of the metamorphic basement and variations in thickness of Old Red and Permo-Triassic deposits were quoted as a possible cause of the discrepancies. New gravity modelling across the Inner Moray Firth Basin has been carried out to further investigate both the regional gradient and the residual low.

3.2 Modelling the Basin

Considering that the shape of the basin and the basement ridge within it were elongated enough, it was decided that two-dimensional gravity models across the basin along some of the deep seismic lines

FIGURE 3/5

Residual gravity map of the Inner Moray Firth Basin. Dashed line: observed gravity. Solid line: residual anomaly ($g_{res} = g_{obs} - g_{calc}$). Contours at 5mGal intervals. After Chesher and Bacon (1975).

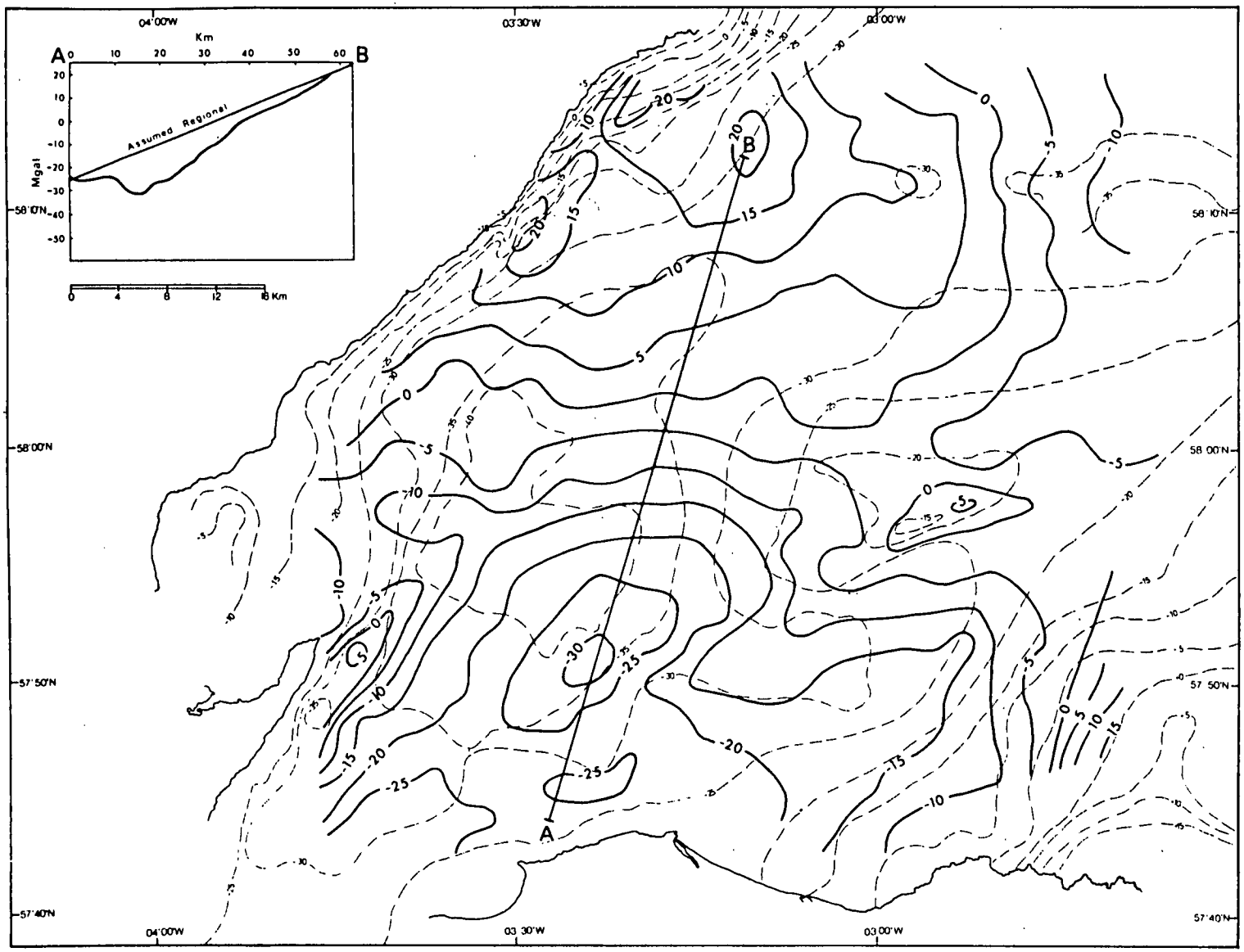
04°00'W
03°30'W
03°00'W
58°10'N
58°00'N
57°50'N
57°40'N
A
B
Km
0 10 20 30 40 50 60
20
10
0
-10
-20
-30
-40
-50
Mgal
Assumed Regional
0 4 8 12 16 Km

would be sufficient to reveal the structure of the deepest parts of the basin. As the most characteristic line across the basin, the seismic line 6 was chosen as the first to be modelled. The procedure of modelling includes the following stages: regional gravity reduction; definition of the densities to be used; use of the seismic information to define the depth to the different layers on individual lines; stripping the Mesozoic sediments' gravity effect along individual lines and, finally, interpretation of the remaining gravity anomalies in conjunction with any other available information, such as the geology summarised in chapter 2.

3.2.1 Regional gravity reduction

The first and probably the most difficult stage during the modelling was the removal of the regional gravity field. A commonly applied technique for the solution of this problem is frequency filtering. This includes first the conversion of the spatial domain data into the frequency domain by using Fourier transformation, then the removal of the low frequencies, which normally constitute the regional field. Finally the remaining frequencies are transformed into the spatial domain again. A description of this method is given in the book " Gravity and magnetics in oil prospecting" (Nettleton, 1976). The main disadvantage of the method is that it is purely mathematical and does not take into account any geological information. By removing gravity anomalies of greater wavelength than a certain limit, it is possible to remove information about a deep seated body of "local" dimensions which produces an anomaly corresponding to the removed wavelength. The same is true in the case of the effect of shallow sediments widely spread over an area. In both cases the interpretation of the residual anomalies after the removal of the regional field becomes questionable, since the residual anomalies could be misleading.

In the present case, having decided to produce two-dimensional models, the removal of a first degree, linear regional gravity field from the area was thought to be adequate. The determination of the plane representing the regional gravity field could have been done by least square fitting to the gravity values of the area. However,

again the method is purely mathematical and the result would have been biased by the extensive low over the Firth as well as the presence of huge granitic and basic intrusions of the surrounding areas, thus producing residual anomalies of shape and amplitude different from the true anomalies. The determination of the plane representing the regional field over the area was done by finding the linear gravity field along two long gravity profiles crossing the area and then from their slopes and the value of the regional field at their cross point to determine the regional plane. This method is probably as effective as the above described method, bearing in mind the interpreter's knowledge of the regional geology.

The position of the two profiles and their extent was dictated by the trend of the basin and the availability of IGS gravity data. The two profiles are marked on the Sub-Pleistocene geological map of the British Isles (inside back cover) so a quick comparison of the gravity field along the profiles (figure 3/6) with the geology of the area is convenient.

The first profile includes multi-channel seismic line 6 and is about 750km long; its end coordinates are 60°N, 4°58'W and 53°53'N, 0°31'E. The north-west end of this profile is at the edge of the Continental Shelf which follows roughly the 200m depth contour line, whereas the south-east end of it lies in the southern North Sea off the coast of Hull. The prominent features along this profile are:

a. A gravity high of +62mGal at 60km, which is thought to represent a ridge of Lewisian rocks.

b. The area of relatively low gravity related to the West Orkneys Basin complex between 70 and 140km.

c. A gravity gradient of 0.35mGal/km between 140 and 190km. This gradient is thought to reflect, at least partly, the gravity effect of the Moine Thrust.

FIGURE 3/6

Long gravity profiles through the Moray Firth. Vertical axis: observed gravity in mGal. Horizontal axis: distance in km. Dashed line: First degree regional interpretation of the profiles across the area of the basin.

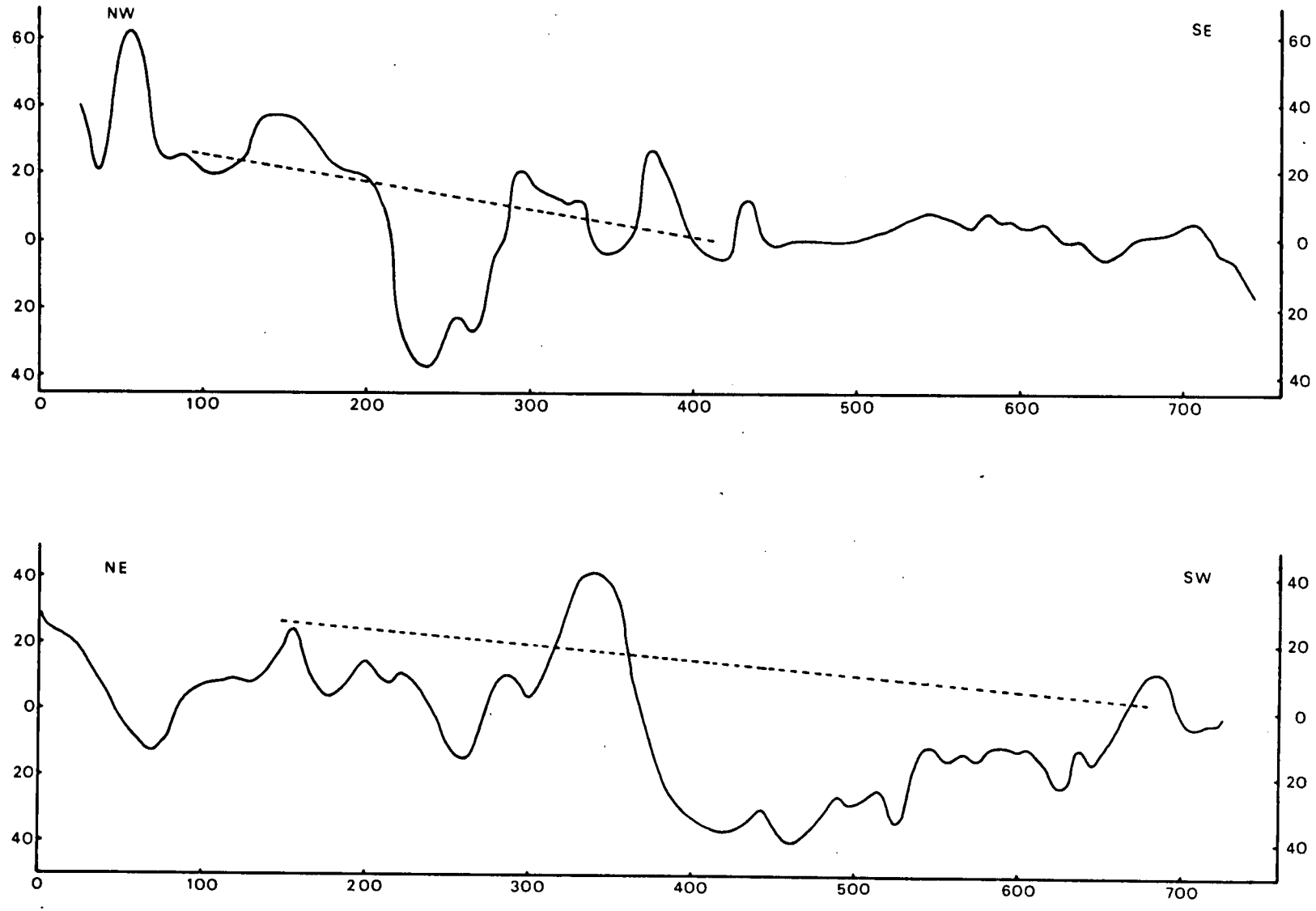
NW
SE
NE
SW
60
40
20
0
20
40
0
100
200
300
400
500
600
700

d. The large gravity low between 215 and 280km, which corresponds to the Moray Firth Mesozoic Basin.

e. The gravity low at 350km, which represents the granites of the Aberdeenshire area.

f. Two gravity highs at 375 and 430km; they probably represent Devonian or Carboniferous volcanics, since they occur on the offshore extension of the Midland Valley.

g. The area of positive gravity values between 520 and 620km, which coincides with the Mid North Sea High.

The chosen linear regional gravity field for the area of and around the Moray Firth is drawn on the profile. The gradient along this line is about 0.10mGal/km. It is noteable that a long wavelength gravity high like that associated with the North Sea graben (Donato and Tully, 1981) is not seen in the Inner Moray Firth area. This has implications for the deep crustal structure of the area, which will be discussed in the last chapter.

The second profile is at an angle of 66° to the first one and follows the trend of the basin; the end coordinates of it are 61°N, 02°E and 56°N, 06°W. The main features of this profile are:

a. The combination of the gravity high at 0km and the gravity low at 70km, which is due to the combined effect of the thick sediments within the Viking Graben and crustal thinning beneath it (Donato and Tully, 1981).

b. The area of positive gravity between 100 and 230km reflecting the East Shetland Plateau.

c. The gravity lows at 260km and 300km representing two sedimentary basins, the youngest sediments being of Permo-Triassic age.

d. The gravity high at 340km, which corresponds to the Caithness Ridge.

e. The extended area of low gravity between 370 and 660km which represents the Moray Firth Basin at first (370-490km) and the granitic intrusions of the Grampian Highlands (490-660km).

f. The gravity high at 675km, reflecting the Devonian volcanics of the Oban area.

The linear regional interpretation of this profile over the area of interest has a slope of 0.045mGal/km.

Gravity profiles along the modelled lines A'A", B'B", C'C" and D'D" (figure 3/3) are shown in figure 3/7. Drawn on these profiles is the linear regional interpretation of them, which is in accordance with the regional gravity plane defined by the two gradients along the two long profiles described above. These regional lines are the adopted zero gravity levels for the computed anomalies in the models.

3.2.2 Density information

Density measurements on rocks from the area around the Moray Firth, the general lithologies of which have been discussed in chapter 2, have been considered. Table I summarises the density information classified into six different formations. Under the term "basement" Moinian and Dalradian rocks have been included. The density value used in the modelling for the basement is 2720kg/m^3 which is close to the average value from the measured specimens. For granites a density of 2620-2640kg/m^3 has been adopted. This value again is near the mean measured while Telford et al (1976) have proposed 2640kg/m^3 as representing the average granite density. Only the measured densities from the Foyers area (Baria and McCann, 1973) are considerably higher than the values used. A density value of 2620kg/m^3 has been chosen as representative of the whole Old Red Sandstone succession under the Moray Firth. This is higher than the average value of 2550kg/m^3 derived from wells 13/22-1 and 13/24-1 which nevertheless represents the density of the topmost part of Devonian sediments under the Moray Firth, presumably of the Upper Old

Location	Formation / Reference	Basement	Granite	ORS	Permo-Trias	Jurassic	Cretaceous
Foyers Inverness-shire	Baria & McCann Report 21	2.69-2.72	2.69-2.73	2.64-2.68	-	-	-
Orkneys	McCann Report 12	2.64-2.97	2.64-2.68	2.27-2.77	-	-	-
Orkneys	McQuillin Geophys. Pap. No.4	-	2.57-2.61	2.25-2.71	-	-	-
Grudie	Foster Report 105	-	2.49-2.65	-	-	-	-
Ross & Cromarty	Foster Report 81	-	2.59-2.63	-	-	-	-
Elgin	Fenning	2.63-2.77	-	2.24-2.54	2.34-2.62	2.23-2.40	-
Moray Firth	Well logs	-	-	2.55	2.45-2.55	2.35-2.55	2.20-2.45
Turriff Aberdeenshire	Ashcroft & Wilson	2.56-2.82	2.54-2.72	2.32-2.66	-	-	-

TABLE 1: Summary of density information

FIGURE 3/7

Extended gravity profiles along the modelled lines and the adopted zero gravity level for the modelling (dashed line). The profiles run from NW (left) to SE (right). Vertical axis: observed gravity in mGal. Horizontal axis: distance in km. AA', BB', CC' and DD' indicate the extent of the modelled profiles.

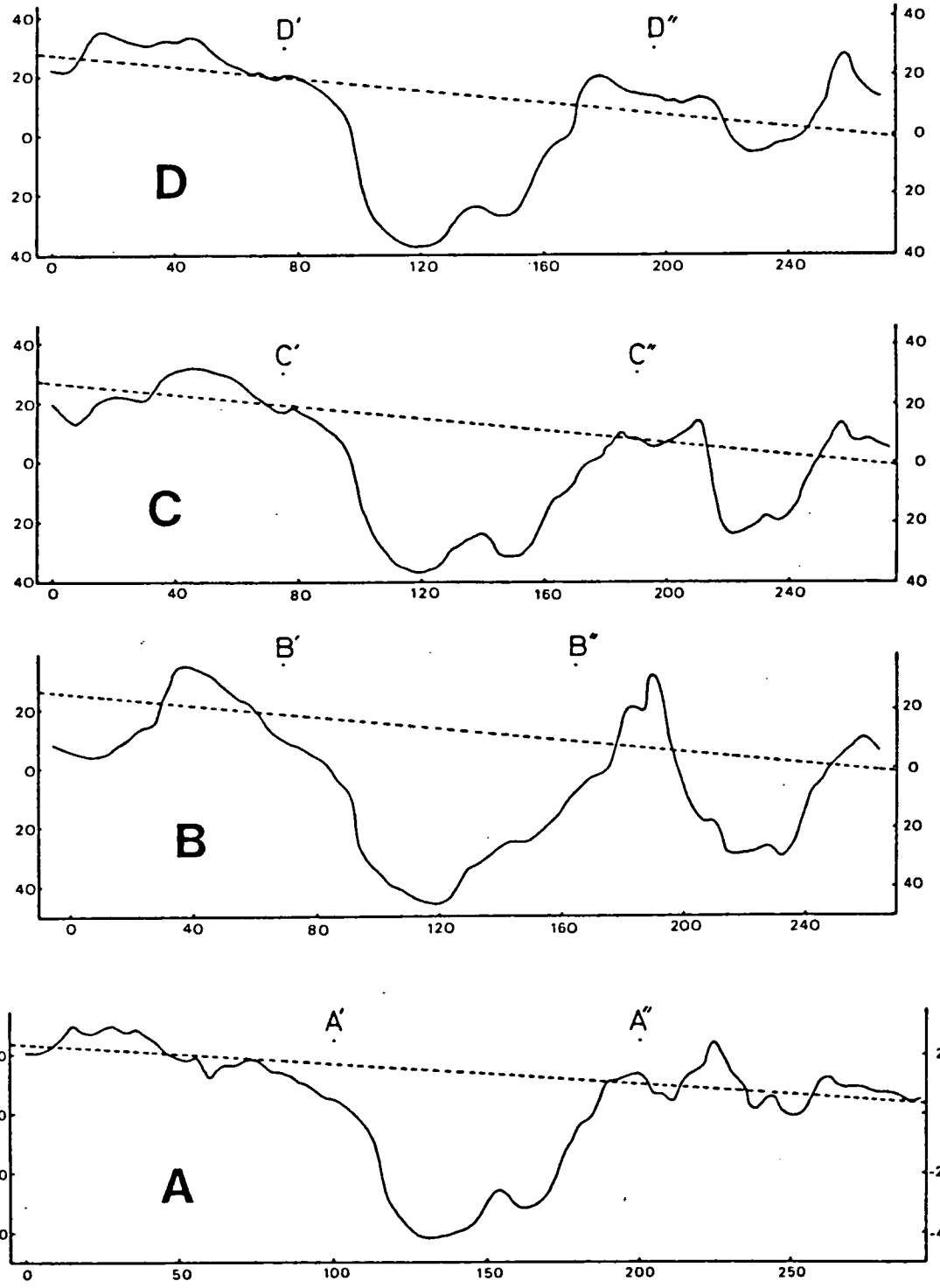
D'
D''
D
C'
C''
C
B'
B''
B
A'
A''
A

Sandstone succession. The very low density values of 2240-2320kg/m^3 shown on the table correspond to a layer of high porosity (20-25%) within the Upper Old Red Sandstone and their occurrence is rare compared to other Devonian layers with densities higher than 2400kg/m^3. In their interpretation of the Turriff Old Red Sandstone Basin, Ashcroft and Wilson (1976) used a density of 2590-2620kg/m^3 for the sediments; although their average measured density is 2470kg/m^3, they suggest that the values used may reasonably be considered minimum values since the density probably increases with depth in the Old Red Sandstone.

The main source of density information for the Mesozoic sediments is the data from exploration wells in the outer Moray Firth area. For the Permo-Triassic layer, which consists mainly of sandstone, a density of 2520kg/m^3 has been chosen for the modelling. This value is close to the value proposed by Fenning (1968) for the Elgin area and to the average value derived from wells 13/17-1 and 13/22-1. The density averaged over the full depth range of Jurassic in wells 12/22-1, 13/17-1 and 13/22-1 is about 2440kg/m^3 and this value was used in the modelling. Only two Jurassic specimens were measured by Fenning (1968) in the Elgin area, one of sandstone the other of mudstone which gave densities of 2400kg/m^3 and 2230kg/m^3 respectively. It is recalled that the Jurassic succession consists mainly of shales and sandstones and therefore the mudstone specimen density is not characteristic of the succession. The range of 2200-2450kg/m^3 density values for the Lower Cretaceous is derived from the wells 12/22-1, 13/17-1, 13/22-1 and 13/24-1. The value adopted for the modelling of this layer is 2320kg/m^3 and represents the average value from these wells. All the values referred to above and in Table I represent saturated density values.

3.2.3 Seismic input

The interpretation of Chesher and Bacon (1975) has been used as a guide for the identification of the different horizons on the actual seismic lines. The conversion of the two-way travel time to the different horizons into depth in kilometres was done by using seismic velocity spectra through the formula $D = \frac{T}{2} \times V$, where D is the depth to the specific horizon, T the two-way time to this

horizon at a certain shotpoint for which the average velocity V to this reflector is known. The velocity spectra give the average velocity to every strong reflector in the seismic record at shotpoints spaced about 3km apart. The error involved in the estimation of these velocities can be as high as 20% if the reflectors' dip is very steep. In the present case the base Cretaceous and base Jurassic reflectors are dipping smoothly generally and the error involved is thought to be about 10% and no more than 15%. The depth to the two reflectors calculated from the velocities is therefore affected to the same degree. The conversion of the two-way time to depth was made in this way for all the lines except for line 14 for which no velocity data were available.

The converted depths were granted to the Geophysics Department of Edinburgh University to be used in a regional gravity reduction project which will eventually cover the whole United Kingdom area. They were also used for the calculation of the gravity effect of the post-Triassic sediments (see section 3.2.4) and the construction of the profile A (figure 3/3) not running along a seismic line (see page 67). The constructed depth contour map to the base of Jurassic is shown in figure 3/8. A printed copy, reduced in scale, of seismic lines 5 and 6 is in the pocket inside the back cover (Plate I). Seismic line 3 is shown in figure 3/9. A letter V on top of a record indicates the location of a velocity analysis.

On seismic line 3 (figure 3/9) the fault controlled Central Ridge can be seen between shotpoints 180 and 220. The main Mesozoic basin extends north-west of the ridge. The Mesozoic strata are seen to dip uniformly towards the Great Glen Fault, reaching their maximum thickness at shotpoint 670. It is worth noting the change in thickness of the sediments, notably between horizons F and C, which occurs at about shotpoint 560. The change is seen to be associated with a normal fault downthrowing to the north-west. To the south-east of this fault and up to the Central Ridge these sediments have a uniform thickness, the layers being almost parallel although normal faulting often occurs. Between this fault and the Great Glen Fault the reflectors sag and layers are more variable in thickness. This

FIGURE 3/8

Depth to the base of Jurassic. Contours at 1km intervals.

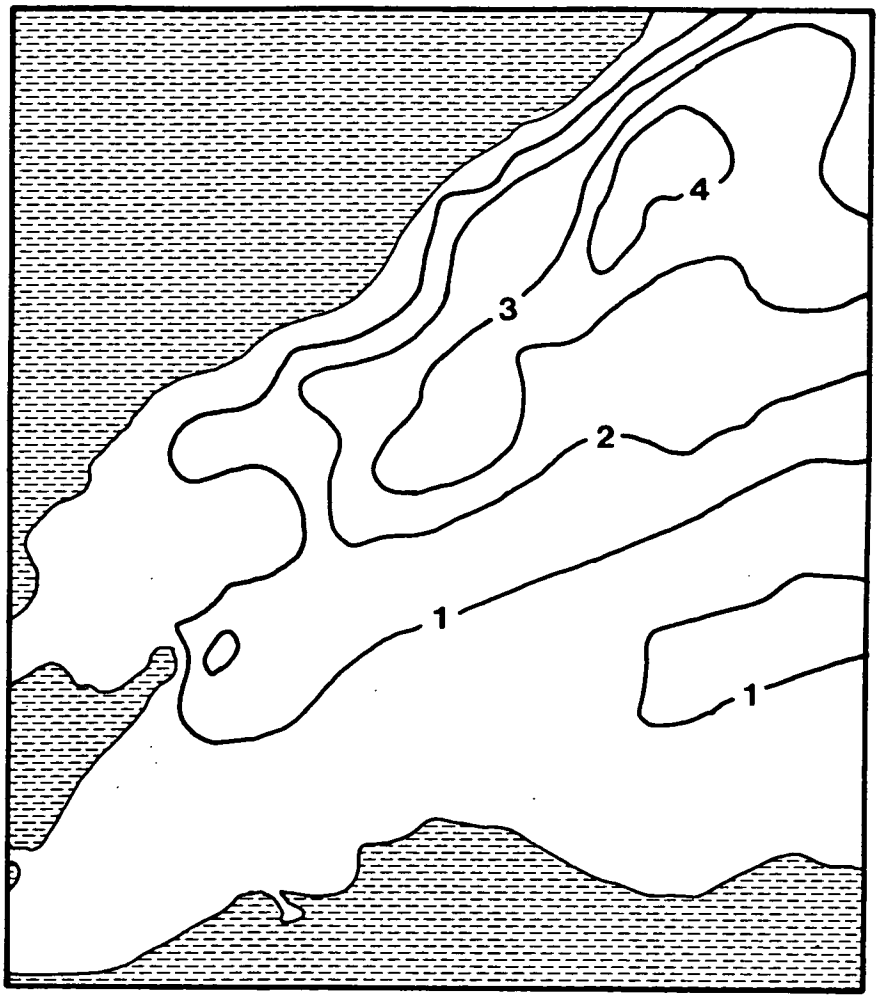
4
3
2
1
1

FIGURE 3/9

IGS deep seismic reflection line 3. Colour key: green, Horizon B (base Cretaceous); brown, Horizon C (Mid-Jurassic); blue, Horizon D; yellow, Horizon E (base Jurassic); red, Horizon F (base? Permo-Trias). Section is in two parts running from NW (left) to SE (right); first part SPs 909-440, second part SPs 480-16 (see figure 3/4 for location of the line).

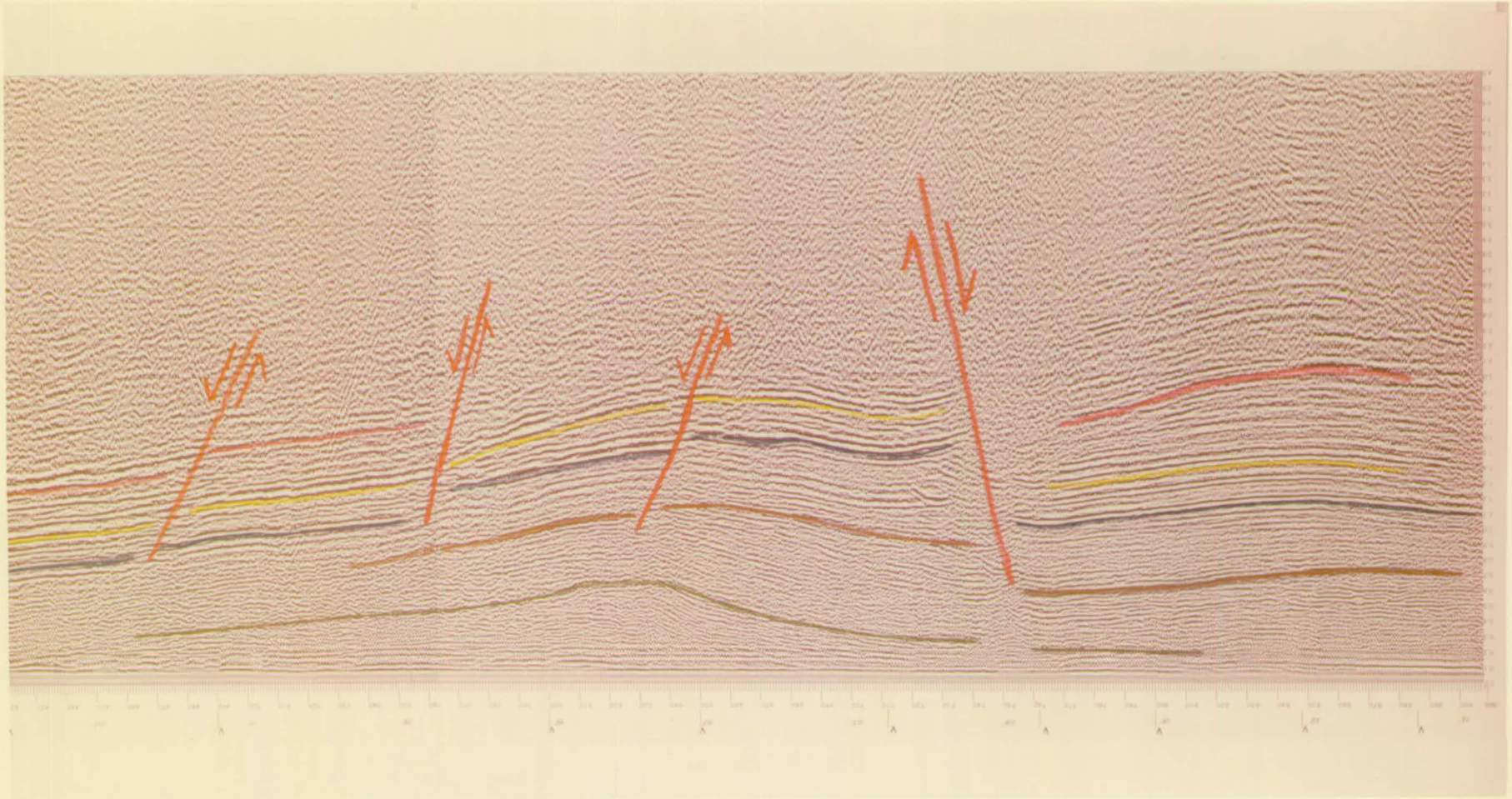

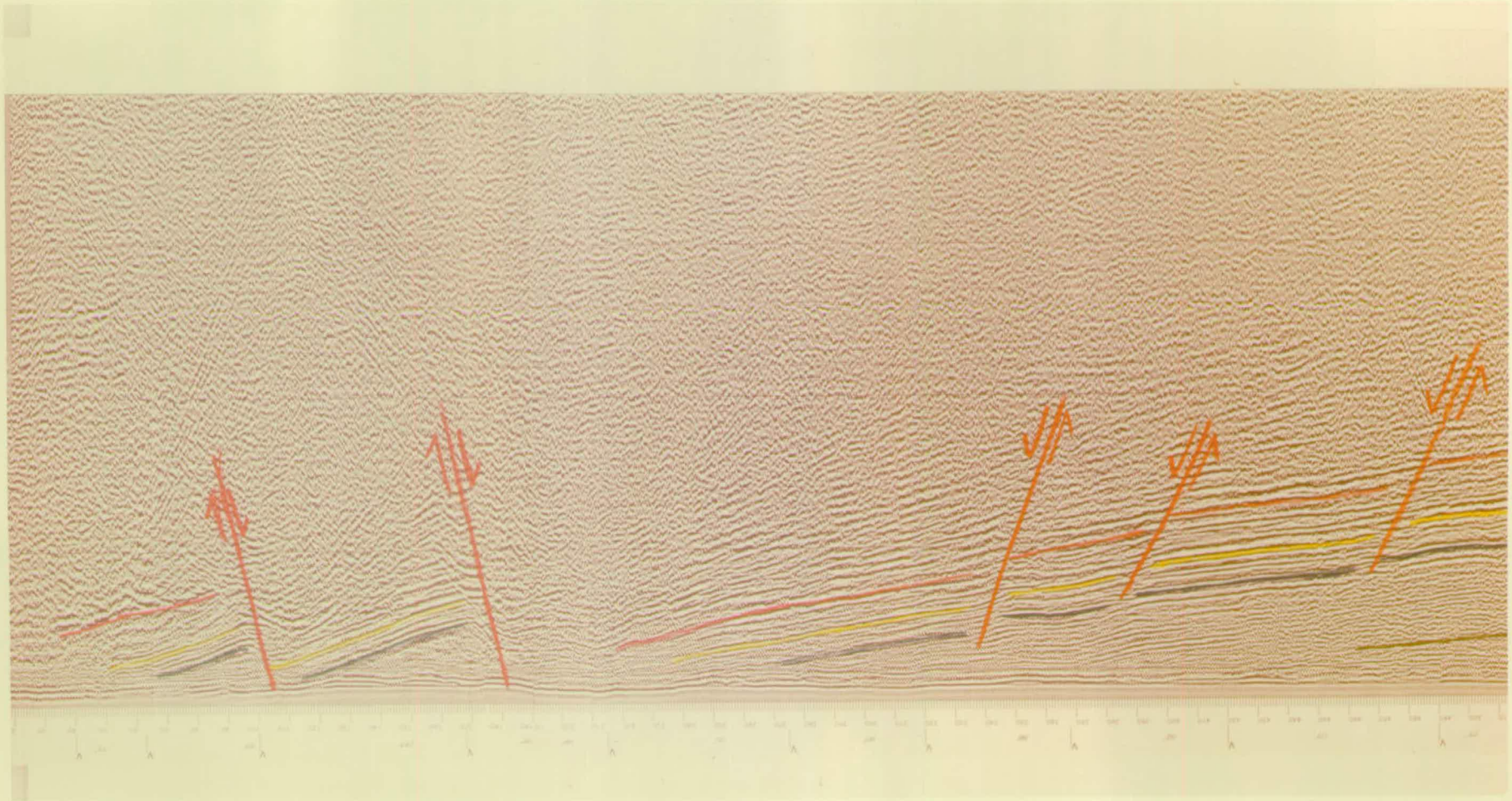

change is accompanied by a migration of the deepest point of the reflectors. Thus horizon B is deepest at shotpoint 615, while horizon C is at shotpoint 630 and horizon E at shotpoint 670. In addition to these changes horizon F cannot be followed north-west of this fault. To the south-east of the Central Ridge the sub-basin can be seen between shotpoints 180 and 100. We can note in this area that horizon F again cannot be followed and that the basement shows a character of north-westwards tilting blocks, one between shotpoints 180 and 100, the other between shotpoints 100 and 45. The implication of the changes of the sediments' character, as described above, is discussed at the end of the chapter (3.2.6). The existence of Old Red Sandstone sediments is indicated by the seismic reflectors occurring between the Great Glen Fault and the north-west end of the line at depths of 2.0 to 3.0s two-way time. The strength and the curvature of these reflectors excludes the possibility of them being multiples of other reflectors higher up the section. These reflectors are not observed elsewhere in the section.

Seismic lines 5 and 6 (Plate I, inside back cover) are quite similar. The Central Ridge is clearly shown between shotpoints 670 and 840 on line 5 and 760 and 550 on line 6. The ridge is shown to be tilted to the north-west (more clearly on line 6). The post-Triassic sediments are seen to thicken from south-east to north-west. The relative thickness change is greater for the Jurassic (layer between red and blue lines) than the Lower Cretaceous (layer between blue and green lines) sediments. The Jurassic sediments on top of the ridge are thinner than the equivalent sediments on either side of it. It is worth noting on seismic line 6 the occurrence of the Beatrice Oilfield in the neighbourhood of shotpoint 990. Oil has been trapped there by the normal fault downthrowing to the south-east (at shotpoint 970) while migrating upwards within the Lower-Middle Jurassic layer (Linsley et al, 1980). It is also worth noting a pocket of sediments on seismic line 5, occurring between shotpoints 950 and 1050 and at depths 1.5 to 2.0s two-way time. It is possible that this sediment pocket represents an embayment of the Devonian topography filled up with Permo-Triassic sediments.

3.2.4 Gravity interpretation

Using all the velocity analyses, detailed shapes for the base of Lower Cretaceous and of Jurassic for all the lines have been obtained. The depths to these horizons along seismic line 14 were extrapolated from the depths at the crosspoints of this line with seismic lines 1, 2, 3 and 4. The gravity effect of the post-Triassic sediments was then calculated from the two-dimensional models using the densities referred to above. A contour map showing the gravity effect of the post-Triassic sediments is shown in figure 3/10. The calculated values were then subtracted from the observed gravity (corrected for regional changes as described in 3.2.1) and the "residual" gravity values were finally contoured. The contour map produced is shown in figure 3/11. Superimposed on this map are the main tectonic features of the basin, namely the location of the Central Ridge and the Great Glen and Helmsdale Faults.

Before advancing to the significance of the features shown on the map the possible error of the residual values is discussed. The following sources of error may have influenced the "residual" gravity map shown: (i) error in the calculated depth of the two horizons introduced by any error in the velocity values derived from spectra analysis. This error depends on the slope of the two horizons and is thought to be less than 10% on the smoothly dipping reflectors over most of the area but it can be up to 15% over zones of steep dips mainly along the Great Glen Fault. (ii) There is an error introduced through the uncertainty associated with the density values used in the model. The densities presented in 3.2.2 (Table 1) give an indication of the density variation for the Cretaceous and Jurassic strata. The average densities for these sediments referred to on page 50 have been derived from Formation Density Logs in the wells examined using the following procedure. The mean density value of different sedimentary formations (having generally the same density and being of the same lithology) was weighted according to the formation's thickness and then the different formation densities were averaged. The uncertainty on reading the density from the logs was $\pm 20 kg/m^3$. Although the average densities calculated in this way

FIGURE 3/10

Gravity effect of the post-Triassic sediments. Contours at 5mGal intervals.

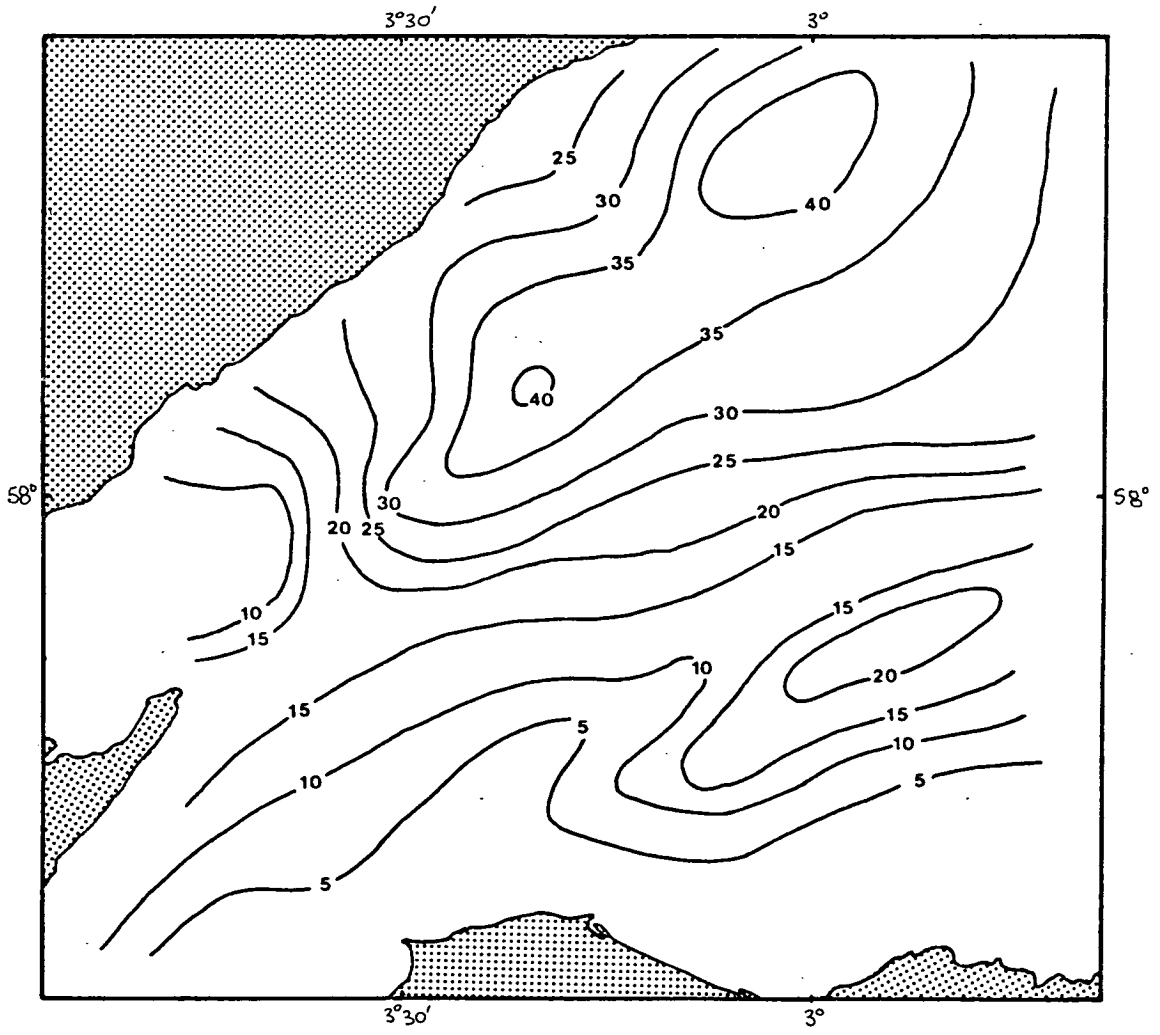
3°30'
3°
58°
25
30
35
40
35
40
30
25
20
30
25
20
15
10
15
15
20
15
10
5
15
10
5
3°30'
3°

FIGURE 3/11

Residual gravity map of the Inner Moray Firth Basin. Thick solid lines: main normal faults of the area. The location of the Central Ridge is indicated by the stippled area. Contours at 5mGal intervals.

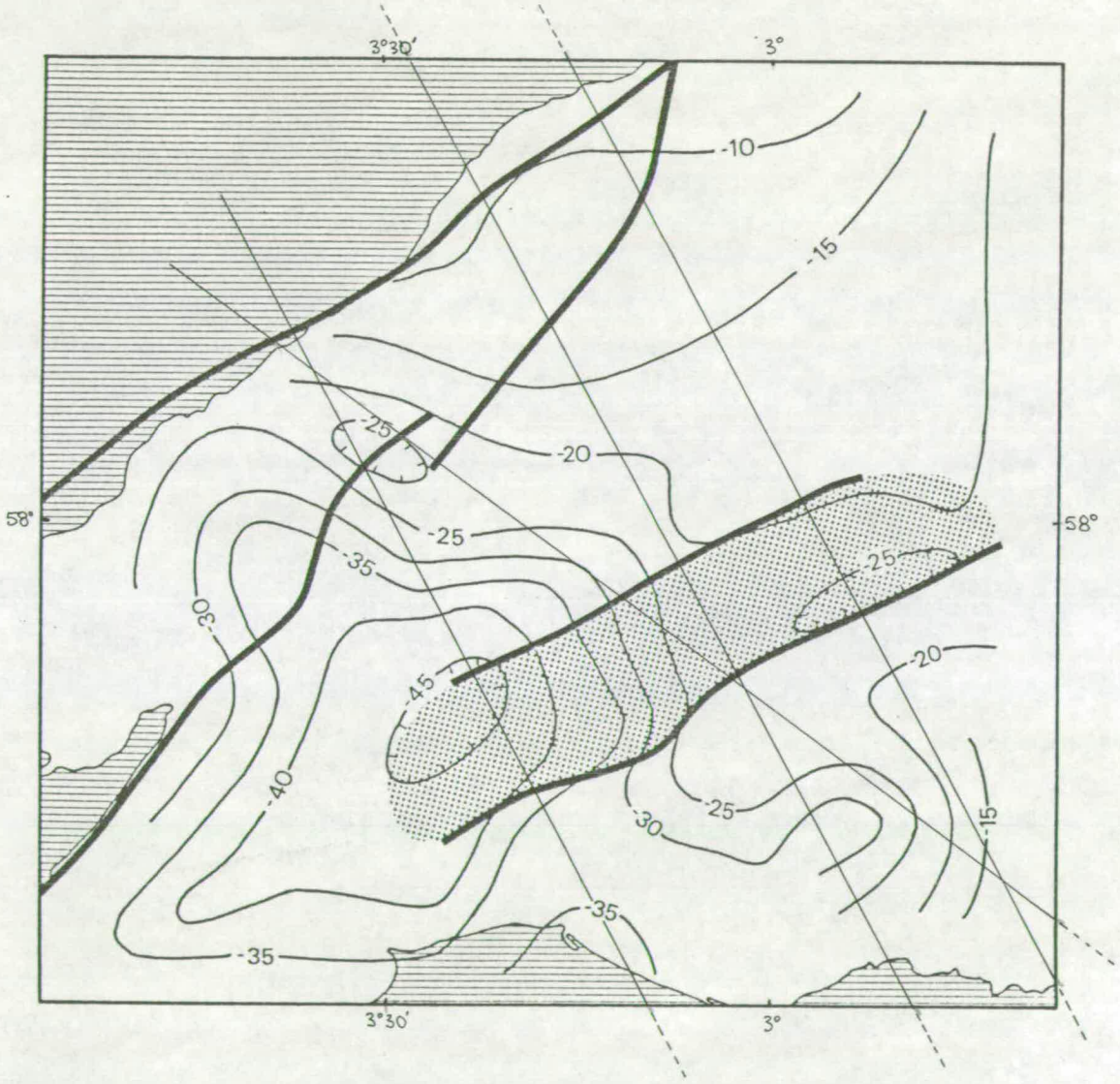
3°30'
3°
58°
-10
-15
-20
-25
-30
-35
-40
-45
-25
-20
-25
-15
-35
-35
3°30'
3°
58°

are well defined, the problem which arises is how well these densities represent strata of the same age in the Inner Moray Firth Basin. There is not an easy answer to this question. The lithology of the wells was checked against the lithology of the Cretaceous and Jurassic strata in the Inner Moray Firth Basin and found to be similar. On the basis of this agreement it is thought that the error of the densities used in the model is probably no greater than $\pm(30\text{-}40)kg/m^3$. This error introduces an error of ±10-15% in the calculated gravity effect of the post-Triassic sediments, since the density contrasts used for Cretaceous and Jurassic layers are -400 and $-280kg/m^3$ respectively. (iii) Finally there is the error introduced by the use of two-dimensional models, which assumes prisms of infinite length extending either side of the profile which of course does not reflect the real shape of the basin. A simple way of approaching the real shape is to assume that the prisms extend to an finite length on either side of the profile. If Y is the length of a prism on one side of the profile (half of the total prism's length) and ρ the depth to the axis of the prism, then the ratio of the gravity effect of such a prism g to that of an infinite length prism g_∞, calculated by the two-dimensional model, depends on the ratio Y/ρ and it is:

$$\frac{g}{g_\infty} = \frac{1}{\sqrt{1+(\rho/Y)^2}}$$

This ratio is known as "end correction" (Nettleton, 1976) and for Y/ρ values of 2, 3 and 4 it is 0.89, 0.95 and 0.97 respectively. Taking into account that the average depth to the base of Jurassic in the basin is about 2km and that the sediments extend more than 6km either side of the profiles (except from the profiles running very close to the coastline) it is concluded that the gravity effect of the post-Triassic sediments has been overestimated by less than 5%.

In addition to the errors described above, it should be noted that the observed values are defined with an accuracy of ±1-2mGal.

The main features of the "residual" map are two gravity lows over the north-eastern and south-western ends of the Central Ridge. The regional gravity map of the area (Hussain and Hipkin, 1981) shows similar features. The calculated gravity effect of the post-Triassic sediments over these two areas is less than 15 mGal and therefore the maximum error is thought to be about ± 5 mGal.

The two anomalies of the "residual" map are rather of equal dimensions (more so the south-western one). Also the depth to the body causing these anomalies is now deeper. Therefore, the use of two dimensional modelling will produce less accurate results quantitatively, but is thought that the qualitative interpretation of these anomalies by two-dimensional modelling will be valid. The seismic lines 3, 5 and 6 were chosen for interpretation modelling because these either cross the anomalous features (lines 3 and 6) or lie between them (line 5). As mentioned in chapter 2 the base of the Permo-Triassic? layer (horizon F) cannot be followed throughout the seismic lines but according to Chesher and Lawson (in press) it reaches a thickness in excess of 500m near the axis of the basin. On this evidence it was decided to use an average thickness of 500m for this layer. Using the formula $g = 0.042\sigma t$ (Nettleton, 1976) where g is the gravity effect in mGal produced by a horizontal slab of thickness t in km and of density contrast σ in kg/m^3, it is seen that the gravity effect of this layer is about 4mGal. Thus changes of the order of 100 or 200m to the average thickness of this layer do not affect significantly the gravity values of the calculated profile, the total amplitude of the anomaly being over 50mGal.

The first model to be established was that of seismic line 6. After removal of the gravity effect of the Permian-Lower Cretaceous sediments, a gravity anomaly up to -23mGal remained (figure 3/13). To account for this anomaly, it was attributed to the presence of Old Red Sandstone sediments beneath the Mesozoic and an appropriate

FIGURE 3/12

Regional gravity map of the Inner Moray Firth Basin. Contours at 4mGal intervals. See text for way of derivation. After Hussein and Hipkin (1981).

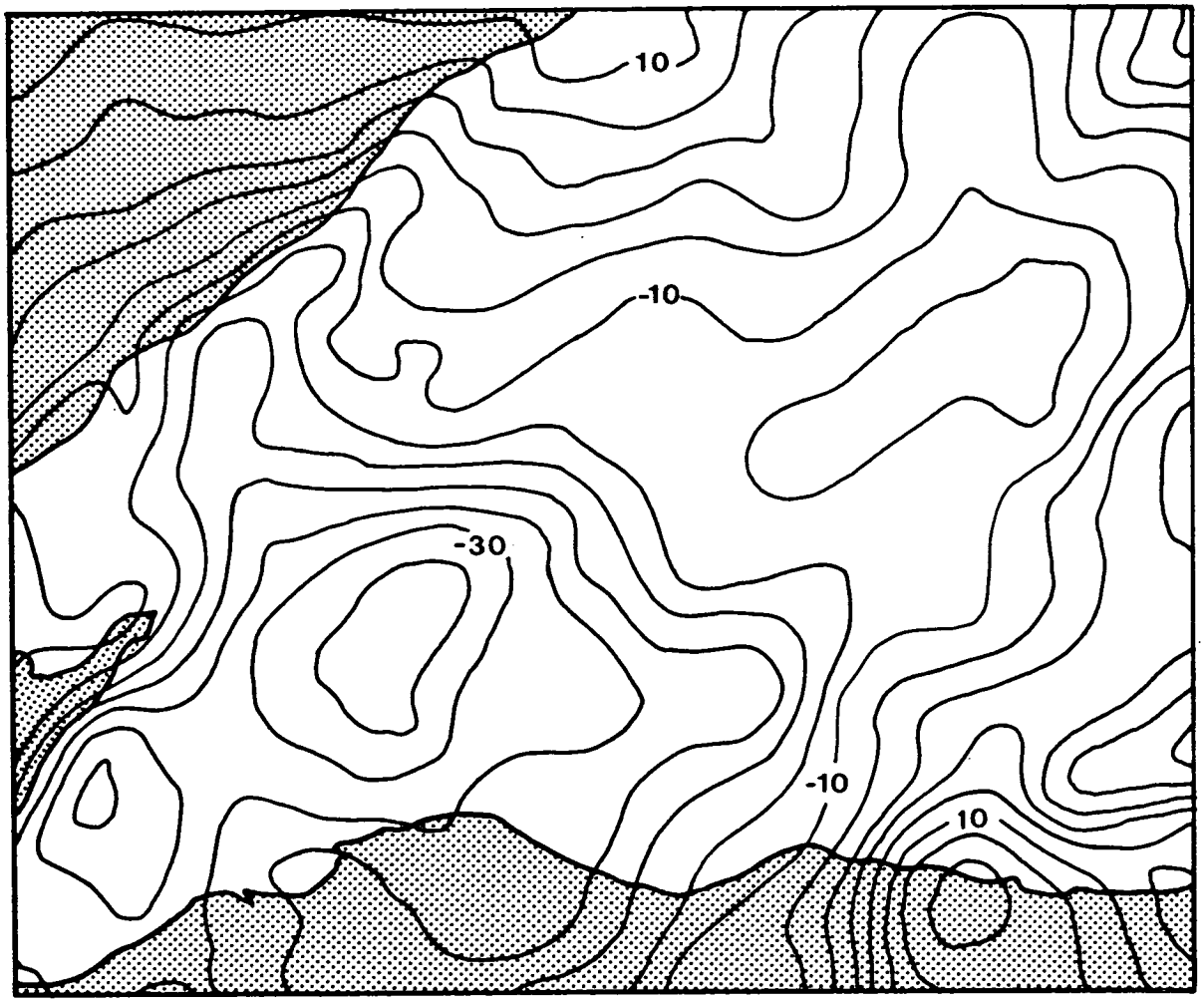
10
-10
-30
-10
10

FIGURE 3/13

Model D'D'' (along seismic line 6): Gravity effect of the Mesozoic sediments. Crosses indicate observed gravity, reduced for regional effect (see figure 3/3 for location of interpreted gravity profiles). Identification and density of layers are as follows: K: Cretaceous (2320kg/m^3); J: Jurassic (2440kg/m^3); P: Permo-Triassic (2520kg/m^3).

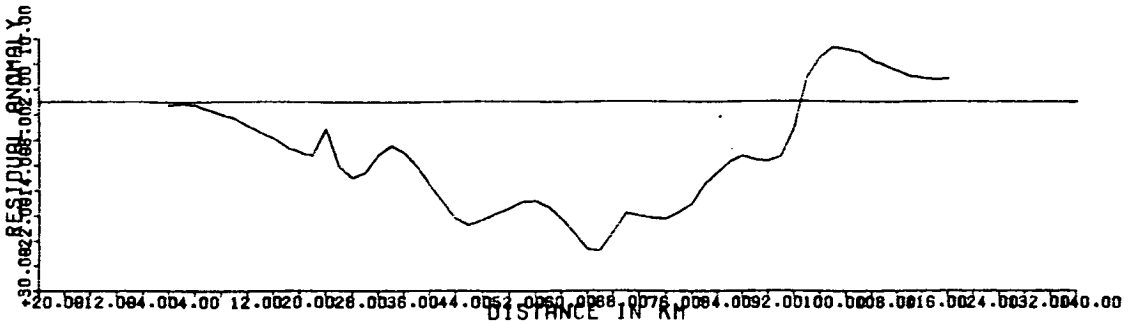
RESIDUAL ANOMALY
DISTANCE IN KM

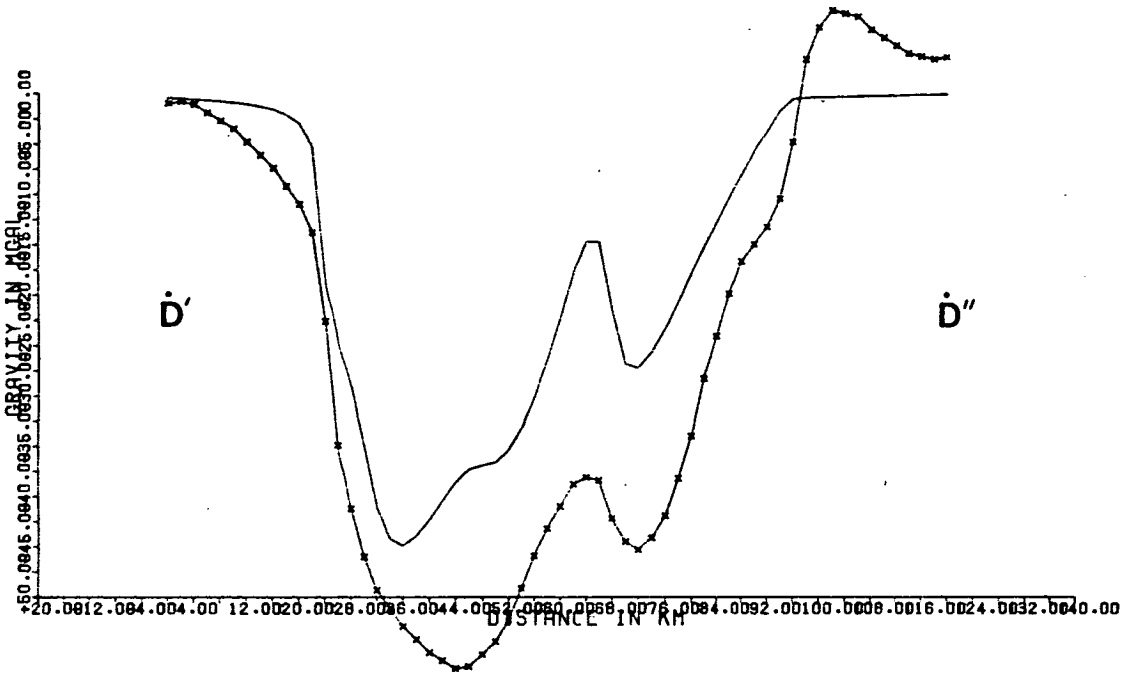
GRAVITY IN MGAL
D′
D″
DISTANCE IN KM

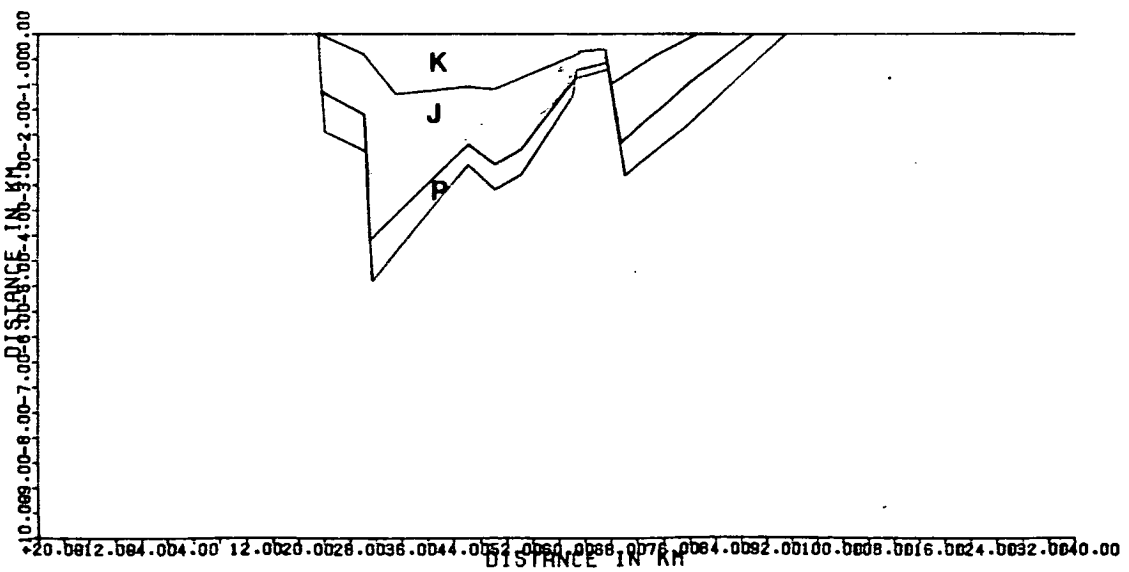
K
J
P
DISTANCE IN KM

additional layer was introduced into the model. In matching the calculated to the observed values a difference of less than 5mGal between them(which is the estimated maximum error of the residual anomaly) was thought to represent an adequate fit. The model constructed with the introduction of the Old Red Sandstone layer (figure 3/14) shows a Devonian basin with a very steep flank to the south and with an increase in depth of 2.5km at the Great Glen Fault. The maximum depth to the bottom of this basin occurs beneath the Central Ridge where it is 9km deep. The Devonian sediments extend beyond the Helmsdale Fault, where another downthrow of 1.5km is indicated, but the thickness there is only a crude estimate and it was mainly incorporated into the model in order to reduce the expected edge effect, the main interest remaining within the limits of the basin.

In the same way a model for seismic line 5 was constructed (figure 3/15). Again the south flank of the Devonian basin is very steep but the maximum depth and thickness now occur to the south-east of the Central Ridge, the maximum depth being 10km. The basement beneath the Old Red Sandstone sediments forms a ridge between 130 and 140km where the overlying sediments thin from 8 to 4km.

The very steep margins of the Devonian basin along with the large indicated thickness of these sediments, which is not justified from any onshore geological evidence, the fact that the shape and position relative to the Central Ridge of the basin changes from one model to the other over a distance of only 10km and mainly the magnetic evidence presented below were the reasons to doubt the idea that the remaining gravity anomaly along the two profiles is totally attributable to Old Red Sandstone sediments.

3.2.5 Magnetic interpretation and final models

The most prominent feature on the aeromagnetic map of the Moray Firth area (figure 3/2) is a curved zone of magnetic highs observed both offshore and onshore. The shape and extent of this zone is well described by the 200nT contour line and is seen to have a north-

FIGURE 3/14

Model D'D" (along seismic line 6): Gravity model attributing the difference between the gravity effect of the Mesozoic sediments and observed gravity to the presence of Old Red Sandstone sediments. Identification and density of layers are as follows: K: Cretaceous (2320kg/m^3); J: Jurassic (2440kg/m^3); P: Permo-Triassic (2520kg/m^3); O: Old Red Sandstone (2620kg/m^3).

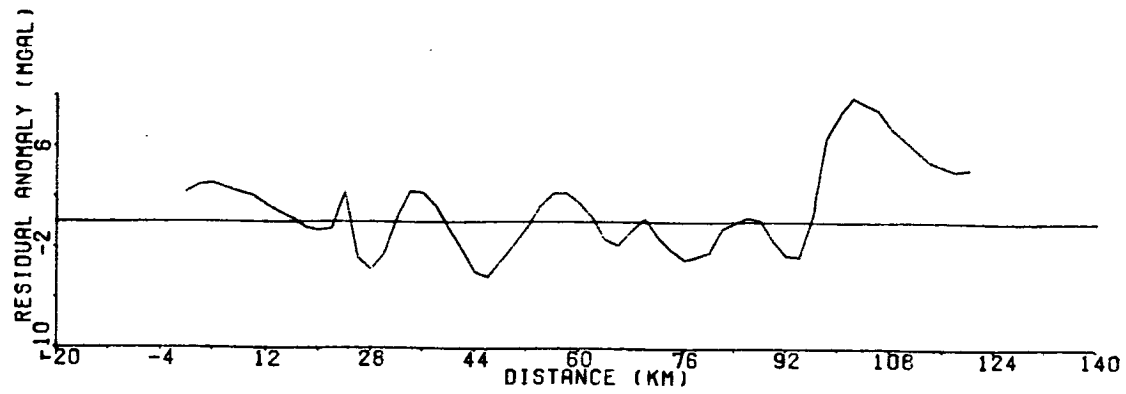

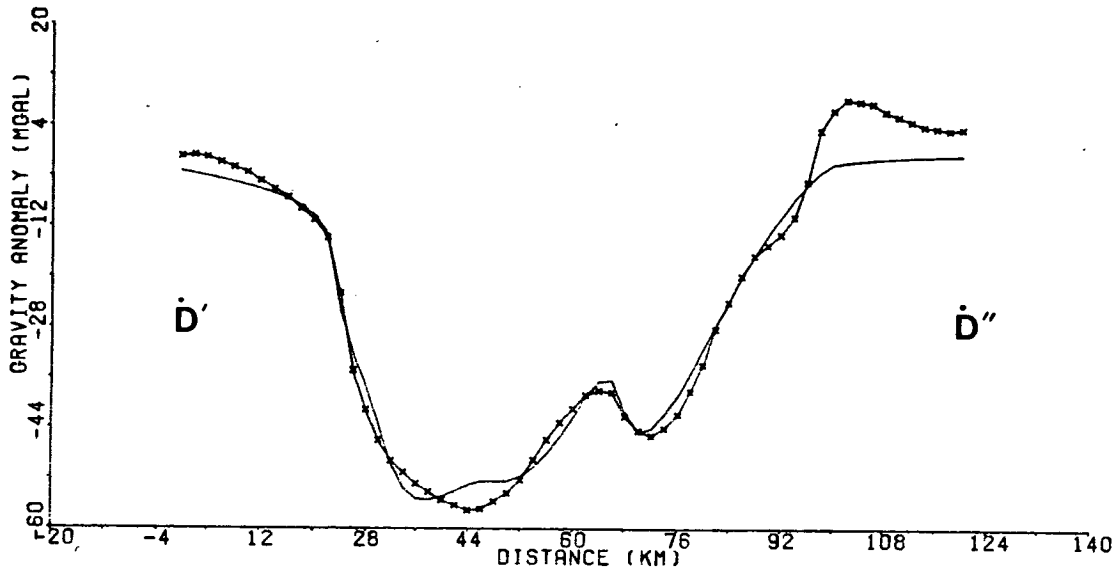

KEY: OBSERVED GRAVITY — CALCULATED GRAVITY

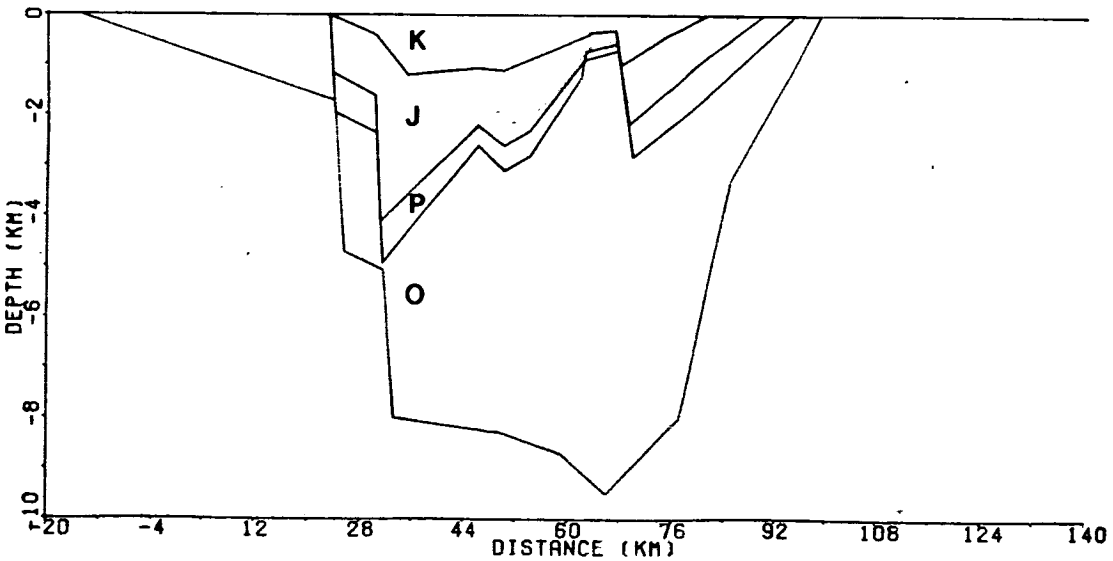

FIGURE 3/15

Model C'C'' (along seismic line 5): Gravity model attributing the difference between the gravity effect of the Mesozoic sediments and observed gravity to the presence of Old Red Sandstone sediments. Identification and density of layers are as follows: K: Cretaceous (2320kg/m^3); J: Jurassic (2440kg/m^3); P: Permo-Triassic (2520kg/m^3); O: Old Red Sandstone (2620kg/m^3).

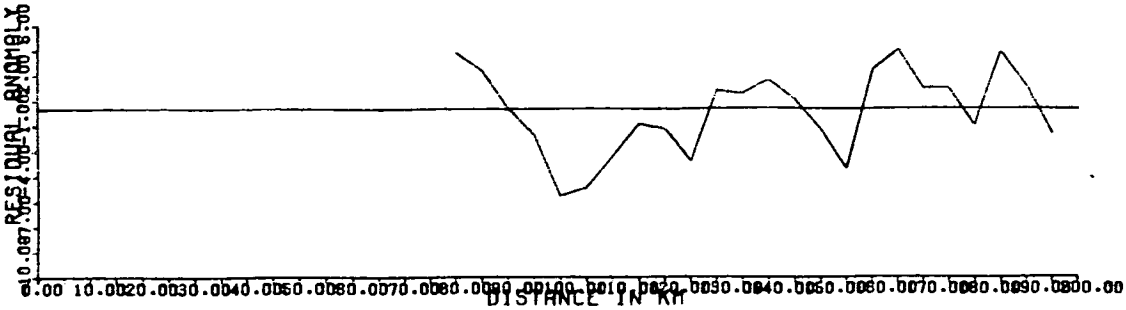
RESIDUAL ANOMALY
DISTANCE IN KM

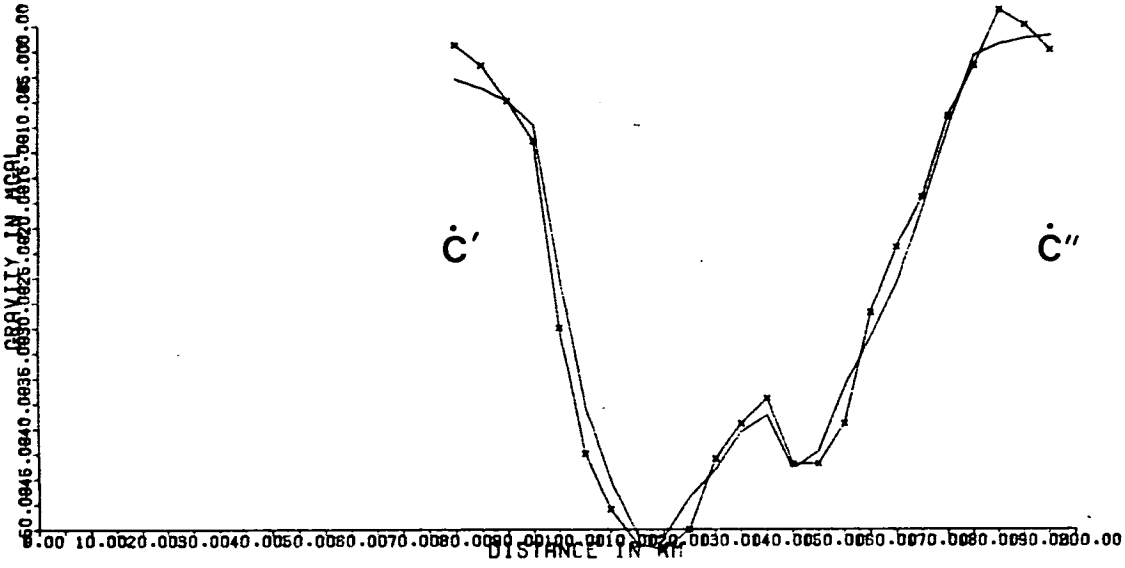
GRAVITY IN MGAL
DISTANCE IN KM
C'
C''

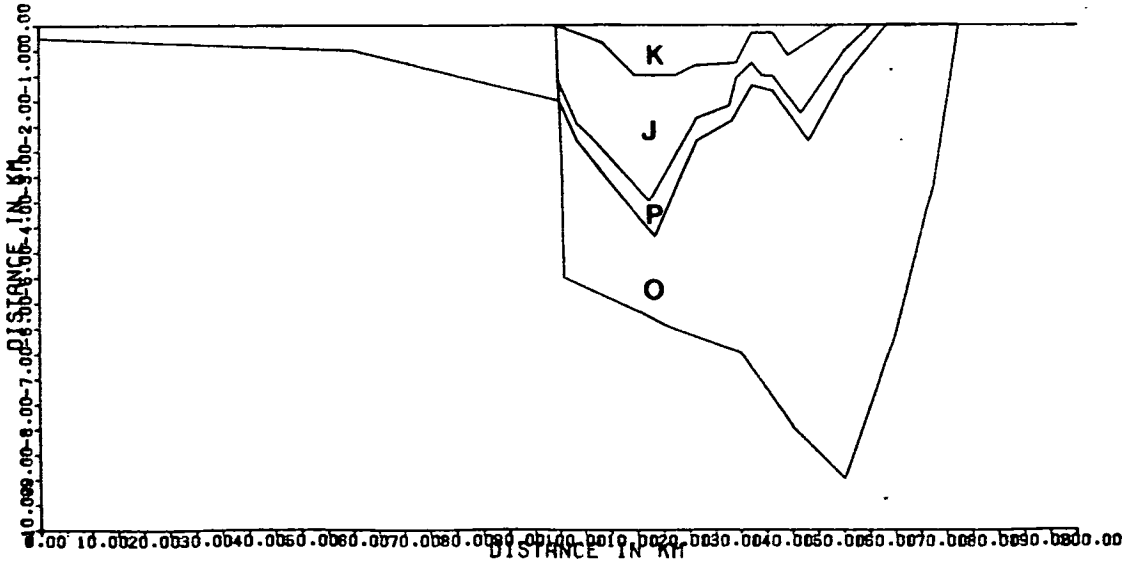
DISTANCE IN KM
K
J
P
O
DISTANCE IN KM

south trend onshore before turning to a north-northeast to south-southwest trend off the coast of the Lossiemouth area. Within this zone two peaks of over 300nT are seen at the north-eastern end and near the middle of the zone and another peak reaching 400nT occurs at the southern end of it. This peak occurs in the neighbourhood of the Ben Rinnes granite. The north-eastern peak occurs over the northeastern part of the Central Ridge in the basin and the middle one crosses the south Moray Firth coast at Lossiemouth. The similarity of the three peaks observed within the 200nT contour line and the continuity of this zone suggest that the cause of the magnetic anomalies over the Central Ridge and at Lossiemouth could be the same as the cause of the Ben Rinnes peak, namely an extensive granitic batholith, but covered by sediments in both cases. The probable extension of granites offshore, deduced from the pattern of the magnetic anomalies on the aeromagnetic map has been proposed as well by Flinn (1969). The possibility that the two 300nT peaks are caused by Old Red Sandstone lavas or Carboniferous volcanics is rather unlikely, since they are associated with negative "residual" gravity anomalies and the presence of volcanics would rather suggest the opposite (positive "residual" anomalies). Volcanics of Carboniferous age have been encountered only in one well in the area farther to the east (well 12/23-1, Linsley et al, 1980) but the location is not associated with any significant magnetic or gravity anomaly.

An estimation of the depth to the top of the body causing the anomaly over the Central Ridge was carried out by using the method introduced by Vaquier et al (1951). This depth was estimated to be 5km. Thus the depth to the top of the body causing the anomaly (assuming that it is of a vertical prismatic shape) does not agree well with the depth of 7km for the basement beneath the Old Red Sandstone sediments indicated by the model of seismic line 6, which crosses the magnetic anomaly at its peak. It was decided then to introduce a granitic body of a simple shape and to try to produce a combined gravity and magnetic model including the Mesozoic sediments, the Old Red Sandstone and the granite. The density of the granite was assumed to be 2640kg/m^3 which is the average

granite density proposed by Telford et al (1976). The susceptibilities used were 25 x 10^{-3} for the metamorphic basement and 43 x 10^{-3} (rationalised system) for the granite. Both these values are within the susceptibility range of the corresponding rocks (Telford et al, 1976). The sediments were treated as effectively non-magnetic. The direction of the magnetisation vector within the different layers was assumed to be the same as the direction of the earth's magnetic field at present.

The final combined gravity and magnetic models of seismic lines 5 and 6 are shown in figures 3/16 and 3/17. The fit between observed and calculated values for both gravity and magnetics is thought to be good for such a simple granite shape, taking into account that no accurate data for the granite's density and the susceptibilities used were available. A constant value of 120nT (DC shift) was removed from the observed magnetic values. The top of the granite is at 2.8km depth in the model of line 6, and 3.5km in line 5 where the magnitude of the anomaly is 60nT less. On both models the granite is 6km thick and its base is at a depth of 9-10km. Because of the very small density contrast between granite and the Old Red Sandstone sediments, the top of the granite cannot be defined more accurately with any degree of reliability. Slight changes in the granite's density will alter the depth to the base of it with no major divergence on the magnetic profiles. The granite in the model of line 5 appears to be wider than in line 6, because line 5 is not perpendicular to the "strike" of the magnetic anomaly while line 6 is. This is the reason for the generally less good fit between observed and calculated magnetic values on the line 5 model.

Another profile has been modelled. It crosses the magnetic anomaly at the same point as line 5 but is perpendicular to its "strike," (line A in figure 3/3). The model along the line A (figure 3/18) indicates again the presence of the granite under the Moray Firth at a depth of 3.5km. It is very similar to the models of lines 5 and 6. The depths to the base of Cretaceous and base of Jurassic for this model have been taken from the depth contour maps constructed for these reflectors.

FIGURE 3/16

Final combined gravity and magnetic model of line C'C'' (along seismic line 5). Identification and density of layers are as follows: K: Cretaceous (2320kg/m^3); J: Jurassic (2440kg/m^3); P: Permo-Triassic (2520kg/m^3); O; Old Red Sandstone (2620kg/m^3); G: Granite (2640kg/m^3).

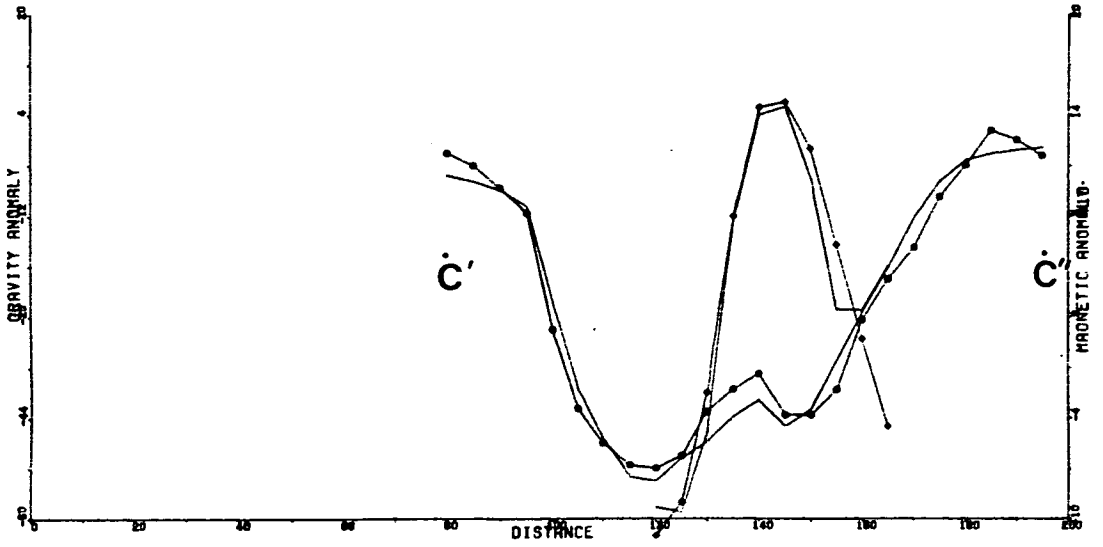

KEY :—— OBSERVED GRAVITY —— OBSERVED MAGNETICS

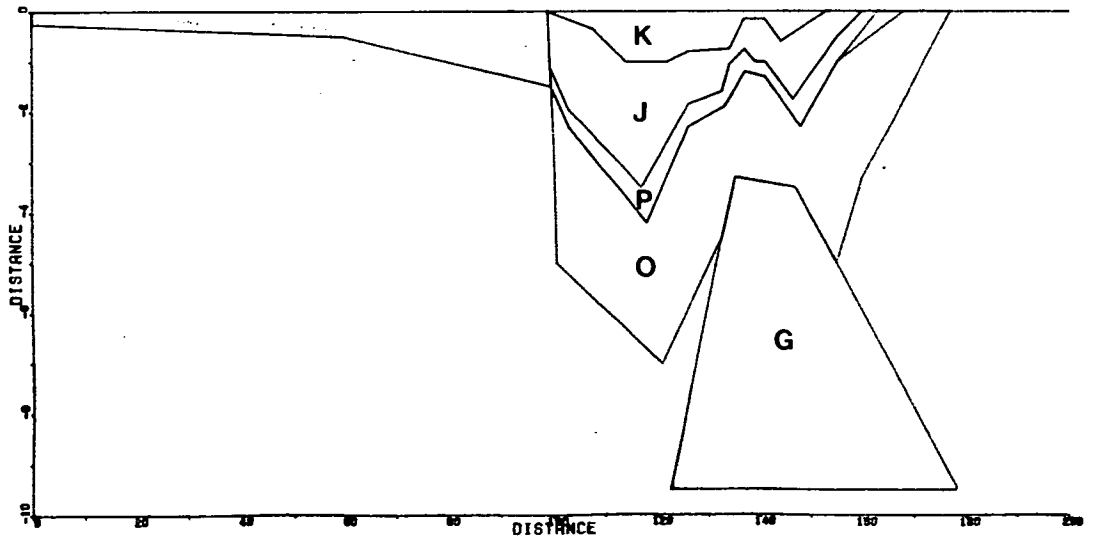

FIGURE 3/17

Final combined gravity and magnetic model of line D'D'' (along seismic line 6). Identification and density of layers are as follows: K: Cretaceous (2320kg/m^3); J: Jurassic (2440kg/m^3); P: Permo-Triassic (2520kg/m^3); O: Old Red Sandstone (2620kg/m^3); G: Granite (2640kg/m^3).

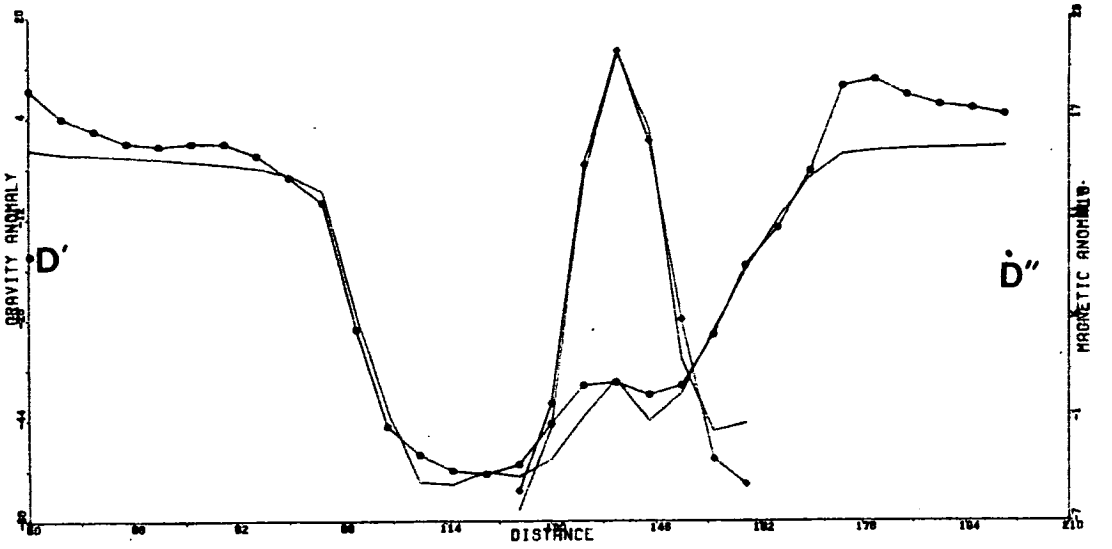

KEY: OBSERVED GRAVITY — OBSERVED MAGNETICS

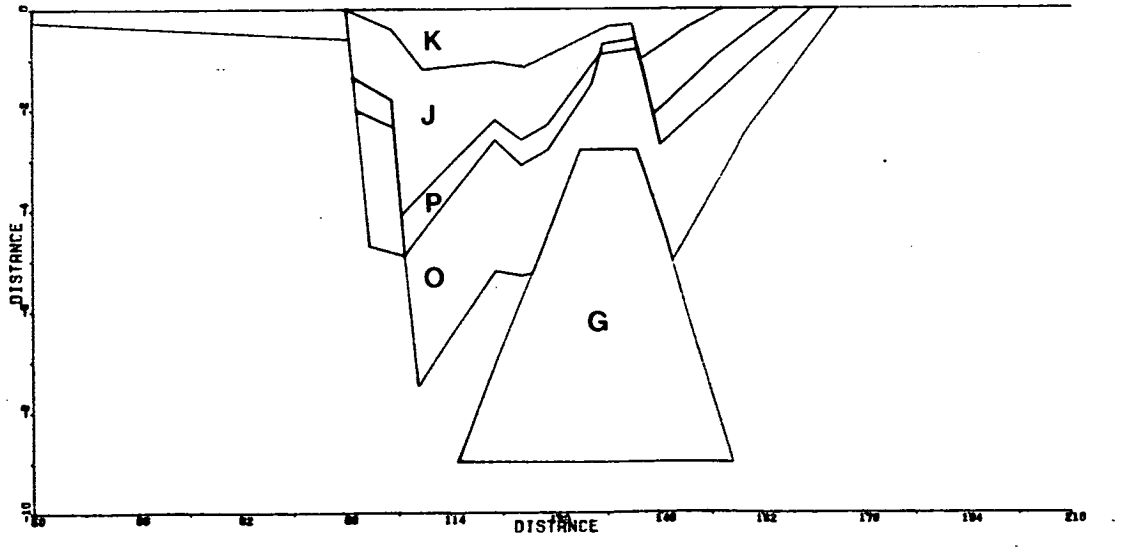

FIGURE 3/18

Final combined gravity and magnetic model of line A'A''. Identification and density of layers are as follows: K: Cretaceous (2320kg/m^3); J: Jurassic (2440kg/m^3); P: Permo-Triassic (2520kg/m^3); O: Old Red Sandstone (2620kg/m^3); G: Granite (2640kg/m^3).

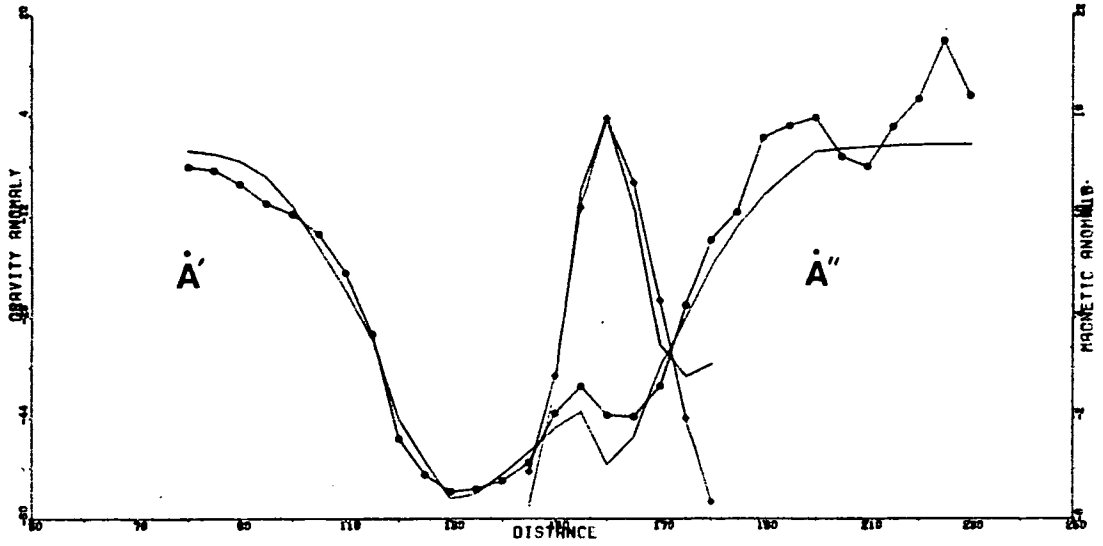

KEY :—— OBSERVED GRAVITY —A— OBSERVED MAGNETICS

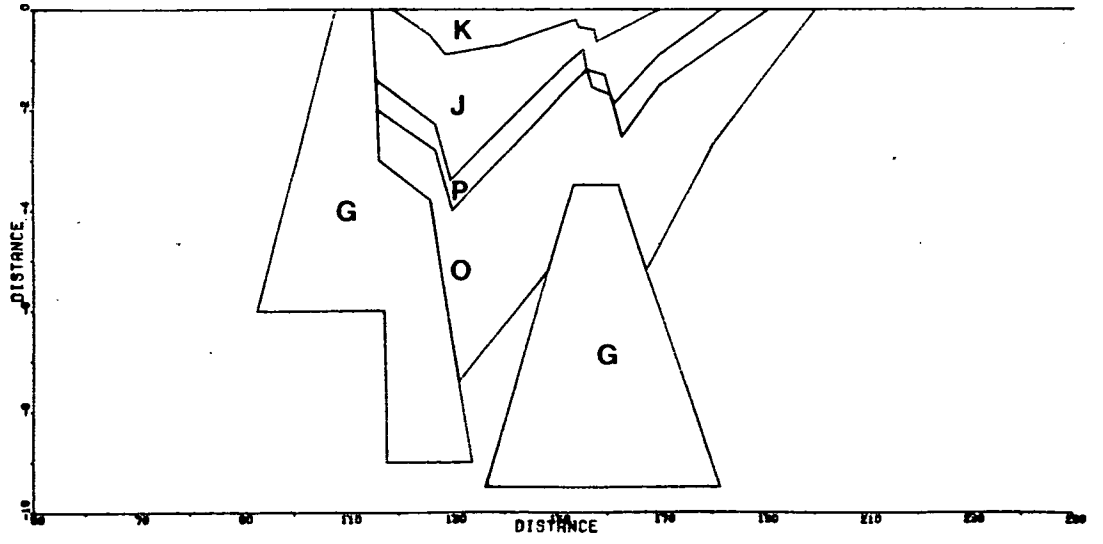

Seismic line 3 was chosen to be modelled because it crosses the part of the basin with the lowest gravity values seen on the residual gravity map (figure 3/11). After the gravity stripping of the Permian-Lower Cretaceous sediments, a gravity anomaly of -42.5mGal remained. It was clear on this occasion that although the remaining gravity low was not associated with a magnetic anomaly closure, it was too large to be attributed to Old Red Sandstone alone. It required more than 12km of these sediments, and the previous models have indicated an average thickness of 3km for this layer. The difference between the expected gravity effect of an Old Red Sandstone layer 3km thick and one 12km thick is about 30mGal, which cannot be attributed to local changes in the basement density or the sediments' density, although it is known that locally onshore Upper Old Red Sandstone with a density of 2300kg/m^3 occurs. The existence of an extensive granite was assumed and the model incorporating it is shown in figure 3/19. The granite is about 12km thick. It rises to only 2km depth near the coast in the Lossiemouth area, thus confirming that the third peak of the magnetic anomalies within the positive magnetic zone running offshore from the Lossiemouth coast is due to another culmination of granite. The granite also seems to be affected by the fault bounding the Central Ridge to the south (at 140km on the model). The fit of the gravity on this model is not as good as in the other models, particularly between 130 and 180km. The simplification of the model, which does not include changes in the Old Red Sandstone thickness due to normal faulting, or density changes within either the granite or the Old Red Sandstone, could produce such differences. On the other hand the fit between calculated and observed magnetic profiles is very good.

3.2.6 Summary

The present work in the Inner Moray Firth Basin has suggested the presence of granite batholiths under the sedimentary cover, thus bridging the interpretations of Collette (1960) and Sunderland (1972). The maximum thickness of the Permian-Lower Cretaceous sediments is suggested to be about 5km and this is more than the previous estimation of 3-4km of Sunderland (1972). The gravity models suggest that the Old Red Sandstone sediments continue beneath the basin having an average thickness of 3km.

FIGURE 3/19

Final combined gravity and magnetic model of line B'B" (along seismic line 3). Identification and density of layers are as follows: K: Cretaceous (2320kg/m^3); J: Jurassic (2440kg/m^3); P: Permo-Triassic (2520kg/m^3); O: Old Red Sandstone (2620kg/m^3); G: Granite (2640kg/m^3).

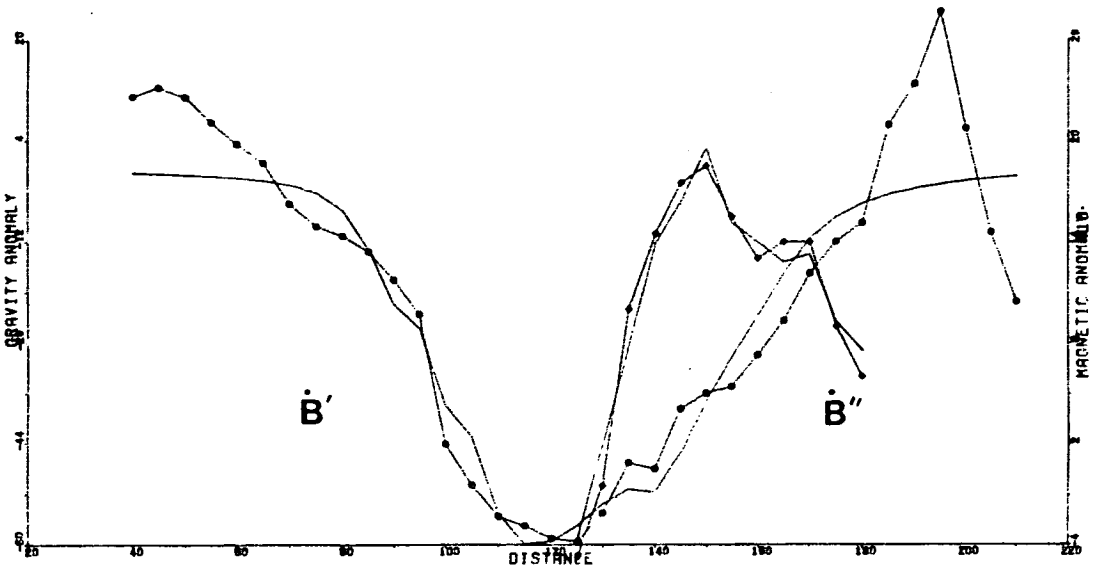

KEY: OBSERVED GRAVITY — OBSERVED MAGNETICS

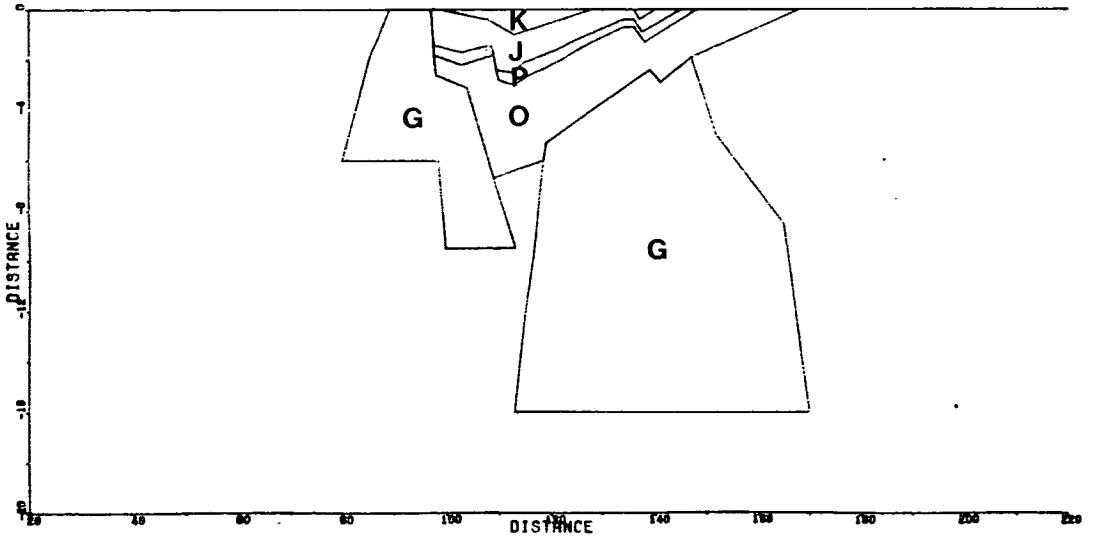

No new results are presented for the detented structure of the Mesozoic fill of the basin, but the disposition of layers is thought to hold significance for the basin's mechanism of subsidence. The relatively uniform thickness of the Jurassic layer on top of the Central Ridge on seismic lines 5 and 6 (Plate I, inside back cover) compared with the significant increase in thickness of the same layer towards the Great Glen Fault, the northwestwards dipping of almost parallel horizons on seismic line 3 followed by a sudden change of these horizons to a sagging shape again towards the Great Glen Fault, the tilted appearance of the Jurassic layer in the south-eastern sub-basin and finally the great difference in throw between the north-western and south-eastern margins of the Central Ridge, all suggest that the basin's area has been subjected to north-westwards tilted movements during the Upper Jurassic-Lower Cretaceous period. This period is characterised by significant normal movements along the major fault lines. The fact that the Jurassic sediments on top of the Central Ridge are thinner than the ones to either side of it, suggest that the ridge was uprising relative to the basin during this period. This uplift is thought to be the result of the buoyant effect of the granite (which underlies the ridge in this region) during a period of crustal tension.

The possibility of the tilted movements of the southern sub-basin being caused by a similar uplift of the Grampian Highlands was considered. Uncertainties in the mid-crustal structure based on LISPB interpretation in the Grampian area led to further investigation of this area described in the following chapter as a means of searching for a possible cause of uplift.

CHAPTER 4

A GEOPHYSICAL INVESTIGATION OF THE GRAMPIAN HIGHLANDS

4.1 Introduction

In the previous chapter it has been shown that the Inner Moray Firth, lying in the same tectonic unit as the Grampian Highlands, is probably underlain by granite batholiths similar to those which crop out in large numbers farther south. The possible relationship of these latter granites to the development of the basin in association with the uncertainty of LISPB experiment results at mid-crustal depths in the Grampian Highlands led to the further investigation of granite batholiths presented in this chapter.

The LISPB (Lithospheric Seismic Profile in Britain) profiles were intended to establish a detailed velocity cross-section which would be useful in solving tectonic problems in the British Isles, in particular, those in the Caledonian orogenic belt. The experiment has been fully described in Bamford et al (1976) and Kaminski et al (1976). The results of the LISPB data interpretation for northern Britain have been described in Bamford et al (1977), Bamford et al (1978) and Assumpcao and Bamford (1978). Here the results of this interpretation in conjunction with regional gravity, magnetic and electromagnetic anomalies over the area are examined and a profile along the LISPB line, modified at mid-crustal depth is proposed.

4.2 Geophysical and Geological Evidence from the Area

4.2.1 Seismic data

The latest model for the crustal structure of northern Britain is shown in figure 4/1. Beneath the superficial layer of low velocity sediments is the layer which represents the metamorphic rocks of the Caledonian belt. In this layer a velocity of 6.0-6.05km/s can be seen below the area of the Grampian Highlands. The depth to the base of the layer in the northern Highlands and the Midland Valley is mainly controlled by the arrival of a P wave phase which has been refracted along the base of this layer. The arrivals of this

FIGURE 4/1

Schematic cross-section through the crust and uppermost mantle along the LISPB line. I: Caledonian belt metamorphics; II: Lower Palaeozoic; III: Pre-Caledonian basement ($v > 6.4$km/s); IV: Pre-Caledonian basement ($v < 6.3$km/s); V: Lower crust; VI: Zone of uncertain relationship between lower crust and uppermost mantle; VII: Upper mantle; VIII: Uncertain structure. Numbers within the layers referred to velocity in km/s. After Bamford et al (1978.

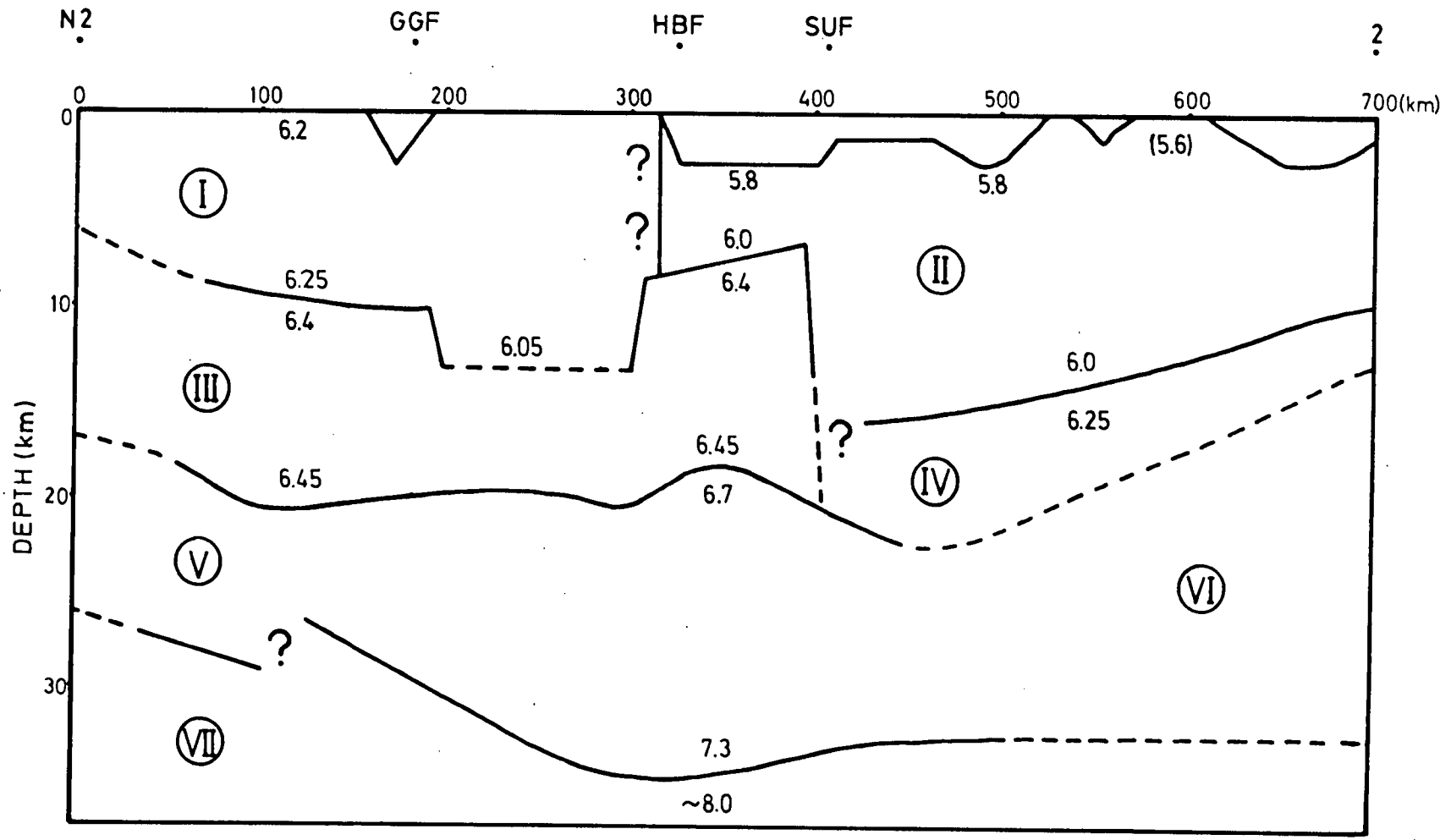
N2
GGF
HBF
SUF
2
0
100
200
300
400
500
600
700(km)
DEPTH (km)
0
10
20
30
6.2
5.8
5.8
(5.6)
I
II
III
IV
V
VI
VII
6.25
6.4
6.05
6.0
6.4
6.0
6.25
6.45
6.45
6.7
7.3
~8.0
?
?
?
?

phase are clearly observed at distances of more than 50km on the profiles 1--→ β (from shotpoint 1 to segment BETA) (Figure 4/2) and E--→ β + α, but degenerate into weaker and delayed arrivals in the region of the Grampian Highlands. According to Bamford et al (1978) this behaviour, and the fact that there is no definite arrival of this phase on the profile 1--→ α, might be caused by a rapid deepening (eg, due to major downfaulting) of the interface which propagates it. This deepening occurs south of the Great Glen Fault and north of the Highland Boundary Fault. The dashed part of this interface (figure 4/1) has been obtained by a ray-tracing program for the weak, delayed and poor quality arrivals within this area, and Bamford et al (1978) suggest that it represents a 'minimum' depth to this interface. The continuation of the pre-Caledonian (Lewisian) basement beneath the Grampian Highlands is based on the observation of the 'Lewisian' velocity of 6.4km/s in arrivals from the Kintail earthquake, which occurred during the LISPB experiment (Kaminski et al, 1976).

4.2.2 Gravity data

Three long gravity profiles have been constructed in order to compare the regional gravity field over the Grampian Highlands with the regional field of the surrounding areas. The three profiles and their positions are shown in figures 4/2 and 4/3.

The first profile (N2-2) is along the LISPB line. It is clear on this profile that there is a considerable decrease of average gravity between the Great Glen and Loch Tay Faults. The mean gravity value between the two faults is -25mGal. The area south of the Loch Tay Fault has a mean gravity value of 0mGal whereas the gravity values north of the Great Glen Fault remain negative for about 50km and then increase steadily until the point N1. The negative values correspond, firstly, to the Old Red Sandstone basin north of the fault (between 160 and 190km) and beyond that the Lairg Granite (between 130 and 160km). The steady increase is due partly to the effect of the Moine Thrust, but mainly to an apparent rapid change in Moho depth (figure 4/1). North of N1 the gravity values decrease due to the effect of the West Orkney Basin Complex and then remain

FIGURE 4/2

Location map of the LISPB and gravity profiles. AB, CD: gravity profiles.
N2, N1, 1, E, 2; LISPB shotpoints.

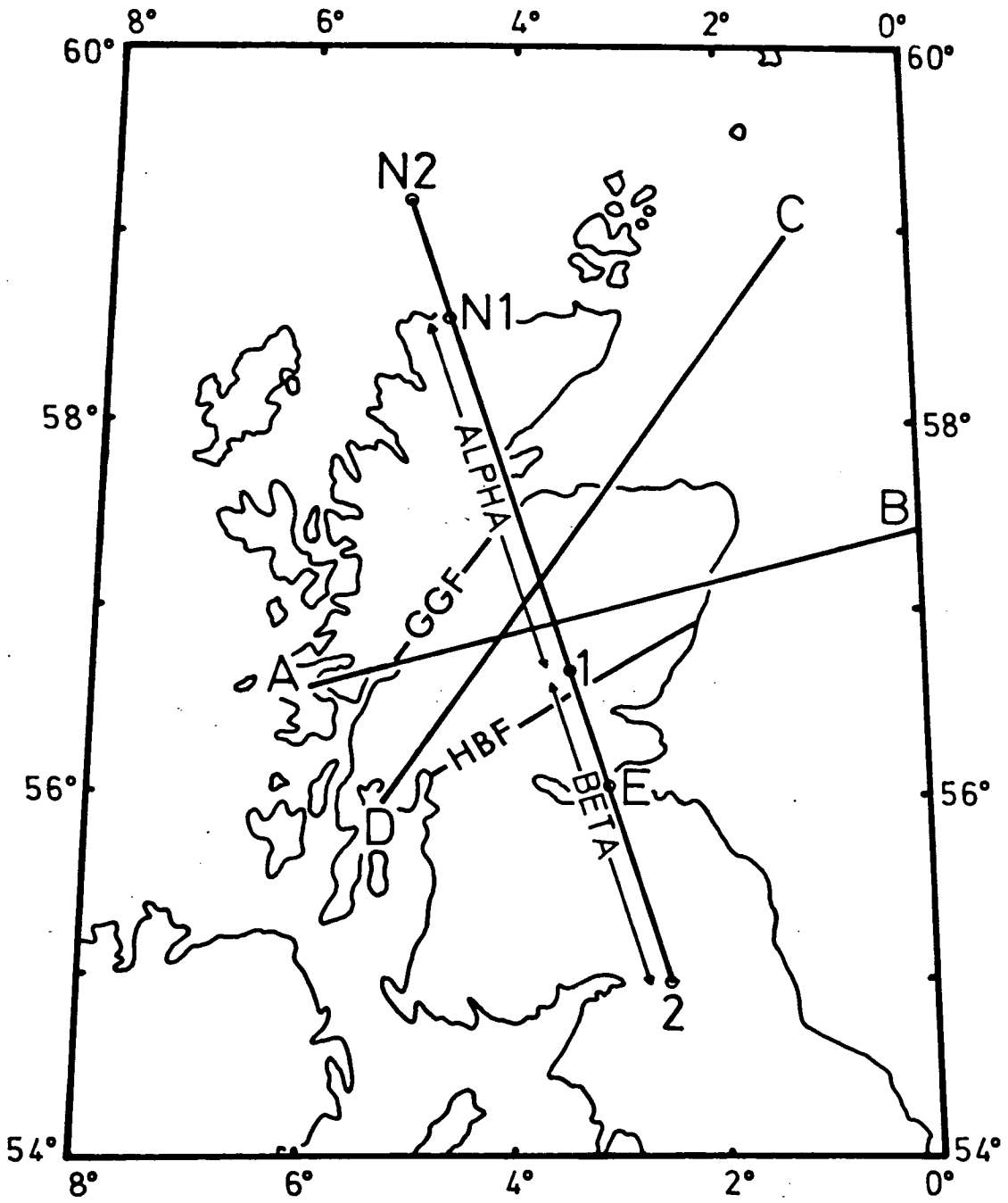
8°
6°
4°
2°
0°
60°
58°
56°
54°
N2
N1
C
B
A
D
E
1
2
ALPHA
BETA
GGF
HBF

FIGURE 4/3

Gravity profiles along the lines N2-2, A-B and C-D (see figure 4/2).

N2, N1, E, 2: LISPB shotpoints.

GGF: Great Glen Fault. LTF: Loch Tay Fault. HBF: Highland Boundary Fault.

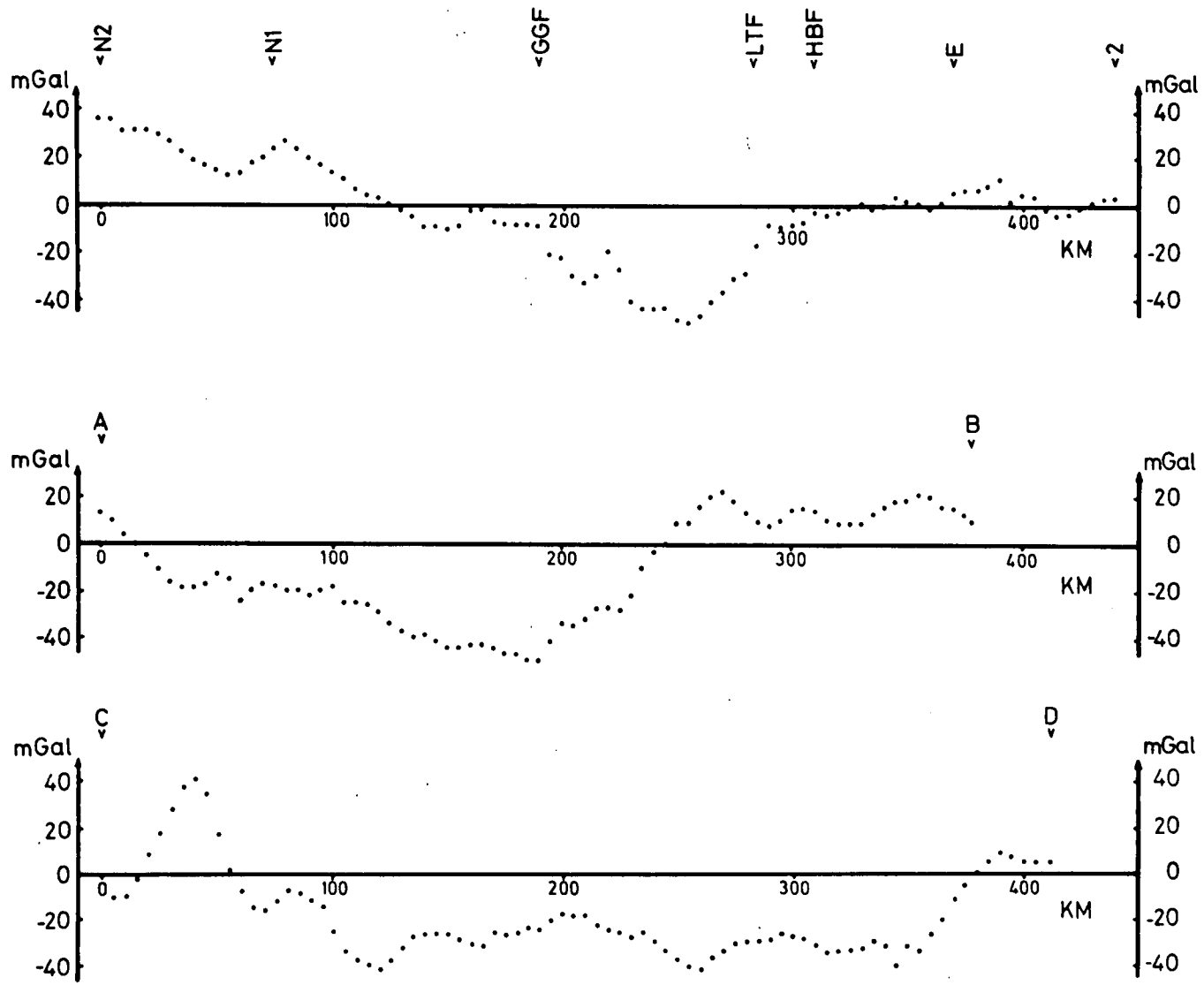
N2
N1
GGF
LTF
HBF
E
2
mGal
40
20
0
-20
-40
0
100
200
300
400
KM
A
B
C
D

stable. Assuming a mean gravity value of +10mGal for the area north of the Great Glen Fault, the Grampian Highlands area then has a mean gravity value of 25-35mGal lower than the areas to the south and to the north.

The second profile (A-B) is perpendicular to the first and crosses the southern part of the Grampian Highlands, avoiding the outcrops of the basin intrusions of the Aberdeenshire region. Again, the mean gravity value in the Grampians is about -30mGal whereas the area east of the coast has a mean value of +10mGal despite the presence of the Palaeozoic and Mesozoic sediments of the North Sea.

The third profile (C-D) is parallel with and south-east of the Great Glen Fault and passes between the outcrops of the large granitic intrusions of the area. The profile crosses the Grampian Highlands and the Moray Firth sedimentary basin. The gravity values over these areas have a mean value of -25mGal. It should be noted here that only part of the gravity low over the Moray Firth Basin can be attributed to the sediments, part of it apparently being due to granitic intrusion (see chapter 3).

4.2.3 Magnetic data

The pattern of the regional magnetic anomalies over northern Britain can be seen on the smoothed aeromagnetic map of Great Britain (Hall and Dagley, 1970). Figure 4/4 shows a simplified geological map of the Grampian Highlands on which the zero countour line from the smoothed aeromagnetic map has been added. It can be seen that the zero contour line south of the Great Glen Fault outlines well the outcrops of the Caledonian granites of the area. North of this zero contour line is a positive magnetic zone which covers a large part of the Grampians area. Anomalies within this zone commonly relate to Caledonian granites. Of the fifteen larger bodies, nine have positive anomalies over them. These are the Strontian, Ben Nevis, Foyers, Monadliath, Cairngorm, Mt Battock, Moor of Rannoch, Mull of Ross and Etive (Hall and Dagley, 1970). In addition to these a connection between the Ben Rinnes Granite and a granite buried under the Moray Firth Basin, inferred from magnetic anomalies,

FIGURE 4/4

Simplified geological map of the Grampian Highlands.
1: Upper Dalradian; 2: Granitic intrusions; 3: Basic intrusions; 4: Sediments (mainly Old Red Sandstone); 5: Moine and Lower Dalradian; 6: Zero magnetic anomaly contour derived from the smoothed aeromagnetic map of Great Britain and Northern Ireland (Hall and Dagley, 1970); 7: Strike slip faults.

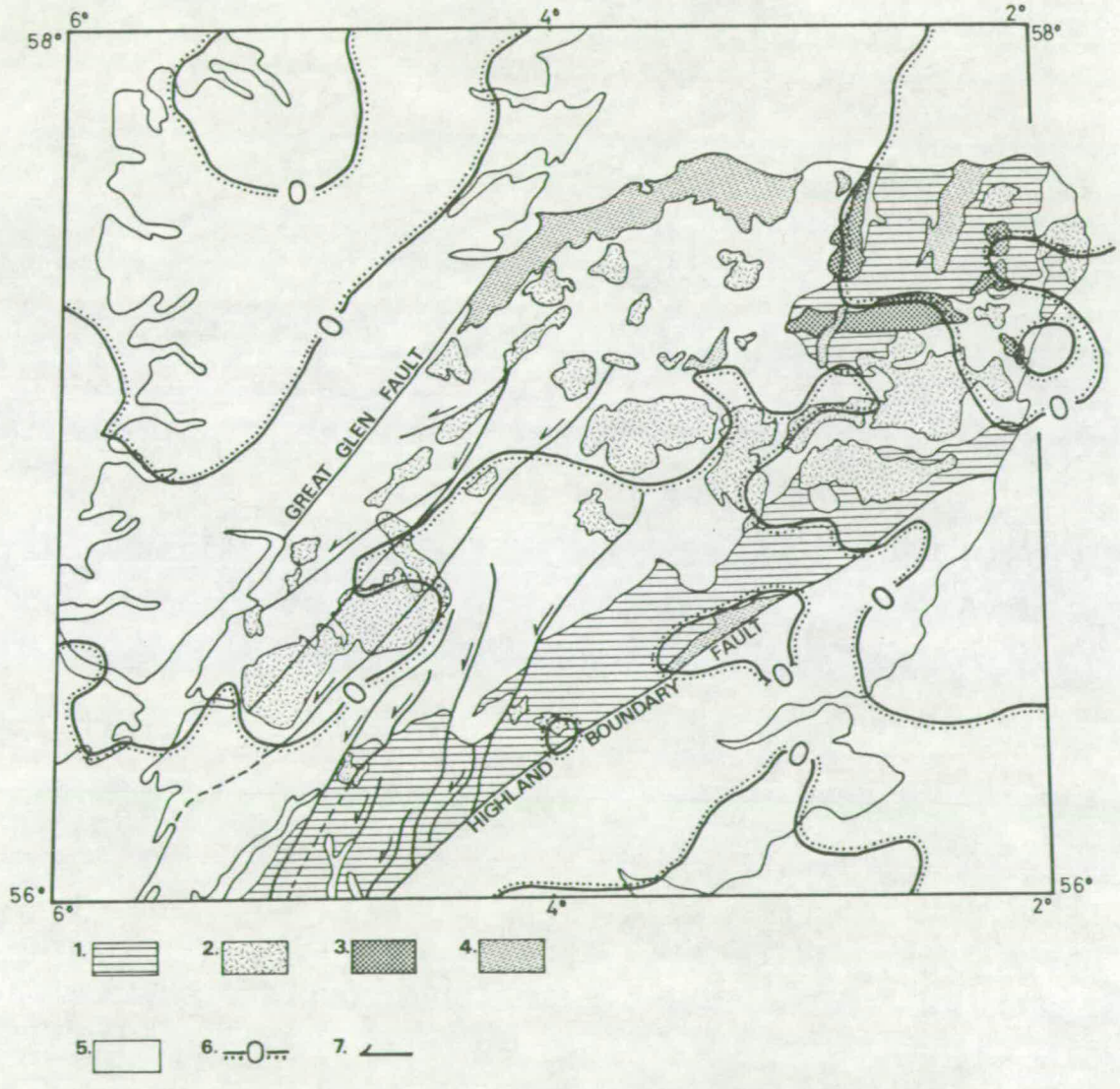
6°
4°
2°
58°
58°
56°
56°
6°
4°
2°
0
0
0
0
0
0
0
GREAT GLEN FAULT
HIGHLAND BOUNDARY FAULT
1.
2.
3.
4.
5.
6.
7.

has been suggested (Flinn, 1969; chapter 3). Hall and Dagley (1970) in three profiles crossing the positive magnetic zone, suggested that this magnetic field could be produced by a normally magnetised sheet-like unit of 9km mean thickness lying at depths varying from 8 to 26km, with an intensity of magnetisation, I = 3 - 4 A/m. This unit is bounded to the north by a vertical plain coinciding with the Great Glen Fault, whereas no boundary to the south has been given.

South of the zero countour line is a negative magnetic zone. This follows the outcrop of the Upper Dalradian which occurs to the south and north-east of the Grampian Highlands (figure 4/4).

4.2.4 Magnetotelluric data

Measurements in the period range 10-1200sec have been made across northern Scotland by E W Mbipom (1980). The preliminary 1-D inversion of the data, along a line parallel and close to the LISPB profile indicates a highly resistive crust (4×10^3-3×10^5 Ω/m) extending to depths of between 5 and 20km in the Grampian Highlands area. This value lies within the resistivity range of 3×10^2-1×10^6 Ω/m for granites (Telford *et al*, 1976). The highly resistive layer is underlain by a less resistive lower crust and upper mantle.

4.2.5 Geological data

The majority of the granitic outcrops of the Grampian Highlands belong to Caledonian granites, which are well known as the 'Newer Granites' or the 'newer igneous rocks'. Brown and Locke (1979) subdivide the Caledonian granites of northern Scotland into two distinctive groups. The first group consists of granites with small gravity and magnetic anomalies. They are pre-Silurian in age, largely syn-tectonic and have isotope ratios consistent with a crustal source of magma, although deeper melt initiation cannot be excluded. They are of small intrusive volume and in the Grampian Highlands are usually found close to the Great Glen Fault and to the north coast of the Buchan area. The second group is

recognised by its association with large negative gravity anomalies caused by large intrusive volumes and, in many cases, significant aeromagnetic anomalies. They are Siluro-Devonian in age and were generated by partial fusion within a subduction zone environment, or within a Caledonian continental underplate.

An implication for the emplacement of the second group of granites is thought to be the formation of the north-east trending faults of the Grampian Highlands (figure 4/4). They are probably the combined result of the uprising magma and the strains produced by displacements along the Great Glen and Highland Boundary Faults. These faults control the transition from the Moinian and Lower Dalradian metamorphic basement in the south of the area. This transition coincides with the southerly limit of the granites which cover 20% of the Moinian-Lower Dalradian area of the Grampian Highlands.

4.3 A Crustal Model for the Grampian Highlands

Summarising the evidence mentioned above, the upper crust in the Grampian Highlands area has the following geophysical characteristics:

1. Low P-wave velocity, thus explaining the delayed arrivals of the seismic waves within the area;

2. lower density than the adjacent layers, to account for the area's regional gravity field of -25mGal;

3. high resistivity, according to the magnetotelluric data;

4. fairly strongly magnetised, to explain the broad positive magnetic zone seen on the smoothed aeromagnetic map;

5. inhomogeneous composition so that seismic waves travelling through it scatter a high percentage of their energy by multiple reflections and refractions.

All these considerations are consistent with the presence of abundant granitic intrusions in the upper crust of the area as is suggested from the solid geology map. These outcrops are probably only the surface expressions of massive plutons occurring extensively throughout the upper crust. In order to check this possibility against the existing evidence, a 2-D crustal model along the LISPB line was constructed with a granitic layer beneath the Grampians. The model, which is a combined ray-tracing, gravity and magnetic one, is shown in figure 4/5.

4.3.1 Ray-tracing model

The only waves to travel through the total thickness of the granitic layer are those generated in the Firth of Forth (shotpoint E, figure 4/2) and reflected from the Moho (phase 'c' in Bamford *et al*, 1978). The actual travel times for these arrivals within the Grampian Highlands, corrected for the topographic effect, were taken from Assumpcao (1978). An average P wave velocity for each layer in the model was taken from Bamford *et al* (1978) and for the granitic layer a velocity of 5.85km/s was assumed.

Accepting that the interface at 20km depth is well defined from the LISPB data, the granitic layer was located above this level. Using a straight-line ray-tracing program a thickness of 10-12km for the granitic layer gives a very good agreement between observed and calculated travel times for the above mentioned arrivals.

4.3.2 Gravity model

Using the vertical thickness derived from the ray-tracing program, a gravity model was attempted. The densities used are shown on the model and are consistent with the density-velocity curve of Nafe and Drake (1963) for the LISPB velocities. For the granitic layer an average density of 2640kg/m^3 was used (Telford *et al*, 1976).

The model indicates a 12km thick granitic layer at depths from 7 to 19km. The lateral extent of this layer seems to be controlled by the Great Glen Fault to the north and the Loch Tay Fault to the south.

FIGURE 4/5

Proposed generalised model along the LISPB line. The numbers within the layers represent the densities in kg/m^3, used in the gravity program. (N2), (2): LISPB shotpoints.

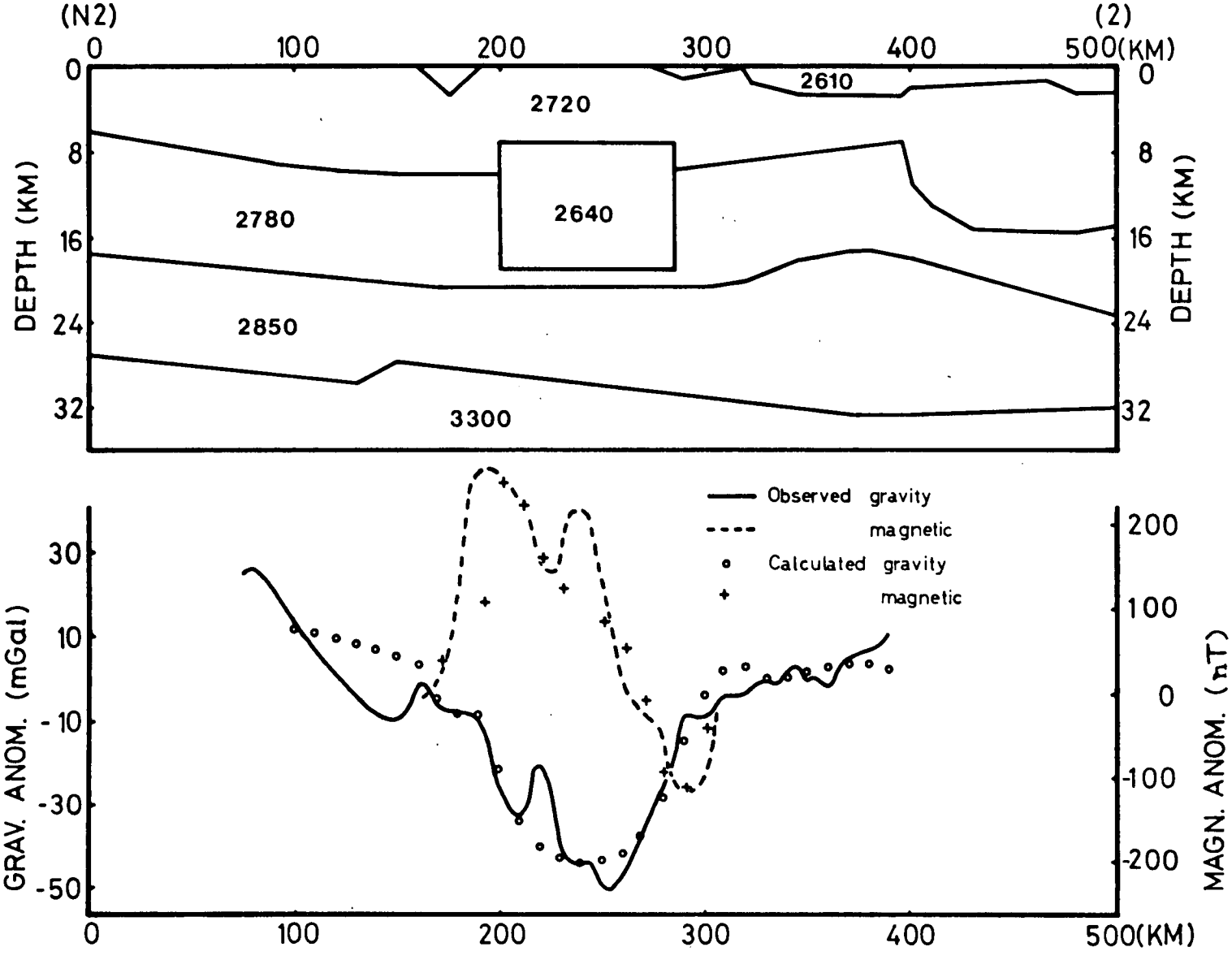
(N2)
(2)
0
100
200
300
400
500(KM)
2610
2720
2780
2640
2850
3300
DEPTH (KM)
8
16
24
32
Observed gravity
magnetic
Calculated gravity
magnetic
GRAV. ANOM. (mGal)
30
10
-10
-30
-50
200
100
0
-100
-200
MAGN. ANOM. (nT)

Between these two faults the calculated mean gravity value is -25mGal with respect to surrounding areas, and is comparable with the observed anomaly.

4.3.3 Magnetic model

Only regional magnetic effects can be attributed to a granitic layer lying deep in the crust. Thus a magnetic profile from the smoothed aeromagnetic map was constructed and a match of this profile was attempted using the model as defined by the gravity program. In order to simplify the model only a uniform intensity magnetisation contrast between the granitic layer and the surrounding basement was used. The best fit between observed and calculated values was obtained when a total magnetisation vector $\vec{M}_T$ of -150nT magnetisation contrast between granite layer and surrounding rocks was assumed (M_T = -150nT) and of a direction of -10° inclination (I_T = 10°, positive downwards) and +20° declination (D_T = +20°, positive eastwards). The inclination and declination of $\vec{M}_T$ were defined with an accuracy of ±5°.

In order to compare the obtained total magnetisation vector $\vec{M}_T$ with the present day's magnetic field direction and palaeopoles known from palaeomagnetic data, a method of projecting different possible directions of the remanent magnetisation vector ($\vec{M}_R$) on the globe and comparing the projections to the palaeopoles was developed. The method, a computer program written to describe how to execute the calculations and the comparison of the above mentioned total magnetisation vector to the known palaeopoles are all described in Appendix II. The comparison suggests that the layer should be of Siluro-Devonian age and that it has an average susceptibility of 9500 x 10^{-6} (rationalised system) and a Koenigsberger ratio Q of 2.24. The latter value means that the remanent magnetisation of the layer is more than double the induced magnetisation. This contradicts the measured values from samples of 6 x 10^{-6} for the remanent and 815 x 10^{-6} (rationalised system) for the induced magnetisation of the Cairngorm Granite (Brown and Locke, 1979). Brown and Locke suggest that this difference may be explained either by differentiation of the magma, changing its composition with depth, or by a change of magnetisation due to contact metamorphic effects in the basement around the plutons.

4.4 Discussion

It must be emphasised that the model in figure 4.5 does not take into account the granite bosses which crop out at the surface (see Brown and Locke, 1979, for details of the geophysical anomalies of these bosses). It only suggests the probable continuous presence of granitic material at mid-crustal depths. The model is best thought of as indicating that an average thickness of approximately 12km of this material exists between the surface and about 20km depth. The existence of granitic plutons at depth explains the low regional gravity over the area. It also explains the scattering of the seismic waves travelling through the area as well as the weak arrivals of little horizontal persistence, observed on some stations of the LISPB experiment (Bamford et al, 1978) since these waves would have been reflected or refracted at the top of the granitic plutons. The model also explains the positive regional magnetic field over the area.

The tectonic implications of the granitic plutons are significant. It is believed that huge volumes of magma of the second group of granites (Siluro-Devonian in age) rose up and once solidified, their buoyant effect produced an uplift and northerly tilt of the whole Grampian area. The boundaries of the uplifted area are thought to be the Great Glen Fault to the north and the Highland Boundary Fault to the south, which existed as major transcurrent faults by the time of the uplift. Through a similar mechanism, it is suggested that a similar uplift of the Southern Uplands area was taking place at the time (Lagios, 1979). The combined effect of these uplifts may have resulted in the initiation of the Midland Valley graben. The contemporaneous accumulation of sediments in the developing valley and the buoyant effect of the granites, reinforced by the erosion of their overlying rocks, probably encouraged the subsidence of the Midland Valley during the Devonian and Carboniferous. The buoyant effect of the granites may well have been present throughout the geological history of the area (see page 2), but was probably most effective during tensional regimes (Bott et al, 1978), for example during the Carboniferous as just discussed and during the Mesozoic when the Inner Moray Firth Basin was developed.

CHAPTER 5

THE GEOLOGY OF THE ST GEORGE'S CHANNEL AREA

5.1 Introduction

This chapter, like the chapter for the Moray Firth Basin, presents a brief summary of geological information known for the St George's Channel Basin area. This basin has generally been examined together with its north-eastern extension, the Cardigan Bay Basin, and this approach is maintained in the summary presented here.

The first author to predict that a Triassic basin would be found beneath Cardigan Bay was O T Jones (1952, 1956), who based his argument on the radial drainage of Wales towards the Bay, the shape, dimension and orientation of which are closely similar to the Triassic filled Cheshire Basin. Blundell et al (1968) reported briefly on the findings of seismic and gravity surveys across Cardigan Bay and St George's Channel, made by the University of Birmingham between 1965 and 1967. The survey revealed the presence of a long (120km) and narrow (30km) basin beneath the St George's Channel-Cardigan Bay area. An estimated maximum sediment thickness in the basin of 3500 to 6700m was suggested, the estimation being based on the gravity anomaly over the area and observed seismic refraction velocities. A shallow unconformity was traceable throughout the area surveyed. The strata below the unconformity were slightly folded and the top 100m of these sediments in the Cardigan Bay area were thought to be of Mesozoic or early Tertiary age.

A deep reflection seismic survey of the area, carried out in 1968 for the Institute of Geological Sciences, confirmed the existence of a deep sedimentary basin and for the first time it was suggested that salt tectonic features were present in the south-western part of the area (Bullerwell and McQuillin, 1969). In a full report of the interpretation of the geophysical data collected by Birmingham University between 1964 and 1969 (Blundell et al, 1971) the infill of the basin beneath Quaternary deposits in the Cardigan Bay and

beneath both Quaternary and Tertiary deposits in St George's Channel areas was thought to be of Mesozoic age. This age interpretation was based on refraction velocities and the reflective character of the strata as well as comparison of these characteristics with those of neighbouring areas of better established geological knowledge. Notably, Blundell et al concluded that the Upper Cretaceous Chalk of the Nymphe Bank, south of Ireland, did not extend into the Cardigan Bay. Subsequently, Dobson et al (1973) on the basis of additional seismic and gravity data collected by the University of Wales, Aberystwyth, and the results of the Institute of Geological Sciences (IGS) sea-floor coring programme, re-examined the earlier surveys and refined the structural interpretation of the area. They also reassessed the stratigraphic identification of the seismic horizons, and whilst agreeing with the inferred Jurassic-Triassic component of the basin fill, they postulated the additional presence of chalk and possibly Lower Cretaceous beds in the St George's Channel region.

The first deep offshore well in the basin, 106/24-1, was drilled by Arco Oil Producing Inc in 1974, following a growing interest in the hydrocarbon prospects of the area. The results were geologically interesting, although economically disappointing, showing 155m of Quaternary, 535m of Tertiary and 2000m of Middle and Upper Jurassic, the well ending within Bajocian strata at 2775m depth. Subsequently, other wells were drilled by Hydrocarbons Great Britain (HGB)/Denimex (well 106/28-1), Texaco/HGB (well 103/2-1) in 1977 and HGB (well 107/21-1) in 1978. The position of these wells and their stratigraphic correlation are shown in figures 5/6 and 5/2. Based on information from these wells and commercial deep seismic surveys in the area between 1971 and 1977, Barr et al (1981) presented an up-to-date account of the geology of the area. This paper, unless otherwise stated, is the source of information for this chapter. In brief, it is seen that a Triassic-Jurassic succession is overlain directly by Tertiary or younger strata.

5.2 Stratigraphy of the Basin

5.2.1 Pre-Permian

The only well which encountered formations older than the Triassic

FIGURE 5/1

Simplified solid geology map of the St George's Channel Basin. After Whittington et al (1981).

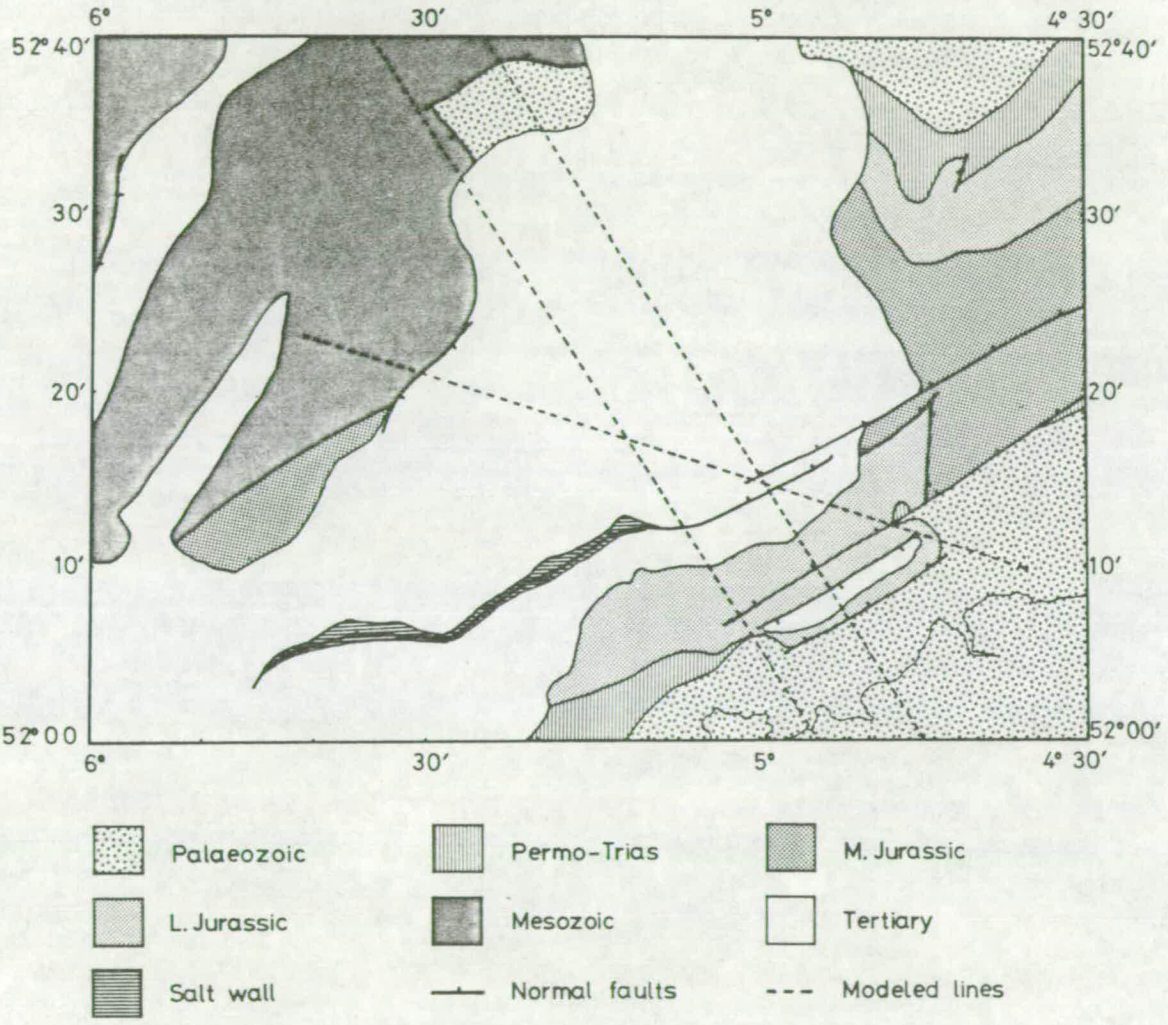
6°
30′
5°
4° 30′
52°40′
30′
20′
10′
52°00
Palaeozoic
Permo-Trias
M. Jurassic
L. Jurassic
Mesozoic
Tertiary
Salt wall
Normal faults
Modeled lines

is the well 103/2-1, which is the westernmost well along the southern margin of the basin. It was terminated in Upper Carboniferous Coal Measures (Barren Red Measures) of Westfalian D age. Carboniferous strata are known to occur around the margin of the basin; for example to the north of the basin they occur in Anglesey, on the adjacent Welsh mainland along the trend of the Dinorwic Fault system and north of the Lleyn Peninsula in the IGS sea floor core 71/53. To the south of the basin Carboniferous strata occur in a syncline surrounded by Palaeozoic rocks of the Pembrokeshire massif, whilst farther away to the south-east there is the full Carboniferous succession of the South Wales coalfield. Barr et al (1981), based on the distribution of Carboniferous outcrops around the basin and the fact that the deep seismic records indicate a depth of some 10,000m in the centre of the basin, suggest that much of the basin may have a pre-Permo-Triassic floor of Carboniferous, including Coal Measures. This however contradicts up-to-date palaeogeographic reconstructions of the area during Carboniferous times, which indicate an elevated landmass (St George's Landmass, Wales-Brabant Landmass) covering the area during much of the Carboniferous (for further details see: Anderton et al, 1979. "A Dynamic Stratigraphy of the British Isles," the chapter on the Carboniferous).

Older, Lower Palaeozoic and Precambrian formations make up the surrounding Welsh borderlands and extend into the offshore areas as St Tudwal's Arch, the continuation of the Lleyn Peninsula, and as the Cardigan coastal shelf along the south-eastern margin of the basin (sub-Pleistocene geology map of the British Isles, inside back cover). In the case of St Tudwal's Arch the Permo-Triassic sediments onlap onto the Palaeozoic basement ridge, whilst to the south and east the Permo-Mesozoic formations appear to be always in fault contact with the older basement rocks (Barr et al, 1981). These older basement rocks are of Silurian or Ordovician age. The Irish Sea Geanticline to the north-west of the basin, probably consists of Cambrian and Precambrian rocks, similar to those occurring in North Wales and Anglesey, covered by thin Mesozoic sediments. This is indicated by the similarity of the magnetic anomaly pattern over these areas. Palaeozoic and Precambrian

rocks are often associated with intrusive and volcanic rocks.

5.2.2 Permo-Trias

Rocks of established or inferred Triassic age have been reported from the lowermost interval of the Mochras borehole (Woodland, 1971), from the IGS sea floor sample stations 71/47 and 71/55 on the extension of the Lleyn Peninsula, and in offshore wells 103/2-1 and 106/28-1. The latter two wells contain the most complete Triassic succession so far found in the basin, ranging from Rhaetian to Middle Triassic. Rhaetic beds (up to 51m) in the wells consist of claystones with occasional sandstone. Below them 455m of claystone with traces of anhydrite represent the "Upper Keuper Shales." These are underlain by up to 825m of anhydritic mudstones interbedded with layers of halite up to some 20m in thickness, equivalent to the "Keuper Saliferous Beds." On average halite layers amount to 35% of the sequence. These in turn are underlain by up to 580m of mudstones, representing the "Lower Keuper Shales," generally similar to the beds above the saliferous unit. The saliferous beds may have been the origin of the salt for the intrusive structures west of Strumble Head on the southern margin of the basin (figure 5/1). However, seismic evidence suggests the possibility of a deeper salt section within the Permo-Trias (Barr et al, 1981). The lowermost beds in the wells consist of sandstone and anhydritic mudstones, which are inferred to be of Middle Triassic age. In well 103/2-1 some 249m of this unit were penetrated resting unconformably on older formations. The total thickness of Triassic rocks penetrated in the wells amounts to 2025m, which represents only the Upper to Middle Trias. The extent to which Lower Triassic and Permian deposits, comparable to those of the Cheshire and Irish Sea Basins, may occur in Cardigan Bay remains speculative. However, it is quite possible that some representatives of these may be present in the deeper, axial parts of the basin. (Barr et al, 1981.)

5.2.3 Jurassic

Strata of Middle and Lower Jurassic age subcrop below the Recent and Pleistocene deposits over the inner parts of Cardigan Bay

(Penn and Evans, 1976) as seen in figure 5/1. The results from deep wells (figure 5/2) show that farther westward, along the basin axis, the Upper Jurassic appears and the Middle Jurassic section thickens dramatically. The thickest well section of Jurassic sediments is that of well 106/24-1, in which all the stages from Lower Purbeckian to Bajocian are represented and have a total thickness of just under 2000m. If we assume that the thickness of Lower Jurassic is similar to the Lias of the Mochras borehole (1305m), then a thickness of 3800m or more for the whole Jurassic is indicated. This is considerably in excess of the maximum known thickness of some 1500m for the Jurassic of the British land area (Bennison and Wright, 1969), and moreover, exceeds that so far reported in the North Sea Jurassic province (Brooks and Chesher, 1975, various authors in Woodland, 1975).

Upper Jurassic: The presence of Upper Jurassic in the deeper, western parts of the Cardigan Bay-St George's Channel Basin had been postulated on the basis of the seismic survey data (Blundell et al, 1971, Dobson et al, 1973) and was confirmed by the results of the deep wells 106/24-1 and 107/21-1. The total thickness of the section in well 106/24-1 is 1498m, which compares with a thickness of some 800m in the Isle of Purbeck, the thickest known section on land. The lithologies are mainly shales and mudstones. The shales are anhydritic in places. The depositional environments range from lagoonal, brackish, locally restricted (anhydrite deposition) to marginal marine. The sequence becomes increasingly marine towards the base of the formation (Oxfordian and Callovian times).

Middle Jurassic: Both the Bathonian and Bajocian subdivisions of the Middle Jurassic are represented in the basin. In well 107/21-1 a complete Bathonian-Bajocian section is encountered with a total thickness of 963m. This thickness bears out the earlier estimation of Penn and Evans (1976) of 850m for the sequence in the vicinity of St Tudwal's Arch, and is the thickest known in the British Isles. The lithology consists mainly of shales interbedded with limestone layers that were deposited in a shallow marine environment. The Bajocian sandstones and interbedded mudstones in wells 106/24-1 and 107/21-1, appear to be marine in origin, although in the absence of cores, no more precise depositional environment can be attributed.

FIGURE 5/2

Stratigraphic correlation diagram of the exploration wells in the St George's Channel Basin, the geological section based on IGS sea-floor sampling data (Penn and Evans, 1976), and the Llanbedr (Mochras) borehole. After Barr et al (1981).

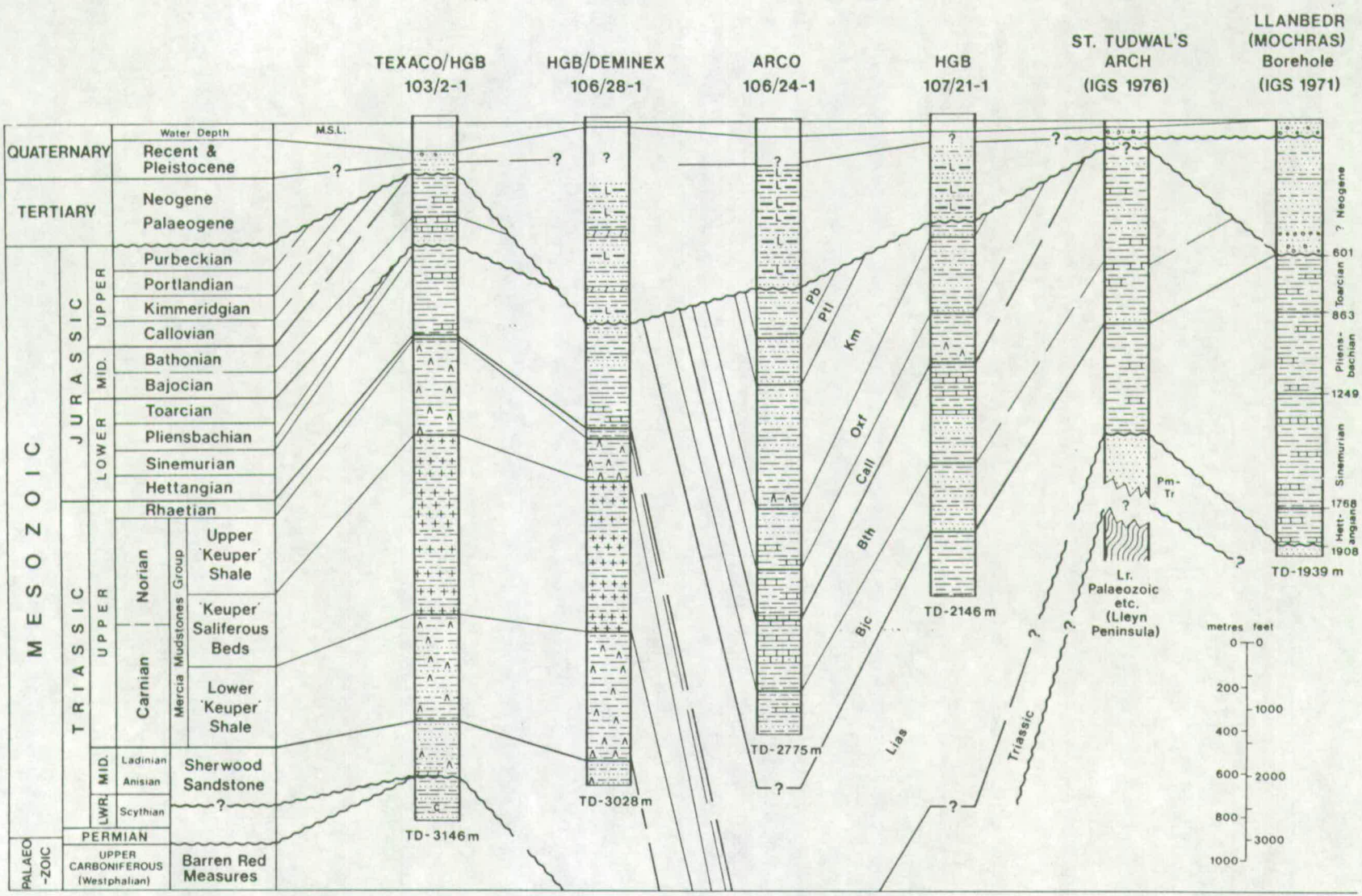
TEXACO/HGB 103/2-1
HGB/DEMINEX 106/28-1
ARCO 106/24-1
HGB 107/21-1
ST. TUDWAL'S ARCH (IGS 1976)
LLANBEDR (MOCHRAS) Borehole (IGS 1971)
Water Depth
M.S.L.
QUATERNARY
Recent & Pleistocene
TERTIARY
Neogene
Palaeogene
MESOZOIC
JURASSIC
UPPER
MID.
LOWER
Purbeckian
Portlandian
Kimmeridgian
Callovian
Bathonian
Bajocian
Toarcian
Pliensbachian
Sinemurian
Hettangian
Rhaetian
TRIASSIC
UPPER
Norian
Carnian
Mercia Mudstones Group
Upper 'Keuper' Shale
'Keuper' Saliferous Beds
Lower 'Keuper' Shale
MID.
Ladinian
Anisian
LWR.
Scythian
Sherwood Sandstone
PERMIAN
PALAEO-ZOIC
UPPER CARBONIFEROUS (Westphalian)
Barren Red Measures
TD-3146m
TD-3028m
TD-2775m
TD-2146m
TD-1939 m
Pb
Ptl
Km
Oxf
Call
Bth
Bjc
Lias
Triassic
Pm-Tr
Lr. Palaeozoic etc. (Lleyn Peninsula)
? Neogene
Toarcian
Pliens-bachian
Sinemurian
Hett-angian
601
863
1249
1768
1908
metres feet
0 0
200 1000
400
600 2000
800
1000 3000

Lower Jurassic: The best documented sequence for the Lower Jurassic (Lias) is that encountered in the Mochras borehole. The sequence is represented by 1305m of siltstones and mudstones, thin limestone bands and is the thickest Liassic sequence known anywhere in Britain (Woodland, 1971). The thick sequence is wholly marine, but still probably of a fairly shallow shelf environment. Offshore the Lias is present in wells 103/2-1 and 106/28-1, where it is represented by 393 and 482m of section respectively. There are also some 290m of Lias in well 107/21-1. The lithologies in the wells are mainly argillaceous and comparable to those described in detail in the Mochras borehole (Woodland, 1971), being of similar open marine facies type, although probably not of a deep water environment. Based on the seismic data, the Lias along the basin axis would be expected to maintain and possibly exceed the thickness of the Mochras borehole. The abrupt change in lithology, from the argillaceous Lias to the arenaceous and dolomitic beds at the top of the underlying Trias, along with the fact that sedimentation at the base of the Lias is condensed, suggests an interval of non deposition and erosion prior to the Liassic marine incursion (Barr et al, 1981).

5.2.4 Quaternary and Tertiary

A thin layer of Recent and Pleistocene (glacial) deposits cover the entire area. The recent sediments include muds, sands and gravels, locally up to some 50m in thickness. The Pleistocene consists of glacial till of varying composition from stiff boulder clays to outwash gravels.

The Tertiary sequences are assumed to include representatives of the Neogene and Paleogene, although only the latter has been positively identified. The Tertiary of the Mochras borehole is thought to be of Neogene age (Woodland, 1971), but elsewhere the presence of Neogene is uncertain. Blundell et al (1971) have assigned the uppermost horizontally stratified layers recorded by sparker surveys (layer 1 in Blundell et al, 1971) as being of Neogene age. These surveys also indicate an angular unconformity inferred to be the Neogene-Paleogene boundary. This unconformity is better seen on the

deep seismic record of IGS line 6 (figure 5/3). Dobson et al (1973) on the other hand have interpreted this unconformity as the boundary between Chalk and Paleogene (figure 5/4).

In the deep offshore wells, the uppermost parts of the borehole are not usually logged and sampled so that stratigraphic identification is not possible. Thus in the wells, the upper 150 to 200m of the Tertiary section may be of Neogene age, but the major part of the sequence (some 700m) is of Paleogene age, consisting of a varied sequence of shelf deposits.

As evidenced in all the wells the Tertiary rests with marked unconformity on the older formations, and perhaps one of the more important results is that the underlying Mesozoic is of Jurassic age. This does not necessarily mean that the entire Cretaceous is absent as Barr et al (1981) propose. A look at figures 5/6 and 5/7 reveals that the wells are located on the south-east flank of the basin. Seismic line 6 (figure 5/3) and the interpretation of its western end by Dobson et al (1973) (figure 5/4) reveal also a change in the character of the unconformity from angular on the flanks of the basin to a disconformity followed by a considerable sagging towards the centre of the basin. The preservation of younger Mesozoic sediments towards the axis of the basin is apparent from a comparison of wells 106/24-1 and 107/21-1. In well 106/24-1 which is closer to the axis of the basin than well 107/21-1, youngest Mesozoic rocks are of Lower Kimmeridgian age. Extrapolating towards the basin's axis and taking into account the quite high sedimentation rate during the Upper Jurassic (55m/My in well 106/24-1) and the known deposition of Lower Cretaceous sediments farther south, it is suggested here that sediments of Cretaceous age should be present along the axial parts of the basin. This suggestion is in agreement with the change in the unconformity's character mentioned above (figure 5/4). The strong reflector above the angular unconformity, referred to as "Base Chalk" in the same figure, is thought to represent an early Tertiary event.

FIGURE 5/3

IGS deep seismic reflection line 6. Section is shown in two parts running from the west (left side) to east (right side). See figure 6/3 for location.

LINE 6

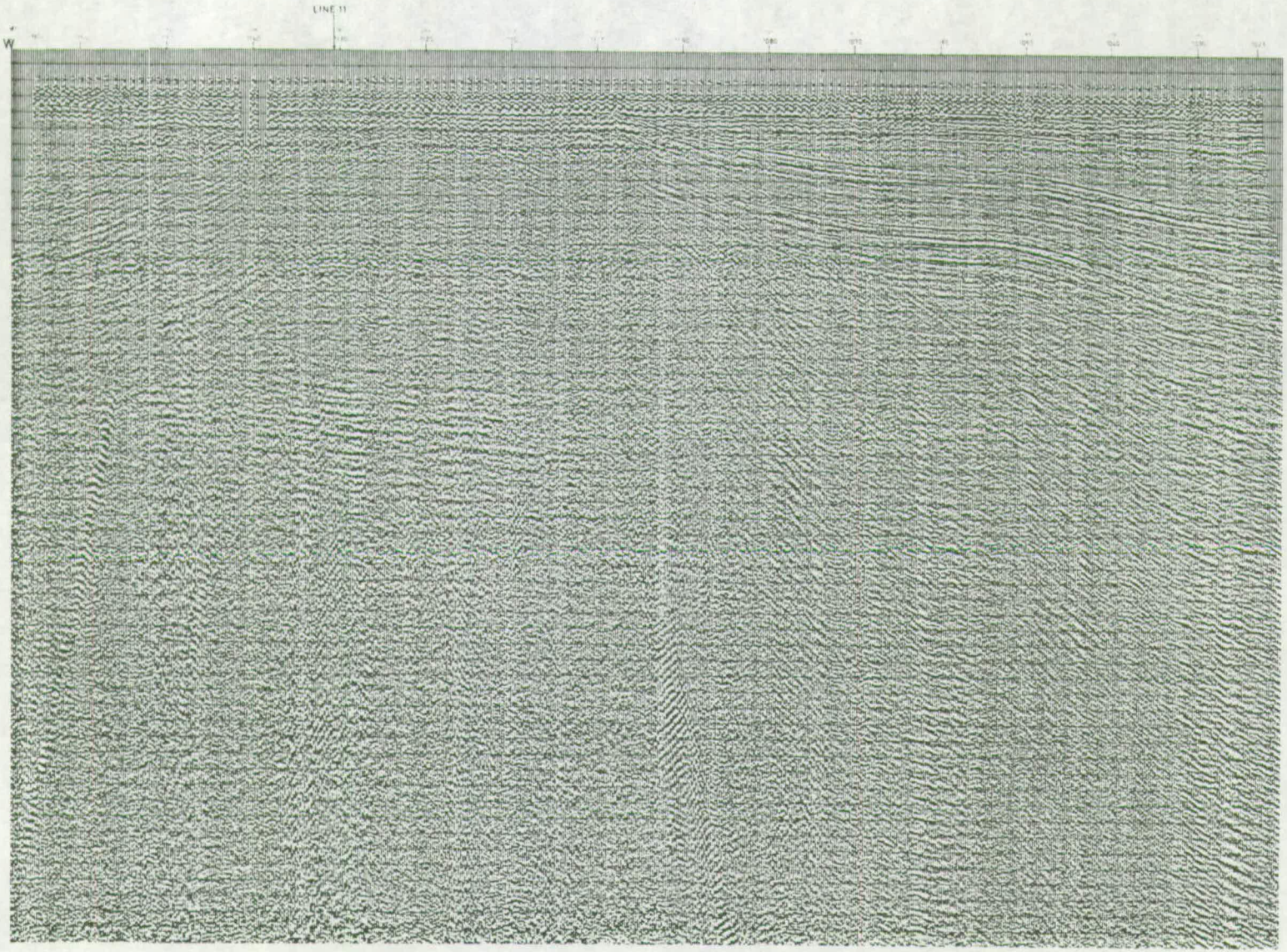

BREAK IN SHOOTING

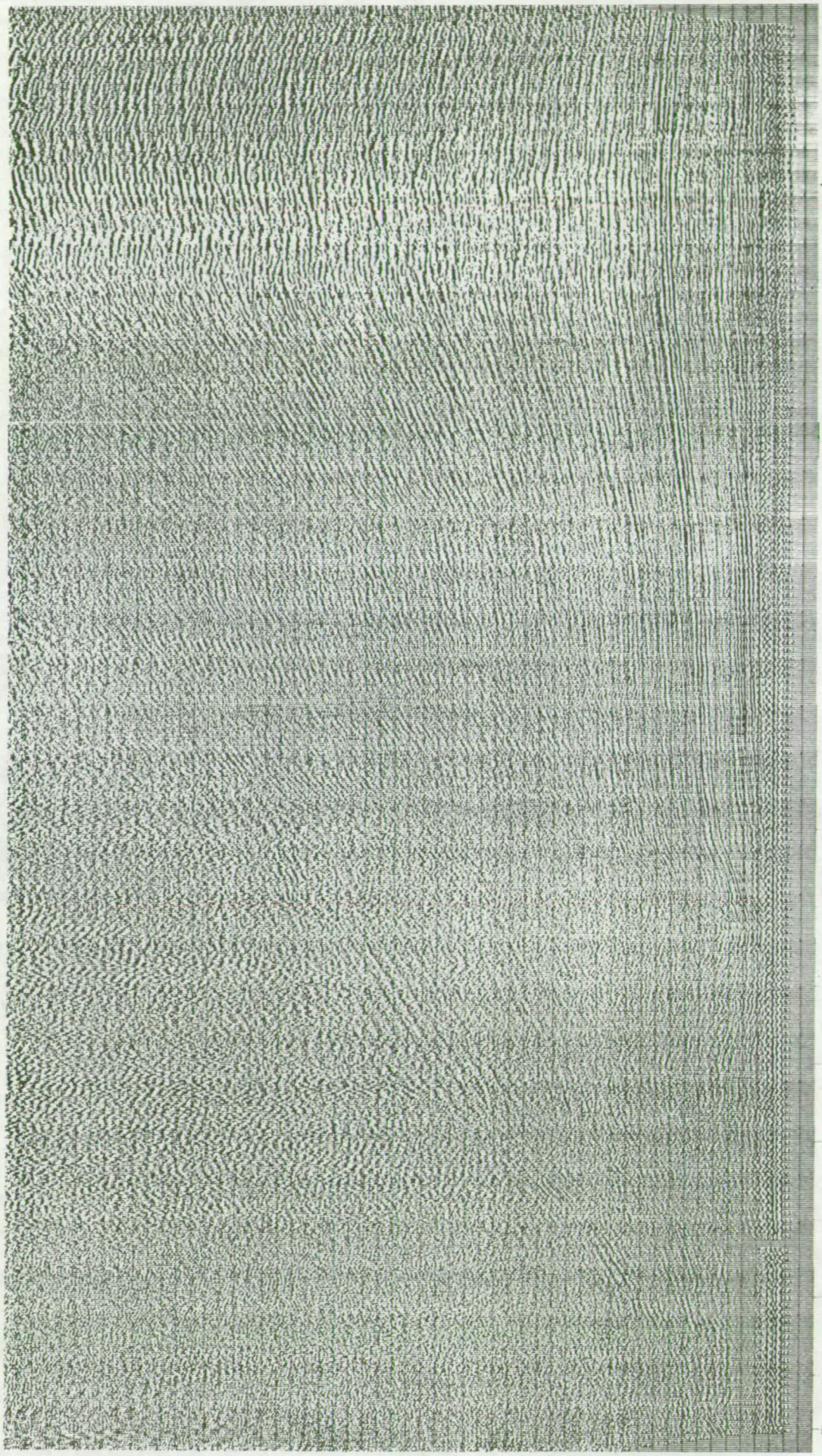

LINE 6

FIGURE 5/4

Interpretation of the western end of IGS seismic line 6. After Dobson et al (1973).

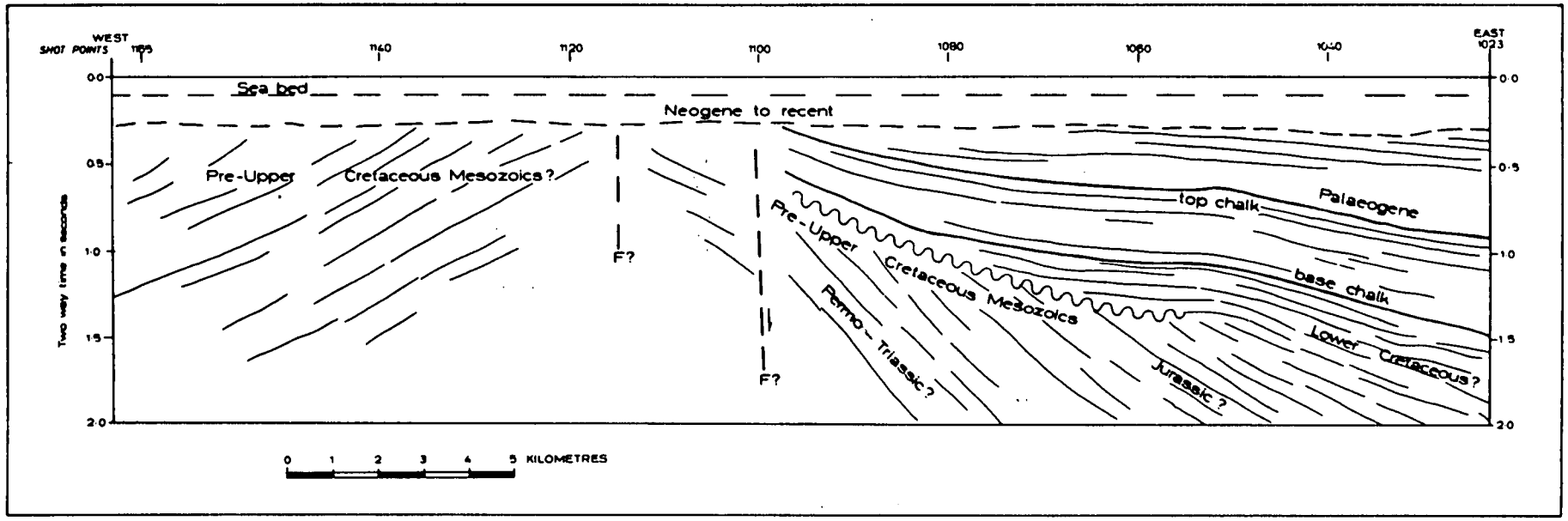
WEST
SHOT POINTS
1180
1160
1120
1100
1080
1060
1040
EAST
1023
0·0
Sea bed
Neogene to recent
0·5
Pre-Upper Cretaceous Mesozoics?
F?
F?
top chalk
Palaeogene
Pre-Upper Cretaceous Mesozoics
base chalk
Lower Cretaceous?
Permo-Triassic?
Jurassic?
1·0
1·5
2·0
Two way time in seconds
0 1 2 3 4 5 KILOMETRES

5.3 The Structure of the Basin

5.3.1 Regional structure

The St George's Channel Basin and its co-extensive Cardigan Bay Basin are the north-western extension of the Celtic Sea Basin (figure 1/1). The relation of the basin to the surrounding area is shown in figure 5/5. To the northwest, the basin margin is defined by the Palaeozoic Tuskar Rock Platform of southeastern Ireland, by the Irish Sea Geanticline, and by the Palaeozoic ridge of the Lleyn Peninsula and its offshore extension as St Tudwal's Arch. To the east, the basin margin is formed by the fault-controlled coastline of central Wales with outcropping Lower Palaeozoic rocks to the east, including the Harlech Dome. To the southeast, the margin comprises the Cardigan and St Bride's Bay coastal shelves, made up of the offshore continuation of the Lower Palaeozoic terrain of central and southeastern Wales, and delimited by the southwestern extension of the Bala Fault system. The location of the Bala Fault has been argued recently (figure 1 in Whittington et al, 1981) but further discussion follows later in this chapter. At the north-eastern end of Cardigan Bay, a structural sub-unit has been recognised as the Tremadoc Bay Sub-basin on the basis of its localised Tertiary fill (Blundell et al, 1971). The St George's Channel and Cardigan Bay Basins are separated only by a saddle structure extending southward from St Tudwal's Arch. The basin communicates with the Central Irish Sea and Caernarvon Bay Basins through two narrow troughs, the Carnsore and Bardsey Island Troughs respectively.

The whole basin structure can be regarded as having a half-graben form with the more stable platform area to the northwest, including the Irish Sea Geanticline and the Lleyn Peninsula, and with a zone of major subsidence to the southeast along the Bala Fault system (Barr et al, 1981). The general trend of the basin is Caledonoid and following the earlier suggestions of O T Jones and T N George, Woodland (1971) inferred that the original basin formation was a product of the Caledonian orogeny, and thus was already in existence in Carboniferous times. As has already been mentioned, whether or

FIGURE 5/5

Structural regions of the south Irish Sea. After Dobson et al (1973).

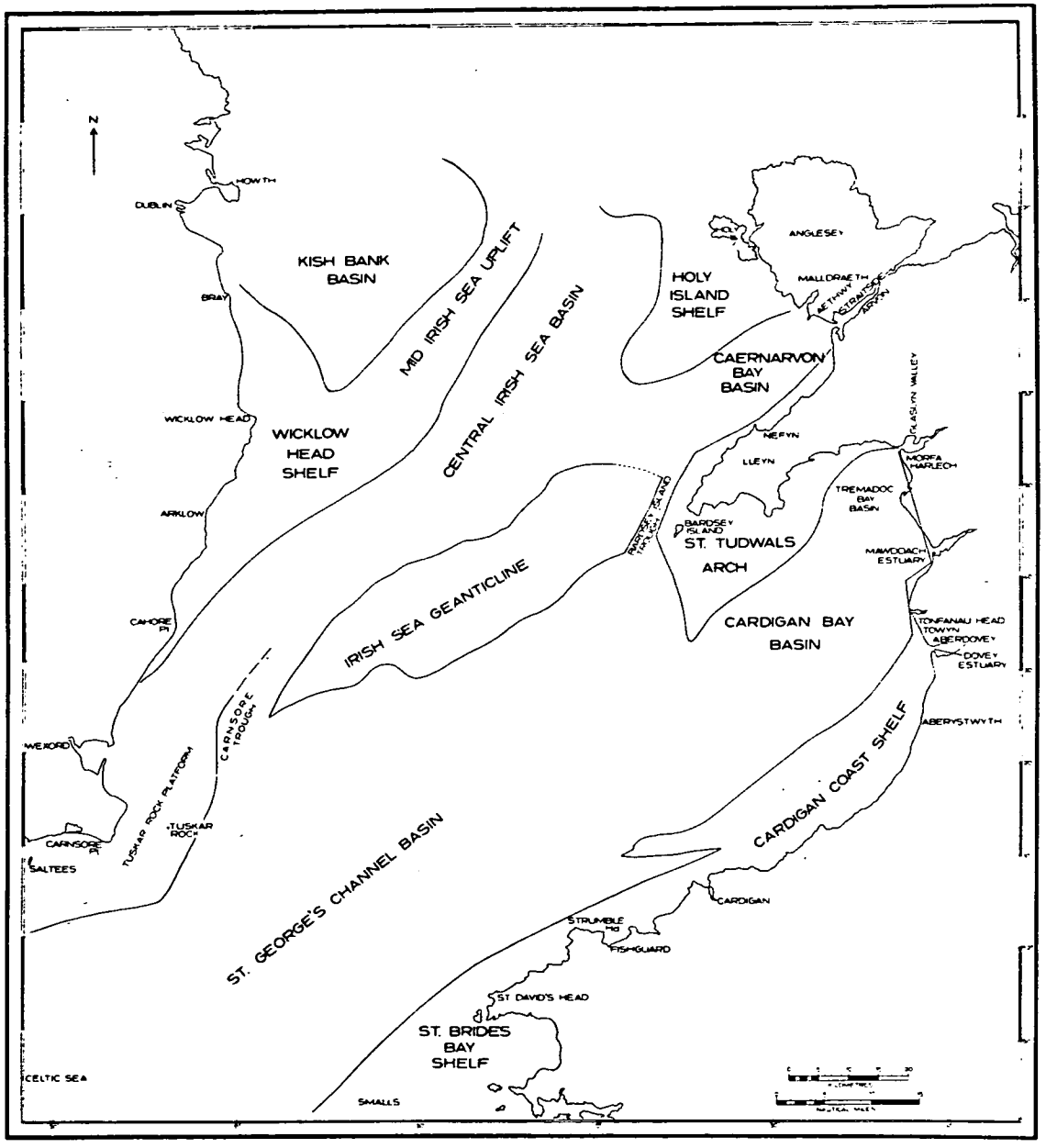
N
DUBLIN
HOWTH
BRAY
WICKLOW HEAD
ARKLOW
CAHORE PT
WEXFORD
CARNSORE PT
SALTEES
TUSKAR ROCK PLATFORM
CARNSORE TROUGH
TUSKAR ROCK
KISH BANK BASIN
MID IRISH SEA UPLIFT
CENTRAL IRISH SEA BASIN
WICKLOW HEAD SHELF
IRISH SEA GEANTICLINE
ST. GEORGE'S CHANNEL BASIN
CELTIC SEA
HOLY ISLAND SHELF
ANGLESEY
MALLORAETH
CAERNARVON BAY BASIN
NEFYN
LLEYN
BARDSEY ISLAND
ST. TUDWALS ARCH
TREMADOC BAY BASIN
MAWDDACH ESTUARY
CARDIGAN BAY BASIN
TONFANAU HEAD
TOWYN
ABERDOVEY
DOVEY ESTUARY
ABERYSTWYTH
CARDIGAN COAST SHELF
CARDIGAN
STRUMBLE HD
FISHGUARD
ST DAVID'S HEAD
ST. BRIDES BAY SHELF
SMALLS

not there was any considerable subsidence and sedimentation in late Palaeozoic times has not yet been proved, but certainly the basin's form has continued to be dominated by Welsh Caledonian lineaments during its major subsidence and infilling (Mesozoic times) to the present day. The sub-Pleistocene offshore geology of the St George's Channel Basin and the major faults within it are shown in figure 5/1.

To the southwest the basin is continued into the Irish Celtic Sea Basin. To the northeast, the system of St George's Channel, Cardigan Bay and Tremadoc Bay Basins, is closed by the Mochras, Mawdach Estuary and Tonfanau Faults which follows the mid-Welsh coastline (Dobson et al, 1973). However, these are evidently late faults, possibly of mid-Tertiary age, and it seems probable that originally the basin may have extended considerably to the east of the present coastline across some parts of the North Wales Lower Palaeozoic complex (Woodland, 1971). Whether it may ever have extended farther eastward to link up with the Cheshire Basin is a matter for speculation, although at least during Jurassic times it seems entirely possible that it did so, as for example, suggested in the Bathonian palaeogeographic reconstruction in figure 2 by Penn and Evans (1976).

5.3.2 Structure within the basin

A large number of independent surveys dating from 1969, both by the Institute of Geological Sciences and various oil companies, comprise the seismic control in the Cardigan Bay area. The discussion which follows is based on the interpretation by Barr et al (1981) which incorporated data from the following companies: Amoco (UK) Exploration Co., Arco Oil Producing Inc., British Gas Corporation and its subsidiary Hydrocarbon Great Britain Ltd., Denimex Oil and Gas (UK) Ltd., and Texaco Production Services Ltd. The data quality varied considerably from poor to occasionally good, the reflection quality being very dependent on the particular area. Seismic lines shot in areas where Tertiary beds overlie Upper and Middle Jurassic sections provided the best reflection quality, especially in areas of least tectonic complexity. In places, the seismic coverage was poor or

even absent, as for example along the southeastern margin of the basin and around the St Tudwal's Arch extension, and this inhibited mapping of horizons in these areas. In the latter area also, correlation of the picked seismic reflections with sea-bottom geological information was sometimes difficult (Barr et al, 1981).

In the axial part of the basin, deep reflections at depths of 5 seconds (two-way time), although these could be multiples, imply a sedimentary section thickness in excess of 10,000m assuming an average seismic velocity of 4.0km/s to these reflectors (see figure 5/3, IGS line 6). Multiple reflections problems were most acute in these areas within the intra-Tertiary horizons, and in places these reflections mask the base Tertiary unconformity event. The eastern and southeastern margins of the basin are tectonically complex, with severe faulting affecting the whole section. The correlation of events in this area is uncertain.

The structure within the basin is illustrated by two isochron maps (figures 5/6 and 5/7), for the top Middle Jurassic and an intra-Permo-Triassic event. The former map ties up to wells 106/24-1 and 107/21-1 at depths -2124m and -861m respectively, whereas the intra-Permo-Triassic event cannot be correlated with the wells within the main St George's Channel Basin, as these are terminated within the Jurassic. It is believed, though, that this horizon reflects the structural configuration of the deeper section of the basin. In the deepest parts of the basin, depths to these reflectors are approximately 4400m and 9000m respectively. Lateral correlation from the wells 106/28-1 and 103/2-1, which penetrate the Triassic section, into the basin is difficult; this is due to the fact that they are separated from the main basin by major faulting associated with salt intrusion and that the quality of the seismic data in the region of these wells is poor.

Apart from the main basinal form, structural features are generally fault-related, as in the region of well 107/2-1, or are a function of faulting and associated salt intrusion, as near wells 106/28-1 and 106/24-1. The main Strumble Head salt feature is a salt wall, the subcropping extent of which is shown in figure 5/1. This wall

FIGURE 5/6

Seismic structure map in two-way time on near-top Middle Jurassic. After Barr *et al* (1981).

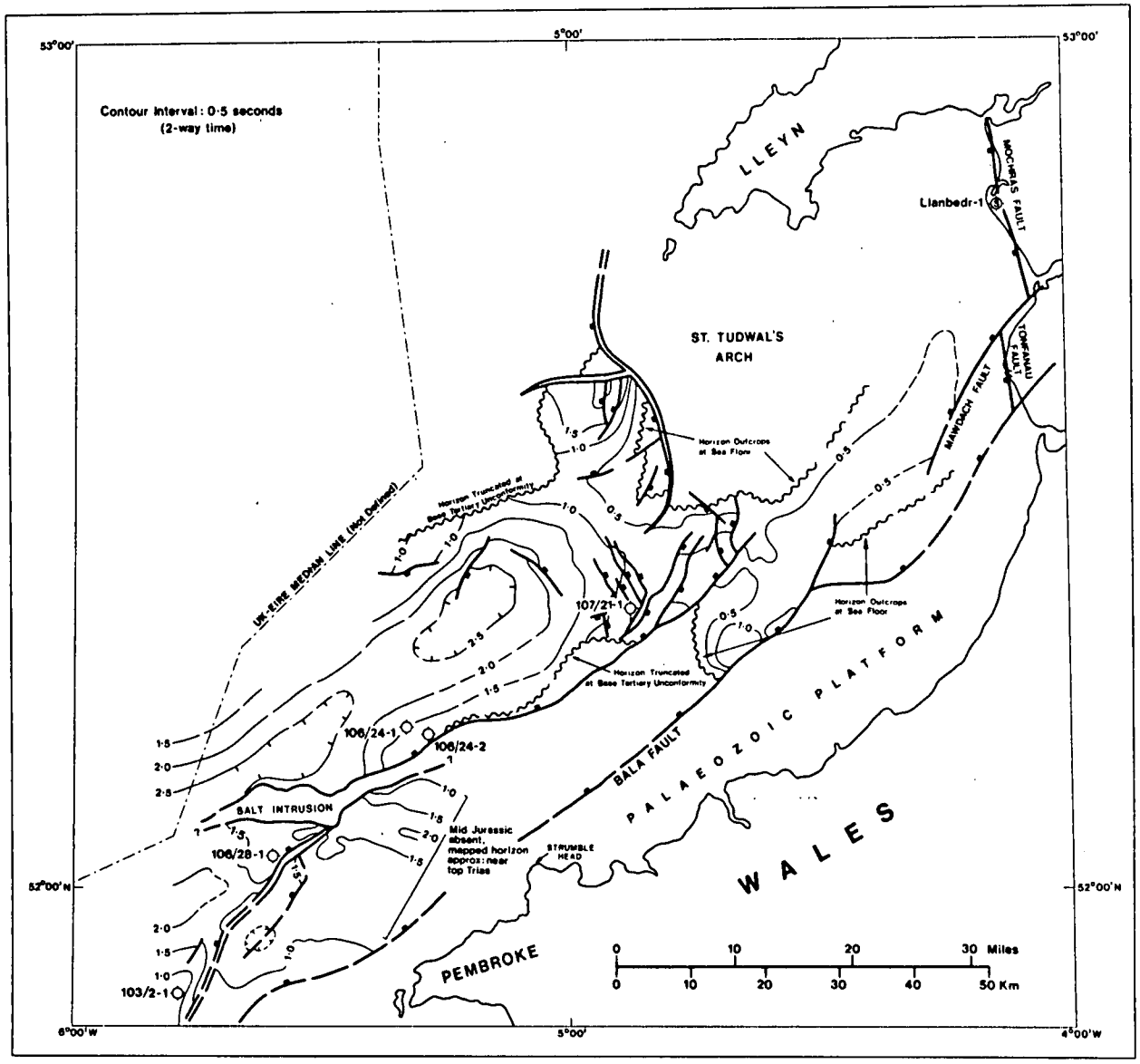
Contour Interval: 0·5 seconds
(2-way time)
53°00'
5°00'
4°00'W
52°00'N
LLEYN
Llanbedr-1
MOCHRAS FAULT
TONFANAU FAULT
MAWDACH FAULT
ST. TUDWAL'S ARCH
Horizon Outcrops at Sea Floor
Horizon Truncated at Base Tertiary Unconformity
UK-EIRE MEDIAN LINE (Not Defined)
107/21-1
106/24-1
106/24-2
106/28-1
103/2-1
BALT INTRUSION
Mid Jurassic absent, mapped horizon approx: near top Trias
BALA FAULT
PALAEOZOIC PLATFORM
WALES
STRUMBLE HEAD
PEMBROKE
0 10 20 30 Miles
0 10 20 30 40 50 Km

FIGURE 5/7

Seismic structure map in two-way time on the "intra-Permo-Triassic" event. AB, CD modelled profiles. After Barr et al (1981).

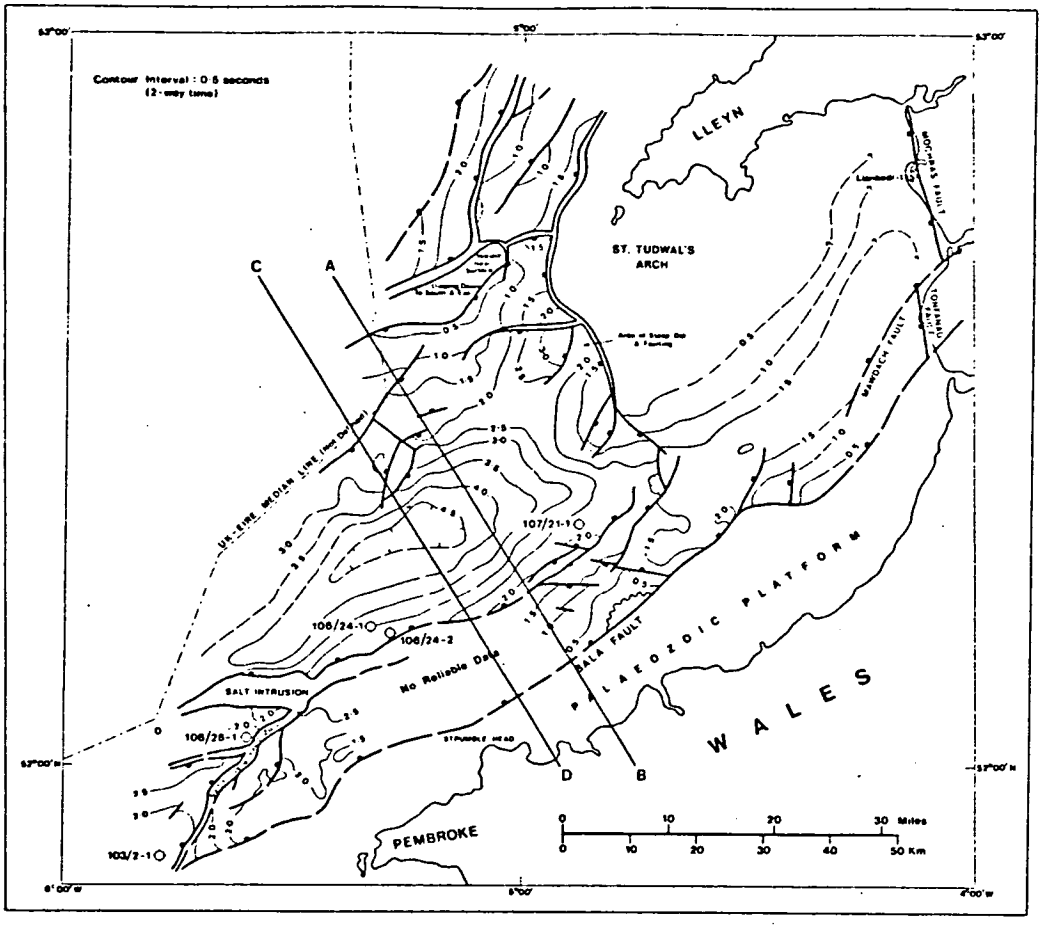
Contour Interval : 0·5 seconds
(2-way time)
LLEYN
ST. TUDWAL'S ARCH
C
A
D
B
107/21-1
106/24-1
106/24-2
No Reliable Data
SALT INTRUSION
106/28-1
103/2-1
BALA FAULT
PALAEOZOIC PLATFORM
WALES
PEMBROKE
0 10 20 30 Miles
0 10 20 30 40 50 Km

displaces Jurassic and younger horizons, but the intruded salt masks reflection data from deeper levels. It is therefore uncertain from the geophysical evidence whether or not the salt has penetrated from geologically deeper horizons than those just mentioned. Drilling has already proved the presence of salt in the Upper Triassic in the southwestern part of St George's Channel Basin (figure 5/2), which may be the origin of the Strumble Head salt intrusion. It does not however rule out the possibility of the occurrence of a salt section deeper in the Permo-Triassic. The exact nature of the relationship between the Strumble Head feature and the Palaeozoic basement edge is impossible to ascertain owing to the very low density and poor quality of the seismic data in this area.

It is assumed that the Bala Fault defines the edge of the Palaeozoic platform, and thus the southeastern margin of the basin following the earlier interpretations of Blundell et al (1971) and Dobson et al (1973). More recently, as already mentioned, Whittington et al (1981) show the Bala Fault as continuing south-westwards close to the axis of the Cardigan Bay Basin to join up with the major fault which is associated with the Strumble Head salt wall. Barr et al (1981)agree that a major fault controls the salt intrusion and extends for some distance northeastwards but say that they cannot link this fault to the Bala Fault on the basis of the available seismic data. They believe that it is debatable which of the sub-parallel faults to the southeast of the basin is the dominant one and they suggest that the most likely one, is that which defines the basin's margin, downthrowing the Mesozoic sediments to the north against the Palaeozoic platform to the south.

5.4 Summary

Up to the present research in the St George's Channel-Cardigan Bay area has revealed the presence of a very deep sedimentary basin, its thickness being in excess of 10km. The fill of the basin consists of sediments of Permo-Triassic to Quaternary age with the notable exception of Cretaceous strata, the presence of which has not yet been proved. The oldest Mesozoic sediments encountered in wells are of Middle Triassic age resting unconformably on

Upper Carboniferous strata, at the south-westernmost part of the area (well 103/2-1). Despite the presence of Carboniferous strata in this area, their presence under the basin farther to the north-west is questionable, since the latter region lies in the area occupied by the St George's landmass during the Carboniferous (Anderton et al, 1979). Older than Carboniferous rocks beneath the basin are thought to be similar to those occurring in Wales, namely Ordovician and Silurian rocks. These rocks are in fault contact with the Mesozoic sediments of the southern and south-eastern margin of the basin. It is not clear if the north-western margin of the basin is of onlap type against the Irish Sea Geanticline or if it is faulted. In a recent paper (Nutt and Smith, 1981) the existence of a major transcurrent fault active in Devonian and pre-Devonian times and running roughly along the north-western margin of the basin has been proposed. In such a case a subsidence to the south-east of the fault during the Mesozoic would be expected, the fault line being a line of weakness in the upper crust, due to the weight of the accumulating sediments and the tensional regime of that period. Such a subsidence against that fault would also agree with the steep gravity gradient observed in this area (see next chapter). The Irish Sea Geanticline is thought to consist of rocks similar to those of the Lleyn and Pembrokeshire Peninsulas and those of North Wales and Anglesey, probably being associated with volcanics and intrusions. The areas associated with igneous activity around the basin seem to have resisted subsidence throughout their history, forming prominent ridges between sedimentary basins (Bott, 1968).

The sediments within the basin show an exceptionally thick Jurassic succession, the thickest known in the British Islands area, the reasons for such an accumulation of sediments in a narrow basin are not yet known. Beds of halite occur in the mid-Upper Triassic, whereas the layers immediately above and below the saliferous layers contain beds of anhydrite. It is not known if the halite forming the salt wall seen within the basin (figure 5/1) comes only from the mid-Upper Triassic layer or if salt from deeper layers has also migrated upwards as Barr et al (1981) suggest. The salt wall is seen

to be associated with a normal fault running through the basin. No tight folding has been observed in the Mesozoic sediments, the only strata to form smooth open folds being of Tertiary age. These sediments rest with an angular unconformity over the margins of the basin on the Mesozoic rocks, thus suggesting a period of non deposition and erosion prior to their deposition.

CHAPTER 6

GEOPHYSICAL INVESTIGATION OF THE ST GEORGE'S CHANNEL BASIN

6.1 Introduction

The first geophysical observation in the Irish Sea was in 1923 when a gravity measurement was taken on board S.S. Nestor using a barometric gravimeter. The Free-Air anomaly value of -25mGal measured south-west of Anglesey (Duffield, 1924) was an early indication of a mass deficit beneath part of the Irish Sea. The next expedition was again to survey gravity by the Geology and Geophysics Department, University of Cambridge in 1946, during which a measurement located on the north-west flank of the St George's Channel Basin gave a Bouguer anomaly of -37mGal and as a probable explanation of this low gravity value the existence of a deep Triassic basin was suggested (Browne and Cooper, 1950).

In 1956 M N Hill reported (discussion after Powell, 1956) that on two out of three refraction stations across the South Irish Sea there was little doubt that a thick layer of rocks occurred with a medium velocity similar to velocities associated with New Red Sandstone formations found elsewhere. This layer at the most easterly station (position 59°20'N, 04°49'W), lay below 700ft (213m) of low-velocity material and was approximately 5000ft (1524m) thick. Below this layer a high velocity layer was found, the velocity being similar to that of Palaeozoic formations. At the station in the middle of the Irish Sea (position 52°32'N, 05°18'W) the low-velocity cover material was 1100ft (335m) thick and the medium-velocity layer approximately 1900ft (579m) thick. Again the velocity of the bottom layer was similar to those found in Palaeozoic formations. The third station was near the Irish coast (position 52°41'N, 05°49'W) and there the low-velocity layer was 230ft (70m) thick, whereas the medium-velocity layer appeared to be absent. Beneath the layer of low-velocity there was a layer with a velocity higher than that of the middle layer and lower than the velocity of the bottom layer at the two other stations. In the light of this evidence Hill suggested the existence of a Trias basin centred in Cardigan Bay. The velocities for the two uppermost layers at the first two stations were given later by O T Jones

(in discussion after Griffiths et al, 1961) and were 7000 and 6000ft/sec (2134 and 1829m/sec) for the low velocity middle layer. Seismic refraction surveys in the Tremadoc Bay Basin to the north-east of Cardigan Bay (Griffiths et al, 1961; Blundell et al, 1964) indicated the existence of three layers with different velocities in that area. The top layer had a similar velocity to that of Jones (1830-2440m/sec) and was interpreted as consisting mainly of Tertiary or Mesozoic clays. The middle layer had a slightly higher velocity than the one of Jones (3960m/sec) and was thought to represent Ordovician rocks. The bottom layer had a velocity of 5180m/sec and was considered to consist of Cambrian strata similar to those of the Harlech Dome.

An underwater gravity meter traverse across the south Irish Sea between Arklow and Cardigan was made from RRS Shackleton by M H Bott in 1961. The traverse is on line with the three refraction stations of M N Hill. In a combined interpretation of the gravity traverse, the refraction results and surface ship magnetic measurements along the same line, Bott (1968) suggested the existence of a sedimentary basin, possibly mainly Triassic, under Cardigan Bay. The north-western margin of the basin was thought to be the south-western extension of the magnetic rocks beneath the Lleyn Peninsula. The probable existence of a second basin to the west of this magnetic ridge was noted. The gravity anomaly associated with the main basin had an amplitude of -60mGal over Cardigan Bay. Since the seismic model appeared to be insufficiently deep to explain the whole of this gravity anomaly, Bott proposed different ways of accounting for the discrepancy. The most interesting one, which will be returned to later, is that the observed seismic basement could be a layer of salt or Carboniferous limestone.

The Cardigan Bay gravity anomaly is superimposed on a high regional gravity field of +40mGal. This regional field is +20mGal higher than comparable regional fields over the adjacent land areas of Ireland and Wales. The possible interpretation of the high regional Bouguer characteristic of much of the Irish Sea had been reviewed by Bott (1964), and the idea of a thinner crust was that which agreed

best with seismic evidence for the north-eastern part of the Irish Sea (Agger and Carpenter, 1964). Interpreting the magnetic anomalies of the south Irish Sea as seen on the aeromagnetic map of the area (figure 6/1), Bott recognised three different magnetic belts: the North Wales positive (NWP), the South Wales positive (SWP) and the Cardigan Bay negative (CBN) belts. The two positive belts were related to the centres of Ordovician vulcanism and to shallow Precambrian rocks. It was thought that they were caused at least in part, by variably magnetic igneous rocks occurring throughout the underlying crust and reaching the surface to cause the rough magnetic topography. The intervening belt of negative anomalies over Cardigan Bay was thought to be formed by a basement relatively deficient in intrusions underlying the sedimentary cover. The sharp truncation of the rough magnetic field at the Harlech Fault suggests, however, that the quiet magnetic field may be simply due to the deeper burial of basement beneath the sedimentary basin.

Detailed geophysical surveys across Cardigan Bay and St George's Channel were carried out between 1964 and 1969 by the University of Birmingham (Blundell et al, 1968; 1971). An unconformity at varying depths below the seabed was traced across the whole area surveyed, separating beds of negligible dip above from folded strata below. This unconformity was at a depth of 30 to 60m beneath Cardigan Bay. The region was divided into four areas according to the characteristics of the strata beneath the unconformity (figure 6/2). The central area B covered Cardigan Bay and the St George's Channel areas and had a north-east to south-west trend. Seismic refraction data suggest the presence of two layers in this area with velocities 2.3 and 3.5km/s. The base of the 2.3km/s layer reached depths of 1000m and the 3.5km/s layer had a thickness in excess of 2000m at the centre of the area. The north-west and south-east boundaries of this area were thought to be faulted judging from their strong diffraction patterns on profiler records, a view further reinforced by the steep gravity gradients associated with these boundaries. The downthrow side of the faults was towards the axis of this area. The gravity map of the south Irish Sea (figure 2 in Blundell et al, 1968) indicated an elongated gravity

FIGURE 6/1

Magnetic map of the Irish Sea region. Contours at 50 gamma (nT) interval. From Bott (1968).

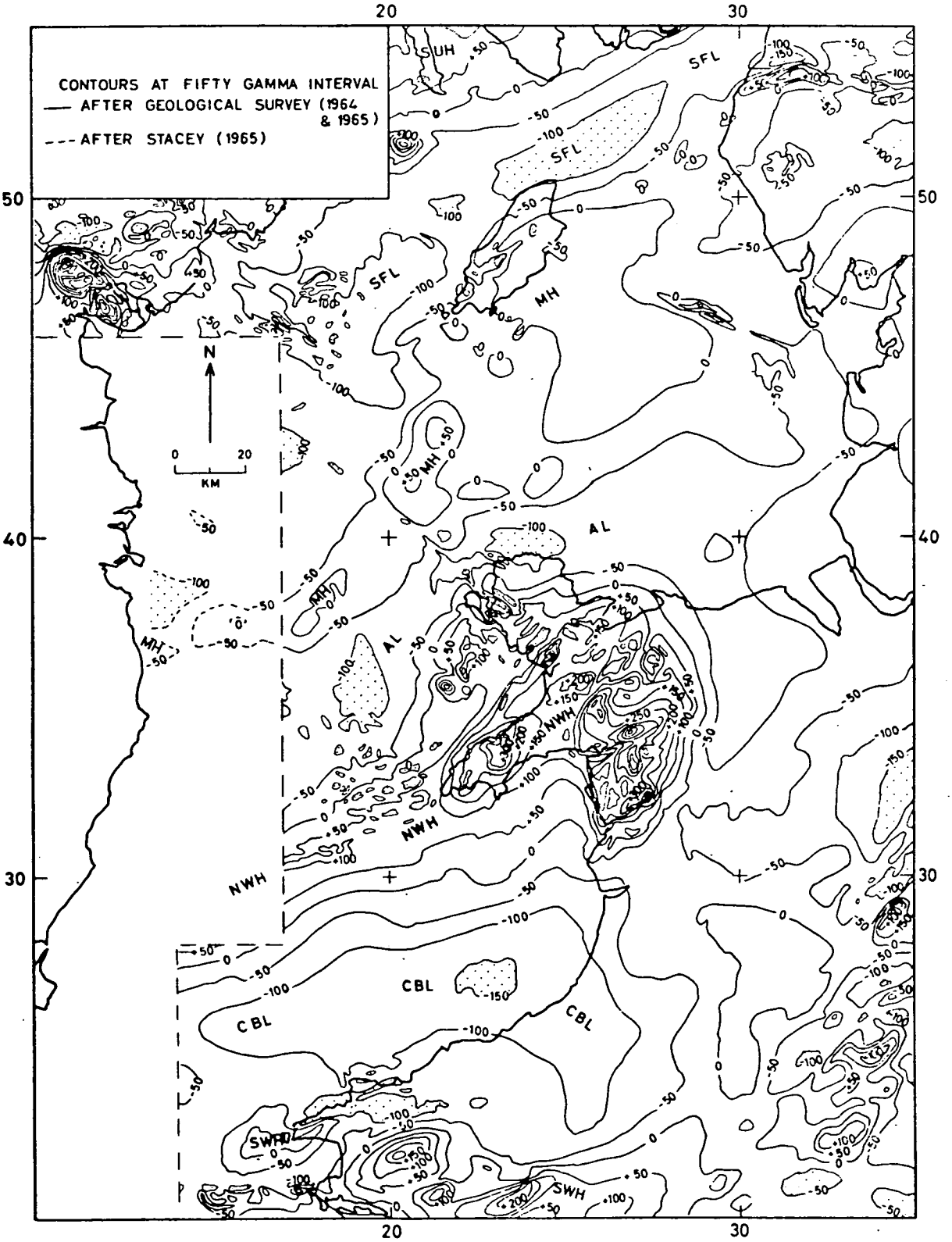
CONTOURS AT FIFTY GAMMA INTERVAL
— AFTER GEOLOGICAL SURVEY (1964 & 1965)
--- AFTER STACEY (1965)
N
0 20
KM
20
30
50
40
30
SUH
SFL
MH
AL
NWH
CBL
SWH

FIGURE 6/2

South Irish Sea areas with different reflective characteristics on seismic profiler (sparker) records. After Blundell *et al* (1971).

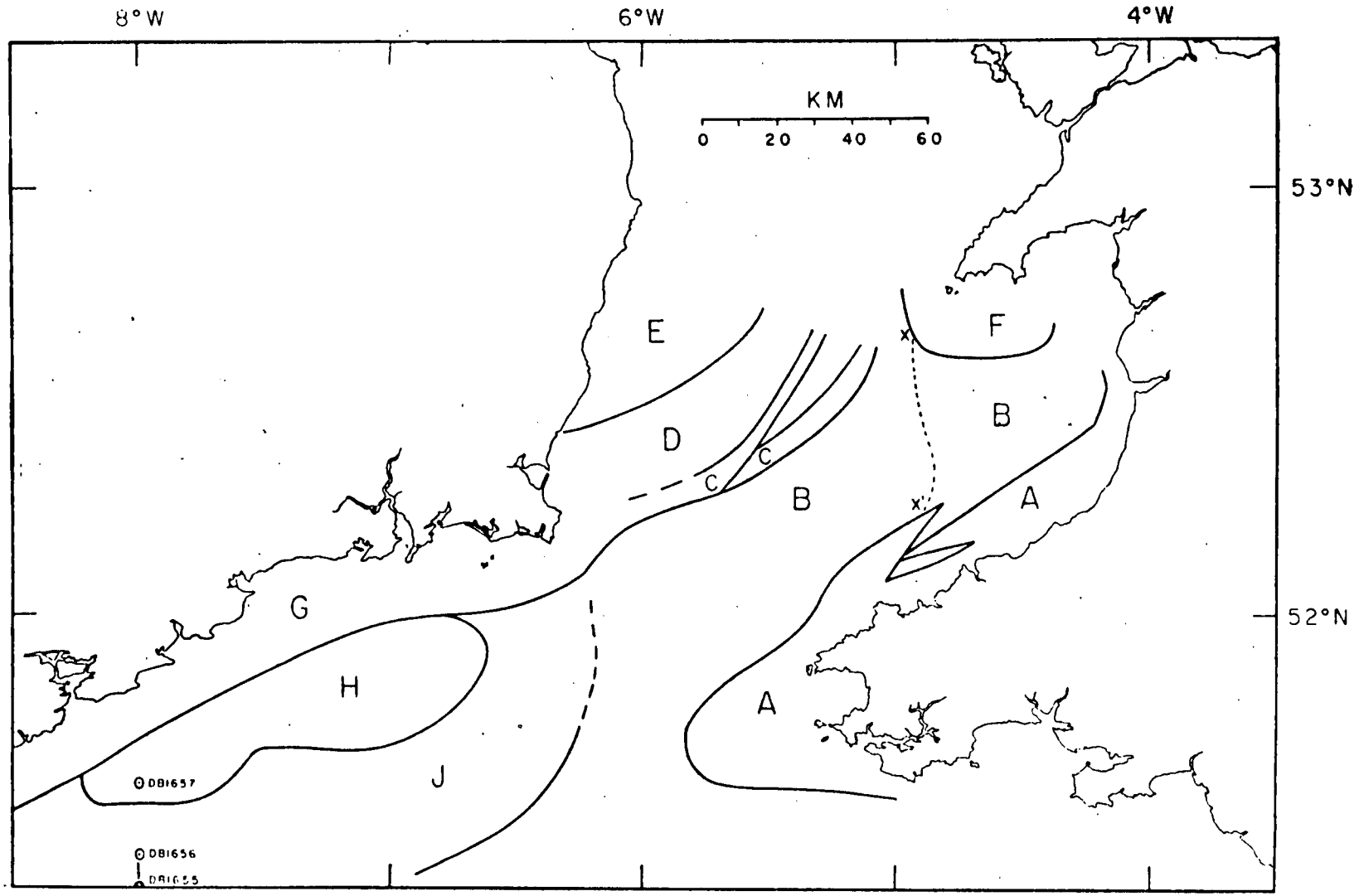
8°W
6°W
4°W
53°N
52°N
KM
0 20 40 60
E
F
D
C
C
B
B
A
G
H
J
A
DB1657
DB1656
DB1655

low covering the Cardigan Bay area, with a minimum value of -32mGal. Assuming an average density between 2200 and 2400kg/m^3 for the sediments, which is consistent with their velocities, Blundell et al, (1968) suggested that the maximum depth of the basin should be between 3500 and 6700m. The upper 1000m or so of the folded sediments in the Cardigan Bay Basin were thought to be Jurassic or Tertiary in age according to their character on the seismic profile records and their physical properties (velocity-density). The areas to the north-west and to the south-east of the basin (areas C and A) were penetrated generally less than 100m by the seismic profiler and the observed structures were complex. The seismic velocities of the rocks were between 4.4 and 5.4km/s. The area south-east of the basin seemed to form an extension of the Lower Palaeozoic succession of Wales, the faulted boundary being probably associated with the Bala Fault, whereas the area north-west of the basin was thought to represent a Precambrian ridge linking the outcrops of Rosslare in Ireland with those of Anglesey and Lleyn. Finally the gravity low over Tremadoc Bay was thought to represent a smaller subsidiary sedimentary basin controlled by the same major structures.

A fuller report by Blundell et al (1971) recognised four different layers according to their velocities from the refraction lines. The first layer had an average velocity of 1.8km/s, which corresponded to a density of 2100kg/m^3. The layer was thought to be possibly of Pleistocene age and was separated by an unconformity from the station beneath it. It was found that the layer thickened considerably in the St George's Channel area where as much as 200m of horizontally stratified sediments were deposited. The second layer had an average velocity of 2.3km/s. This velocity was similar to that of Tertiary from the Mochras Borehole and from elsewhere, so an average density of 2300kg/m^3 was chosen to represent this layer. The sediments comprising this layer were shown on the profile records to be well bedded and to form open folds and their reflecting character suggested that they consisted of clays and shales. By comparing two distinct unconformities on profile records south of Ireland with the two unconformities shown on the IGS deep reflection records (Bullerwell and McQuillin, 1969) over the south Irish Sea area, Blundell et al (1971) suggested that a Palaeogene age for the

strata of this layer is most consistent with their reflection and refraction records. Up to 2km of these sediments were thought to be present in the central part of the basin, indicating an extended subsidence during the Tertiary. This subsidence was thought to be caused by rifting, a probability strengthened by the presence of the 7.3km/s layer at the base of the crust and by Tertiary vulcanicity nearby. The third layer had an average velocity of 3.5km/s with a range from 3.0 to 4.0km/s. The velocity values within this layer were more variable than those in the previous layer and it was thought that it might represent at least two different layers. The average velocity of this layer was compatible with the Lias in the Mochras Borehole and therefore an average density of 2500kg/m^3 for this layer was assumed. Layer 3 was detected near to the surface in Cardigan Bay where it underlies layer 1 but plunges to depths beyond the detectable range of the refraction seismic method used in the St George's Channel Basin area. Gravity interpretation indicated a total thickness of about 6km at the centre of the basin. This layer was thought to consist of Jurassic and Permo-Triassic sediments, the presence of the latter being supported by the presence of a structure of salt plug appearance shown on line 10 of the IGS deep seismic survey. Although layer 3 was suggested to represent a more complete sequence of Mesozoic rocks than the Lias of the Mochras Borehole, the presence of any considerable thickness of chalk was rejected, on the basis of the absence of its typical reflection characteristics. Finally, the fourth layer had an average velocity of 4.9km/s and was observed on only a few profiles near the coast. Its velocity was more compatible with those of the Palaeozoic succession in Wales. Blundell et al (1971) also recalculated the data of Griffiths et al (1961) from the Tremadoc Bay area, and showed that the then interpreted layer 2 of 4.0km/s could equally well be of 3.5km/s (thus being compatible with layer 3 in the Cardigan Bay and St George's Channel areas) and that it should extend to 2000m beneath Mochras (the Mochras Borehole terminates at 1908m within the Permo-Trias).

In 1973 a progress report of the continuing investigation of the south Irish Sea by the University College of Wales, Aberystwyth, was

published (Dobson et al, 1973). The Bouguer anomaly gravity map produced covered the area between 4° and 6°30'W longitude and 51°50' and 53°20'N latitude. Where possible the isogals offshore were tied to the land gravity contours of Griffiths and Gibb (1965) for Wales, and those of Murphy (1962) for Ireland. Apart from the dominant Welsh Caledonoid trend, a subsidiary grain at right angles to this and a maximum value of +45mGal at two locations within the south Irish Sea were the general features of the gravity map. Magnetic surveys were carried out in three marine areas, two of which had been previously covered by the Aeromagnetic Map of Great Britain, Sheet 2 (1:625,000, IGS 1965). A combined marine magnetic and aeromagnetic map was constructed at 25 gamma (25nT) contour interval in the areas covered by the marine surveys (St George's Channel, Tremadoc and Barmouth Bays). On this map the Cardigan Bay "low" magnetic belt (CBN in Bott, 1968) could be seen to continue south-westwards towards Carnshore Point and then turn southwards into the Celtic Sea. The North Wales "high" magnetic belt (NWP in Bott, 1968) also extended south-west, but off the Irish coast there was a noticeable lack of high magnetic relief evident in the north-eastern part of the feature, and although a peak of 100 gamma (100nT) was seen, the contours were very smooth. This peak probably represents a Palaeozoic volcanic ridge covered by relatively thin Mesozoic sediments since it is associated with high gravity values of up to 40mGal (figure 6/3).

Sparker profile surveys by the Aberystwyth group covered the south-western part of the St George's Channel and the Tremadoc and Barmouth Bays, as well as the inshore parts of Cardigan and Barmouth Bays. Strong reflections down to 0.5sec two-way travel time were obtained from these surveys. The results of the sparker profiling are complementary to the deep seismic reflection records, which showed little information above the 0.5sec level. Correlation and identification of the sparker recorded interfaces with those obtained by previous refraction studies was made as well. The continuous acoustic velocity and density logs of the Mochras Borehole were combined by Dobson et al (1973) to give an acoustic impedance log for the Tertiary and Lias, from which an analysis of probable

FIGURE 6/3

Bouguer gravity map of the St George's Channel- Cardigan Bay area. Thick solid line indicates the location of the IGS seismic line 6. Prepared using published IGS Bouguer gravity data. Contours at 5mGal interval.

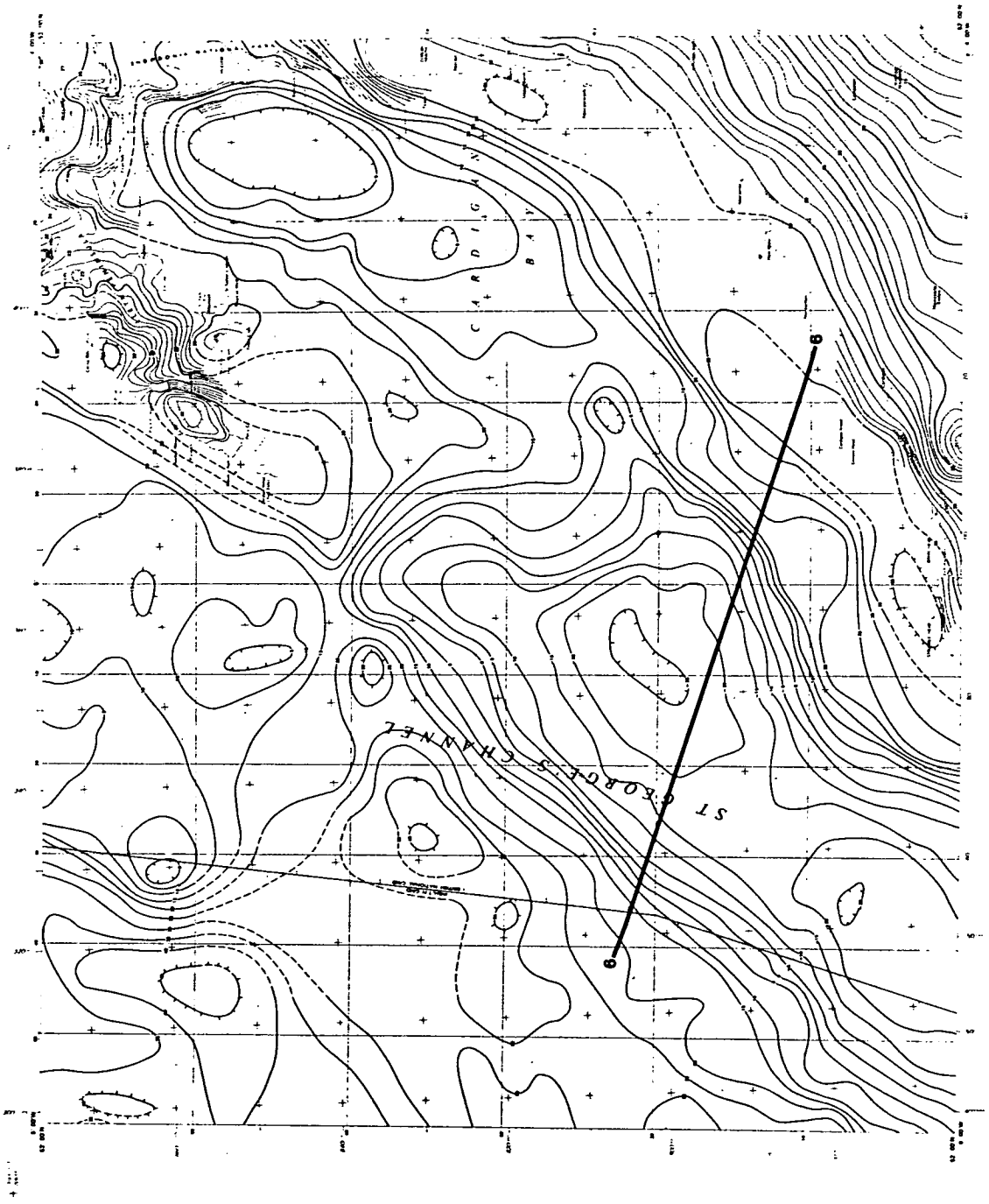
CARDIGAN BAY
ST GEORGE'S CHANNEL
6
6

reflecting horizons then a comparison with the actual records was made. The reflection characteristics of the Permo-Triassic and Liassic rocks allowed the boundaries of these rocks subcropping under Recent deposits to be inferred in the Cardigan Bay area. The Permo-Triassic rocks were seen to subcrop beneath the Tertiary to the south-west of the area and to crop out around the Lower Palaeozoic rocks of St Tudwal's Arch. No seismic evidence was obtained to indicate the subcrop here of rocks of age younger than Permo-Triassic but older than the Lower Palaeozoic. The subcropping Liassic rocks are of Lower Lias age and are distinguished on the seismic records from the Middle Jurassic strata which subcrop beneath Quaternary deposits in the central part of Cardigan Bay (figure 5/1).

6.2 Gravity Models across St George's Channel Basin

The St George's Channel Basin is sufficiently elongate for two-dimensional gravity models across it to be considered adequate in revealing the structure of the deepest part of the basin. As a starting point the modelling of IGS deep reflection line 6 was considered. Preliminary results of this modelling showed a discrepancy between the wavelength of the calculated and observed gravity anomalies, the latter being wider (figure 6/4). There were, nevertheless, certain problems on continuing modelling this line or other lines from the same survey. The line is at an angle of about 45^{o} to the axis of the basin and identification of horizons beneath the clearly shown angular unconformity was extremely difficult if not impossible due mainly to the poor quality of the records. In addition, it was thought that the appearance of more information in the form of a detailed sub-Pleistocene map of the area (Whittington *et al*, 1981) and of the two-way travel time contour maps (figures 5/6 and 5/7) accompanied by released deep-well data (Barr *et al*, 1981) would enable the construction of two-dimensional models at right angles to the axis of the basin. The procedure is the same as in the Moray Firth Basin, including the following stages: regional gravity reduction; seismic information to define the different layers; choice of densities for these layers; stripping the gravity effect of the above layers and, finally,

FIGURE 6/4

Preliminary model along seismic line 6. Horizontal axis: distance in km. Numbers within the layers indicate density in kg/m^3. Identification of layers is as follows: T: Tertiary; J?: Jurassic?; P?: Permo-Triassic?

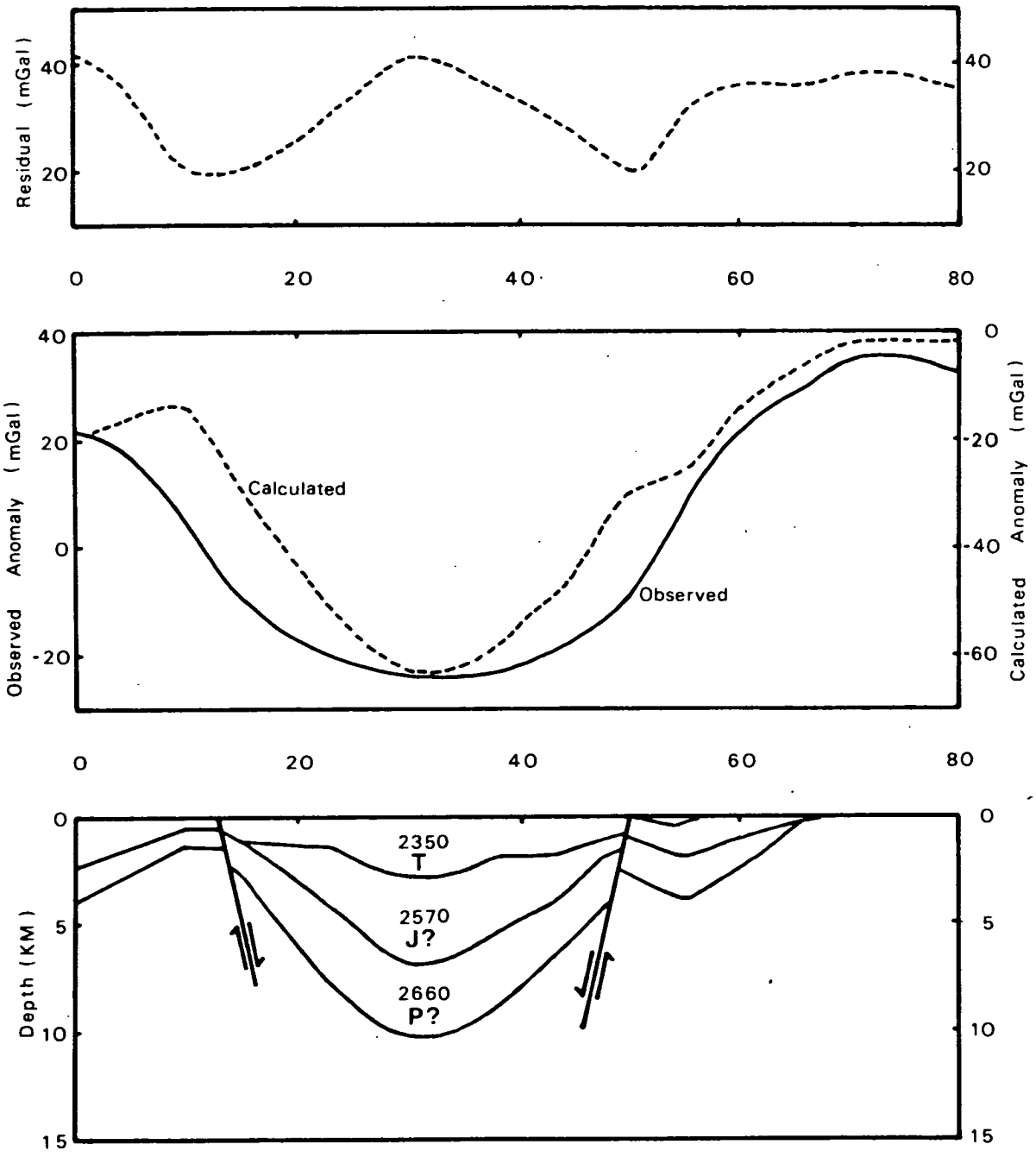
Residual (mGal)
40
20
0
20
40
60
80
Observed Anomaly (mGal)
Calculated Anomaly (mGal)
Calculated
Observed
-20
-40
-60
Depth (KM)
2350
T
2570
J?
2660
P?
5
10
15

interpretation of the remaining gravity anomalies in conjunction with any other available information.

6.2.1 Regional gravity reduction

As in the Moray Firth Basin case, two long gravity profiles have been constructed to reveal the regional gravity changes over the area. The fact that the Irish Sea is an area of regional high gravity and suggestions for the cause of the regional high have already been mentioned in the introduction to this chapter. What is attempted now is the better definition of the regional anomaly's amplitude and wavelength. The location of the two profiles is shown on the Sub-Pleistocene geological map of the British Isles (back cover), to allow a quick comparison of the gravity and known geology along them. The direction of the profiles and their length (figure 6/5) were dictated by the trend of the St George's Channel Basin and the availability of gravity data.

The first profile is 750km long with a SW-NE strike; its end coordinates are 49°30'N, 8°W and 55°N, 2°W. The profile runs from the South West Approaches area to northern England near Newcastle. The main features of this profile are:

(a) A broad gravity low covering the Celtic Sea between 90 and 270km.

(b) The large gravity low of 60mGal amplitude between 300 and 410km, bounded by the gravity highs corresponding to the Pembrokeshire and Lleyn Peninsulas.

(c) A gravity low between 520 and 610km, representing the south part of the Irish Sea Basin.

(d) An area of relatively high gravity between 610 and 650km representing the Palaeozoic rocks of Cumbria.

(e) A gravity low centred at 700km, related to the Northumberland Carboniferous Basin.

FIGURE 6/5

Long gravity profiles through the south Irish Sea area and their location. Dashed line denotes an interpretation of the regional field.

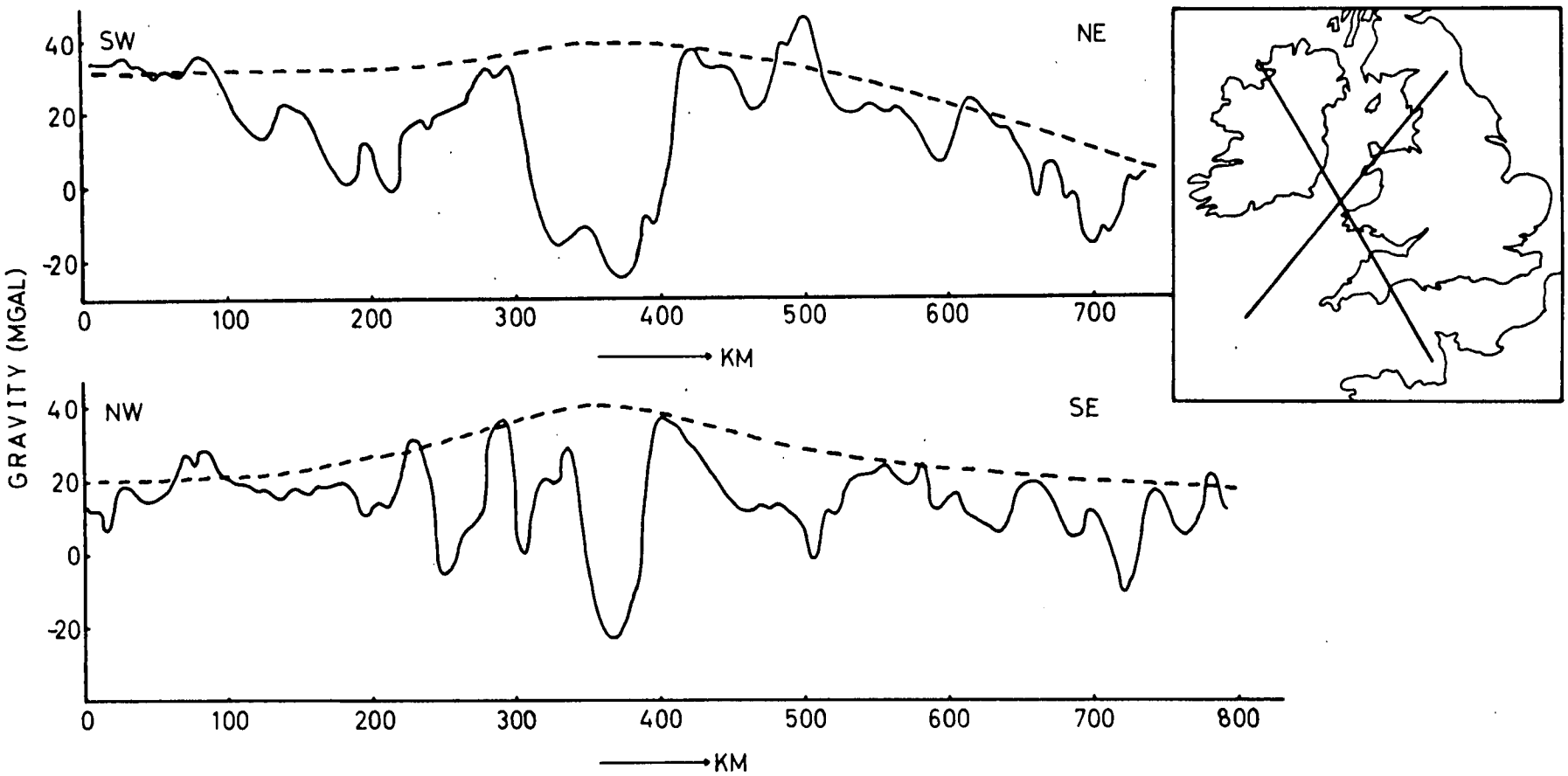
SW
NE
NW
SE
40
20
0
-20
GRAVITY (MGAL)
0
100
200
300
400
500
600
700
800
KM

The second profile is 800km long, striking NW-SE; its end coordinates are $54^{o}44'N$, $8^{o}47'W$ and $49^{o}04'N$, $2^{o}W$. The profile runs from the north-west coast of Ireland to Jersey Island. The most prominent features along this profile are:

(a) A gravity high of +30mGal at 225km, representing a Palaeozoic ridge intruded by intermediate and basic igneous rocks near the south-east coast of Ireland.

(b) A series of gravity highs and lows between 225 and 400km, representing Palaeozoic ridges and post-Palaeozoic basins, the most prominent being the St George's Channel Basin of more than 60mGal amplitude.

(c) The Bristol Channel Basin low between 440 and 530km.

(d) A low related to the Cornwall granite at 630km.

(e) An area of low gravity between 670 and 730km, related to the English Channel Basin.

(f) Two lows related to the Channel Islands' granites.

The regional interpretation of the two profiles (figure 6/5) shows a quite stable regional value of about 40mGal over the south Irish Sea. The gravity profiles across the St George's Channel Basin which were selected for modelling were corrected for regional gravity changes in a similar way to the first regional gravity profile, with which they are parallel. Due to the importance of the regional gravity high over the area in association with a high velocity layer at the base of the crust (Blundell and Parks, 1969), a more detailed investigation of it was carried out and is described at the end of this chapter.

6.2.2 Initial seismic input and densities

The only horizon which can be recognised and followed throughout the

IGS survey is the unconformity horizon which corresponds to the base of the Tertiary. The depths to this horizon used in the models are extrapolated from the IGS survey lines and they are converted to depth in kilometres by using an average velocity of 2.2-2.4km/s. This velocity is indicated by refraction data (Blundell et al, 1971). The average sonic velocities at 50m intervals from Mochras Borehole for the Tertiary sediments there (the first 600m) are not conclusive. They have a wide range of 1.86-3.02km/s with an average value of 2.41km/s, but a sudden increase from 2.34km/s to 2.71km/s occurs at 400m. The density used for the Tertiary layer is 2250kg/m^3 and is the same as the average Tertiary density in the Mochras Borehole. The average density indicated by well data is about 2200kg/m^3.

The seismic input for the next two deeper layers is provided by the two-way travel time isochron contour maps to the top of Middle Jurassic and to the unidentified horizon within the Triassic, referred to as "Permo-Triassic event," shown in figures 5/6 and 5/7. The velocities used to convert the two-way time in sec to depth in km are shown in the table below:

Two-way Time sec	Velocity km/sec	Formation
0.0-1.5	$\bar{v}$ = 2.4	U Jurassic
1.5-2.0	$\bar{v}$ = 2.6	
2.0-2.5	$\bar{v}$ = 2.8	
0.0-0.5	$\bar{v}$ = 3.1	M-L Jurassic
1.0-1.5	$\bar{v}$ = 3.3	
2.0-2.5	$\bar{v}$ = 3.6	and
3.0-3.5	$\bar{v}$ = 3.8	
4.0-4.5	$\bar{v}$ = 4.0	U Triassic?

The velocities for the lower layer cover the range of 3.0-4.0km/s measured by Blundell et al (1971) for their layer 3. The range 2.4-2.8km/s is also observed on some refraction profiles. Average

sonic velocities from well data agree with the velocities used. The density assumed for the Upper Jurassic layer is 2400kg/m^3 and has been derived from the well data. For the Middle-Lower Jurassic and Triassic? layer a density of 2600kg/m^3 has been used. This value is in agreement with well data and the average Lias density from the Mochras Borehole (2560kg/m^3). The density assumed for the Palaeozoic basement is 2730kg/m^3. The same density has been used for the Palaeozoic strata of the area by Blundell et al (1971) and is in agreement with density measurements of Palaeozoic rocks in Wales (Gibb, 1961; Griffiths and Gibb, 1965).

6.2.3 The gravity models

The location of the models constructed is shown in figure 5/7. The gravity effect of the three layers in the first model (AB) and its comparison with the observed gravity (reduced for regional effect) are shown in figure 6/6. It is immediately apparent that whereas the fit between observed and calculated values is very good at the ends of the profile (-1mGal at 5 and 75km), where the profile lies over Palaeozoic basement (figure 5/1), and at the centre of the basin (-3mGal at 40km) considerable differences occur over the flanks of the basin and near the south-east end of the profile between 60 and 70km. These differences reach 15mGal over the north-western flank of the basin, 18mGal over the south-eastern flank and 13mGal between 60 and 70km and always the observed anomaly is more negative than the calculated. Overall the calculated anomaly seems to be narrower than the observed.

One way of explaining the differences is to assume that thicker sediments, older than the "Triassic event" are present under the flanks and near the south-eastern end of the basin but not under the centre of the basin. Using again the approximate formula $g = 0.042\ t\sigma$ (see chapter 3), in order to make up the 16.5mGal (the average gravity difference over the two flanks) 1.5km of sediments of 2480kg/m^3 (σ = 250kg/m^3) density are needed, or 2.5km of sediments of 2570kg/m^3 (σ = 160kg/m^3) density or 4km of sediments having a density of 2630kg/m^3 (σ = 100kg/m^3). These sediments must be of either Triassic, Permian, Carboniferous or Devonian age. The known

FIGURE 6/6

Gravity model along line AB. Bottom horizon represents the "intra-Permo-Triassic" event. See figure 5/7 for location of profile. Identification and density of layers are as follows: T: Tertiary (2250kg/m^3); u-J: Upper Jurassic (2400kg/m^3); lm-J, u-T?: Lower-middle-Jurassic and (?) Upper Triassic (2600kg/m^3); M: Mesozoic (2400kg/m^3).

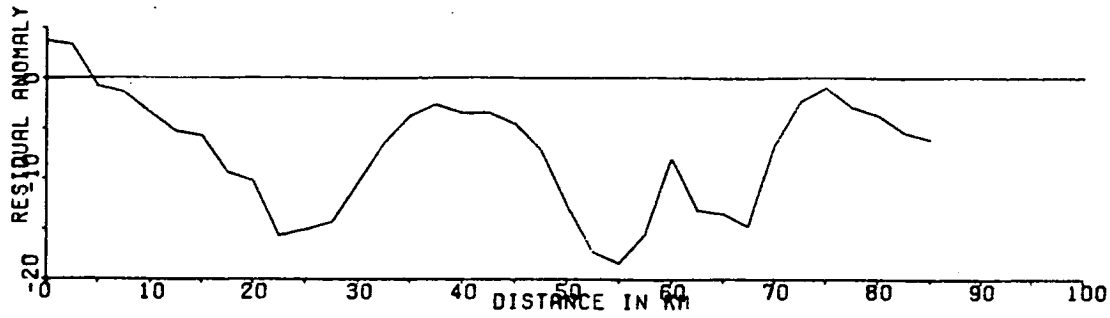
RESIDUAL ANOMALY
10
0
-10
-20
0
10
20
30
40
50
60
70
80
90
100
DISTANCE IN KM

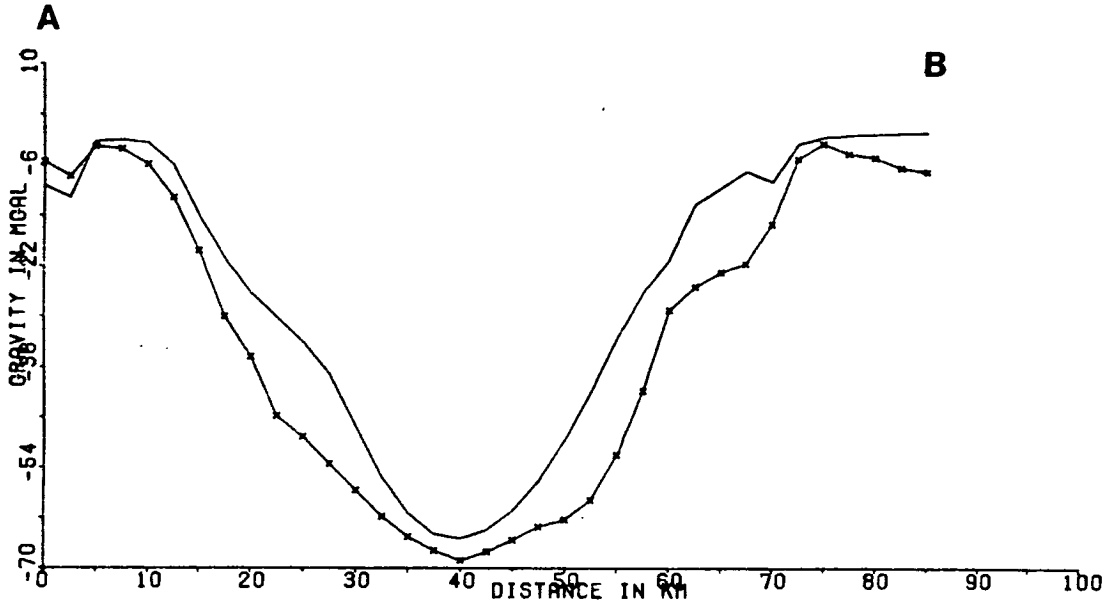
A
B
GRAVITY IN MGAL
10
-6
-22
-38
-54
-70
0
10
20
30
40
50
60
70
80
90
100
DISTANCE IN KM

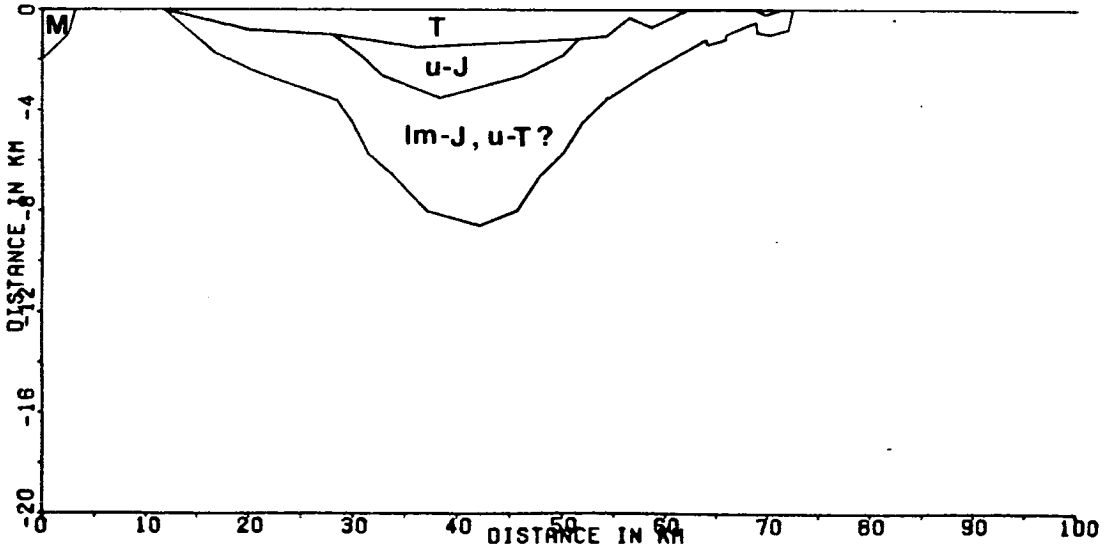
M
T
u-J
Im-J, u-T?
DISTANCE IN KM
0
-4
-8
-12
-16
-20
0
10
20
30
40
50
60
70
80
90
100
DISTANCE IN KM

densities for sediments of these ages in the area are as follows:

Triassic: (2550-2650)kg/m^3 (well data, Irish Sea)

Permian: 2650kg/m^3 (J Cornwell, pers. commun., S Wales)

Carboniferous: 2650kg/m^3 (Gibb, 1961, Wales; Thomas and Brooks, 1973, S Wales)

Devonian (Old Red Sandstone): 2550kg/m^3 (Gibb, 1961, Wales)

It is apparent that at least 2.5 to 3.0km of sediments are needed beneath the flanks to make up the observed difference, whereas no significant thickness of the same sediments should be present under the centre of the basin. The most likely geological model which could explain these differences (figure 6/7a) involves a ridge at the centre of a narrow deep graben. Since the profile lies near the centre of the St George's landmass, Carboniferous sediments of such thickness can be excluded (see also chapter 5). The existence of Permo-Triassic sediments of the order of 4km under the flanks only, and in addition to the Permo-Triassic sediments already included in the model, is questionable since no similar thicknesses have been reported in other Irish Sea basins (Colter and Barr, 1975; Jenner, 1981) and this hypothesis is not in agreement with data on sedimentation rates for this period (see also chapter 7), therefore the Permo-Triassic solution can also be excluded. There is no evidence against or for the additional presence of Devonian age rocks under the flanks, although in the author's opinion the fact that the two maxima of the gravity difference are only 30km apart is against this model also. Furthermore, there is no evidence in the available deep seismic records to support these geological models. Therefore, the presence of thicker sedimentary sections under the flanks of the basin as the cause of the difference between observed and calculated anomalies is not considered to be satisfactory and another more acceptable hypothesis is sought.

The alternative hypothesis favoured here is that the difference is due to salt migration from the centre to the flanks of the basin.

FIGURE 6/7

Geological models to explain lower gravity under the flanks of the basin.

a. The basement forms a graben with a horst at centre.

b. Basement with lateral density differentiation. $\rho_1 > \rho_2$

c. Tightly folded basement with two sediment pockets under the flanks of the basin.

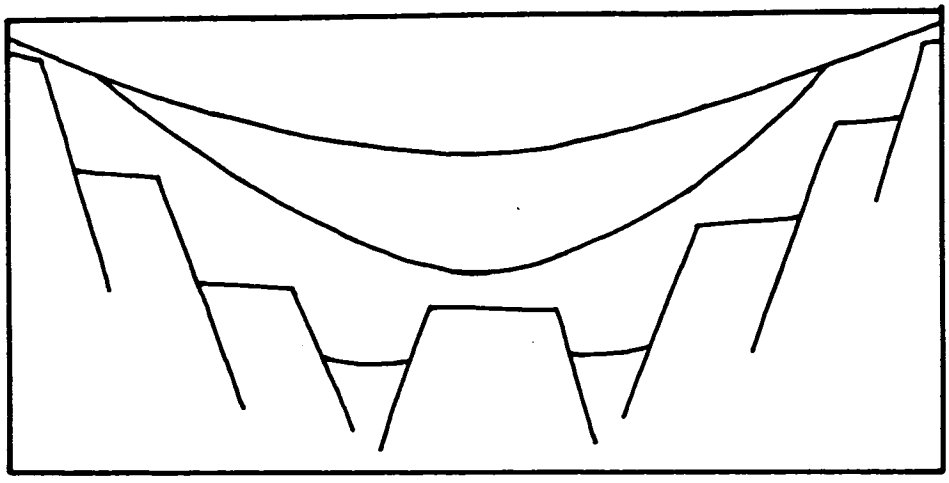

a

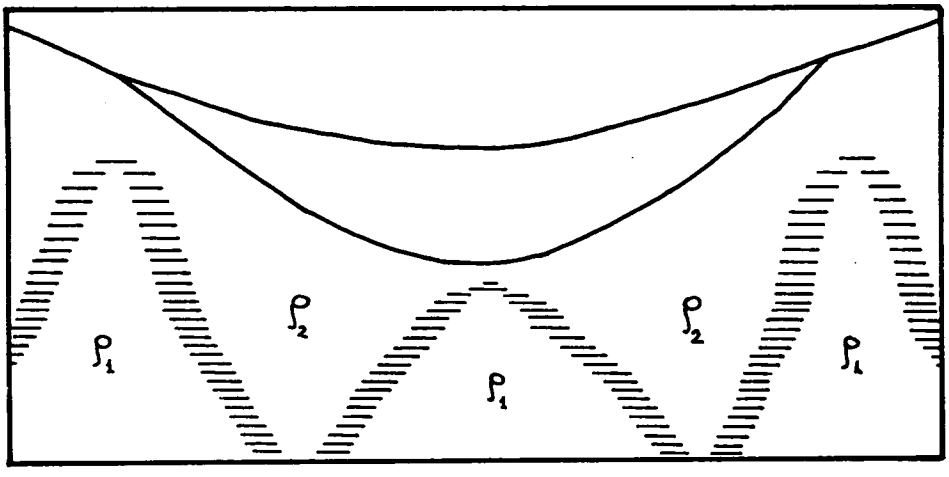

b

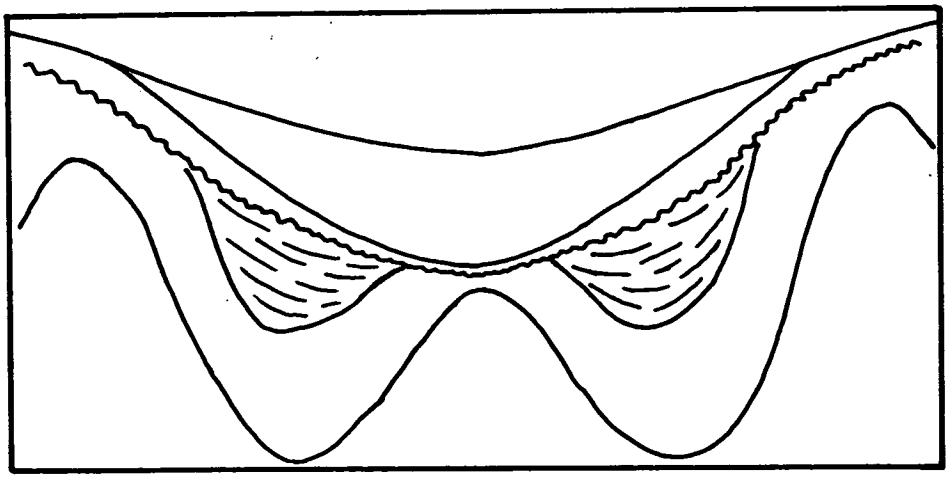

c

Such salt migration has been reported in the past for the Mansfield Basin in Germany, the Ebro Basin in Spain and the Transylvanian Basin in Rumania (Trusheim, 1960). The obvious evidence for such a movement is the presence of the salt wall in the south-eastern flank of the basin, but no apparent evidence, immediately related to salt structures, is seen in the north-western flank. Using the same approximate formula as above it was estimated that a maximum thickness of 700 and 850m of pure halite of 2080kg/m^3 density is needed to make up the observed gravity differences over the flanks of the basin. The quoted density for halite is indicated by well data.

The same order of differences was observed in the second model constructed with end coordinates 52°40'N, 5°35'W and 52°N, 4°55'W (figure 6/8). In order to verify the hypothesis of salt migration and to model it, supplementary information was requested from the Phillips Petroleum Company in the form of any seismic indication for such a movement and of spot depths to the lower observed strong horizon at the intersection points of their seismic survey with the two profiles. The company kindly provided a seismic section, shown in figure 6/9, from a north-south striking seismic line in the eastern part of the basin and all the available spot depths as requested. On this seismic section it is immediately apparent that there is a thickening of the assumed saliferous layer from the centre of the section towards the south, where the layer is associated with the formation of a salt structure, presumably the extension of the salt wall eastwards. Although some thickening of the same layer is observed in the northern part of the section, it is not so extensive as in the southern part and this is because the section crosses the north-eastern margin of the basin and not the north-western, where a similar thickening of the layer might be expected. It seems likely that salt migration has been caused by the difference in pressure from the sediments accumulating above the saliferous beds between the flanks and the centre of the basin. The rising temperature of the salt as its depth of burial was increased at the centre of the basin, is thought to have added to its mobility.

- FIGURE 6/8

Gravity model along line CD. Bottom horizon represents the "intra-Permo-Triassic" event. See figure 5/7 for location of profile. Identification and density of layers are as follows: T: Tertiary (2250kg/m^3); u-J: Upper Jurassic (2400kg/m^3); lm-J, u-T?: Lower-middle-Jurassic and (?) upper Triassic (2600kg/m^3); M: Mesozoic (2400kg/m^3).

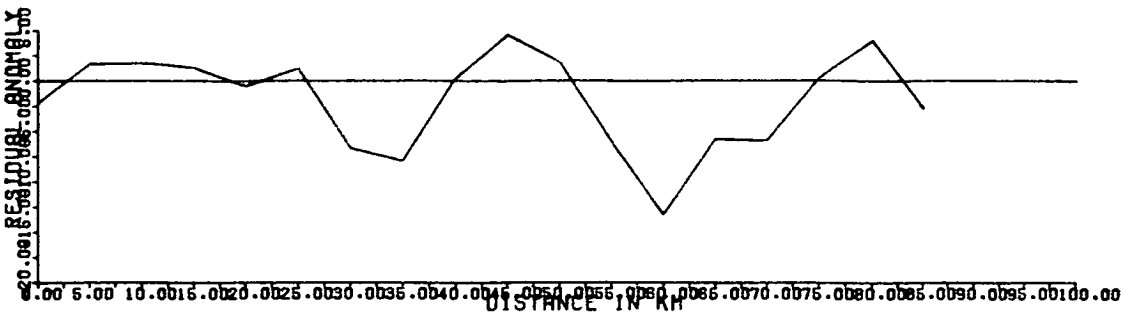
RESIDUAL ANOMALY
DISTANCE IN KM

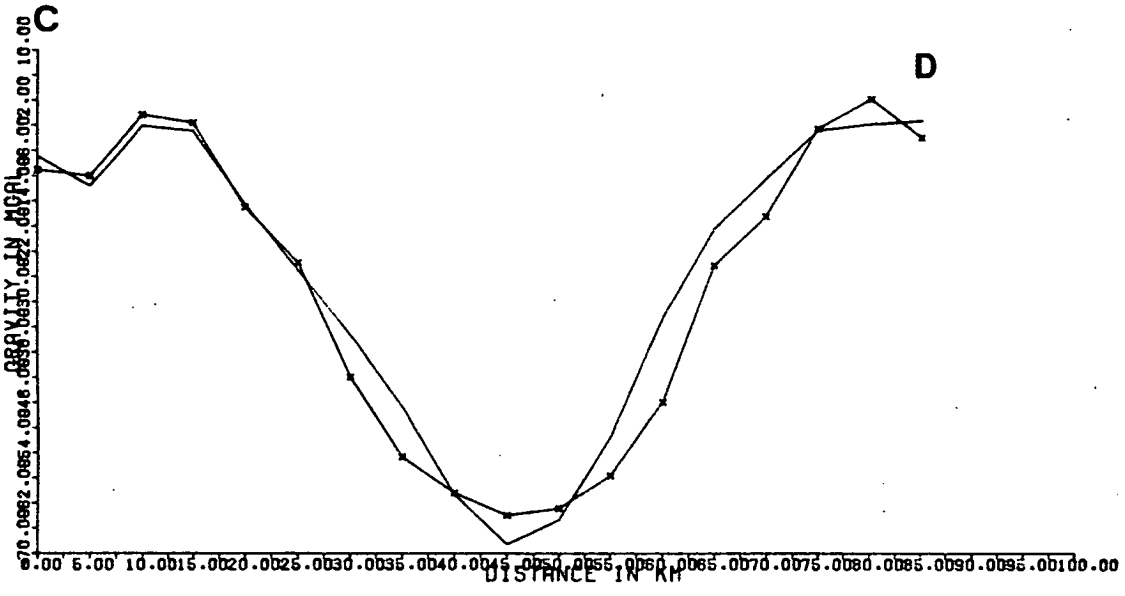
C
D
GRAVITY IN MGAL
DISTANCE IN KM

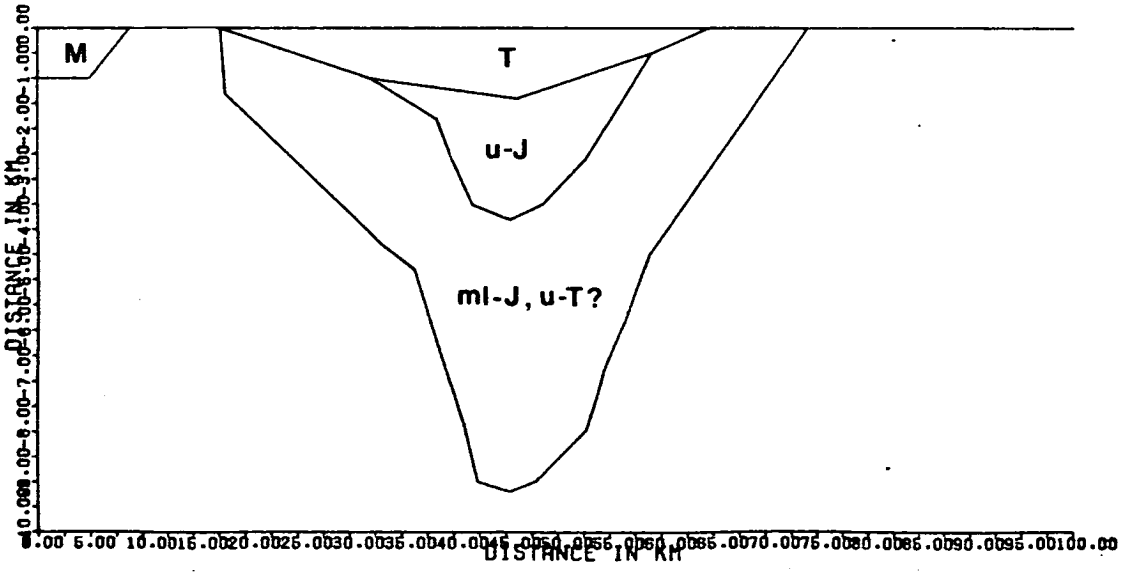
M
T
u-J
ml-J, u-T?
DISTANCE IN KM

FIGURE 6/9

N-S seismic section at the eastern part of the basin showing the saliferous layer (indicated by the two arrows) to thicken over the southern flank of the basin. Courtesy: Phillips Petroleum Company.

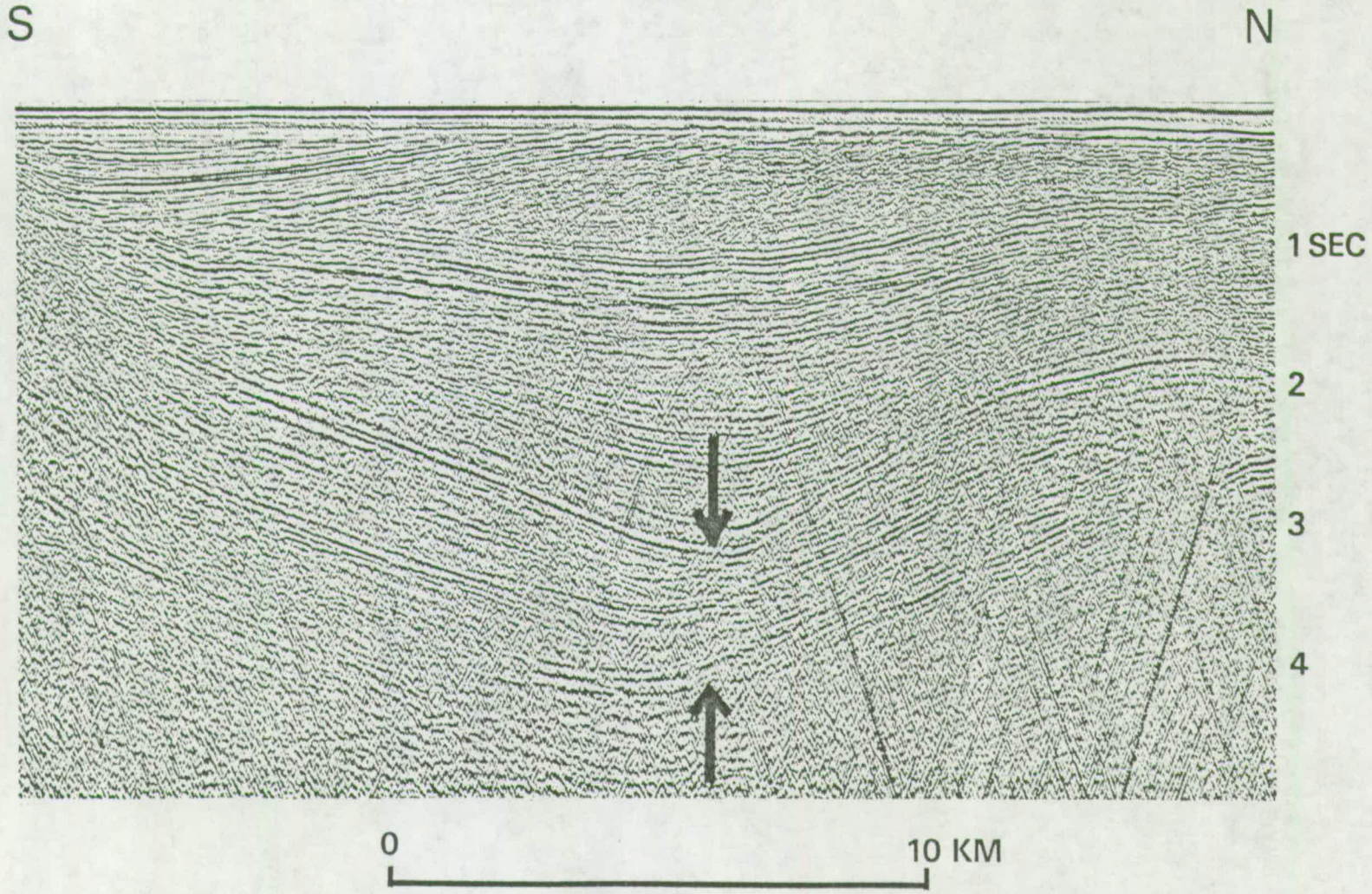
S
N
1 SEC
2
3
4
0
10 KM

The spot depths to the lowest observed horizon are shown on the models. It was possible to interpolate between them to form the base of the basin only on the first profile and there only for the south-eastern part where spot depths were available. As a means of modelling the effect of migrated halite, a "salt excess" interval was introduced in the upper part of the layer bounded by the "Permo-Triassic event" and the lowest observed horizon. This was done to ease modelling for it is realised that the salt may be distributed throughout the lowest layer introduced in the model. The shape of the "salt excess" layer on both the flanks of the basin is chosen to match the observed gravity differences. The good fit between observed and calculated gravity values at the centre of the basin before, and on the flanks after the inclusion of the "salt excess" layers (figure 6/10) implies that the lowest layer in the model has no significant effect and therefore its average density is similar to the one used for the basement (2730kg/m^3). Assuming that the saliferous beds within the basin occur only or mainly in the middle "Keuper shales" sequence as in wells 103/2-1 and 106/28-1 (figure 5/2) then the density of 2730kg/m^3 is consistent with the occurrence of anhydritic mudstones in the lower "Keuper shales" sequence in these wells. The total depth of the basin indicated by the model is over 10km which is 50% more than the estimation of Blundell et al (1971) and agrees well with the estimation of Barr et al (1981).

6.3 The Regional Gravity High over the Irish Sea

In order to find out the lateral extent of the high regional gravity values observed over the southern (Blundell et al, 1971) and northern Irish Sea (Bott, 1964) fourteen long gravity profiles were constructed. These profiles range from 550 to 700km in length and cover the area between 49° and 55°N and 0° to 10°W (figure 6/11). The data used to compile the profiles were: (1) gravity maps published by the Institute of Geological Sciences, (2) unpublished marine gravity data collected by the same Institute, (3) gravity map of Ireland published by the Dublin Institute for Advanced Studies, (4) Bouguer anomaly gravity map of Wales (Griffiths and Gibb, 1965), (5) Bouguer anomaly map of the North Celtic Sea (Davey, 1970) and (6) the gravity map of

FIGURE 6/10

Final model along line AB. The dots on the bottom horizon are the spot depths to the lowest observed reflective horizon. Provided by the Phillips Petroleum Company. Identification and density of layers are as follows: T: Tertiary (2250kg/m^3); u-J: Upper Jurassic (2400kg/m^3); lm-J, u-T?: Lower-middle-Jurassic and (?) upper Triassic (2600kg/m^3); m-T?: Middle Triassic and (?) the rest of Permo-Triassic (2730kg/m^3); M: Mesozoic (2400kg/m^3); S: Salt excess (2080kg/m^3).

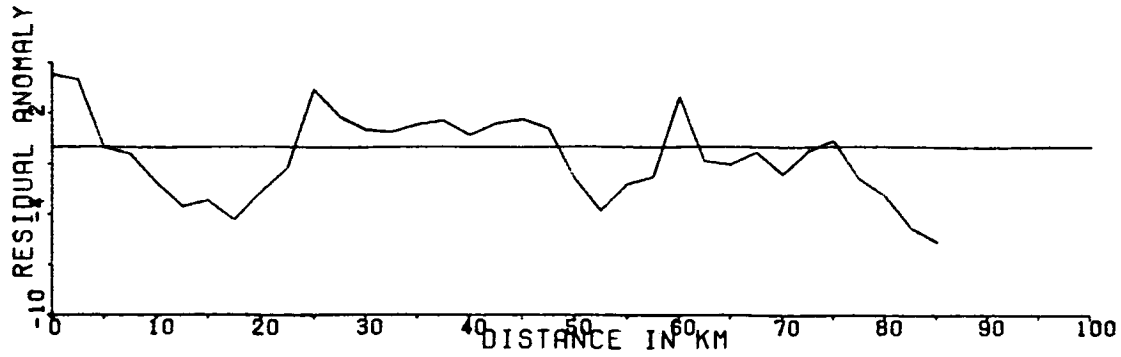
RESIDUAL ANOMALY
2
-1
-10
0
10
20
30
40
50
60
70
80
90
100
DISTANCE IN KM

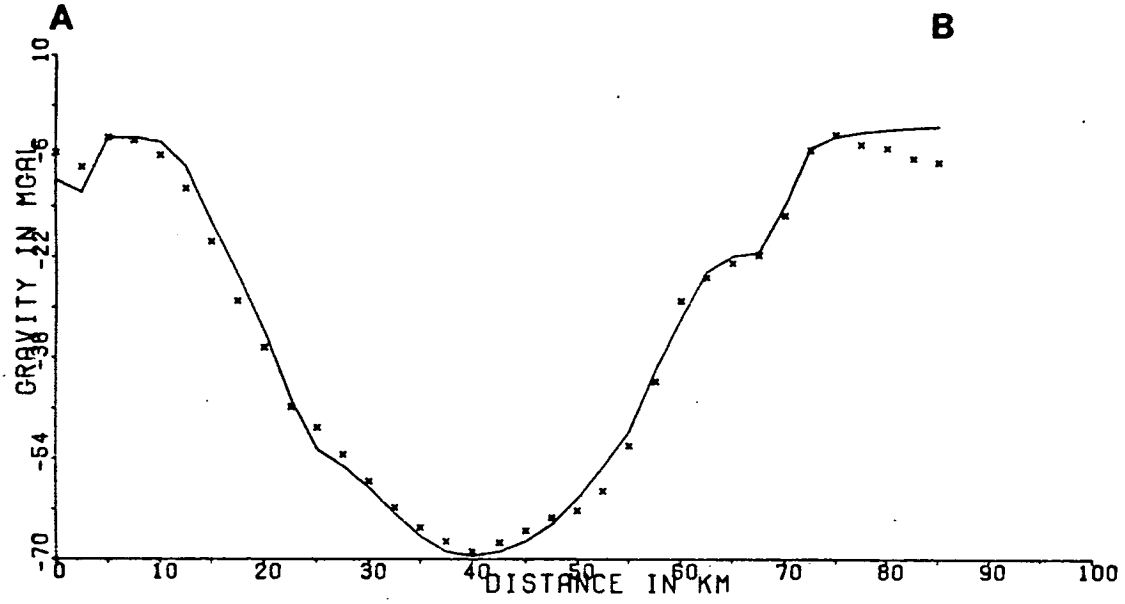
A
B
GRAVITY IN MGAL
10
-22
-38
-54
-70
0
10
20
30
40
50
60
70
80
90
100
DISTANCE IN KM

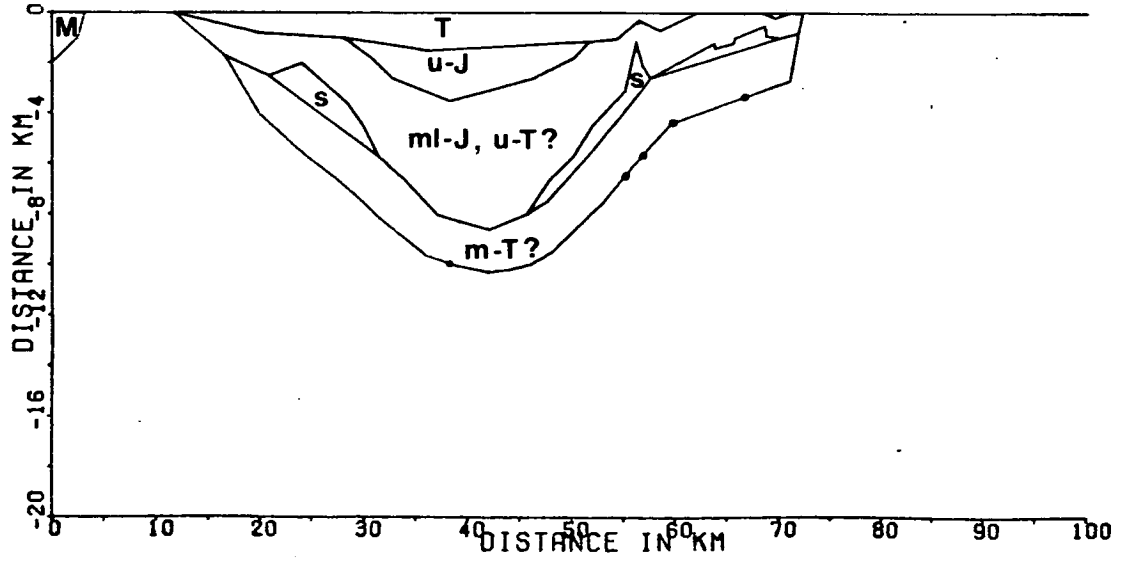
M
T
u-J
s
s
ml-J, u-T?
m-T?
DISTANCE IN KM
0
-4
-8
-12
-16
-20
0
10
20
30
40
50
60
70
80
90
100
DISTANCE IN KM

FIGURE 6/11

Location of the long gravity profiles constructed for the study of the regional gravity field of the Irish and Celtic Sea areas.

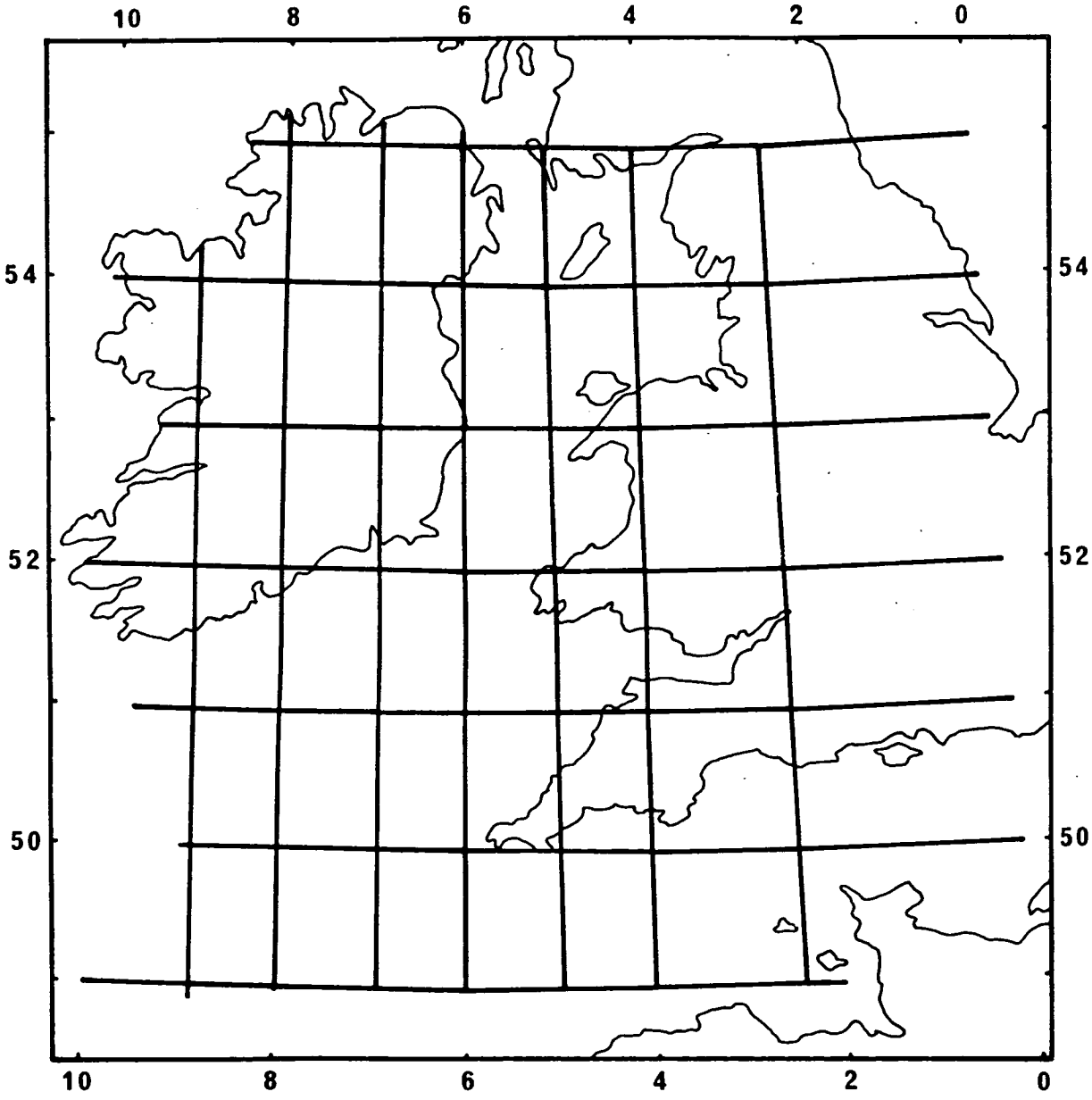
10
8
6
4
2
0
54
52
50

the south Irish Sea and Nymphe Bank (Blundell et al, 1971). Each profile was interpreted individually to find a regional curve and then the regional gravity values at the cross points of the profiles were checked against each other. Some of the profiles constructed are shown in figure 6/12, After the cross points were adjusted so their difference was of the order ±1mGal, the values of the regional field were posted and contoured (figure 6/13). A very long wavelength regional gravity effect was then removed. This effect is on average 0.01mGal/km in a direction away from the edge of the Continental Shelf and is thought to reflect the gradual increase of crustal thickness. It was best observed on the gravity profile running along 49°N. A similar very long wavelength regional change away from the Continental Edge is seen in the Moray Firth, see figure 3/6. The "residual" regional values were then contoured and the map produced is shown in figure 6/14. Although it can be argued that the interpretation of the long gravity profiles is subjective, the whole procedure, including the adjustment of the regional values at the cross points of the profiles and the smoothing during the contouring, reduces considerably the possibility of vast errors.

The final map (figure 6/14) shows clearly a regional gravity anomaly of +25mGal amplitude over the whole Irish Sea. The pattern of the anomaly is an elongated one, striking north-south over the Irish Sea/ Bristol Channel area before it turns to a north-east to south-west direction west of the Cornwall Peninsula. The cause of this regional anomaly is thought to be the 7.3km/s layer at the base of the crust, as has already been proposed (Blundell et al, 1971). The existence of the 7.3km/s layer in the south Irish Sea was confidently reported by Blundell and Parks (1969). The layer was reported to have a thickness of 5.5km, its base being at 29.9km. Another refraction experiment carried out in the north Irish Sea was not conclusive. It is described by Agger and Carpenter (1964) and was carried out for the calibration of the UKAEA seismometer array at Eskdalemuir. The line of charges fired in the northern Irish Sea runs from north Anglesey to the Solway Firth and was effectively unreversed. The interpretation of the Pg and Pn arrivals lacked the support of a good control of the near the surface layers and in view of all these uncertainties the crustal profile which was produced with thickness

FIGURE 6/12

Four of the constructed long gravity profiles. Vertical axes: observed gravity in mGal. Horizontal axes: distance in degrees of longitude or latitude. Dashed lines: interpreted regional field.

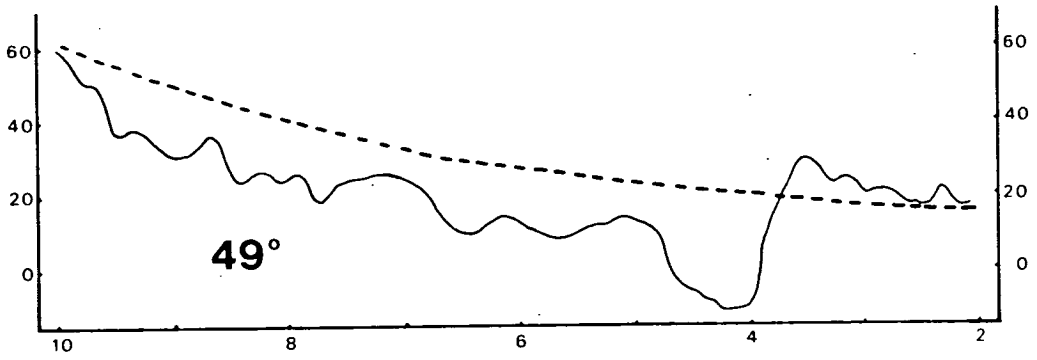
60
40
20
0
49°
10
8
6
4
2
60
40
20
0

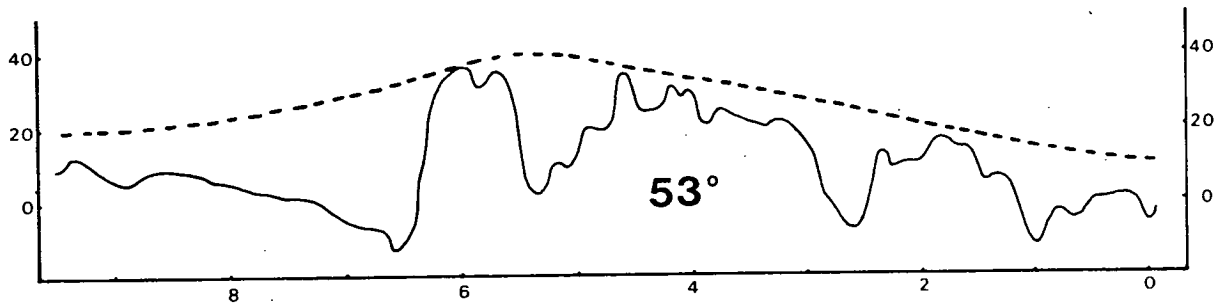
40
20
0
53°
8
6
4
2
0
40
20
0

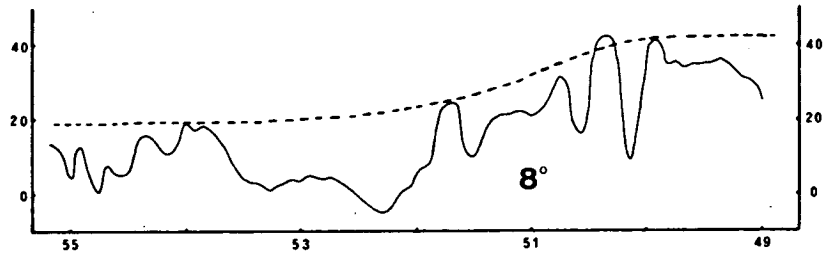
40
20
0
8°
55
53
51
49
40
20
0

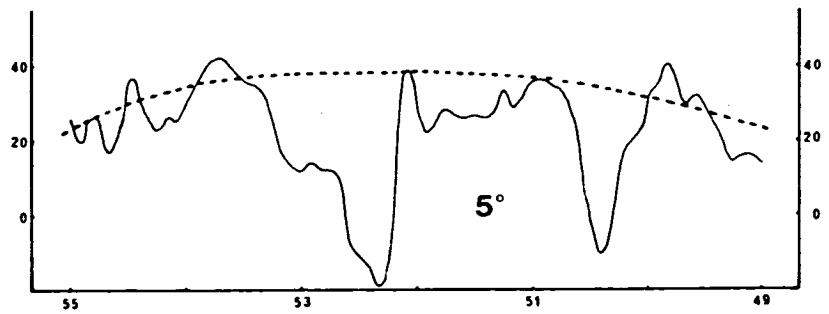
40
20
0
5°
55
53
51
49
40
20
0

FIGURE 6/13

Regional gravity map of the Irish and Celtic Sea areas. Contours at 5mGal intervals.

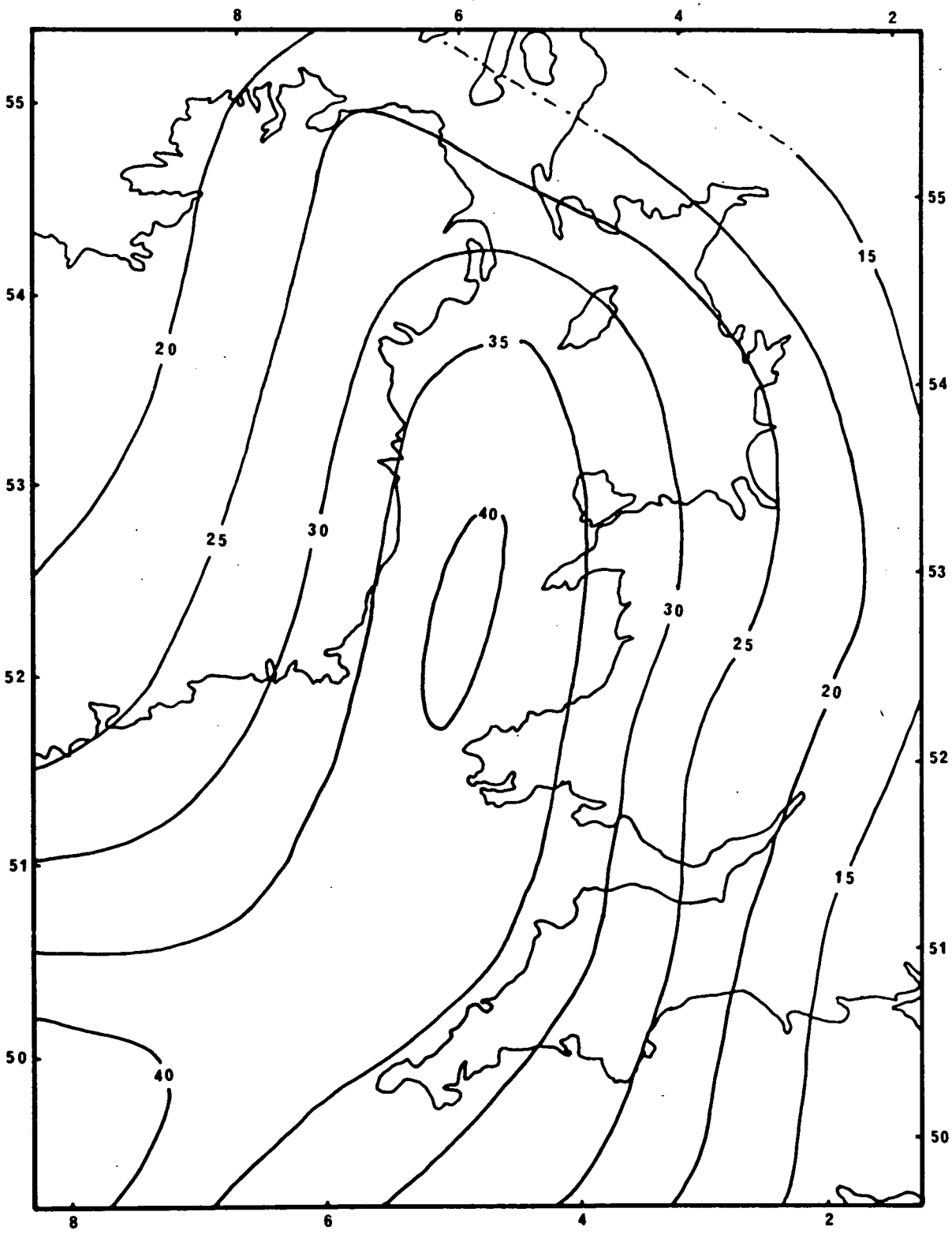
8
6
4
2
55
54
53
52
51
50
15
20
25
30
35
40

FIGURE 6/14

Regional anomaly gravity map of the Irish and Celtic Sea areas. Solid line: regional anomaly in mGal. Dashed line: thickness of the high velocity-high density layer at the bottom of the crust in km.

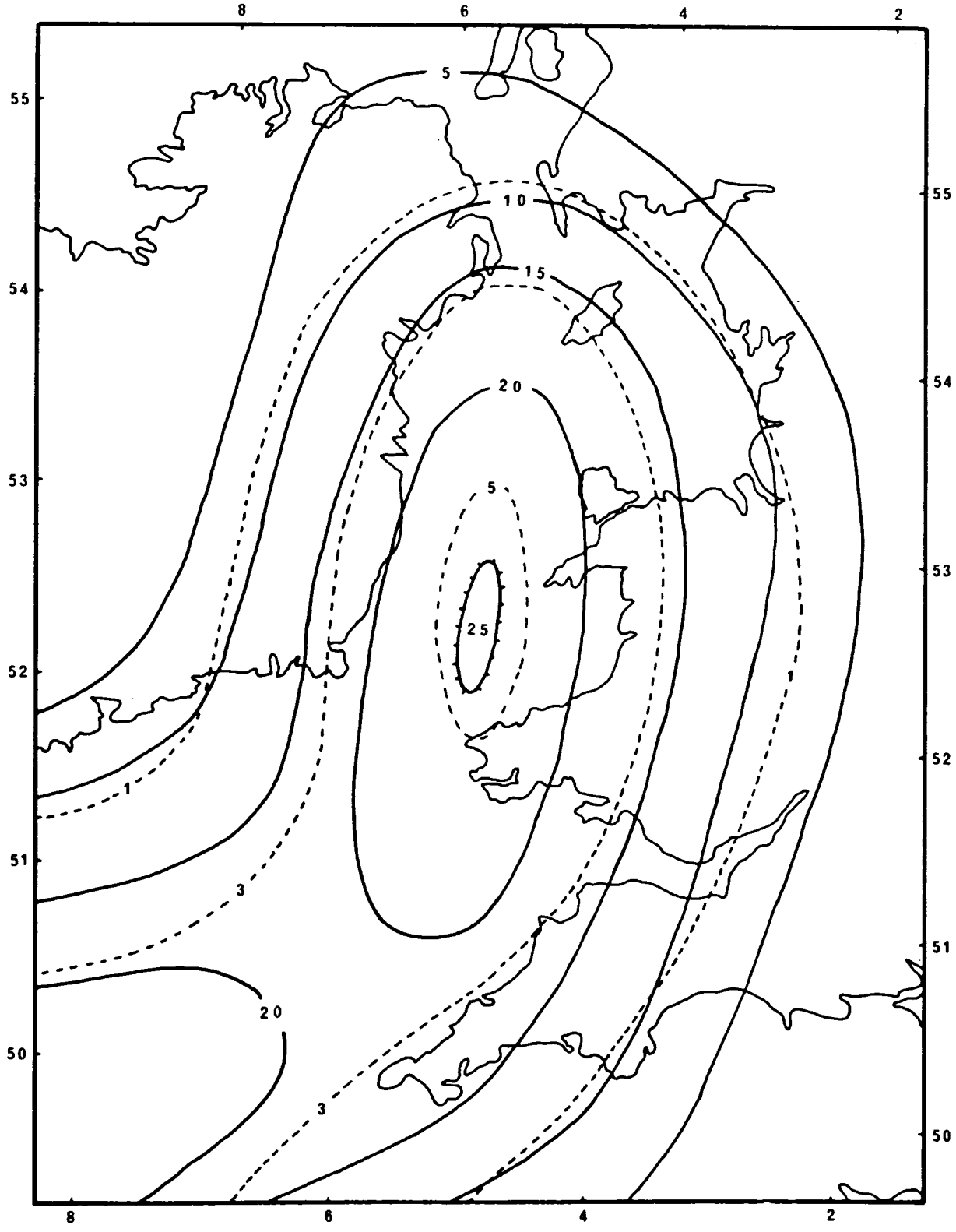
8
6
4
2
55
54
53
52
51
50
5
10
15
20
5
25
1
3
20
3

ranging between 23 and 34km becomes questionable.

A three dimensional model of the 7.3km/s layer was attempted assuming its base at a constant depth of 30km. The density adopted for this layer is 3000kg/m^3 indicated by the velocity-density curves (Ludwig et al, 1971). A density of 2850kg/m^3 was assumed for the lower crust. The resulting model is shown in figure 6/14. The edge effect imposed by the program used in the modelling did not permit the contouring of the layer's thickness to be completed towards the margins of the area. The model suggests a maximum thickness of 5.5km for the layer at the centre of the south Irish Sea and this is the same as the thickness indicated by the refraction data.

CHAPTER 7

CONCLUSIONS AND DISCUSSION

7.1 The Inner Moray Firth Basin

7.1.1 Introduction

Previous geophysical and geological work in the Inner Moray Firth Basin has defined in broad terms the extent, structure and history of the basin during the Mesozoic. The geophysical work presented in chapter 3 added the following to previous knowledge of the basin: (i) there is a difference between observed gravity over the basin and the gravity effect of the Mesozoic sediments which have a maximum thickness of 4.5km against the Great Glen Fault in the north-eastern part of the basin. This difference was explained as due to the presence of Old Red Sandstone sediments under the basin having an average thickness of 3km and to the presence of granite intrusions in the basin area. One granite intrusion is situated beneath the Central Ridge at the centre of the basin. Another granite intrusion in the inner part of the basin, calculated to be 12km thick, explains the discrepancy between the calculated gravity effect of the sediments (both Mesozoic and Old Red Sandstone) and the observed gravity in that area, first noted by Chesher and Bacon (1975). (ii) The Great Glen Fault shows a net throw of 2.5km in the north-eastern part of the basin. The throw decreases south-westwards towards the inner part of the basin, ie, the fault acted as a hinge fault in Mesozoic times. (iii) The long gravity profile across the basin shows no regional gravity high indicative of substantial crustal thinning under the area.

7.1.2 The formation of the Mesozoic Basin

In the light of the results summarised above, a renewed discussion of the formation of the basin is warranted.

The Inner Moray Firth Mesozoic basin overlies the southern part of the Orcadian Old Red Sandstone basin and although it has been the subject of later erosion is not thought to have extended much farther onshore, the high grounds of the Grampian and Northern Highlands having operated as physical boundaries for the basin. The boundaries of the Mesozoic basin are the Wick Fault to the north, the Great Glen and Helmsdale Faults to the north-west, the south boundary being partly fault controlled by the Banff Fault at its south-easternmost part, the rest being of onlap type on the Old Red Sandstone sediments of the south coast of the Moray Firth. To the east the basin continues into the outer Moray Firth Basin which is the extension of the Buchan-Witchground graben system (figure 2/9). Since the Wick and Banff Faults form the north and south boundary faults of this graben system and its extension westwards, it is logical to infer that the formation of the Inner Moray Firth Basin is related to the formation of the North Sea grabens.

The development of the Mesozoic Basin started during late Permian-early Triassic times, as evidenced by the age of the oldest Mesozoic sediments in the basin (see chapter 2). During this period extensional movements allowed the rapid subsidence of a complex graben and trough system in the North Sea area (Ziegler, 1978). The crustal fracture along the Buchan and Witchground grabens, defined as one arm of a triple junction by Whiteman et al (1975) and underlain by thinned crust (Christie and Sclater, 1980; Donato and Tully, 1981) is thought to have propagated westwards defining the lines of the Wick and Banff Faults. It is logical therefore to assume that the Inner Moray Firth Basin was formed as a result of the extensional mechanism responsible for the formation of the major North Sea grabens. McQuillin et al (in preparation) define the direction of the tensional forces during the late Permian-early Triassic times as a NE-SW one and propose the formation of a graben system between the Wick and Banff Faults. Extensional movements alone allow a maximum subsidence within the graben of just under 2km. The estimation of this subsidence is based on a post Permo-Carboniferous dextral movement of 7-8km along the Great Glen Fault. According to McQuillin et al this movement is restricted to the part of the fault south-west of Wick, the junction of the Wick and Great Glen Faults

being sealed. The 7-8km dextral movement corresponds to an average (pulling apart) extension δL = 5.35km between the two faults. The present distance between the two faults is L + δL = 86km. If D is the initial thickness of the crust and δD the total subsidence of the graben, then $\delta D/D = \delta L/L$ assuming that there is no crustal thinning beneath the developed graben. The NW-SE long gravity profile crossing the Inner Moray Firth Basin (figure 3/6) does not show a regional gravity high associated with crustal thinning similar to the North Sea grabens (Donato and Tully, 1981). In contradiction to this, Smith and Bott (1975), based on the results of a refraction line running from Peterhead to just north of Wick, suggest depths to the base of the crust of 22.0, 22.8 and 29.4km for the south-eastern, middle and northwestern parts of this line, implying that a substantial crustal thinning occurs beneath the basin. This crustal thinning corresponds to a gravity anomaly of the order of +100mGal, which as just mentioned is not observed over the area. In the absence of gravity support for such a substantial thinning under the basin, it is thought that a thickness of D = 29-30km is a good representation of the depth to the base of the crust under the Inner Moray Firth area. This crustal thickness is expected to produce a graben of 1.85km maximum subsidence, assuming no crustal thinning under it. McQuillin et al assume a crustal thickness of 32km, the same as under the East Shetland Plateau (Christie and Sclater, 1980), and therefore, since the extension factor is 1.066, they predict a maximum graben thickness of 2.00km. The E-W extension produced an additional subsidence of the order of 0.10km only.

Let us now compare the typical graben formation predicted by purely extensional mechanism, to the shape and total thickness of the Inner Moray Firth Basin as revealed by the deep seismic data. IGS seismic line 6 is the furthermost NW-SE running line and a depth conversion of it is shown in figure 7/1. It is seen from this section that the average thickness to the base of Jurassic is about 2.0km and that the basin is rather of a half-graben shape, tilted to the north-west, than of a symmetrical graben shape with similar throw at both margins. In order to estimate the maximum thickness of the basin we should add an average thickness of 0.5km of

Permo-Triassic sediments as well as an average thickness of 1.0km of post-Lower Cretaceous sediments eroded off during a regional uplift of the Scottish Highlands (Neville George, 1966). The total maximum thickness of the basin is thus estimated to have been 3.5km along the seismic line 6. The basin is thought to be thicker farther to the east where Upper Cretaceous and Tertiary sediments are preserved. It is seen therefore that the extensional model for the formation of the basin does not explain either the tilted shape of the basin or its total thickness, the predicted maximum subsidence of the basin being about half of the maximum estimated thickness. In addition to these differences the curve representing the subsidence of the basin has been plotted on the diagram of the predicted subsidence of grabens having different extension factors β (McKenzie, 1978). The base of Jurassic has been taken as the time of initiation of the basin since this is the lowest horizon recognisable within the basin. The three subsidence points plotted on the diagram correspond to the base Middle Jurassic, base Cretaceous and the intra-Lower Cretaceous event of the interpretation of seismic line 6 by Chesher and Bacon (1975), at a point where the depth to the base of Jurassic is the same as the average depth to this horizon throughout this seismic line. It is clear that the extension factor $\beta = 1.066$ is too small to produce the total observed subsidence of the basin and also that the basin subsided at a greater rate than the value of $\beta = 1.066$ would indicate. Indeed the slope of the basin's subsidence curve is similar to the one predicted for basins having an extension factor of $\beta = 4.0$ (figure 7/2). An additional mechanism to account for the differences referred to above was therefore sought.

The additional mechanism to be examined is that of a north-eastwards tilted Grampian Highlands due to the uplifting effect of the extensive granites which occur within this block. The significance of these granites in producing uplift is not known, but the extent of their outcrops (see the Sub-Pleistocene geology map, inside back cover) and their gravity effect, as seen on the Regional Gravity Map of Northern Britain, warrant further investigation. The uneven mass distribution of a tectonic unit can produce a torque within it.

FIGURE 7/1

Depth conversion of IGS seismic line 6. From McQuillin *et al* (in preparation).

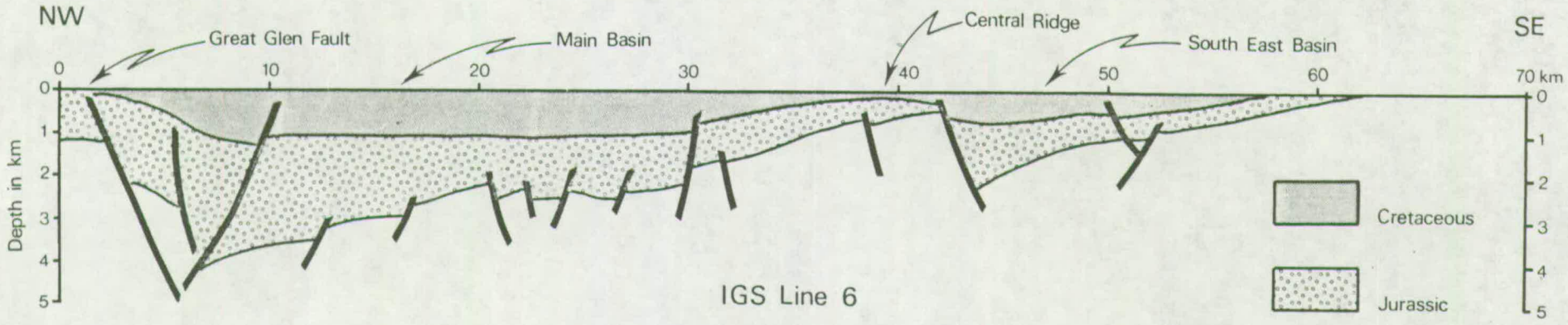
NW
SE
Great Glen Fault
Main Basin
Central Ridge
South East Basin
0
10
20
30
40
50
60
70 km
Depth in km
0
1
2
3
4
5
Cretaceous
Jurassic
IGS Line 6

FIGURE 7/2

Subsidence of a developing through extension graben as a function of t, where t is in My. Left vertical axis: depth of the graben when it is filled by water. Right vertical axis: thickness of sediments (having a density of 2500kg/m^3) filling the graben. 1: Subsidence curve for the Inner Moray Firth Basin. 2: Subsidence curve for the St George's Channel Basin assuming initiation at the beginning of the Permian. 3: Subsidence curve for the St George's Channel Basin assuming initiation at the beginning of the middle Triassic. Redrawn from McKenzie (1978).

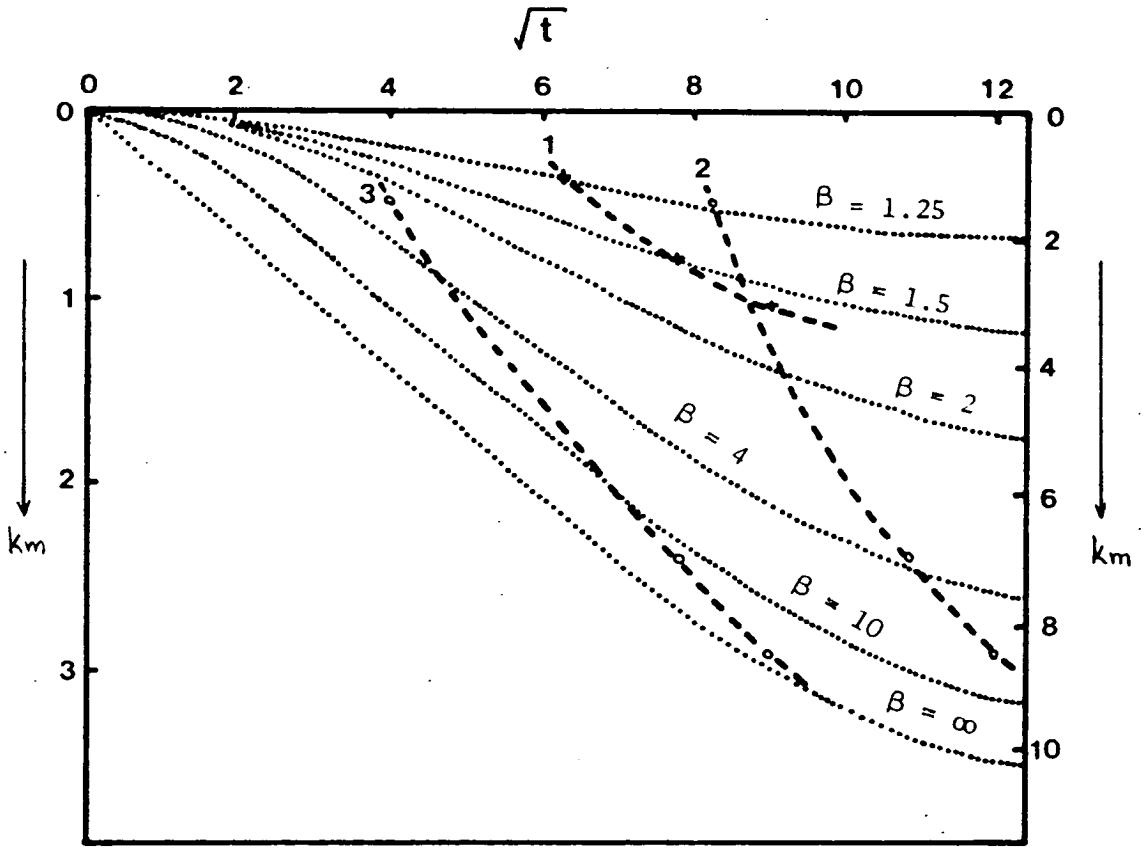
√t
0
2
4
6
8
10
12
1
2
3
β = 1.25
β = 1.5
β = 2
β = 4
β = 10
β = ∞
km
km

FIGURE 7/3

The extent of the Grampian Highlands tectonic unit as examined here. The dotted line divides the unit into two areas of different gravity values: positive to the north-east and negative to the south-west. The stippled areas have moved (in the vertical direction) on a reverse way than their regional gravity field suggests. 1: Wick Fault. 2: Banff Fault. CMD: Centre of mass of deficit masses. CMU: Centre of mass of whole tectonic unit. CME: Centre of mass of mass excesses.

If the tectonic unit is not in isostatic equilibrium, then this torque will tend to tilt the tectonic unit until equilibrium is reached. The uneveness of the mass distribution within a tectonic block is reflected in its gravity field. It is possible to outline the distribution and estimate the magnitude of the mass deficit and excess within the block from the gravity anomalies over the block. The total torque on the block can be calculated from the magnitude of the mass excess and deficit and their distribution relative to the centre of mass of the block. The procedure to calculate the total torque, if there was any when the basin started developing, includes the definition of the block's boundaries, reconstruction of the block's gravity field at the beginning of the Permo-Triassic and using this, calculation of the centres of the mass anomalies, and finally the calculation of the total torque the two mass anomalies would produce.

The boundaries of the Grampian Highlands tectonic unit onshore are the Highland Boundary and Great Glen Faults. In defining the offshore boundaries of the unit, the Highland Boundary Fault line was extended to the point where it meets the western margin of the Central Graben and then round the Halibut Horst to meet the Wick Fault which is thought to represent the northern boundary of the unit. The south-western boundary of the unit is difficult to define with any accuracy because both the Great Glen and the Highland Boundary Faults run offshore in the Malin Sea. The boundary shown in figure 7/3 was chosen in such a way as to avoid the Tertiary igneous activity which has affected the western part of Scotland and which would probably disturb the Permo-Triassic gravity picture of the area.

In order to reconstruct the gravity field of the unit the gravity effect of the post Permo-Triassic sediments should be compensated for and the effect of the mass eroded from the onshore area taken into account. The regional gravity map of Northern Britain (Hussein and Hipkin, 1981), which is a smoothed version of the Bouguer anomaly map (using a 4km filter) and in which the post-Triassic sediments of the Inner Moray Firth have been compensated for (using

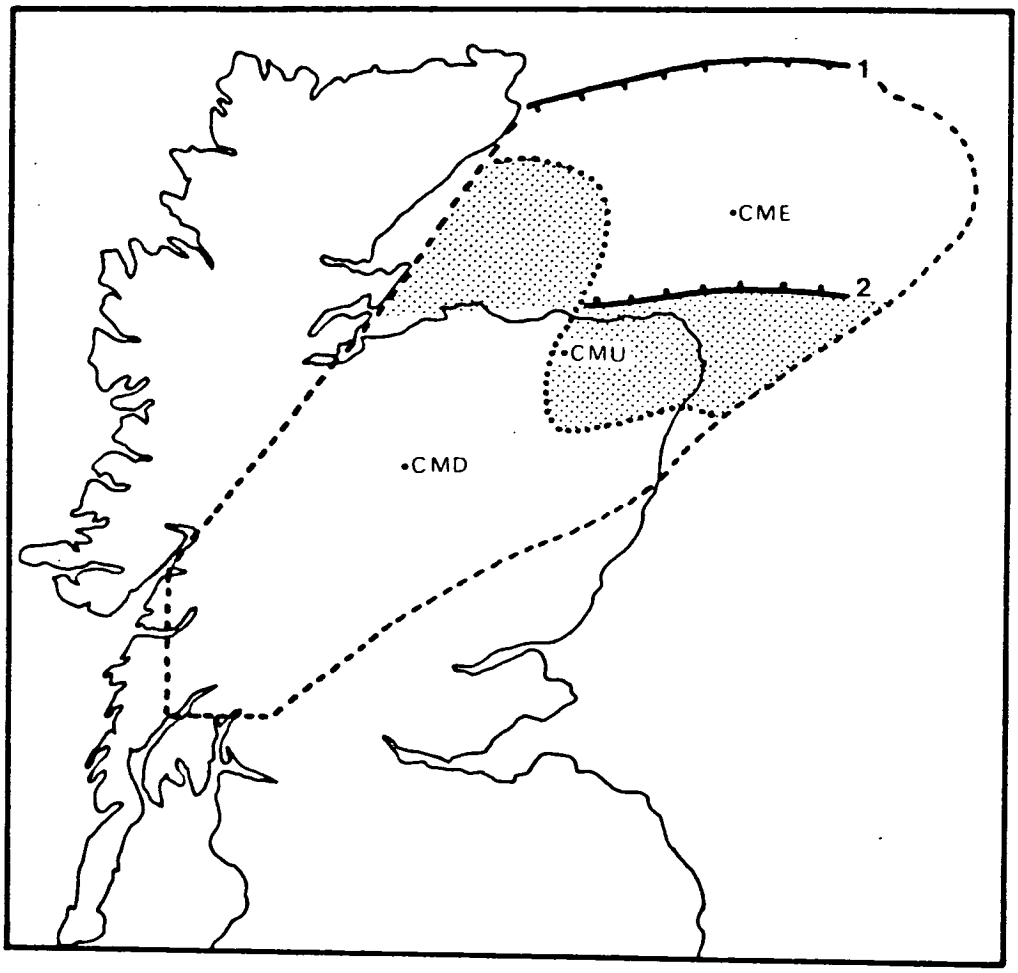
1
2
•CME
•CMU
•CMD

a density contrast of 300kg/m^3) was used as the gravity information source for the onshore part of the tectonic unit and the part of the offshore area west of a N-S line running through Fraserburgh. For the rest of the unit to the east of this line the published IGS Bouguer anomaly maps corrected for regional changes due to crustal thinning under the North Sea (Donato and Tully, 1981) were used and the gravity effect of the sediments was estimated using a density contrast of 400kg/m^3, taking into account the presence of Upper Cretaceous and Tertiary sediments in this area. The area was divided in squares of 10km side and the gravity values over each square were averaged. No estimation of the gravity effect of the eroded off masses from the onshore area has been made.

The total mass deficit and excess, corresponding to areas of negative and positive regional gravity values respectively, as well as their centre of mass, were calculated in the method described by Grant and West (1965), and found to be:

$$M_D = 11.13 \times 10^{15}\text{kg} \text{ and } M_E = 7.33 \times 10^{15}\text{kg}$$

The corresponding centres of mass deficit and mass excess as well as the centre of mass of the whole tectonic unit are shown in figure 7/3. No "tailing off" corrections (see Nettleton, 1976, page 214) have been applied on the calculations which also assume that the zero gravity contour represents the absolute limit of the deficit and excess masses. The estimated deficit and excess masses indicate a net mass deficit over the whole tectonic unit $M_D = 3.80 \times 10^{15}$kg. More significantly the centres of the deficit and excess masses lie on either side of the tectonic unit's centre of mass, thus the uplifting and downwarping forces corresponding to these masses produce a torque which tends to tilt the whole block to the north-east. The magnitude of this torque is: $T = (M_D.X_D + M_E.X_E).g = 1.53 \times 10^{21}$Nm. If we assume that the tectonic unit is represented by a rigid block floating in the lower crust, then as the block tilts an opposite torque is developed and tends to stop further tilting. The way of estimating this opposite torque is described in Appendix III. The angle φ at which

equilibrium occurs is estimated to be $\varphi = 0.14^{o}$. This angle produces a net downthrow between the unit's centre of mass and its north-eastern margin of the order of 400m or 130m at the junction of the Wick and Great Glen Faults. Thus, the mechanism of whole block tilting under the influence of the distribution of the deficit and excess masses within it does not adequately explain the difference between the extensional mechanism's predictions and the actual shape and total subsidence of the basin.

An alternative hypothesis which takes into account the mass distribution within the tectonic unit is one which assumes that the unit consists of two blocks, one having a mass deficit of M_D, the other a mass excess of M_E, moving vertically and independently. Supporting evidence for this hypothesis is the distribution of the gravity values over the tectonic unit, as seen on the Regional Gravity Map of the British Isles, Northern Sheet (Hussein and Hipkin, 1981). Practically the whole of the onshore area (apart from its north-eastern part) and the inner part of the basin has negative regional gravity values (therefore indicating mass deficit) whereas the rest of the area has positive values (thus indicating mass excess). The two areas of generally negative and positive regional gravity values are shown in figure 7/3. If we assume that the deficit and excess masses are concentrated within the upper crust and that the two blocks were kept at the same level at a certain time (for example due to compressional forces), and then leave the two blocks to move freely, it is expected that the mass deficit area will rise within the upper crust to reach hydrostatic equilibrium whereas the mass excess area will subside pushing downwards the rigid part of the crust beneath it until the whole subsiding block reaches an equilibrium by floating into a denser ductile material, for example the lower crust. As the mass excess block subsides sediments will accumulate on it. The height Y to which the mass deficit block will rise and the total subsidence of the mass excess block (which is equal to the thickness of the accumulated sediments) t are given by the following formulae (see Appendix III for derivation):

$$Y = \frac{M_D}{S_D} \cdot \frac{1}{\rho_u} \qquad \text{and} \qquad t = \frac{M_E}{S_E} \cdot \frac{1}{\rho_f - \rho_s}$$

where M_D, M_E, S_D and S_E are the deficit and excess masses and their corresponding lateral extent, ρ_u and ρ_s the upper crustal and accumulating sediments' density, and ρ_f the density of the material in which the subsiding dense block floats. The lateral extent of the anomalous mass cannot be defined with accuracy. The best indication for the boundary of the anomalous body is the gravity gradient around the anomaly. If we assume that the body is of prismatic shape with nearly vertical sides, then the steepest gradient roughly outlines the anomalous body. It is therefore reasonable to assume that the whole anomalous mass is a vertical prism of surface S defined by the steepest gravity gradient. The steepest gradient around the negative anomalies onshore is about -15 to -20mGal, whereas offshore the steepest gradient of the positive anomalies is not as clear and is roughly between +10 and +20mGal. The table shown below assumes that the positive anomalous mass (mass excess) extent is defined by the +10, +15 and +20mGal contours and leaves the rigid block beneath it to float into material ranging in density from 2850kg/m^3 (typical lower crust density) to 3300kg/m^3 (mantle density). The numbers in the table represent the maximum thickness in kilometres of the accumulated sediments having a density of 2400kg/m^3. For comparison the subsidence of the whole positive area (this assumes that the mass excess is evenly distributed throughout the area of positive gravity values) has been included in the left-hand column of the table.

TABLE 1

Predicted Maximum Subsidence of a Vertical Column Containing a Mass excess $M_E = 7.33 \times 10^{15}$kg, floating in material of density ρ_f and covered by sediments of density $\rho_s = 2400 kg/m^3$. S_E is the cross sectional area of the column

$\rho(Kg/m^3)$	$S_E(m^2)$			
	1.84×10^{10} ($g \geqslant$ 0mGal)	1.31×10^{10} ($g \geqslant$ +10mGal)	0.98×10^{10} ($g \geqslant$ +15mGal)	0.58×10^{10} ($g \geqslant$ +20mGal)
$\rho_f = 2850$	0.89	1.24	1.66	2.81
$\rho_f = 3000$	0.66	0.93	1.25	2.11
$\rho_f = 3150$	0.53	0.75	1.00	1.69
$\rho_f = 3300$	0.44	0.62	0.83	1.40

It is seen from the table that this mechanism predicts an additional subsidence of the developing basin of the same order as the difference between estimated maximum basin subsidence and the extensional mechanism model.

As geological evidence for the differential vertical movements of two blocks characterised by positive and negative gravity values respectively, we can refer to the presence of the Banff Fault. This fault is thought to be a result of the extensional mechanism and roughly divides the Grampian Highlands tectonic unit into two parts: to the north of it is the area of positive gravity values whereas to the south-west of it is the negative gravity values area. It is interesting to note that the fault dies out to the west where it reaches the area of extensive granitic material under the innermost

part of the Moray Firth. Thus, it is thought that the presence of this fault facilitated the subsidence of the area north of it. It is also interesting to see that two areas, the innermost part of the Moray Firth and the north-east corner of the Grampian Highlands (the two areas are shown in figure 7/3) show a vertical movement, the reverse of that expected by their gravity field. The north-eastern part of the Grampian Highlands south of the Banff Fault of positive gravity values being attached to the block of negative gravity values has remained at a higher level than the positive gravity area north of the fault. In a similar way the innermost part of the Moray Firth of negative gravity values is attached to both the negative and positive gravity values blocks. As a result this area is dragged down by the block north-eastwards of it and is pushed up by the block to the south of it, the combined result being the north-eastward tilting of the inner part of the basin. The uplift of the negative gravity values block is estimated to be 300m if we assume that the anomalous mass is outlined by the -15mGal contour line and that it rises freely within an upper crust of 2720kg/m^3 density. The comparison of this value with that of the present day average topography of the central Grampian Highlands (the average level is of the order of 1km) is thought to be a further indication that additional uplift of the area occurred as a part of a much wider region.

From the above discussion it is concluded that the Moray Firth basin is the combined result of the extensional mechanism, responsible for the development of the North Sea graben system, and of a subsidence mechanism due to differential distribution of anomalous masses within the upper crust over the whole Grampian Highlands tectonic unit.

The subsidence of the inner basin follows a similar history to that of the North Sea grabens until the Lower Cretaceous although certain significant differences exist. The period between Permo-Trias and Lower Cretaceous is characterised by a rifting phase in the North Sea grabens with normal fault development and subsidence along these faults. This was accompanied by crustal thinning (though notably not beneath the Inner Moray Firth - see below), and doming of the area to produce the predominant unconformities

observed in these grabens. The Triassic sequence is not as well developed in the Moray Firth as in the North Sea, as the former was at the margin of a broadly subsiding area during this period (a few hundred metres of Triassic sediments in the Inner Moray Firth Basin (Chesher and Lawson, in press) compared with about 3km in the North Sea (Ziegler, 1978)). During the Jurassic and Lower Cretaceous the sedimentation in both the Inner Moray Firth Basin and the North Sea grabens is quite similar. The Kimmerian unconformities are present in the basin but to a lesser extent than in the graben. The high subsidence rate during the Upper Jurassic observed along the marginal faults of the grabens in the North Sea, resulting from a tensional NE-SW regime in the crust, is also observed against the Great Glen Fault in the Moray Firth.

Whatever the similarities and differences in the development of the Inner Moray Firth Basin and the North Sea grabens up to the Lower Cretaceous their history afterwards is distinctively different. In the North Sea a phase of broad regional subsidence during the period Upper Cretaceous to the end of the Tertiary is recognised, whereas in the Inner Moray Firth, although relatively thin Upper Cretaceous sediments are thought to have been deposited, these were eroded off during the Tertiary. The broad subsidence of the North Sea during this period has been explained in terms of gravity pulling from the loading of the cooling magma of a thinner crust under the grabens (Donato and Tully, 1981), or by thermal cooling in response to stretching (Christie and Sclater, 1980). As already mentioned (chapter 3) the gravity results indicate no shallowing of the Moho under the Inner Moray Firth Basin. The presence of a very narrow zone of crustal thinning or a narrow dense intrusion can not be ruled out, but their effectiveness in driving subsidence would in any case be limited.

The internal structure of the basin was influenced by the presence of granite batholiths in the basement under the basin. The role of these batholiths in supporting the Central Ridge horst which divides the basin into two sub-basins has already been mentioned. The thick batholith in the innermost part of the basin is thought to have restricted the rapid subsidence of this area, resulting

in a basement platform covered by gently dipping parallel layers of sediments which turn to a more sagging shape close to the Great Glen Fault (see photograph of seismic line 3, figure 3/9). The uniform thickness of the layers over this platform and their north-westwards dip indicate the type of differential movements described above. The differentiation of subsidence along the Great Glen Fault resulted in the deepest part of the basin forming at about the cross section of seismic line 6 and the fault, and not in the inner part of the basin.

7.2 The St George's Channel Basin

7.2.1 Introduction

The gravity modelling across the St George's Channel Basin has led to a better understanding of its structure and evolution. The results of this interpretation may be viewed as follows: (i) The basin reaches a thickness of 10-11km. About 5km of these sediments lie between the top Middle Jurassic and the "Permo-Triassic event" horizons. (ii) The most important result in this study was the interpretation of the difference in wavelength between observed and calculated gravity anomalies across the basin in terms of salt migration from the centre to the flanks of the basin (chapter 6). On the south-eastern flank, the salt has intruded the walls of a normal fault and formed the salt wall seen to outcrop under the Quaternary cover in the south-western part of the basin (figure 5/1). The model in figure 6/10 suggests that the net throw of the south-easternmost fault to bound the basin is 2.5-3.0km. (iii) The regional gravity investigation of the south-western British Isles revealed the broad extent of high regional gravity previously reported for the north and south Irish Sea as well as the amplitude of the regional anomaly. The anomaly covers the whole Irish Sea trending N-S before turning to ENE-WSW direction and has an amplitude of 25mGal. This anomaly is interpreted as due to an intrusion of dense material at the base of the crust, reaching a thickness of over 5km under the south Irish Sea, as originally proposed by Blundell et al (1971). The implications of this regional gravity anomaly and its cause are discussed below.

7.2.2 The formation and development of the basin

The origin of the basin goes back to late Carboniferous times. During the Carboniferous the southern Irish Sea area was part of the St George's landmass which extended into Ireland and Wales and provided detritus to the Carboniferous basins around it. From the latest Carboniferous times, depositional basins adopted a new style, being mostly fault controlled troughs separated from each other by discrete horsts or massif blocks. Movements occurred along old structural lines inherited from the Caledonian and earlier periods of deformation and also from structures newly formed during the Hercynian orogeny. These blocks and basins (one of them is the St George's Channel Basin) resulted from differential movements within the basement (Anderton et al, 1979). No reason for the cause of these differential movements was given by Anderton et al. During the same period uplift started affecting much of the area north of the Hercynian front. An erosional phase during latest Carboniferous to early Permian times is evidenced by the substantial unconformity between Carboniferous and Permian rocks in the northern Irish Sea (Kish Bank, Irish Sea and Cheshire Basins) and between Carboniferous and Triassic rocks in the southern Irish Sea (St George's Channel Basin, Bristol area). The difference in age of the sediments above the unconformity in the north and south is thought to be due to the additional uplifting effect of the Hercynian front in the latter.

Let us consider the formation of the basin as the result of lateral extension of the crust. If we assume that the bottom of the crust is defined by the top of the high-velocity layer (see chapter 6), then an average thinning of δD = 2.75km extended for a distance of $L + \delta L$ = 300-450km (from western Ireland to the east of Wales, see figure 6/14. Assuming that the thinning of the crust occurs only at the base of it and that the initial thickness of the crust was 30km, then from the relationship $\delta D/D = \delta L/L + \delta L$ an extension δL = 39km is calculated and therefore an extension factor β = 1.10 (where $\beta = (L+\delta L)/L$). If we assume that the thinning at the base of the crust is accompanied by similar thinning and consequent sedimentation

at its top, then an extension factor $\beta = 1.18$ is estimated (see Appendix III for derivation). In the second case a wide geosyncline basin is expected with a maximum thickness of 3.7km, assuming an average sediment density of 2500kg/m^3. Subsidence data from the St George's Channel Basin, based on the model shown in figure 6/10 have been plotted on the diagram of predicted subsidence of basins formed as a result of extensional mechanism for different values of β (figure 7/2). Two different curves have been produced. Curve 2 assumes beginning of the basin at early Permian times (as suggested by the age of the sediments above and below the unconformity in the northern Irish Sea), whereas curve 3 assumes a mid-Triassic time for the beginning of the basin (as suggested by the age of the oldest sediments in well 103/2-1). Both curves indicate much quicker subsidence of the basin than basins with larger extension factor β. The total thickness of the basin (about 10km) is also a lot larger than the maximum predicted thickness of basins with similar extension factor (1.6km for $\beta = 1.25$).

It is seen from the above discussion that the basin cannot be explained as the result of a pull-apart extension mechanism. Yet the sequence of events, as described at the beginning of this paragraph, in association with the existence of the high velocity layer at the bottom of the crust (Blundell and Parks, 1969), suggest that the area may have been related to rift system development. Lower Permian time is a period of rifting in NW Europe (Ziegler, 1978). It is thought that the intrusion of hot light mantle material at the base of the crust shortly after the latest Carboniferous resulted in an uplift and doming of the Irish Sea area accompanied by fracture of the upper crust and the development of block and basin tectonics. The age of the doming period can be concluded from the age difference of the sediments above and below the Carboniferous-Permian unconformity. The youngest known Carboniferous sediments below the unconformity are of Stephanian age in the Kish Bank Basin (Jenner, 1981), whereas the oldest Permian rocks are of a probable Lower to Middle Permian age in the Irish Sea and Cheshire Basins (Colter and Barr, 1975). Thus an early Permian age is the most probable period for the doming of the Irish Sea area.

During the Upper Permian and Lower Triassic there was sedimentation mainly in the northern basins of the Irish Sea, but the rate of sedimentation during this period was much lower than at later times (Colter and Barr, 1975). The reason for this low sedimentation rate is thought to be the slow subsidence of the newly formed basins in association with the arid climate of the area during the period. The slow subsidence may reflect local stress conditions in the Irish Sea area that prevented the lateral expansion of the crust and consequently significant vertical movements along the normal faults which controlled the development of the basins (figure 7/4).

The subsidence rate gradually increased and reached its maximum probably during the period late Triassic to early-mid Jurassic times. The rapid subsidence after mid-Triassic times is thought to be the result of the development of a tensional regime in the crust during the period (Ziegler, 1978) coupled with the gravity pulling effect of the cooling high velocity-high density layer at the base of the crust. The presence of a tensional regime during the Upper Triassic is supported by the fissure deposits in E-W trending fractures in Carboniferous limestones in the Mendips and South Wales (Anderton et al, 1979). The sedimentation rate remained at high level during the whole Jurassic in the southern Irish Sea area due partly to a transgression of the sea from the south during the Lower Jurassic, which persisted throughout the period. As already mentioned (chapter 5) there are no proven Cretaceous sediments in the Irish Sea, and the Tertiary sedimentation (as seen on the sub-Pleistocene geology map of the British Isles, inside the back cover) is restricted to the southern Irish Sea only. The subsidence rate of the Irish Sea area due to the loading effect of the high density layer at the base of the crust is expected to increase with time after the doming phase, to reach a maximum and then to decrease again in a similar way with the North Sea grabens (Donato and Tully, 1981). It is not possible to time exactly the maximum subsidence rate in the St George's Channel Basin because the centre of the basin has suffered an additional subsidence due to the migration of salt from this part of the basin and also because no single well (figure 5/2) contains a complete section of Triassic to Tertiary sediments to allow a comparison to

FIGURE 7/4

Normal faulting and basins' location around the south Irish Sea.
1: Solway Basin; 2: Irish Sea Basin; 3: Cheshire Basin;
4: Kish Bank Basin; 5: Cardigan Bay Basin; 6: St George's Channel
Basin; 7: Bristol Channel Basin; 8: Hercynian Thrust front line.

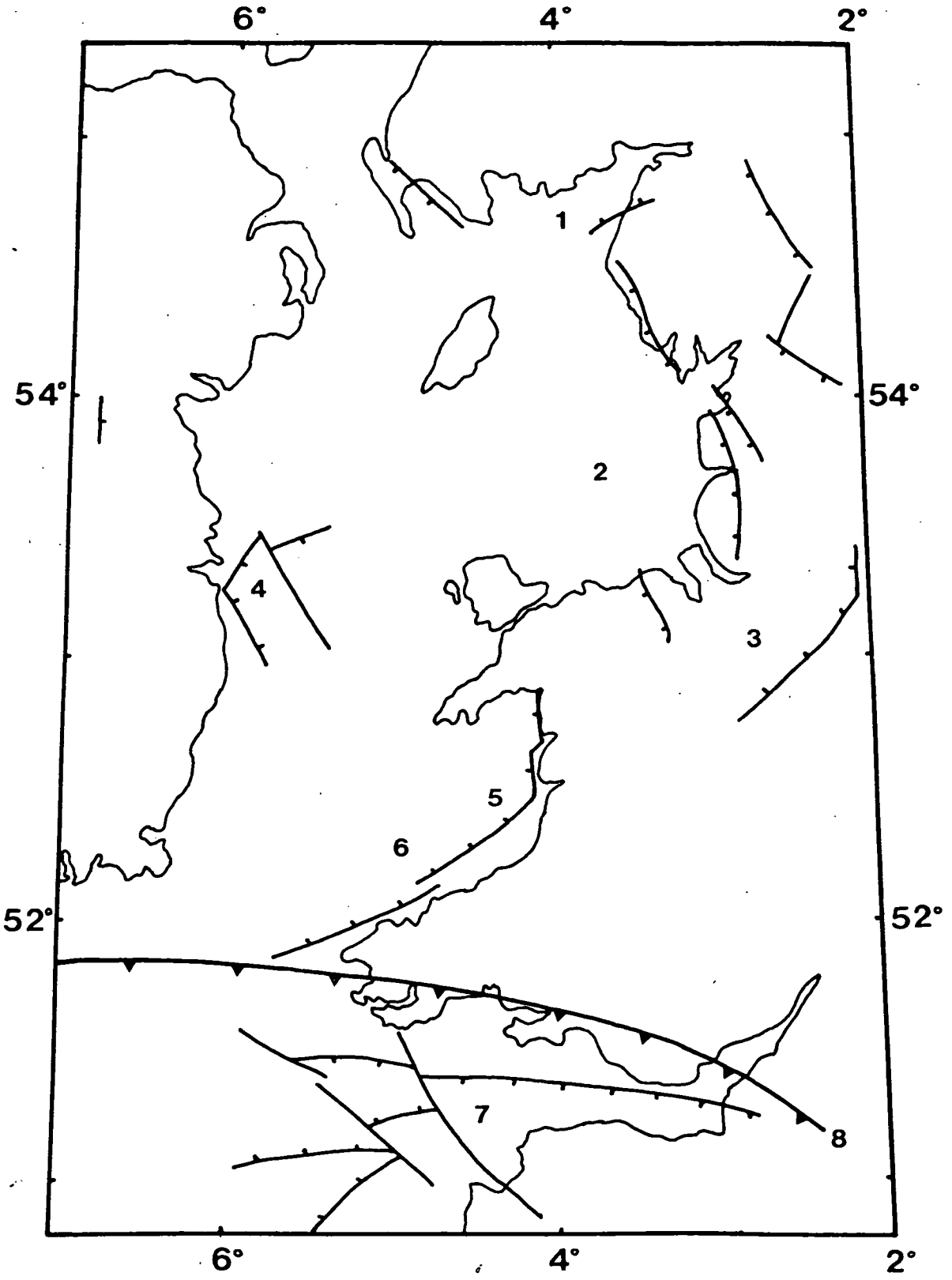
6°
4°
2°
54°
52°
1
2
3
4
5
6
7
8

be made. The very thick Upper Triassic sequence indicated by wells 103/2-1 and 106/28-1 is thought again to be biased by the migration of the salt at this layer from the centre to the flank of the basin where the two wells are located. Judging from the model of figure 6/10, a Lower Jurassic time is probably the best estimation for the maximum sedimentation rate and therefore the maximum subsidence rate. This is about 90Ma after an assumed early Permian doming period. For comparison the corresponding time between doming and maximum subsidence rate for the Central and Viking Grabens in the North Sea is 85 and 55Ma respectively. The comparison is seen to be quite good in the case of the Central Graben, the dimension (width) of which resembles better that of the Irish Sea rather than that of the Viking Graben. Thermal subsidence is not taken into account here, but it could not have been very important because sedimentation in the Permian-Lower Triassic period does not reveal the rapid pulse expected immediately after doming has ceased.

The St George's Channel Basin formed as explained above, is the deepest known in the western UK area. The basin is bounded by the St Tudwal's Arch to the north-east, the extension of the Pembrokeshire Peninsula to the south-west, the Irish Sea Geanticline to the north-west and the Pembrokeshire Peninsula to the south-east. The last of these boundaries is clearly fault controlled by the Bala Fault system. Of the other margins the north-east margin is shown on the two-way time seismic structure maps (figures 5/6, 5/7) to be faulted, the south-west margin is probably of onlap type over the Palaeozoic ridge and the north-west margin shows faulting at its deepest structural levels near its north-east end. There is little information on the south-west part of the north-western margin. The inconclusiveness of the seismic data in this part of the basin as well as the complex fracture pattern observed in the north-eastern part are probably both a result of the migration of salt towards the north-western margin of the basin. The steep gravity gradient across the north-west flank of the basin on the modelled profiles, along with the presence of the extremely thick sedimentary sequence against it would suggest the north-west margin of the basin is indeed fault controlled and similar to the south-east. The existence of

intra-basin faults in the south-eastern part of the basin and the salt's migration towards the flanks and intrusion into one of the faults is thought to have facilitated the further subsidence of the central part of the basin in that it produced an additional sagging at the centre of the basin. These features could have encouraged additional accumulations of sediments there and consequently further sagging due to the additional weight of the sediments and so on, resulting in the shape of the basin as seen in the models. The shape is apparently that of a syncline, but no compressional tectonics are envisaged. The history of the basin and its relation to the palaeo-environments from Triassic onwards is discussed in Barr et al (1981).

The change of trend of the regional gravity anomaly from N-S over the Irish Sea to ENE-WSW south of Ireland (figure 6/13) is suggested to be due to the presence of a separate rift system running in the latter direction. This fracturing is thought to have occurred during Upper Jurassic-Lower Cretaceous times and to be associated with the opening of the Atlantic. Similar fractures of an Atlantic continental margin are observed in South America (Urien and Zambrano, 1973). The existence of this rift explains the restriction to the south Irish Sea of sedimentation during the Tertiary as well as the absence of any Cretaceous sediments.

7.3 Comparison of the Moray Firth and St George's Channel Basins

The two basins share some common features. Both were initiated during Permo-Triassic times having a Caledonide trend and exhibit continuous subsidence during the Jurassic. Both are fault controlled at one of their margins, the Moray Firth Basin by the Helmsdale-Great Glen Fault system, the St George's Channel Basin by the parallel faults of the Bala Fault system, whereas the facing margin seems to be of onlap type over the older sediments of the north coast of the Grampian Highlands in the former case and over the Irish Sea Geanticline in the latter case. Both areas finally have suffered an erosional period in late Mesozoic-early Tertiary times, but while no further subsidence and sedimentation after this period is observed in the Inner Moray Firth Basin, the St George's Channel Basin was the subject of considerable subsidence during the Tertiary and

Quaternary times.

Despite the common features and similar subsidence history during most of the Mesozoic, the two basins show two totally different mechanisms for their initiation. The Inner Moray Firth Basin has been developed as the combined result of an extensional mechanism and of differential vertical movements of two blocks of positive (subsidence) and negative (uplift) gravity values respectively. On the other hand, it is thought that the St George's Channel Basin resulted from the intrusion of light mantle material at the base of the crust and the subsequent doming and fracture of the crust, followed by localised subsidence of individual basins against more stable upthrusting blocks. The difference of the two mechanisms is probably reflected in the difference of the maximum depth of the two basins. The subsidence of the narrow St George's Channel Basin against the Palaeozoic ridges of the Pembrokeshire Peninsula and the Irish Sea Geanticline was helped by a ductile flow on a relatively small scale in the lower crust (Bott, 1976), whereas in the Inner Moray Firth Basin case the frictional forces on the walls of the Great Glen Fault acted always against subsidence of the basin. The result is that the St George's Channel Basin is about two and a half times deeper than the Inner Moray Firth Basin, being about half in width. Thus although both basins subsided during a tensional regime, the subsidence of the former basin was much faster.

Further research in the two areas can define better the significance of these factors controlling the subsidence of the two basins and help to a better understanding of the development of small individual sedimentary basins.

REFERENCES

AGGER, H.E. & CARPENTER, E.W. 1964. A crustal study in the vicinity of the Eskdalemuir seismological array station. Geophys. J.R. astr. Soc., vol. 9, pp. 69-83.

ANDERTON, R., BRIDGES, P.H., LEEDER, M.R. & SELLWOOD, B.W. 1979. A Dynamic Stratigraphy of the British Isles. George Allen & Unwin Ltd., London, 301pp.

ARKELL, W.J. 1933. The Jurassic System in Great Britain. Clarendon Press, Oxford.

ARTEMJEV, M.E. & ARTYUSHKOV, E.V. 1971. Structure and isostasy of the Baical rift and the mechanism of rifting. J. Geophys. Res., vol. 76, pp. 1197-1211.

ASHCROFT, W.A. & WILSON, C.D.V. 1976. A geophysical survey of the Turriff Basin of Old Red Sandstone, Aberdeenshire. Jl. Geol. Soc. London, vol. 132, pp. 27-43.

ASSUMPCAO, M. 1978. Studies of crustal shear waves and Poisson's ratio. PhD Thesis, University of Edinburgh.

ASSUMPCAO, M. & BAMFORD, D. 1978. LISPB-V. Studies of crustal shear waves. Geophys. J.R. astr. Soc., vol. 54, pp. 61-73.

BACON, M. & CHESHER, J.A. 1975. Results of recent geological and geophysical investigations in Moray Firth, Scotland. Norges geol. Unders., vol. 316, pp. 99-104.

BAMFORD, D., FABER, S., JACOB, B., KAMINSKI, W., NUNN, K., PRODEHL, C., FUCHS, K., KING, R. & WILLMORE, P.L. 1976. A lithospheric seismic profile in Britain - I. Preliminary results. Geophys. J.R. astr. Soc., vol. 44, pp. 145-160.

BAMFORD, D., NUNN, K., PRODEHL, C. & JACOB, B. 1977. LISPB-III. Upper crustal structure of northern Britain. Jl.Geol. Soc. London, vol. 133, pp. 481-488.

BAMFORD, D., NUNN, K., PRODEHL, C. & JACOB, B. 1978. LISPB-IV. Crustal structure of northern Britain. Geophys. J.R. astr. Soc., vol. 54, pp. 43-60.

BARIA, R. & McCANN, D.M. 1973. Density, porosity and sonic velocity determination on selected rock types from Foyers, Inverness-shire. Engineering Geology Unit, Inst. Geol. Sci., Rep. No. 21.

BARR, K.W., COLTER, V.S. & YOUNG, R. 1981. The geology of the Cardigan Bay-St George's Channel Basin (pp. 432-443) in Petroleum Geology of the Continental Shelf of North-West Europe. Illing, L.V. and Hobson, G.D. (editors). Heyden & Son, London.

BENNISON, G.M. & WRIGHT, A.E. 1969. The Geological History of the British Isles (pp. 406). Edward Arnold, London.

BERRIDGE, N.G. & IVIMEY-COOK, H.C. 1967. The geology of a Geological Survey borehole at Lossiemouth, Morayshire. Bull. Geol. Surv. Gt. Br., vol. 27, pp. 155-169.

BLUNDELL, D.J., KING, R.F. & WILSON, C.D.V. 1964. Seismic investigations of the rocks beneath the northern part of Cardigan Bay, Wales. Q. Jl. geol. Soc. London, vol. 120, pp. 35-50.

BLUNDELL, D.J., DAVEY, F.J. & GRAVES, L.J. 1968. Sedimentary basin in the south Irish Sea. Nature, vol. 219, pp. 55-56.

BLUNDELL, D.J., DAVEY, F.J. & GRAVES, L.J. 1971. Geophysical surveys over the south Irish Sea and Nymphe Bank. Jl Geol. Soc. London, vol. 127, pp. 339-375.

BLUNDELL, D.J. & PARKS, R. 1969. A study of the crustal structure beneath the Irish Sea. Geophys. J.R. astr. Soc., vol. 17, pp. 45-62.

BOTT, M.H.P. 1964. Gravity measurements in the north-eastern part of the Irish Sea. Q. Jl. geol. Soc. London, vol. 120, pp. 369-396.

BOTT, M.H.P. 1968. The geological structure of the Irish Sea Basin (pp. 93-115) in Geology of Shelf Seas. Donovan, D.T. (Editor). Oliver and Boyd, Edinburgh.

BOTT, M.H.P. 1971. Evolution of young continental margins and formation of shelf basins. Tectonophysics, vol. 11, pp. 319-327.

BOTT, M.H.P. 1976. Formation of sedimentary basins of graben type by extension of the continental shelf. Tectonophysics, vol. 36, pp. 77-86.

BOTT, M.H.P., ROBINSON, J. & KOHNSTAMM, M.A. 1978. Granite beneath Market Weighton, East Yorkshire. Jl. Geol. Soc. London, vol. 135, pp. 535-543.

BRIDEN, J.C. & DUFF, B.A. Pre-Cenozoic palaeomagnetism of stable Europe and the British Isles. Rep. International Dynamics Commission, no. 10 (in press).

BROOKS, J.R.V. & CHESHER, J.A. 1975. Review of the offshore Jurassic of the northern North Sea (pp. 1-24) in Jurassic Northern North Sea Symposium. Finstad, K.G. and Selley, R.C. (Editors). Vol. 2, Stavanger, September 1975.

BROWN, G.C. & LOCKE, C.A. 1979. Space-time variations in British Caledonian granites: some geophysical correlations. Earth Planet Sci. Lett., vol. 45, pp. 69-79.

BROWNE, B.C. & COOPER, R.I.B. 1950. The British submarine gravity surveys of 1938 and 1946. Phil. Trans. Roy. Soc., vol. 242A, pp. 243-310.

BULLERWELL, W. & McQUILLIN, R. 1969. Preliminary report on a seismic reflection survey in the southern Irish Sea (7pp). Inst. Geol. Sci., rep. no. 69/2.

BUROLLET, P.F., BYRAMJEE, R. & COUPEY, C. 1969. Contribution a l'etude sedimentologique des terrains Devoniens du Nord-Est de l'Ecosse. Notes mem. Cie. Fr. Pet., no. 9.

CHESHER, J.A. 1977. A review of the offshore geology of the Moray Firth (pp. 60-71) in The Moray Firth Area Geological Studies. Gill, G. (Editor). Inverness Field Club.

CHESHER, J.A. & BACON, M. 1975. A deep seismic survey in the Moray Firth (13pp). Inst. Geol. Sci., rep. no. 75/11.

CHESHER, J.A., DEEGAN, C.E., ARDUS, D.A., BINNS, P.E. & FANNIN, N.G.T. 1972. IGS marine drilling with m.v. "Whitethorn" in Scottish waters, 1970-71 (25pp). Inst. Geol. Sci., rep. no. 72/10.

CHESHER, J.A. & LAWSON, D. The geology of the Moray Firth. Inst. Geol. Sci. (in press).

CHRISTIE, P.A.F. & SCLATER, J.G. 1980. An extensional origin for the Buchan and Witchground Grabens in the North Sea. Nature, vol. 283, pp. 729-732.

COLLETTE, B.J. 1960. The gravity field of the North Sea (pp.47-96) in Gravity Expeditions 1948-1958, Volume 5. Bruins, G.J. (Editor). Delft.

COLTER, V.S. & BARR, K.W. 1975. Recent developments in the geology of the Irish Sea and Cheshire Basins (pp. 61-73) in Petroleum Geology of the Continental Shelf of North-West Europe, Vol. 1: Geology. Woodland, A.W. (Editor). Applied Science Publ., London.

DAVEY, F.J. 1970. Bouguer anomaly map of the North Celtic Sea and entrance to the Bristol Channel. Geophys. J.R. astr. Soc., vol. 22, pp. 277-282.

DEWEY, J.F. & PANKHURST, R.J. 1970. The evolution of the Scottish Caledonides in relation to their isotopic age pattern. Trans. R. Soc. Edinb., vol. 68, pp. 361-389.

DOBSON, M.R., EVANS, W.E. & WHITTINGTON, R. 1973. The geology of the south Irish Sea (35pp). Inst. Geol. Sci., rep. no. 73/11.

DONATO, J.A. & TULLY, M.C. 1981. A regional interpretation of North Sea gravity data (pp. 65-75) in Petroleum Geology of the Continental Shelf of North-West Europe. Illing, L.V. (Editor). Heyden, London.

DONOVAN, D.T. 1963. The Geology of British Seas. Inaugural Lecture, University of Hull.

DONOVAN, R.N., ARCHER, A., TURNER, P. & TARLING, D.H. 1976. Devonian palaeogeography of the Orcadian Basin and the Great Glen Fault. Nature, vol. 259, pp. 550-551.

DOWNIE, C., LISTER, T.R., HARRIS, A.L. & FETTES, D.J. 1971. A palynological investigation of the Dalradian rocks of Scotland (30pp). Inst. Geol. Sci., rep. no. 71/9.

DUFFIELD, W.G. 1924. The problem of measuring gravity at sea. Mon. Not. R. Astron. Soc., Geophys. Suppl., vol. 1, pp. 161-204.

EVANS, D., CHESHER, J.A., DEEGAN, C.E. & FANNIN, N.G.T. 1980. The offshore geology of Scotland in relation to the IGS shallow drilling programme, 1970-1978. Inst. Geol. Sci., rep. no. 81/12.

FENNING, P.J. 1968. Geophysical investigations (pp. 140-53) in Peacock, J.D., Berridge, N.G., Harris, A.L. and May, F. The Geology of the Elgin district. Mem. Geol. Surv.

FLINN, D. 1969. A geological interpretation of the aeromagnetic maps of the continental shelf around Orkney and Shetland. Geol. J., vol. 6, pp. 279-292.

FOSTER, A. 1975. Density and porosity determinations on four samples from Ardgay, Ross and Cromarty. Engineering Geology Unit, Inst. Geol. Sci., rep. no. 81.

FOSTER, A. 1977. Density and porosity determinations on six samples of granite from Grudie, Scotland. Engineering Geology Unit, Inst. Geol. Sci., rep. no. 105.

FUCHS, K. 1974. Geophysical contributions to taphrogenesis (pp. 420-432) in Approaches to Taphrogenesis. Illies, J.H. and Fuchs, K. (Editors). Schweizerbart, Stuttgart.

GEOLOGICAL SURVEY OF GREAT BRITAIN. 1964. Aeromagnetic map of part of Great Britain and Northern Ireland, Sheets 7 and 8.

GEOLOGICAL SURVEY OF GREAT BRITAIN. 1965. Aeromagnetic map of Great Britain, 1/625,000, sheet 2.

GIBB, R.A. 1961. Gravity measurements in Wales. PhD Thesis, University of Birmingham.

GRANT, F.S. & WEST, G.F. 1965. Interpretation Theory in Applied Geophysics. McGraw-Hill Book Company.

GRIFFITHS, D.H. & GIBB, R.A. 1965. Bouguer gravity anomalies in Wales. Geol. J., vol. 4, pp. 335-342.

GRIFFITHS, D.H., KING, R.F. & WILSON, C.D.V. 1961. Geophysical investigations in Tremadoc Bay, North Wales. Q. J. geol. Soc. London, vol. 117, pp. 171-191.

HALL, D.H. & DAGLEY, P. 1970. Regional magnetic anomalies: an analysis of the smoothed aeromagnetic map of Great Britain and Northern Ireland. Inst. Geol. Sci., rep. no. 70/10.

HALLAM, A. 1965. Jurassic, Cretaceous and Tertiary sediments in The Geology of Scotland. Craig, G.Y. (Editor). Oliver and Boyd, Edinburgh.

HALLAM, A. 1975. Jurassic Environments. Cambridge University Press.

HEISKANEN, W.A. & VENING MEINESZ, F.A. 1958. The Earth and its Gravity Field. McGraw-Hill, New York.

HUSSAIN, A. & HIPKIN, R.G. 1981. Regional gravity map of the British Isles, Northern sheet. Department of Geophysics, University of Edinburgh.

INSTITUTE OF GEOLOGICAL SCIENCES. 1968. Aeromagnetic map sheets 13 and 14.

IRVING, E. 1977. Drift of the major continental blocks since the Devonian. Nature, vol. 270, pp. 304-309.

IRVING, E. & PULLAIAH, G. 1976. Reversals of the geomagnetic field, magnetostratigraphy and relative magnitude of Palaeosecular variation in the Phanerozoic. Earth Science Reviews, vol. 12, pp. 35-64.

JENNER, J.K. 1981. The structure and stratigraphy of the Kish Bank Basin (pp. 426-431) in Petroleum Geology of the Continental Shelf of North-West Europe. Illing, L.V. and Hobson, G.D. (Editors). Heyden and Son, London.

JOHNSON, M.R.W. 1975. Morarian orogeny and Grenville belt in Britain. Nature, vol. 257, pp. 301-2.

JOHNSTONE, G.S. 1978. British Regonal Geology. The Grampian Highlands. Third Edition, HMSO, Edinburgh.

JONES, O.T. 1952. The drainage system of Wales and the adjacent regions. Q. Jl. geol. Soc. London, vol. 107, pp. 201-225.

JONES, O.T. 1956. The geological evolution of Wales and the adjacent regions. Q. Jl. geol. Soc. London, vol. 111, pp. 323-352.

JUDD, J.W. 1873. The secondary rocks of Scotland. First paper. Q. Jl. geol. Soc. London, vol. 29, pp. 97-195.

KAMINSKI, W., BAMFORD, D., FABER, S., JACOB, B., NUNN, K. & PRODEHL, C. 1976. A lithospheric seismic profile in Britain - II. Preliminary report on the recording of a local earthquake. J. Geophys., vol. 42, pp. 103-110.

KENT, P.E. 1949. A structure contour map of the surface of the buried Pre-Permian rocks of England and Wales. Proc. Geol. Assoc., vol. 60, pp. 87-104.

KENT, P.E. 1977. The Mesozoic development of aseismic continental margins. Jl. Geol. Soc. London, vol. 134, pp. 1-18.

KENT, P.E. 1977. Mesozoic vertical movements in Britain and the surrounding continental shelf (pp. 309-324) in Crustal Evolution in Northwestern Britain and Adjacent Regions. Bowes, D.R. and Leake, B.E. (Editors). Seel House Press, Liverpool.

KENT, P.E. 1980. Tectonics of the northwest European Continental Shelf. Nature, vol. 286, pp. 201-202.

LAGIOS, E. 1979. Gravity and other geophysical studies relating to the crustal structure of south-east Scotland. PhD Thesis, University of Edinburgh.

LEE, G.W. & PRINGLE, J. 1932. A synopsis of the Mesozoic rocks of Scotland. Trans. Geol. Soc. Glasgow, vol. 19, pp. 158-224.

LINSLEY, P.N., POTTER, H.C., McNAB, G. & RACHER, D. 1980. The Beatrice Field, Inner Moray Firth, UK North Sea. A.A.P.G. Mem. 30, pp. 117-129.

LUDWIG, W.J., NAFE, J.E. & DRAKE, C.L. 1971. Seismic refraction (pp. 53-84) in The Sea, Vol. 4, part 1. Maxwell, A.E. (Editor). Wiley Interscience, New York.

McCANN, D.M. 1972. Density, porosity and sonic velocity determinations on selected rocks from the Orkney Islands. Engineering Geology Unit, Inst. Geol. Sci., rep. no. 12.

McELHINNY, M.W. 1973. Palaeomagnetism and Plate Tectonics. Cambridge University Press.

McKENZIE, D. 1978. Some remarks on the development of sedimentary basins. Earth Planet. Sci. Lett., vol. 40, pp. 25-32.

McQUILLIN, R. 1968. Geophysical surveys in the Orkney Islands. Inst. Geol. Sci., Geophys. paper no. 4.

McQUILLIN, R., DONATO, J.A. & TULSTRUP, J. Dextral displacement of the Great Glen Fault as a factor in the development of the Inner Moray Firth Basin. Earth Planet. Sci. Lett. (in prep.).

MBIPOM, E.W. 1980. Geoelectric studies of the crust and upper mantle in northern Scotland. PhD Thesis, University of Edinburgh.

MURPHY, T. 1962. Gravity anomaly map of Ireland. Geophys. Bull., No. 22, Dublin Inst. Adv. Studies.

MYKURA, W. The Old Red Sandstone in Geology of Scotland (2nd Edition) Craig, G.Y. (Editor). In press.

NAFE, J.E. & DRAKE, C.L. 1963. Physical properties of marine sediments (pp. 794-815) in The Sea, Vol. 3. Hill, M.N. (Editor). Interscience, New York.

NETTLETON, L.L. 1971. Elementary gravity and magnetics for geologists and seismologists. Soc. Explor. Geophys. Monogr. Ser. 1, Tulsa.

NETTLETON, L.L. 1976. Gravity and Magnetics in Oil Prospecting. McGraw-Hill Book Company, New York.

NEVILLE GEORGE, T. 1966. Geomorphic evolution in Hebridean Scotland. Scott. J. Geol., vol. 2, pp. 1-34.

NOTT, M.J.C. & SMITH, E.G. 1981. Transcurrent faulting and the anomalous position of pre-Carboniferous Anglesey. Nature, vol. 290, pp. 432-494.

PANKHURST, R.J. 1970. The geochronology of the basic igneous complexes. Scott. J. Geol., vol. 6, pp. 83-107.

PEACOCK, J.D., BERRIDGE, N.G., HARRIS, A.L. & MAY, F. 1968. The geology of the Elgin District. Mem. Geol. Surv.

PENN, I.E. & EVANS, C.D.R. 1976. The Middle Jurassic (mainly Bathonian) of Cardigan Bay and its palaeogeographical significance (8pp). Inst. Geol. Sci., rep. no. 76/6.

PHEMISTER, J. 1960. British regional geology. Scotland: The Northern Highlands. Inst. Geol Sci. rep.

POWELL, D.W. 1956. Gravity and magnetic anomalies in north Wales. Q. Jl. geol. Soc. London, vol. 111, pp. 375-397.

SMITH, P.J., BOTT, M.H.P. 1975. Structure of the crust beneath the Caledonian Foreland and Caledonian Belt of the north Scottish shelf region. Geophys. J.R. astr. Soc., vol. 40, pp. 187-205.

SPEIGHT, J.M. & MITCHELL, J.G. 1979. The Permo-Carboniferous dyke-swarm of northern Argyll and its bearing on dextral displacement of the Great Glen Fault. Jl. Geol Soc. London, vol. 136, pp. 3-11.

STACEY, A.P. 1965. Marine magnetic survey off the coast of County Dublin. MSc Dissertation, University of Durham.

SUNDERLAND, J. 1972. Deep sedimentary basin in the Moray Firth. Nature, vol. 236, pp. 24-25.

SYKES, R.M. 1975. Jurassic stratigraphy in northern Scotland. Scott. J. Geol., vol. 2, pp. 51-78.

TANNER, P.W.G., JOHNSTONE, G.S., SMITH, D.I. & HARRIS, A.L. 1970. Moinian stratigraphy and the problem of the Central Ross-shire inliers. Bull. Geol. Soc. Am., vol. 81, pp. 299-305.

TELFORD, W.M., GELDART, L.P. SHERIFF, R.E. & KEYS, D.A. 1976. Applied Geophysics. Cambridge University Press.

THOMAS, M.D. & BROOKS, M. 1973. The geological significance of a negative gravity anomaly in the South Wales Coalfield. Geol. J., vol. 8, pp. 189-206.

TRUSHEIM, F. 1960. Mechanism of salt migration in northern Germany. Bull. Am. Ass. Pet. Geol., vol. 44, pp. 1519-1540.

URRIEN, C.M. & ZAMBRANO, J. 1973. The geology of the basins of the Argentine continental margin (pp. 135-166) in The Ocean Basins and their Margins, Vol. 1, Nairn, A.E.M. and Stehli, F.G. (Editors). Plenum, New York.

VAQUIER, V., STEENLAND, N.C., HENDERSON, R.G. & ZIEDZ, I. 1951. Interpretation of aeromagnetic maps. Geol. Soc. Am., Memoir 47.

VENING MEINESZ, F.A. 1950. Les graben africains, resultat de compression ou de tension dans la croute terrestre. Bull.Inst. R. Colon. Belge, vol 21, pp. 539-552.

WALCOTT, R.I. 1970. Flexural rigidity, thickness and viscosity of the lithosphere. J. Geophys. Res., vol. 75, pp. 3941-3954.

WATSON, J.V. 1975. The Lewisian Complex in A Correlation of the Precambrian Rocks in the British Isles. Spec. Rep. Geol. Soc. London, 6.

WESTOLL, T.S. 1964. The Old Red Sandstone of north-eastern Scotland. Adv. Sci., vol. 20, 446pp.

WHITEMAN, A.J., NAYLOR, D., PEGRUM, R.M. & REES, G. 1975. North Sea troughs and plate tectonics. Tectonophysics, vol. 26, pp. 39-54.

WHITTINGTON, R.J., CROKER, P.F. & DOBSON, M.R. 1981. Aspects of the geology of the south Irish Sea. Geol. Jl., vol. 16, pp. 85-88.

WINCHESTER, J.A. 1974. The zonal pattern of regional metamorphism in the Scottish Caledonides. Jl. Geol. Soc. London, vol. 130, pp. 509-524.

WOODLAND, A.W. (Editor). 1971. The Llanbedr (Mochras Farm) Borehole (115pp). Inst. Geol. Sci. rep. no. 71/18.

WOODLAND, A.W. 1975. Petroleum and the Continental Shelf of North-West Europe, Vol 1: Geology. Applied Science Publishers, London, 501pp.

ZIEGLER, P.A. 1978. North Sea rift and basin development (pp. 249-277) in Tectonics and Geophysics of Continental Rifts. Ramberg, I.B. and Neumann, E.R. (Editors). NATO Advances Study Institute, Series C, Math, Phys. Sci. No. 37,

APPENDIX I

PARTICIPATION IN MGU GEOPHYSICAL SURVEY PROJECTS AT SEA

The author took part in two regional surveys with the Marine Geophysics Unit of the Institute of Geological Sciences on board m.v. Sperus in the summers of 1978 and 1979, as part of his training. Both surveys covered the SW Approaches area.

The first survey covered the period 22 May to 13 July 1978 and consisted of four legs. The scope of the project (project 78/04) was to extend the regional survey of the SW Approaches to the south and west of the Scilly Isles out to Continental Shelf edge. The survey was carried out using shallow seismic, sidescan sonar, gravity and magnetic techniques on a skewed 7km by 12.5km grid. During leg 1, on which the author took part, from 24 May to 5 June, 208km of gravity lines, 122km of sidescan and 1553km of regional survey were run and the quality of the data was good.

The second survey (project 79/12) was a regional geophysical survey of the SW Approaches to the British Isles, which was run during the period 7 May to 6 June 1979. The project was designed to infill the regional coverage obtained in 1978 in the area $50^{o}10'N$-$48^{o}N$, $11^{o}W$-$7^{o}W$ and to run a number of lines on the Haig Fras sheet of the IGS 1:250,000 map series using shallow seismic profiling, gravity and magnetic methods. In addition, a detailed survey of part of the area was to be run using the Huntec Deep Tow Boomer system. The author took part in the second part of the second leg from 1-6 June and during this time 1178km of line were covered with all the equipment in use. The quality of the collected data was again good.

Gravity data collected during the two surveys have been used for the compilation of the regional gravity map of the Irish and Celtic Seas, presented in chapter 6.

The author also attended a special training course on the

Stratigraphic Interpretation of Seismic Data organised by the American Association of Petroleum Geologists for the Continental Shelf Division of the Institute of Geological Sciences.

APPENDIX II

ON THE AGE AND MAGNETISATION OF BODIES CAUSING MAGNETIC ANOMALIES: THE GRAMPIAN HIGHLANDS REGIONAL ANOMALY EXAMPLE

1. Introduction

The consequences of determining the total magnetisation vector M_T within a body are examined. By applying a method based on vector analysis, conclusions about not only the age of the anomaly but also the susceptibility and the Q ratio of the magnetic body may be reached. The analytical description of this method is followed by an example of its use on the regional magnetic anomaly of the Grampian Highlands. In this example, a Siluro-Devonian age and a susceptibility corresponding to average igneous rocks is indicated for the body causing the anomaly. This geophysically derived conclusion is consistent with the known geology of the area.

2. Mathematical Description of the Method

The total magnetisation vector $\vec{M}_T$ of a body is the sum of the induced magnetisation vector $\vec{M}_I$ and the remanent magnetisation vector $\vec{M}_R$. The equation

$$\vec{M}_T = \vec{M}_I + \vec{M}_R \qquad (1)$$

imposes two restraints on the vector $\vec{M}_R$. Firstly it must lie on the plane formed by the vectors $\vec{M}_T$ and $\vec{M}_I$ and secondly it must form a closed triangle with them. The mathematical expression of these two restraints follows..

2.1 The common plane restraint

The vector $\vec{M}_R$, lying on the plane of the vector $\vec{M}_T$ and $\vec{M}_I$, will be perpendicular to their cross product $(\vec{M}_T \times \vec{M}_R)$. The angle ϑ between any two vectors $\vec{A}$ and $\vec{B}$ is expressed through their direction cosines *l*, *m*, *n* as follows:

$$\cos\vartheta = l_A l_B + m_A m_B + n_A n_B \qquad (2)$$

The equivalent equation for the vectors M_R and $(M_T \times M_I)$, therefore is:

$$\cos 90^o = l_R(m_I n_T - n_I m_T) + m_R(n_T l_I - l_T n_I) + n_R(l_T m_I - m_T l_I) \qquad (3)$$

On a system of Cartesian co-ordinates at a point G on the globe (the Y axis pointing to the true north), the direction cosines of a vector can be expressed in terms of its inclination I (positive downwards) and its declination D (positive eastwards) by the equation

$$\begin{aligned} l &= \cos I \sin D \\ m &= \cos I \cos D \\ n &= \sin I \end{aligned} \qquad (4)$$

If the directions of the vectors $\vec{M}_T$ and $\vec{M}_I$ are known, then by substituting the corresponding values in equation (3) and dividing by $\cos I_R$ ($I_R \neq \pm 90^o$) a relation of the following form is obtained:

$$A\sin D_R + B\cos D_R + C\tan I_R = 0 \qquad (5)$$

where

$$\begin{aligned} A &= \cos I_T \cos D_T \sin I_I - \sin I_T \cos I_I \cos D_I \\ B &= \sin I_T \cos I_I \sin D_I - \cos I_T \sin D_T \sin I_I \\ C &= \cos I_T \cos I_I \ (\sin D_T \cos D_I - \cos D_T \sin D_I) \end{aligned} \qquad (6)$$

Equation (5) is the mathematical expression of the first restraint.

2.2 The closed triangle restraint

If $(\hat{IT})$, $(\hat{IR})$ and $(\hat{TR})$ are the angles formed by the vectors $(\vec{M}_I, \vec{M}_T)$, $(\vec{M}_I, \vec{M}_R)$ $(\vec{M}_T, \vec{M}_R)$ respectively then the relation between these angles, when the vectors $\vec{M}_T$, $\vec{M}_I$ and $\vec{M}_R$ form the closed triangle, is

$$(\hat{IR}) = (\hat{IT}) + (\hat{TR}) \qquad (7)$$

By combining equations (7), (2) and (4) the above relation becomes:

$$\cos^{-1}J + \cos^{-1}K + \cos^{-1}L = 0 \tag{8}$$

where

$$\begin{aligned} J &= \cos I_I \cos I_T (\sin D_I \sin D_T + \cos D_I \cos D_T) + \sin I_I \sin I_T \\ K &= \cos I_T \cos I_R (\sin D_T \sin D_R + \cos D_T \cos D_T) + \sin I_T \sin I_R \\ L &= \cos I_R \cos I_I (\sin D_R \sin D_I + \cos D_R \cos D_I) + \sin I_R \sin I_I \end{aligned} \tag{9}$$

Thus the mathematical expression of the second restraint is equation (8).

2.3 The Palaeopole Corresponding to I_R and D_R

Consider a magnetic anomaly centred at the point $G(\lambda_G,\varphi_G)$, where λ and φ indicate latitude and longitude respectively. If $P(\lambda_p,\varphi_p)$ is the position of the pole at the time the body acquired its remanent magnetisation and if the present geographic north pole (true north) is at the point N on the globe, then the following equations derive from spherical trigonometry:

$$\cos(\hat{GOP}) = \sin\lambda_p \sin\lambda_G + \cos\lambda_p \lambda \cos_G \cos(\varphi_p - \varphi_G) \tag{10}$$

$$\cos(\hat{NGP}) = \frac{\sin\lambda_P - \sin\lambda_G \cos(\hat{GOP})}{\cos\lambda_G \cos(\hat{GOP})} \tag{11}$$

where the point O represents the centre of the earth. The angle $(\hat{NGP})$ is equal to the declination D_R of the vector $\vec{M}_R$. The angle $(\hat{GOP})$ is related to the palaeolatitude λ_R of the point G through the equation:

$$\lambda_R = 90^o - (\hat{GOP}) \tag{12}$$

Equations (10) and (11) solved for $\cos(\varphi_P - \varphi_G)$ and $\sin\lambda_P$, therefore become:

$$\sin\lambda_P = \cos D_R \cos\lambda_R \cos\lambda_G + \sin\lambda_R \sin\lambda_G \tag{13}$$

$$\cos(\varphi_P - \varphi_G) = \frac{\sin\lambda_R - \sin\lambda_P \sin\lambda_G}{\cos\lambda_P \cos\lambda_G} \tag{14}$$

Assuming a geocentric dipole magnetic field during the period in which the remanent magnetisation was acquired, we can further replace λ_R through its corresponding I_R from the equation

$$\lambda_R = \tan^{-1}(\tfrac{1}{2}\tan I_R) \tag{15}$$

Thus, for every pair of values (I_R, D_R) which satisfies equations (5) and (8) knowing the location of the magnetic anomaly we can define the position of the palaeopole P through the equations (13), (14) and (15).

2.4 Susceptibility and Q Ratio

For any valid direction of the vector $\vec{M}_R$ knowing the direction of the vectors $\vec{M}_T$ and $\vec{M}_I$, it is possible to calculate the susceptibility of the body causing the anomaly and its Q ratio.

Applying the sine law on the triangle of the vectors $\vec{M}_T$, $\vec{M}_I$ and $\vec{M}_R$ we obtain:

$$\frac{M_I}{\sin(\hat{TR})} = \frac{M_T}{\sin(\hat{IR})} = \frac{M_R}{\sin(\hat{IT})} \tag{16}$$

where M_T, M_I and M_R are the magnitudes of the corresponding vectors. If H is the present-day strength of the earth's magnetic field at G, k the susceptibility and Q the Koenigsberger's ratio of the body causing the anomaly, then:

$$k = \frac{M_T}{H} \cdot \frac{M_I}{M_T} \tag{17}$$

and

$$Q = \frac{M_R}{M_I} \tag{18}$$

we can replace the ratios M_I/M_T and M_R/M_I from equation (16) and then k and Q become:

$$k = \frac{M_T}{H} \cdot \frac{\sin(\hat{TR})}{\sin(\hat{IR})} \tag{19}$$

and

$$Q = \frac{\sin(\hat{IT})}{\sin(\hat{TR})} \tag{20}$$

From equations (19) and (20) it is seen that if the direction of the vectors $\vec{M}_T$, $\vec{M}_I$ and $\vec{M}_R$ and the magnitude of the vector $\vec{M}_T$ are known, then the susceptibility and the Q ratio can be found.

3. The Age Correlation

For any given direction of the vectors $\vec{M}_T$ and $\vec{M}_I$ an infinite number of vectors $\vec{M}_R$ can satisfy the restraints in 1.1 and 1.2 above. We can obtain a finite number of vectors $\vec{M}_R$ by the method described below, and then we can compare the poles corresponding to these vectors (as described in 2.3 above) to palaeopoles known from palaeomagnetic data.

3.1 The numerical approximation

The vector $\vec{M}_T$ is defined by its magnitude (M_T), inclination (I_T) and declination (D_T). Usually the vector $\vec{M}_T$ derives as the result of modelling a magnetic anomaly and a range for both I_T and D_T is obtained rather than a pair of values (I_T,D_T). In the numerical approximation considered here, the ranges of I_T and D_T are sampled at 1^o intervals. For every pair of I_T and D_T different values of I_R ($-90^o < I_R < +90^o$) and D_R ($0^o \leqslant D_R \leqslant 360^o$), again at 1^o intervals, are substituted in equations (5) and (8). The values of I_R and D_R which satisfy both these equations are then converted to their corresponding pole position through the equations (13), (14) and (15). This position is then compared to the known palaeopoles, as shown in Table 1 (the south poles, not shown in the table), are also

considered for comparison. If the pole lies within the acceptable range of a known palaeopole (Table 1), then the ratios $\sin(\hat{TR})/\sin(\hat{IR})$ and Q are calculated from the equations (4), (2) and (20). The values of I_I and D_I, used in the procedure described above, depend only on the latitude and longitude of the magnetic anomaly and are therefore known.

3.2 The known palaeopole

The meaned position of the north pole during the period Cambrian to Lower Tertiary is shown in table 1. The poles for the periods Carboniferous to Lower Tertiary have been derived by averaging the pole positions given at 10my intervals (Irving, 1977). The Cambrian, Ordovician and Siluro-Devonian poles have been derived by averaging known pole positions for these periods (tables, 3, 4 and 5 in, Briden and Duff, in press). The polarity bias column has been compiled from an unpublished geomagnetic reversal time-scale (D Smythe, IGS, Edinburgh, personal communication) for the periods Permian to Lower Tertiary and from figure 13 of Irving and Pullaiah (1976) for the rest periods. The column ($\Delta\lambda p$, $\Delta\varphi p$) of table 1 gives the range of the known palaeopole positions, within which any calculated palaeopole is considered to be a valid solution for the corresponding period. It is an indication of the accuracy with which the average pole positions have been calculated. It is chosen to give more than 80% probability for the known palaeopoles to lie within this range. The number of valid solutions calculated for every period is shown under column n. If the calculated pole was compared with a north (south) palaeopole, then the indication N(R) is given in the next column.

4. The Grampian Highlands Example

An example of using the method described above is given here. The chosen anomaly is the regional magnetic high zone, which covers a major part of the Grampian Highlands area (Hall and Dagley, 1970). In the two-dimensional interpretation of this anomaly (chapter 4) it has been suggested that the body causing the anomaly is a 12km thick "granitic" layer at mid-crustal depth. The best fit between

Period	North Pole		Polarity bias	$\Delta\lambda_p, \Delta\varphi_p$	n	P	Suscept. range 10^3 (rat. system)	Mean Suscept. 10^3 (rat. system)	Q
	λ_p	φ_p							
L. Tertiary	78.0	180.6	42%N	$\pm 5^o$	7	R	258-758	508	1.02
Cretaceous	71.7	163.2	77%N	$\pm 5^o$	8	R	133-389	261	1.06
Jurassic	66.2	149.1	77%N	$\pm 5^o$	-	-	-	-	-
Triassic	48.8	149.8	75%N	$\pm 5^o$	10	R	37-109	73	1.52
Permian	44.1	162.3	18%N	$\pm 5^o$	8	R	28-82	55	1.82
Carboniferous	36.3	162.6	15%N	$\pm 5^o$	3	R	17-50	33	2.61
Siluro-Devonian	5.7	145.4	50%N	$\pm 10^o$	26	N	0-19	9.5	2.24
Ordovician	10.5	182.5	35%N	$\pm 10^o$	-	-	-	-	-
Cambrian	53.7	348.2	25%N	$\pm 10^o$	-	-	-	-	-

TABLE 1

(λ_p, φ_p): latitude and longitude of the known north palaeopole; $(\Delta\lambda_p, \Delta\varphi_p)$: range of λ_p and φ_p respectively within which any calculated pole is acceptable; n: the number of acceptable calculated poles for the corresponding period; P: the polarity of the calculated poles for each period; Q: the Koenigsberger ratio.

observed and calculated values was obtained when a total magnetisation vector $\vec{M}_T$ of -150nT magnetisation contrast with the surrounding rocks (M_T = -150nT) and of a direction of $I_T = -10^o$ and $D_T = 20^o$ was assumed for the layer. The same fit was obtained if the vector $-\vec{M}_T$ (M_T = 150nT, $I_T = 10^o$, $D_T = 200^o$) was assumed. The inclination and declination of M_T were defined with an accuracy of $\pm 5^o$.

4.1 Description of the results

The results obtained are summarised in table 1. Valid solutions for the period Siluro-Devonian, Carboniferous, Permian, Triassic, Cretaceous and Lower Tertiary have been obtained. Of these only the Siluro-Devonian solutions are of normal polarity, the rest are of reversed polarity. The Q ratio in the last column represents the average of the (n) Q ratios for the corresponding period. The susceptibility range for each period derives from equation (19) by multiplying the average of the $\sin(\hat{TR})/\sin(\hat{IR})$ ratios for the period with range of the ratio M_T/H, which depends on the calculated polarity of the same period.

Knowing that the "granitic" layer causing the anomaly is surrounded by metamorphic rocks with a susceptibility range of 0.0-72.9 x 10^{-3} SI (table 2), then a magnetisation range of (0-290)nT is obtained for these rocks if we assume that they were magnetised in a magnetic field of similar strength to the present day (H = 50000nT). This range can be considered a maximum magnetisation range for these rocks, since the present magnetic field on the earth is stronger than that of any previous period (McElhinny, 1973). This magnetisation range results in a range for the total magnetisation within the "granitic" layer of (0-140)nT in the case of the normal polarity (magnetisation contrast of -150nT) and of (150-290)nT in the case of the reverse polarity (magnetisation contrast of +150nT). In the case of normal polarity it is assumed that the layer is not diamagnetic, so negative magnetisation is not possible. The column of the susceptibility range indicated for each period was derived by using these total magnetisation ranges, as described above.

Rock Type	Susceptibility x10^3 (rat. system)		Density (Kg/m^3)	
	Range	Average	Range	Average
Granite	0.0- 50.3	2.5	2500-2810	2640
Rhyalite	0.3- 37.7		2350-2700	2520
Dolerite	1.3- 37.7	17.6		
Diabase	1.0-163.4	56.5	2500-3200	2910
Basalt	0.3-182.2	75.4	2700-3300	2990
Peridotite	95.5-196.0	163.4	2780-3370	3150
Andesite		169.6	2400-2800	2610
Av. acid Ign.	0.0- 82.1	8.2	2300-3110	2610
Av. var. Metam.	0.0- 72.9	4.4	2400-3100	2740
Av. basic Ign.	0.6-122.0	32.7	2090-3170	2790

TABLE 2

Densities and susceptibilities of various rocks.

It is possible now to compare with calculated susceptibility ranges and their mean value in table 1, with known ranges and average susceptibilities of different rocks shown in table 2. For simplicity we can compare the mean values in table 1 with the average values in table 2. Immediately it is apparent that the mean susceptibilities for the Lower Tertiary and Cretaceous periods are far too high to be considered as realistic, thus these solutions are rejected. The Triassic solution gives a mean susceptibility comparable to the average susceptibility of basalts but a reverse polarity is indicated, within a period known to be of mainly normal polarity. The Triassic solution is therefore rather unlikely. We can further reduce the number of remaining valid solutions by considering geophysical and geological information for the area.

4.2 Geophysical and geological considerations

Of the remaining solutions the mean susceptibility for the Permian is compatible with the average susceptibility of Diabase, and the mean susceptibility for the Carboniferous is compatible with the average susceptibility of basic igneous rocks. The average density of both these rocks is higher than average density of the various metamorphic rocks (table 2). A regional gravity high over the area would then be expected were these rocks present, but is not observed, in fact there is a regional gravity low (chapter 4). On the basis of the gravity criterion the Permian and Carboniferous solutions are rejected. In the same way the Triassic solution can also be rejected.

The last valid solution, the Siluro-Devonian, has a mean susceptibility comparable with the average susceptibility of acid igneous rocks. The corresponding average density (table 2) is lower than the average density of metamorphic rocks and therefore the gravity criterion is satisfied. Furthermore, the existence of a layer of acid igneous rocks at mid-crustal depths, is consistent with the numerous granites which outcrop in the Grampian Highlands.

We conclude therefore that the only possible age for the "granitic" layer is Siluto-Devonian, that its mean susceptibility is 9.5×10^{-3} (rationalised system) and its Koenigsberger ratio is about 2.24.

EDINBURGH FORTRAN(G) COMPILER VERSION 50.16

```
      C PROGRAM TO ESTIMATE THE AGE, SUSCEPTIBILITY AND Q RATIO OF
      C A BODY CAUSING A MAGNETIC ANOMALY, WHEN ITS TOTAL MAGNE-
      C TIZATION IS KNOWN, BY COMPARING THE POLES CORRESPONDING TO
      C THE REMANENT MAGNETIZATION VECTOR'S DIRECTION TO KNOWN PA-
      C LAEOPOLES FROM PALAEOMAGNETIC DATA.
      C
            DIMENSION X(25,2),Y(25,2)
            REAL LP, MP, NP,  LT, MT, NT,  LR, MR, NR
            REAL IP, DP,  IT, DT,  IR, DR
            REAL LTG, LNG
            REAL ITLLM, ITINCR, ITULM,  DTLLM, DTINCR, DTULM
            REAL LATP, LONP,  LATG, LONG
            REAL IPP, DPP,  ITT, DTT,  IRR, DRR
            REAL LNLM, LTLM
      C
      C DEFINITION OF THE INPUT DATA
      C  LATG,LONG: LATITUDE AND LONGITUDE OF POINT G, WHERE THE
      C         MAGNETIC ANOMALY IS CENTERED.
      C  IP,DP: INCLINATION AND DECLINATION OF THE EARTH'S MAGNETIC
      C         FIELD AT POINT G.
      C  ITLLM,ITINCR,ITULM: LOWER LIMIT, INCREMENT STEP AND UPPER
      C         LIMIT OF THE TOTAL MAGNETIZATION VECTOR'S
      C         INCLINATION.
      C  DTLLM,DTINCR,DTULM: LOWER LIMIT, INCREMENT STEP AND UPPER
      C         LIMIT OF THE TOTAL MAGNETIZATION VECTOR'S
      C         DECLINATION.
      C  LNLM,LTLM: THE RADIUS OF THE ACCEPTABLE RANGE FROM THE
      C         KNOWN PALAEOPOLES (IN DEGREES) FOR THE LONGITUDE
      C         AND LATITUDE RESPECTIVELY.
      C  NDATA: NUMBER OF PERIODS FOR WHICH NORTH AND SOUTH PALAEO-
      C         POLE COORDINATES WILL BE ENTERED.
      C  X(II,JJ),Y(II,JJ), JJ=1,2 : LATITUDE AND LONGITUDE OF THE
      C         NORTH AND THEN SOUTH PALAEOPOLES OF EACH PERIOD.
      C
            READ(05,100) LATG, LONG
            READ(05,100) IP, DP
            READ(05,101) ITLLM, ITINCR, ITULM
            READ(05,101) DTLLM, DTINCR, DTULM
            READ(05,104) LNLM, LTLM
            READ(05,102) NDATA
            DO 1000 II=1,NDATA
            READ(05,103) (X(II,JJ),Y(II,JJ),JJ=1,2)
       1000 CONTINUE
      C
            CF=0.017453293
      C
      C CONVERSION OF THE INDUCED MAGNETIZATION VECTOR'S INCLINA-
      C TION AND DECLINATION, AND POINT'S G LATITUDE AND LONGITUDE
      C IN RADIANS.  CALCULATION OF THE INDUCED MAGNETIZATION
      C VECTOR'S DIRECTION COSINES.
      C
            IP=IP*CF
            DP=DP*CF
            CSIP=COS(IP)
            IF(LATG.EQ.90.) LATG=89.999
            IF(LATG.EQ.-90.) LATG=-89.999
            LTG=LATG*CF
            LNG=LONG*CF
            CSLTG=COS(LTG)
            SNLTG=SIN(LTG)
      C
            LP=CSIP*SIN(DP)
            MP=CSIP*COS(DP)
            NP=SIN(IP)
      C
            NINC=IFIX((ITULM-ITLLM)/ITINCR+1.0)
```

```
      NDEC=IFIX((DTULM-DTLLM)/DTINCR+1.0)
C
      WRITE(06,300)
      WRITE(07,301)
C
C FIRST DO LOOP TO COVER THE TOTAL MAGNETIZATION VECTOR'S
C INCLINATION RANGE.
C
      DO 111 K=1,NINC
      IT=(ITLLM+(K-1)*ITINCR)*CF
      CSIT=COS(IT)
      SNIT=SIN(IT)
C
C SECOND DO LOOP TO COVER THE TOTAL MAGNETIZATION VECTOR'S
C DECLINATION RANGE.  CALCULATION OF THIS VECTOR'S DIRE-
C CTION COSINES.
C CALCULATION DIRECTION COSINES FOR THE CROSS PRODUCT OF THE
C OF THE TOTAL AND INDUCED MAGNETIZATION VECTORS.
C
      DO 111 L=1,NDEC
      DT=(DTLLM+(L-1)*DTINCR)*CF
      LT=CSIT*SIN(DT)
      MT=CSIT*COS(DT)
      NT=SNIT
      A=MP*NT-NP*MT
      B=NP*LT-LP*NT
      C=LP*MT-MP*LT
C
C THIRD DO LOOP TO GIVE DIFFERENT VALUES AT THE REMANENT MAG-
C NETIZATION VECTOR'S INCLINATION.
C
      DO 111 I=1,180
      IR=(-90.5+I)*CF
      CSIR=COS(IR)
      SNIR=SIN(IR)
      TNIR=TAN(IR)
C
C FOURTH DO LOOP TO GIVE DIFFERENT VALUES AT THE REMANENT
C MAGNETIZATION VECTOR'S DECLINATION.
C
      DO 111 J=1,360
      DR=(-0.5+J)*CF
      CSDR=COS(DR)
      SNDR=SIN(DR)
C
C SATISFACTION OF THE CONDITION THE TOTAL, INDUCED AND REMAN-
C ENT MAGNETIZATION VECTORS LIE ON THE SAME PLANE.  CALCULA-
C TION OF THE REMANENT MAGNETIZATION VECTOR'S DIRECTION
C COSINES.
C
      D=A*SNDR+B*CSDR+C*TNIR
      IF(ABS(D).GT.0.0001)GO TO 111
C
      RL=ATAN(0.5*TNIR)
      CSRL=COS(RL)
      SNRL=SIN(RL)
C
      LR=CSIR*SNDR
      MR=CSIR*CSDR
      NR=SNIR
C
C CALCULATION OF THE ANGLES BETWEEN THE TOTAL, INDUCED AND
C REMANENT MAGNETIZATION VECTORS.  SATISFACTION OF THE CON-
C DITION THAT THEY FORM A CLOSED TRIANGLE.
C
      ATP=LT*LP+MT*MP+NT*NP
      APR=LP*LR+MP*MR+NP*NR
      ART=LR*LT+MR*MT+NR*NT
C
      SUM=ARCOS(ATP)-ARCOS(APR)+ARCOS(ART)
      IF(ABS(SUM).GT.0.00002)GO TO 111
C
```

```
C CONVERSION OF THE REMANENT MAGNETIZATION VECTOR'S INCLINA-
C TION AND DECLINATION TO THE CORRESPONDING POLE'S LONGITUDE
C AND LATITUDE.
C
      LATP=CSLTG*CSDR*CSRL+SNLTG*SNRL
      IF(LATP.GT.1.) LATP=1.
      IF(LATP.LT.-1.) LATP=-1.
      SQ=SQRT(1.-LATP**2)
      IF(SQ.EQ.0.) SQ=0.000001
      LONP=(SNRL-SNLTG*LATP)/(CSLTG*SQ)
      IF(LONP.GT.1.) LONP=1.
      IF(LONP.LT.-1.) LONP=-1.
C
      PLAT=ARSIN(LATP)
      PLAT=PLAT/CF
      PLONA=ARCOS(LONP)+LNG
      PLONA=PLONA/CF
      PLONB=360.+2.*LONG-PLONA
C
C COMPARISON OF THE CALCULATED POLE'S POSITION TO THE KNOWN
C PALAEOPOLES.
C
      DO 2000 KK=1,NDATA
      LLL=1
      IF(ABS(X(KK,LLL)-PLAT).LT.LTLM)GO TO 444
      LLL=LLL+1
      IF(ABS(X(KK,LLL)-PLAT).GT.LTLM)GO TO 2000
  444 CONTINUE
      IF(ABS(Y(KK,LLL)-PLONA).LT.LNLM)GO TO 2222
      IF(ABS(Y(KK,LLL)-PLONB).GT.LNLM)GO TO 2000
 2222 CONTINUE
C
      TPP=ARCOS(ATP)
      RTT=ARCOS(ART)
      PRR=ARCOS(APR)
      SNRT=SIN(RTT)
      SNPR=SIN(PRR)
      SNTP=SIN(TPP)
C
C CALCULATION OF KOENIGSBERGER'S RATIO AND OF THE
C SUSCEPTIBILITY FACTOR.
C
      Q=SNTP/SNRT
      SUSCF=SNRT/SNPR
C
      ITT=IT/CF
      DTT=DT/CF
      TP=TPP/CF
      PR=PRR/CF
      RT=RTT/CF
C
C DEFINITION OF THE OUTPUT FILES.
C              OUTPUT FILE 1
C  X(KK,LLL),Y(KK,LLL): LATITUDE AND LONGITUDE OF KNOWN
C       PALAEOPOLE.
C  PLONA,PLAT,PLONB: LONGITUDE A, LATITUDE AND LONGITUDE B OF
C       THE CALCULATED POLE.
C              OUTPUT FILE 2
C  PR: ANGLE BETWEEN INDUCED AND REMANENT MAGNETIZATION
C       VECTORS.
C  RT: ANGLE BETWEEN REMANENT AND TOTAL MAGNETIZATION VECTORS
C  SUSCF: SUSCEPTIBILITY FACTOR.
C  Q: KOENIGSBERGER'S RATIO Q.
C
      WRITE(06,200) X(KK,LLL), Y(KK,LLL), PLONA, PLAT, PLONB
      WRITE(07,201) PR, RT, SUSCF, Q
C
 2000 CONTINUE
C
  111 CONTINUE
C
  100 FORMAT(2F8.2)
  101 FORMAT(3F8.2)
  102 FORMAT(I3)
  103 FORMAT(4(F5.1,2X))
  104 FORMAT(F5.1,2X,F5.1)
  200 FORMAT(' ',5(F5.1,3X))
  201 FORMAT(' ',3(F7.3,3X),F5.2)
  300 FORMAT(' ','PLATD   PLONG   PLLNA   PALLT   PLLNB')
  301 FORMAT(' ','ANGLEPR   ANGLERT     SUSCF    Q RAT')
C
      STOP
      END
```

APPENDIX III

1. Estimation of the tilting angle of a non uniform floating block

Let us first consider a single block of material floating within a liquid and examine the forces acting on it when in equilibrium and then when it is higher or lower than its equilibrium level. Figure 1 shows these three situations.

If H, S are the height and cross section of the block, ρ_c its density, ρ_f the density of the liquid in which the block floats and Y the part of the block above the surface of the liquid when in equilibrium, then the following equations apply for the cases I, II and III.

(I) Upward force: $F_u = (H-Y)S\rho_f g$

Downward force: $F_d = H S \rho_c g$ (= weight of the block)

Since the block is in equilibrium, $F_d = F_u$ and therefore

$$(H-Y)\rho_f = H\rho_c \qquad (1)$$

(II) If the block moves upwards by dz then the upward force is: $F_u = (H-Y)S\rho_f g - dzS\rho_f g$ and therefore there is a net downward force $F = F_d - F_u$ or $F = Sg\rho_f dz$ (2)

(III) If the block moves downwards by dz' then the upward force is: $F_u = (H-Y)S\rho_f g + dz'S\rho_f g$ and therefore there is a net upward force $F' = F_u - F_d$ or $F' = Sg\rho_f dz'$.

If the block is loaded by material of density ρ_s and thickness dz' in such a way that its new top is the same level as before (case IV), then the upward force is the same as in case III but the downward force is: $F = H S \rho_c g + dz'S\rho_s g$ and therefore, if $\rho_s < \rho_f$, there is a net upward force:

$$F'' = Sg(\rho_f - \rho_s)dz' \qquad (3)$$

Let us now apply the above derived equations (2) and (3) to a block which is tilted by a torque created by density inhomogenities within it while it is floating in a denser material. Figure 2 shows a cross section of the block already tilted and covered by sediments on its downwarped side. As the block tilts around an axis perpendicular to the plane of the page, an element of it of width dx and length L (L is the total width of the block) moves downwards by dz' whereas another equivalent element on the other side of the block will move upwards. The corresponding upward and downward forces on the two block elements will be:

$$dF' = Ldxg(\rho_f - \rho_s)dz' \qquad dF = Ldxg\rho_f dz$$

We can replace dz and dz' with $x\tan\varphi$ (φ is the angle of tilting) and by multiplying the two forces by x we find their corresponding torques towards the axis of rotation. It is:

$$dT' = Ldxg(\rho_f - \rho_s)x^2\tan\varphi \qquad dT = Ldxg\rho_f x^2\tan\varphi$$

The total torque acting on the block will then be:

$$T = dT + dT' \text{ or}$$

$$T = Lg(2\rho_f - \rho_s)\tan\varphi \int_0^A x^2 dx$$

where A is the half length of the block. The total counterbalancing torque acting on the block and trying to return it to its initial position is:

$$T = {}^1/_3 \, L \, g \, (2\rho_f - \rho_s)A^3\tan\varphi \qquad (4)$$

When the block is in equilibrium the above torque is equal to the torque created by the anomalous mass distribution within the block. If M_D, X_D and M_E, X_E are the anomalous masses and the distance of their centre of mass from the centre of rotation of the block, then the torque they create is:

$$T = (M_D X_D + M_E X_E)g \qquad (5)$$

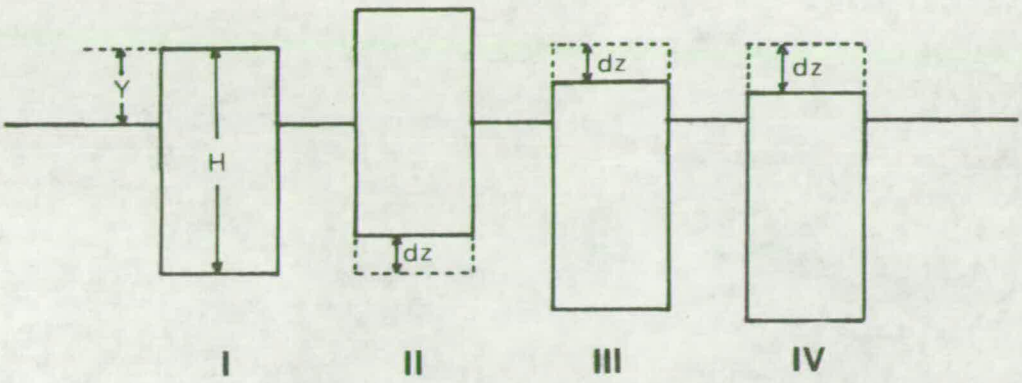

FIGURE 1

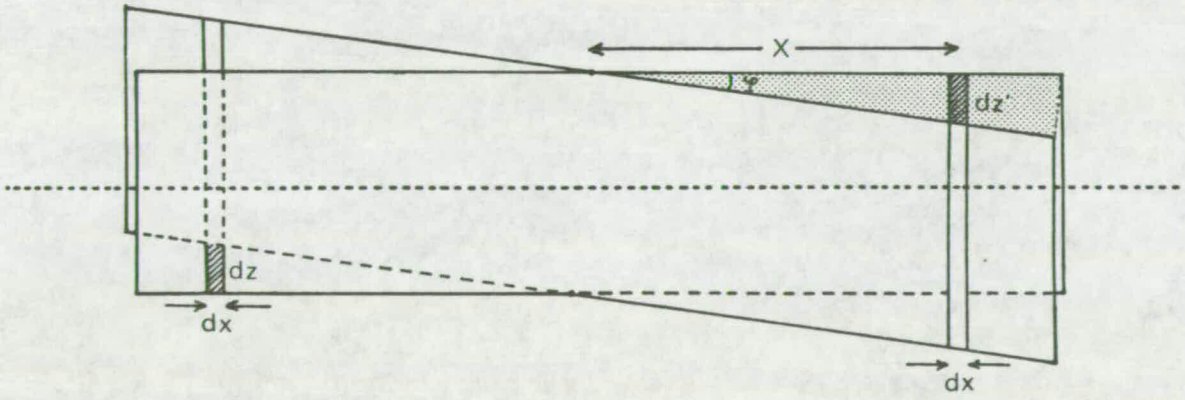

FIGURE 2

From equations (3) and (4) we find the angle φ at which the block attains equilibrium:

$$\tan\varphi = \frac{3(M_D X_D + M_E X_E}{Lg(2\rho_f - \rho_s)A^3} \qquad (6)$$

For the Grampian Highlands tectonic unit the following values were calculated: $M_D = 11.13 \times 10^{15}$kg, $X_D = 78 \times 10^3$m

$$M_E = 7.33 \times 10^{15}\text{kg} \ , \ X_E = 90 \times 10^3\text{m}$$

If we approach the tectonic unit as a block of total length 2A = 360km and width L = 100km floating within the lower crust (density ρ_f = 2850kg/m^3), then an angle of tilting of 0.14^o is estimated.

2. Vertical movements of a crustal block containing an anomalous mass

In the discussion below it is assumed that the anomalous mass is within the upper crust. The cases of a crustal block with a mass deficit and with a mass excess are examined separately.

2.1 Block containing a mass deficit

We can assume, with no loss of generality, that the anomalous mass has the form of a prism having the same cross section as the block and lies midway through it. Then the part of the block above the bottom of the mass deficit can be treated as a block having a mass deficit extending up to the top of the crust and having a mean density less than the surrounding upper crust. Let us, therefore, examine a block consisting of material of density ρ_s (less than the density of the upper crust ρ_u) extending from the surface to a depth H_D, being forces to stay at that level. If the block is left to move freely, then it will rise to a height Y above the surface of the crust. From equation (1), the height Y is:

$$Y = \frac{\rho_u - \rho_s}{\rho_u} \cdot H_D \ . \qquad (7)$$

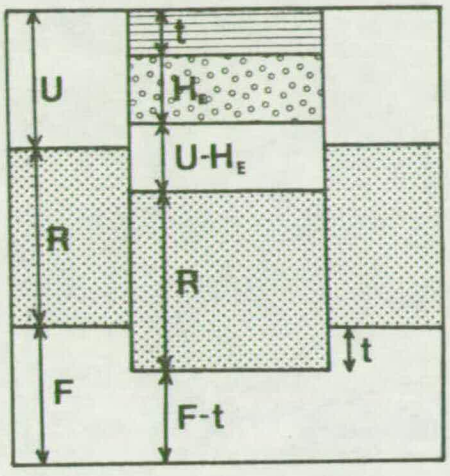

FIGURE 3

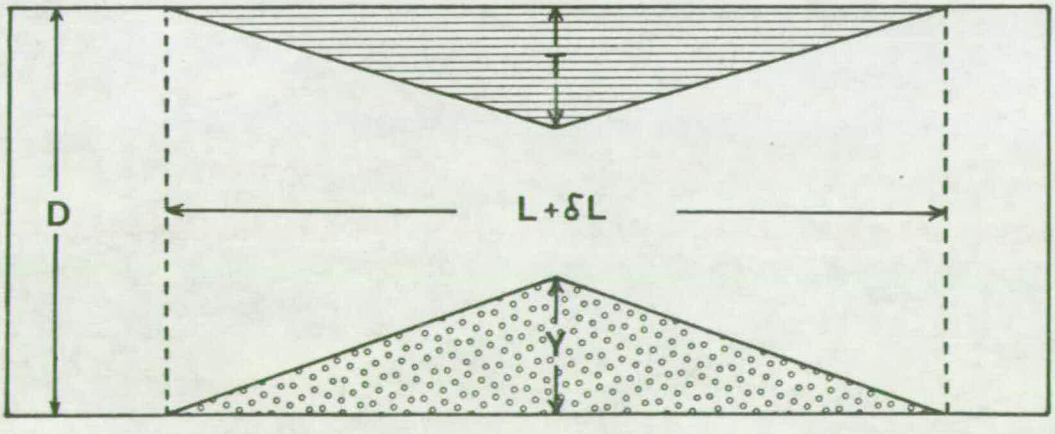

FIGURE 4

Knowing the mass deficit M_D and the surface S_D of the block, we can express the depth H_D:

$$H_D = \frac{M_D}{S_D} \cdot \frac{1}{\rho_u - \rho_s} \tag{8}$$

From equations (7) and (8) the final formula for Y is derived:

$$Y = \frac{M_D}{S_D} \cdot \frac{1}{\rho_u} \tag{9}$$

2.2 Block containing a mass excess

In the same way as with the block containing a mass deficit, we can assume that the mass excess within the corresponding block is concentrated within the topmost part of the upper crust and is represented by a prismatic body of cross section S_E, thickness H_E and density ρ_b greater than the average density of the upper crust ρ_u. Let U be the total thickness of the upper crust, R the thickness of the rigid part of the crust beneath the upper crust having a density of ρ_R and let us also assume that at a depth F below the rigid part of the crust all the density differences have been compensated and that the density of the ductile material between rigid crust and compensation level is ρ_f. Assuming again that the mass excess block is forcefully kept at the top of the crust and then left to move freely in the vertical direction, the block will move downwards pushing the rigid part of the crust beneath it as well. Sediments will accumulate at the top as the block moves down. When the block reaches its equilibrium (figure 3), then the total force per unit area at the compensation level beneath the mass excess block and the adjacent area will be the same:

$$\left[\rho_s t + \rho_b H_E + \rho_u (U - H_E) + \rho_R R + \rho_f (F - t)\right] g = (\rho_u U + \rho_R R + \rho_f F) g$$

and therefore:

$$t = \frac{\rho_b - \rho_u}{\rho_f - \rho_s} \cdot H_E \tag{10}$$

where t and ρ are the thickness and density of the accumulated sediments. The thickness H_E can be expressed in terms of the total mass excess M_E and the cross section of the block as:

$$H_E = \frac{M_E}{S_E} \cdot \frac{1}{\rho_b - \rho_a} \qquad (11)$$

and therefore, the total thickness of the accumulated sediments becomes:

$$t = \frac{M_E}{S_E} \cdot \frac{1}{\rho_f - \rho_s} \qquad (12)$$

3. Estimation of the Irish Sea's extension factor

From figure 6/14 it is seen that the width of the N-S trending crustal thinning beneath the Irish Sea is about 400-450km (from western Ireland to the east of Wales) and is quite symmetrical around its axis. We can approximate this crustal thinning as having an isosceles triangular shape with a base of 425km and a height of 5.5km (figure 4). As already mentioned in chapter 6, this thinning of the crust is filled with material of density $\rho_\ell = 3000 kg/m^3$. Since the base of this layer is at the same level (30km) as the depth to the Moho under the adjacent areas, it is logical to assume that this depth represents a compensation level at which the density differences above it have been equalised. If the crustal thinning at the base of the crust is due to lateral E-W extension and necking of the crust, then a similar shape thinning at the top of the crust is expected. Allowing a long time for this geosyncline type of thinning to be filled with sediments of density ρ_s and maximum thickness T and accepting that the 30km level is at isostatic equilibrium, then we can determine the thickness T of the sediments. Working on the two-dimensional model of figure 4, the sum of the sediments' mass and the mass of the heavy layer at the base of the crust should be the same as a mass of material having the same combined volume but a density equal to the average density of the crust ρ_c. Thus:

$$\tfrac{1}{2}(L + \delta L)T\rho + \tfrac{1}{2}(L + \delta L)Y\rho = \tfrac{1}{2}(L + \delta L)(T + Y)\rho$$

and therefore

$$T = \frac{\rho_\ell - \rho_c}{\rho_c - \rho_s} . Y \qquad (13)$$

The average total thinning of the crust over the distance L + δL is

$$\delta D = \tfrac{1}{2} (T + Y) \qquad (14)$$

Since $\frac{\delta D}{D} \quad \frac{\delta L}{L + \delta L}$ (15)

knowing the densities involved in equation (13) and Y we can find the total extension δL and therefore the extension factor β, from the relation:

$$\beta = \frac{L + \delta L}{L} \qquad (16)$$

If ρ_ℓ = 3000kg/m^3, ρ_c = 2800kg/m^3, ρ_s = 2500kg/m^3, Y = 5500m and D = 30,000m, then it is calculated that β = 1.18.

18 MAR 2002

Dimitropoulos
Ph. D., 1982.
JCM Library

Line No 6

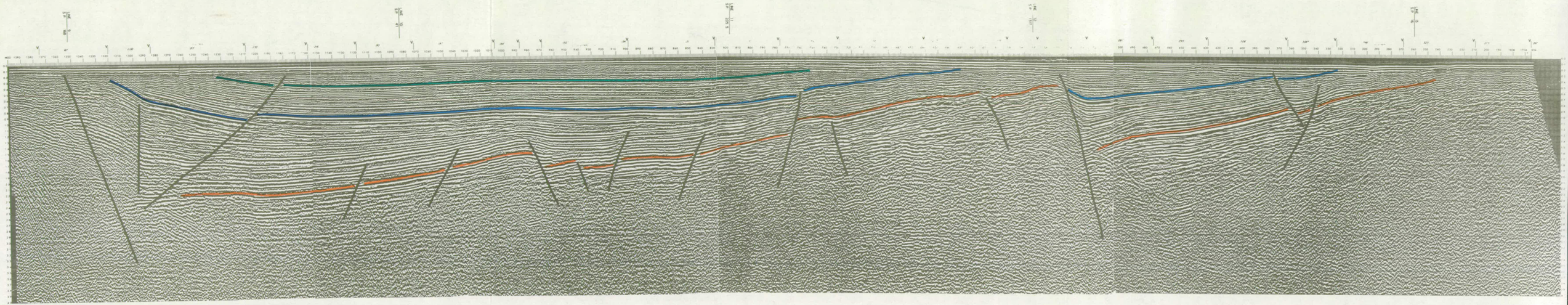

Two-way time in seconds

PLATE I

Seismic Interpretation

Line No 5

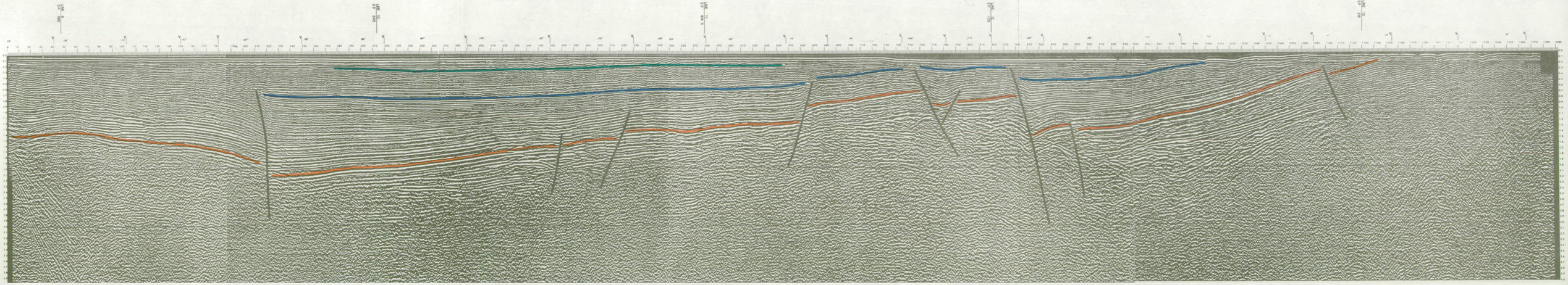

Two-way time in seconds

SUB-PLEISTOCENE GEOLOGY OF THE BRITISH ISLES AND THE ADJACENT CONTINENTAL SHELF

INSTITUTE OF GEOLOGICAL SCIENCES

SECOND EDITION 1979

Austin W. Woodland C.B.E. Director,

Scale 1:2,500,000

Projection: Lambert's Conic Conformal

Kilometres 0 50 100 150 200 250 300

Statute Miles 0 50 100 150 200

Nautical Miles 0 50 100 150 200

INDEX AND EXPLANATION

TERTIARY
- gn — n: Neogene; g: Palaeogene

CRETACEOUS
- k — ku: Upper; kl: Lower

JURASSIC
- j — ju: Upper; jm: Middle; jl: Lower

CARBONIFEROUS
- c: Westphalian-Stephanian; Namurian; Dinantian; Carboniferous is undivided in offshore areas

pt — Permo-Triassic (New Red Sandstone)

Sedimentary basin; Mesozoic (including Permian) Suspected age range e.g. Permian to Jurassic:- p-j

d — Devonian and Old Red Sandstone

Lower Palaeozoic; age indicated offshore where known (e-Cambrian, o - Ordovician, s - Silurian)

Basement undivided: age range pre-Cambrian (a) to Carboniferous, indicated offshore where known Basement, magnetic, metamorphic; Lewisian, (al) where differentiated

IGNEOUS
- Acid
- Intermediate & basic
- Undivided

Geological boundary

Fault

Anticline

Syncline

Depth to base Tertiary in North Sea

500 — Thickness of preserved Triassic in the Southern North Sea

500 — Sediment thickness above base Oligocene in the Rockall-Porcupine Bank area

500 — Bathymetric contours

All depths and thicknesses are in metres

Deep Sea Drilling Project Borehole

Dredge sample

age indicated

Basement deep (greater than about 5km)

Basement at moderate depths (between about 3.5 and 5km)

Relative depths of pre-Permian basement in the North Sea.

Based on work published by the following:-

Denmark: The Instituttet for Teknisk Geologi, Danmarks Tekniske Højskole; the Universitetets Mineralogiske og Geologiske Museum, Copenhagen.

France: The Universities of Caen, Paris and Rennes; the Bureau de Recherches Géologiques et Minières and the Centre National pour l'Exploration des Océans.

Ireland: Geological Survey of Ireland.

Netherlands: The University of Utrecht, the Geologische Stichting, the Koninklijk Nederlandsch Geologisch-Mijnbouwkundig Genootschap, Nederlandse Aardolie Maatschappij B.V.

Norway: University of Bergen, Statens Oljedirektorat, Stavanger.

United Kingdom: The Institute of Geological Sciences; the Institute of Oceanographic Sciences. The Universities of Birmingham, Bristol, Durham, Hull, Liverpool, London (University College) and Wales (Aberystwyth and Menai Bridge).

United States of America: The Deep Sea Drilling Project (including the International Phase of Ocean Drilling)

General: Esso Europe Incorporated, Phillips Petroleum Company and Shell UK Exploration and Production Limited.

NOTE The reliability of geological information in offshore areas is extremely variable and ranges from relatively well proven to speculative.

Compiled by W. Martindale and J. A. Chesher and drawn in the Leeds office of the Institute of Geological Sciences.

Made and published by the Director General of the Ordnance Survey, Southampton, for the Institute of Geological Sciences, Natural Environment Research Council.

4000/79

G.R.WOOD